UNIVERSITAT POLITÈCNICA DE VALÈNCIA

DEPARTAMENTO DE QUÍMICA

CENTRO DE RECONOCIMIENTO MOLECULAR
Y DESARROLLO TECNOLÓGICO

Supramolecular Chemistry
New chemodosimeters and hybrid materials for the chromo-fluorogenic detection of anions and neutral molecules

PhD. THESIS

Submitted by

Sameh El Sayed

PhD. Supervisors

Prof. Ramón Martínez Máñez
Dr. Félix Sancenón Galarza

Valencia, June 2015

RAMÓN MARTÍNEZ MÁÑEZ, PhD in Chemistry and Professor at the *Universitat Politècnica de València*, and FÉLIX SANCENÓN GALARZA, PhD in Chemistry and Lecturer at the *Universitat Politècnica de València*.

CERTIFY:

That the work *"**Supramolecular Chemistry: New chemodosimeters and hybrid materials for the chromo-fluorogenic detection of anions and neutral molecules**"* has been developed by **Sameh El Sayed** under their supervision in the Centro de Reconocimiento Molecular y Desarrollo Tecnológico (IDM) of the *Universitat Politècnica de València*, as a Thesis Project in order to obtain the degree of PhD in Chemistry at the *Universitat Politècnica de València.*

Valencia, 16th June 2015.

Prof. Ramón Martínez Máñez Dr. Félix Sancenón Galarza

" رَبَّنَا إِنَّنَا سَمِعْنَا مُنَادِيًا يُنَادِي لِلْإِيمَانِ أَنْ آمِنُوا بِرَبِّكُمْ فَآمَنَّا ۚ رَبَّنَا فَاغْفِرْ لَنَا ذُنُوبَنَا وَكَفِّرْ عَنَّا سَيِّئَاتِنَا وَتَوَفَّنَا مَعَ الْأَبْرَارِ"

القران الكريم. سورة آل عمران (193)

OUR LORD! VERILY, WE HAVE HEARD THE CALL OF ONE [MUHAMMAD (PBUH)] CALLING TO FAITH: 'BELIEVE IN YOUR LORD,' AND WE HAVE BELIEVED. OUR LORD! FORGIVE US OUR SINS AND REMIT FROM US OUR EVIL DEEDS, AND MAKE US DIE IN THE STATE OF RIGHTEOUSNESS ALONG WITH AL-ABRAR (THOSE WHO ARE OBEDIENT TO ALLAH AND FOLLOW STRICTLY HIS ORDERS, RIGHTEOUS).

SURAT AL IMRAN AYAT NUMBER 193. THE HOLY QURAN.

THE BEST AMONG YOU IS THE ONE WHO DOESN'T HARM OTHERS WITH HIS TONGUE AND HAND.

...PROPHET MOHAMED (ﷺ).

THE MORE I STUDY SCIENCE, THE MORE I BELIEVE IN GOD.

…ALBERT EINSTEIN

LOVE SHOULDN'T PLAY BY THE RULES. IT'S ALL ABOUT CHEMISTRY.

…RACHEL BILSON

THERE ARE NO SECRETS TO SUCCESS; IT IS THE RESULT OF PREPARATION, HARD WORK, AND LEARNING FROM FAILURE.

…COLIN POWELL

بسم الله والصلاة والسلام على رسول الله

اهدى هذا العمل الى....

أبى..... اسال الله ان يتغمده بواسع رحمته وان يجعله من اهل الجنة فقد أدي الامانه.

أمى..... اسال الله ان يبارك لنا فيك ويجزيك خير الجزاء وان يبارك لنا في عمرك.

اخوتى.... ريحاب . داليا . محمد . نورا . أسماء ..... اليكم اهدى هذا العمل.

طارق . سعيد . ساره . منه . ياسمين.

اشكركم جميعا فقد ساهمتم جميعا فيما قد وصلت الية

Acknowledgements

Agradecimientos

الحمد لله رب العالمين حمدا طيبا مبارك فية ملء السموات والارض.
اسأل الله العظيم ان يكون هذا العمل من العلم الذى ينتفع بة فى الدنيا والاخرة.

اتقدم بخالص الشكر والعرفان لكل من ساعد او ساهم فى اخراج هذا العمل. الى اصدقائى فى مصر جميعا شكرا لكم فقد ساهمتم بلا شك فى هذا العمل. خالص الشكر والتقدير الى اصدقائى المصريين فى فالنسيا..... محمد عبد القادر . طارق سلومة . محمد رجب . محمد على . محمد ماهر . عبدالله عبد العظيم . محمد علاء . رامى شلتوت . خالد حربى . أحمد يحيي . الشيخ محمد على . جعفر . محمد ابراهيم . رجب . احمد عزت . عبد الرحمن . احمد شبانة و رحمة و ساندى . أبو بكر الشلقاني . احمد فوزى.

اخى الحبيب . ايمن النجار . شكرا جزيلا على الصحبة الجميلة فى هذة السنوات الاربع واسأل الله العظيم ان يجزيك الخير الكثير وان يبارك لك فيه.

En primer lugar quiero agradecer de todo corazón a mis directores de la Tesis, Ramón Martínez por dejarme formar parte de su gran grupo de investigación, por descubrir como es la investigación y enfrentando a los problemas, encontrando soluciones y experimentando técnicas nuevas. A Félix Sancenón por ser mi mejor maestro, para su enseñanza, su pasión, su gran amistad y ayuda incondicional día día y en cada momento, por momentos inolvidables de risas, dudas, preguntas de química, por escucharme en el Bocho, en Sofra, el Marroquí,.... muchísimas gracias por todos estos años de amistad. Gracias a Juan, Loles, José Vicente y José Luis por vuestras ayudas. A Luis Villaescusa, por muchísimas conversaciones en diferentes temas y por ser mi compañero de vitrina casi cuatros años. ¡MUCHAS GRACIAS!

Cuando he empezado, había tres generaciones en el grupo, primero las personas que acaban de terminar sus tesis, para ellos realmente gracias por haberme ayudado en los primeros días y por darme la confianza y la fuerza de seguir adelante. De ellos quiero agradecer a Elena por el apoyo y hablar amablemente conmigo sobre mi familia y mi tierra. Carmen, por ayudar y explicarme sinceramente cómo resolver mis dudas especialmente en la parte

material. Andrea Bernardos (funny face), de verdad me siento muy agradecido por su ayuda y su encantadora sonrisa. ¡GRACIAS A TODOS!
La segunda generación fueron los investigadores que estaban escribiendo la tesis, quien puede olvidar Estela? eres un crack, muchas gracias por ayudarme y por escucharme. Yolanda, por tu alegría, buen corazón, tu animación de tener una novia española y siempre me has hecho sonreír, Inma Campos, por tu ayuda tanto en el máster como en el laboratorio. Alessando (señor) muchísimas gracias crack por enseñarme mucho de orgánica y por nuestros momentos fuera de laboratorio en Valencia, Pavía y Bérgamo. Maria y Patri, como puedo olvidar a las dos?, son mis favoritas. Maria, por ser siempre muy simpática y maja conmigo, gracias por tu sonrisa increíble cuando te dije una palabra romántica y por nuestras conversaciones. Patri, por desgracia he llegado a Valencia muy tarde y estuviste ocupada, gracias guapa por tratarme como hermano, nunca puedo olvidar tus ojos azules y tu fuerte carácter. Luis Enrique, gracias por tus ayudas y paciencia en enseñarme cómo funcionan las cosas. MUCHAS GRACIAS!

Édgar, amigo mío, de verdad tienes un gran corazón, siempre ofreciendo tu mano y ayudando en todo, muchísimas gracias por tus ayudas, por ser muy amable y para ti espero que llegue todo lo que deseas tanto en la vida profesional como la vida privada y en el campo de fotografía. ¡MUCHAS GRACIAS!

La tercera generación cuando he llegado fueron personas que han empezado en el grupo hace pocos meses como Cris G y Nuria, los que han empezado más o menos conmigo Mar y LLuis y poco después llegó Cris de la Torre. Cris G, la ¡¡Aligera de la Huertaii Chica, tu sabes que mi gusta mucho estar siempre a tu lado, eso porque siempre siento feliz cuando te veo sonriendo. Nuria, chica tan bonita simpática como tú no hay muchas, gracias por tus ayudas y tus deliciosos platos. Mar, guapa, gracias por muchísimas ayudas en el máster y en estos cuatro años sabes que siempre me sentí contento cuando recuerdo tu cara preciosa y tus bromas. Lluiset, mi ha gustado mucho hablar contigo en muchas temas, política, religión, cultura, educación aparte del trabajo y siempre creo que eres un genio. Cris

G, Nuria, Mar, Lluis espero para vosotros di mi corazón todos los buenos deseos en la vida. Cris de la torre, la chica más atleta que conozco hasta ahora te queda solo hacer el IRON MAN, gracias por tus ayudas en el trabajo y por animarme a hacer carreras. Román, un caballero, atleta y electro- electroquímico gracias chico por ser muy majo conmigo.

En mi tercer año en el laboratorio llegaron nuevos chicos, Angela (Angelina Jolie) eres una chica que vale mucho, trabajadora y seguro que llegarás a un nivel muy alto. Cris M, guapa gracias por preocuparte por mí y por tu simpatía. Los Biotecnólogos Irene, Amelia, Alba, Lorena y Monica muchísimo ánimo chicas en vuestro viaje lleno de Biotecnológica. Poco después ii ha llegado Toni, (el tío Toni) un gran chaval, muy amable y simpático, gracias por estar conmigo en tantos momentos alegres además de muchas carreras, nos falta hacer un maratón juntos, como te dije en esa viaje necesitas mucha concentración y ser más paciente enfrente a los problemas....¡GRACIAS CHICOS!

Finalmente quiero agradecer Anita,...bambolina.. eres una chica simpática, agradable y siempre me has hecho sonreír. Además los nuevos que acaban de empezar ya, Santi por tus ánimos de hacer Pádel y Escalar. Bea, por tus ensenarme otro tipo de Castellano....como pitotes.., María Elena, por tus gatos. Marta, por ser la simpática técnica del lab. Luis, por siempre darme chicletes. Elisa, por tu sonrisa. Adrián, por ser amable. ¡GRACIAS CHICOS Y BUENA SUERTE A TODOS!

En Burjassot, había Andrea Barba, Almudena, Inma Candil, Cris S y Alberto gracias chicos por estas fiestas y momentos tan alegres.

Agradezco tamban Laura, Pavel, Rafa, Carolena, Maria Rz, Ana, Hulya, Erick, Kim, Paulina gracias chicos por compartir conmigo momentos felices en ese viaje.

Además de lab 2.6 he tenido unos amigos en otros laboratorios, Dani, Neus y Herme gracias chicos por vuestra amistad y buena compaña.

I think there is some relation between me and India, several times Indian people thought that am from India, i don't know why?? As i love the Indian movies and have various Indian friends. I want to thank Krishanu Sarkar and Ravishankar Bhat for those great and happy moments. Asha Guru, Thank you so much for our conversations, your best wishes for me and reading my hands for future predictions, if it happened i will tell you. iiTHANKSii

During my PhD Thesis stays abroad in Pavia University in Italy i was lucky to be within profesor Murizio Licchell, many thanks prof for your support and help. How could I express my gratitude to you? Many thanks to Valeria y el tío majo Michele you're magic man, also thanks for Greta, Giacomo, Alice, Alessandro, Maduka, Luca, Carlo, Barbra, Agnese, Elisa... iiTHANKSii

Finalmente, gracias a mis amigos en Valencia, Cristian, Carlos, Camelo, Daniel, Roberto, Matteo.

GRACIAS DE TODO CORAZÓN a VALENCIA, ESPAÑA para darme esta gran oportunidad inolvidable.

GRACIAS A TODOS POR VUESTRO APOYO.

Abstract

The present PhD thesis entitled “Supramolecular Chemistry: New chemodosimeters and hybrid materials for the chromo-fluorogenic detection of anions and neutral molecules” is based on the application of supramolecular chemistry and material science principles for the development of optical chemosensors for anions and neutral molecules detection.

The second chapter of this PhD thesis is devoted to the preparation of chemodosimeters for the chromo-fluorogenic detection of fluoride, diisopropyl fluorophosphates (DFP) and hydrogen sulfide. The optical detection of fluoride anion was achieved by using a pyridine derivative containing a t-butyldimethylsilyl ether group. Aqueous solutions of the chemodosimeter were colorless but turned yellow upon addition of fluoride anion. Also a remarkable enhancement in emission was observed only upon the addition of fluoride. The optical changes were ascribed to a fluoride-induced hydrolysis of the silyl ether moiety.

Also a chemodosimeter for the optical recognition of DFP, a nerve agent simulant, was prepared. In this case, the chemodosimeter was based on a stilbene pyridinium derivative functionalized with hydroxyl and silyl ether moieties. Aqueous solutions of the chemodosimeter were colorless changing to yellow upon DFP addition. The optical changes were ascribed to a hydroxyl phosphorylation followed by a fluoride-induced hydrolysis of the silyl ether group. Besides, that probe was implemented in test strips and DFP detection in gas phase was accomplished.

Finally, the fluorogenic recognition of hydrogen sulfide anion was explored. For this purpose different fluorophores were selected and fucntionalized with 2,4-dinitrophenyl ether groups. The prepared probes were neraly non-emissive but remarkable emission enhancements upon addition of hydrogen sulfide were observed. The emission enhancements observed were due to a selective sulfide-induced hydrolysis of the 2,4-dinitrophenyl ether moiety that yielded the free fluorophores. Another set of chemodosimeters equipped with azide and

sulfonylazide moieties were prepared. Again these probes were non-fluorescent but upon addition of hydrogen sulfide an important enhancement in emission was found. The selective response was ascribed to a reduction of the azide and sulfonylazide moieties to amine and sulfonylamide induced by hydrogen sulfide anion. Besides, the viability assays showed that these dosimeters were essentially non-toxic and real-time fluorescence imaging measurements confirmed their ability to detect intracellular hydrogen sulfide at micromolar concentrations.

The third chapter of this PhD thesis was devoted to the preparation of nanoscopic gated materials and their use in sensing protocols. In a first step a gated material for the optical detection of glutathione (GSH) was prepared. For this purpose MCM-41 mesoporous silca nanoparticles were selected as inorganic scaffold. The pores were loaded with safranine O and the external surface was functionalized with disulfide-containing oligo(ethylene glycol) moieties. Dye delivery from aqueous suspensions of the sensory material was only observed in the presence of GSH. The signalling paradigm was ascribed to the selective reduction of the disulfide bond by GSH which induced pore opening and dye release.

Also capped organic-inorganic hybrid materials for the selective detection of hydrogen sulfide were prepared and characterized. In this case the same MCM-41 support was used and charged with $[Ru(bipy)_3]^{2+}$ dye. Then, the external surface was functionalized with Cu(II)-macorcyclic complexes and finally, the pores were capped by the addition of the bulky anion hexametaphosphate. Aqueous suspensions of this material showed negligible dye release whereas in the presence of hydrogen sulfide anion a remarkable colour change was observed. This optical response was ascribed to a demetallation process of the Cu(II) complex induced by hydrogen sulfide.

Resumen

La presente tesis doctoral titulada *"Química supramolecular: Nuevos dosímetros químicos y materiales híbridos para la detección cromo-fluorogénica de aniones y moléculas neutras."* está basada en la aplicación de principios básicos de la química supramolecular y de la ciencia de materiales en el desarrollo de sensores ópticos para aniones y moléculas neutras.

El segundo capítulo de esta tesis doctoral está dedicado a la preparación de dosímetros químicos para la detección cromo-fluorogénica de fluoruro, diisopropil fluorofosfato (DFP) y sulfuro de hidrógeno. Para la detección óptica del anión fluoruro se sintetizó un derivado de piridina funcionalizado con un *t*-butildimetilsilil éter. Las disoluciones acuosas de este sensor son incoloras volviéndose amarillas en cuanto se adiciona el anión fluoruro. Además, la presencia de este anión induce un aumento de fluorescencia significativo. Los cambios de color y de fluorescencia observados son debidos a la hidrolisis de la agrupación silil éter inducida por el anión fluoruro.

En este capítulo también se describe la preparación de un dosímetro químico para la detección de DFP, que es un simulante de agentes nerviosos. Este dosímetro está basado en un estilbeno funcionalizado con una sal de piridinio que contiene grupos hidroxilo y silil éter en su estructura. De nuevo, las disoluciones acuosas de este sensor son incoloras pero se vuelven amarillas en presencia del DFP. Estos cambios de color son debidos a una reacción de fosforilación del grupo hidroxilo con el DFP seguida de una hidrólisis del silil éter inducida por el fluoruro que se libera en el primer paso. La detección de DFP también se produce en fase gas empleando tiras reactivas conteniendo al sensor.

Finalmente se prepararon dos familias de sensores para la detección óptica de hidrógeno sulfuro. La primera familia de sensores consiste en fluoróforos comunes funcionalizados con 2,4-dinitrofenil éteres. Los sensores preparados no presentaron una emisión de fluorescencia importante mientras que, en presencia del anión hidrógeno sulfuro, se observó un aumento significativo. Estos aumentos

en la intensidad de emisión fueron adscritos a la hidrolisis de los grupos 2,4-dinitrofenil éter inducida por el hidrógeno sulfuro. La segunda familia de dosímetros también estaba compuesta por ciertos fluoróforos pero, en este caso, funcionalizados con grupos azida y sulfonilazida. Los dosimétros preparados, siguiendo esta segunda aproximación, tampoco dieron una fluorescencia significativa observándose un aumento de la misma al añadir el anión hidrógeno sulfuro. La respuesta observada fue asignada a reacciones de reducción, de los grupos azida y sulfonilazida, inducidas por el hídrogeno sulfuro. Además, ensayos de viabilidad celular demostraron que las dos familias de dosímetros preparadas no son tóxicas y que se pueden emplear para detectar hidrógeno sulfuro en células en concentraciones micromolar.

El tercer capítulo de esta tesis doctoral está dedicado a la preparación de materiales híbridos nanoscópicos funcionalizados con puertas moleculares y su aplicación en protocolos de reconocimiento. En primer lugar se preparó un material para la detección óptica de glutatión (GSH). Para ello se emplearon nanopartículas de MCM-41 mesoporosas como soporte inorgánico. Los poros del soporte fueron cargados con el colorante safranina O y la superficie externa funcionalizada con oligo(etilenglicol) conteniendo enlaces disulfuro. Al adicionar GSH sobre suspensiones acuosas de dicho material se observó la liberación de la safranina O debido a la hidrolisis del enlace disulfuro de las cadenas de oligo(etilenglicol).

También se prepararon y caracterizaron varios materiales híbridos para la detección selectiva del anión hidrógeno sulfuro. En este caso también se empleó, como soporte inorgánico, sílice mesoporosa MCM-41. Los poros del soporte inorgánico fueron cargados con $[Ru(bipy)_3]^{2+}$ y la superficie externa funcionalizada con varios complejos macrocíclicos de Cu(II). El material sensor final fue obtenido al añadir el anion hexametafosfato, que compleja con los complejos de Cu(II), produciendo un bloqueo de los poros. Al suspender los materiales sensores en agua no se observó liberación de colorante mientras que al añadir hidrógeno sulfuro se observaron cambios de color significativos. Esta respuesta óptica ha

sido adscrita a un proceso de demetalación de los complejos de Cu(II) inducida por el anión hidrógeno sulfuro.

Resum

La present tesi doctoral titulada *"Química supramolecular: Nous dosímetres químics i materials híbrids per a la detecció cromo-fluorogènica d'anions i molècules neutres."* està basada en l'aplicació dels principis bàsics de la química supramolecular i de la ciència dels materials en el desenvolupament de sensors òptics per a anions i molècules neutres.

El segon capítol d'aquesta tesi doctoral està dedicat a la preparació de dosímetres químics per a la detecció cromo-fluorogènica de fluorur, diisopropil fluorofosfat (DFP) i sulfur d'hidrogen. Per a la detecció òptica de l'anió fluorur es va sintetitzar un derivat de piridina funcionalitzat amb un *t*-dibutildimetilsilil èter. Les dissolucions aquoses d'aquest sensor són incolores convertint-se en grogues en el moment en què s'addiciona l'anió fluorur. A més a més, la presència d'aquest anió indueix un augment significatiu de fluorescència. Els canvis de color i de fluorescència observats es deuen a la hidròlisi de l'agrupació silil èter induïda per l'anió fluorur.

En aquest capítol també es descriu la preparació d'un dosímetre químic per a la detecció de DFP, que és un simulant d'agents nerviosos. Aquest dosímetre està basat en un estilbè funcionalitzat amb una sal de piridina que conté grups hidroxil i silis èter en la seua estructura. De nou, les dissolucions aquoses d'aquest sensor són incolores però es converteixen en grogues amb la presència de DFP. Aquests canvis de color són deguts a una reacció de fosforilació del grup hidroxil amb el DFP seguida d'una hidròlisi del silil èter induïda per el fluorur alliberat en el primer pas. La detecció de DFP també es produeix utilitzant tires reactives que contenen el sensor.

Finalment varen ser preparades dues famílies de sensors per a la detecció òptica de sulfur d'hidrogen. La primera família consisteix en fluoròfors comuns funcionalitzats amb 2,4-dinitrofenil èters. Els sensors preparats no presentaren una emissió de fluorescència significativa mentre que, en presencia de l'anió hidrogen sulfur, es va observar un augment significatiu. Aquests augments en la

intensitat d'emissió han sigut adscrits a la hidròlisi dels grups 2,4-dinitrofenil èter induïda per l'hidrogen sulfur. La segona família de dosímetres també estava composada per certs fluròfors però, en aquest cas, funcionalitzats amb grups azida i sulfonilazida. Els dosímetres preparats, seguint aquesta segona aproximació, tampoc donaren una fluorescència significativa observant-se un augment de la mateixa al afegir l'anió hidrogen sulfur. La resposta observada va ser assignada a reaccions de reducció, dels grups azida i sulfonilazida, induïdes per l'hidrogen sulfur. A més a més, assajos de viabilitat cel·lular varen demostrar que ambdues famílies de dosímetres preparades no són tòxiques i poden ser emprades per a detectar sulfur d'hidrogen en cèl·lules a concentracions micromolars.

El tercer capítol d'aquesta tesi doctoral està dedicat a la preparació de materials híbrids nanoscòpics funcionalitzats amb portes moleculars i la seua aplicació en protocols de reconeixement. En primer lloc es va preparar un material per a la detecció òptica de glutatió (GSH). Per a aquest propòsit es varen emprar nanopartícules MCM-41 mesoporoses com a suport inorgànic. Els porus del suport varen ser carregats amb el colorant safranina O i la superfície externa funcionalitzada amb oligo(etilenglicol) que contenia enllaços disulfurs. Al addicionar GSH sobre les suspensions aquoses la lliberació de safranina O va ser observada degut a l'hidròlisi dels enllaços disulfur de les cadenes d'oligo(etilenglicol).

També varen ser preparats i caracteritzats diversos materials híbrids per a la detecció selectiva de l'anió hidrogen sulfur. En aquest cas també es va emprar, com a suport inorgànic, sílice mesoporosa MCM-41. Els porus del suport inorgànic varen ser carregats amb $[Ru(bipy)_3]^{2+}$ i la superfície externa funcionalitzada amb diversos complexos macrocíclics de Cu(II). El material sensor final es va obtindre al afegir l'anió hexametafosfat, que es complexa amb macrocicles de Cu(II), produint un bloqueig dels porus. Al suspendre els materials sensors en aigua no es va observar alliberament de coloronat mentre que al afegir hidrogen sulfur es varen observar canvis de color significatius. Aquesta resposta òptica ha sigut adscrita a

un procés de demetal·lació dels complexos de Cu(II) induïda per l'anió hidrogen sulfur.

Publications

Results of this PhD Thesis and other contributions have resulted in the following scientific publications:

- **Sameh El Sayed,** Alessandro Agostini, Luis E. Santos-Figueroa, Ramón Martínez-Máñez, Félix Sancenón, "*An instantaneous and highly selective chromo fluorogenic chemodosimeter for fluoride anion detection in pure water*", **ChemistryOpen., 2013**, 2, 58-62.

- **Sameh El Sayed,** Cristina de la Torre, Luis E. Santos-Figueroa, Enrique Pérez-Payá, Ramón Martínez-Máñez, Félix Sancenón, Ana M. Costero, Margarita Parra, Salvador Gil, *" A new fluorescent "turn-on" chemodosimeter for the detection of hydrogen sulfide in water and living cells"*, **RSC Adv., 2013,** 3, 25690-25693.

- **Sameh El Sayed,** Lluís Pascual, Alessandro Agostini, Ramón Martínez-Máñez, Félix Sancenón, Ana M. Costero, Margarita Parra, Salvador Gil, *" A Chromogenic Probe for the Selective Recognition of Sarin and Soman Mimic DFP"*, **ChemistryOpen., 2014**, 3, 142-145.

- **Sameh El Sayed,** Cristina de la Torre, Luis E. Santos-Figueroa, Ramón Martínez-Máñez, Félix Sancenón, Mar Orzáez, Ana M. Costero, Margarita Parra, Salvador Gil *" 2,4-dinitrophenyl ether-containing chemodosimeters for the selective and sensitive "in vitro" and "in vivo" detection of hydrogen sulfide"*, **Supramol. Chem.**, **2015**, 4. 244-254.

- **Sameh El Sayed,** Cristina Giménez, Elena Aznar, Ramon Martinez-Manez, Felix Sancenón, Maurizio Licchelli, *" Highly selective and sensitive detection of glutathione using mesoporous silica nanoparticles capped with disulfide-containing oligo(ethylene glycol) chains"*, **Org. Biomol. Chem., 2015,** 13, 1017-1021.

- **Sameh El Sayed**, Cristina de la Torre, Luis E. Santos-Figueroa, Cristina Marín-Hernández, Ramón Martínez-Máñez, Félix Sancenón, Ana M. Costero, Salvador Gil, Margarita Parra, *" Azide and sulfonylazide functionalized fluorophores for the selective and sensitive detection of hydrogen sulfide",* **Sens. Actuators, B., 2015**, 207, 987-994.

- **Sameh El Sayed**, Michele Milani, Maurizio Licchelli, Ramón Martínez-Máñez and Félix Sancenón, "*Hexametaphosphate-capped silica mesoporous nanoparticles containing Cu^{II} complexes for the selective and sensitive optical detection of hydrogen sulfide in water*", **Chem. Eur.J., 2015,** 21**,** 7002 –7006.

- Luis E. Santos-Figueroa, Cristina de la Torre, **Sameh El Sayed**, Félix Sancenón, Ramón Martínez-Máñez, Ana M. Costero, Salvador Gil, Margarita Parra, *"Highly selective fluorescence detection of hydrogen sulfide by using an anthracene-functionalized cyclam–Cu^{II} Complex"*, **Eur. J. Inorg. Chem., 2014,** 41-45.

- Luis E. Santos-Figueroa, Cristina de la Torre, **Sameh El Sayed**, Félix Sancenón, Ramón Martínez-Máñez, Ana M. Costero, Salvador Gil, Margarita Parra, " *A Chemosensor Bearing Sulfonyl Azide Moieties for Selective Chromo-Fluorogenic Hydrogen Sulfide Recognition in Aqueous Media and in Living Cells",* **Eur. J. Org. Chem., 2014,** 1848-1854.

- Alessandro Agostini, Inmaculada Campos, Michele Milani, **Sameh El Sayed**, Lluis Pascual, Ramón Martínez-Máñez, Maurizio Licchelli, Félix Sancenón, " *A surfactant-assisted probe for the chromo-fluorogenic selective recognition of GSH in water",* **Org. Biomol. Chem., 2014,** 12, 1871-1874.

- Cristina Marín-Hernández, Luis E. Santos-Figueroa, **Sameh El Sayed**, Teresa Pardo, M. Manuela M. Raposo, Ramón Martínez-Máñez and Félix Sancenón "*Synthesis and evaluation of the chromo-fluorogenic recognition ability of imidazoquinoline derivatives toward ions",* **Dyes Pigments. 2015.** *Accepted*

Abbreviations

Ala	Alanine
ADP	Adenosine Diphosphate
AMP	Adenosine Monophosphate
ATP	Adenosine Triphosphate
BET	Brunauer, Emmett and Teller model
BJH	Barret, Joyner and Halenda model
BODIPY	Boron-dipyrromethene
CO	Carbon monoxide
$CDCl_3$	Deuterated chloroform
CTABr	Hexadecyltrimethylammonium Bromide
CWA	Chemical Warfare Agents
DNA	Deoxyribonucleic acid
DCNP	Diethyl Cyanophosphate
DCP	Diethyl Chlorophosphate
DFP	Diisopropyl fluorophosphate
DMF	Dimethyl Formamide
DMEM	Dulbecco's Modified Eagle's Medium
DMSO	Dimethylsulfoxide
DLS	Dynamic light scattering
DL-Hcy	Homocysteine
DDT	Dithiothreitol
EA	Elemental Analysis
EDX	Energy Dispersive X-Ray Spectroscopy
ESIPT	Excited State Intramolecular Proton Transfer
EPR	Electron Paramagnetic Resonance
Et_2O	Diethyl Ether
GSH	Glutathione
HEPES	4-(2-Hydroxyethyl)-1-Piperazineethanesulfonic Acid
His	Histidine
HPLC	High Performance Liquid Chromatography
HRMS	High Resolution Mass Spectrometry

IMS	Ion Mobility Spectroscopy
IUPAC	International Union Of Pure And Applied Chemistry
k_a	Association Constant
LOD	Limit of Detection
LUMO	Low Unoccupied Molecular Orbital
MCM	Mobil Composition of Matter
ME	2-Mercaptoethanol
Me-Cys	Methyl-Cysteine
MeOH	Methanol
MS-EI	Electron Impact Ionization Mass Spectrometry
NBD	7-Nitrobenz-2-oxa-1,3-Diazole
NIR	Near Infrared
NMR	Nuclear Magnetic Resonance
NO	Nitrogen Monoxide
PBS	Phosphate Buffered Saline
PET	Photo-Induced Electron Transfer
PEG	Poly(Ethyleneglycol)
PPB	Part Per Billion
PPI	Pyrophosphate
PPM	Part Per Million
P-NMR	Phosphorus Nuclear Magnetic Resonance
PV	Pyrocatechol Violet
RT	Room Temperature
$[Ru(bipy)_3]^{2+}$	Tris(2,2'bipyridyl)Ruthenium(II)
SAMs	Self-Assembled Monolayer Surfaces
SDA	Structure-Directing Agent
SEM	Scanning Electron Microscopy
TBDMSCl	Tertiary Butyl Dimethyl Silyl Chloride
TEM	Transmission Electron Microscopy
TEOS	Tetraethylorthosilicate
Tetryl	2,4,6-Trinitrophenylmethylnitramine
TGA	Thermogravimetric Analysis

UV/Vis	Ultraviolet/Visible spectroscopy
XRD or PXRD	X-Ray Diffraction

Table of Contents

1. General Introduction

1.1 Supramolecular chemistry

Today, supramolecular chemistry (the chemistry beyond the molecules) is a well stablished field inside the chemistry realm. The work presented in this PhD thesis is devoted to the preparation of chemical sensors and sensory hybrid organic-inorganic materials constructed bearing in mind some of the supramolecular chemistry principles. For this reason, main concepts related with supramolecular chemistry and certain applications will be explained in the next pages.

1.1.1 The beginning

Supramolecular chemistry started in the history of chemistry with a series of fundamental discoveries which finally led to the emergence for the first time of the word ''supramolecular chemistry''. This term was coined by Jean-Marie Lehn, who received the Nobel Prize in 1987 together with Donald J. Cram and Charles J. Pedersen for his outstanding research that led to the establishment of this novel branch of chemistry.

However, since XVIII century the formation of molecular aggregates was well known. At this respect, discovery of zeolite by Axel Cronstedt in 1756 and of clathrates ''anomalous ice'' by Joseph Priestley in 1778 were the first examples of molecular aggregates. Remarkable was also the observation of Benjamin Franklin in 1774 about oil spreading on water surface. These were the first signals about the existence of internal forces that can collect molecules in bigger aggregates (supramolecular forces). In XIX century, the intermolecular force principle was demonstrated in 1873 by Van der Waals[1] and the first molecular receptors, the cyclodextrins, were discovered in 1891[2] by Villiers. Then, other important landmarks were the beginning of coordination chemistry in 1893[3] by Alfred

[1] J. D. Van der Waals, *Nobel Lecture: Physics 1901-1921*, **1967**, 255-265.
[2] A. C. R. Villiers, *Hebd. Seances. Acad. Sci.*, **1891**, *112*, 536-538.
[3] a) A. Werner, *Nobel Lecture: Chemistry 1901-1921*, **1966**, 256-269; b) K. Bowman-James, *Acc. Chem. Res.*, **2005**, *38*, 671-678.

Werner and the lock-key model for the enzyme-substrate interaction presented by Emil Fisher in 1894.[4] From all these previous facts, scientists noted the importance of studying the interaction between molecules in chemical and biological processes. A key point in this new chemistry field was the introduction of biological receptor concept coined by Paul Ehrlich in 1906.[5] Besides, the first confirmation about the importance of intermolecular forces was proven by James Watson and Francis Crick in 1953[6] which led to the elucidation of the molecular structure of nucleic acids (DNA) and its significance for information transfer in living organisms. The supermolecule concept was introduced by Lothar Wolf in 1937 to describe the hydrogen-bonded acetic acid dimers,[7] and also the remarkable work of Linus Pauling about the hydrogen bond nature published in 1939.[8]

As stated above, the fathers of supramolecular chemistry are J. M. Lehn,[9] D. J. Cram[10] and C. J. Pedersen.[11] The significant importance of their job was universally recognized in 1987 when they received the Nobel Prize for their fundamental contributions in this new area of chemistry. Nowadays, supramolecular chemistry is a well stablished field inside chemistry and its fundamental concepts have been used for the development of a large number of applications such as chemical sensors for specific recognition of compounds, design of new types of materials, preparation of drugs, developing molecular machinery and the synthesis of highly complex self-assembled structures. In addition supramolecular chemistry has also influenced in the emerging science of nanotechnology and in the development of catalysts.[12]

[4] E. Fischer, *Ber. Dtsch. Chem. Ges*., **1895**, *28*, 1429-1438.
[5] P. Ehrlich, *Nobel Lecture: Physiology or Medicine 1901-1921*, **1967**, 304-320.
[6] J. Watson, F. Crick, *Nobel Lecture: Physiology or Medicine,* **1962**.
[7] K. L. Wolf, H. Frahm, H. Harms, *Z Phys. Chem., Abt. B*, **1937**, *36*, 237–287.
[8] L. Pauling, The Nature of the Chemical Bond, Cornell University, Ithaca, NY, 1st ed., **1939**.
[9] J. M. Lehn, *Nobel Lecture: Chemistry 1981-1990*, **1992**, 444-491.
[10] D. J. Cram, *Nobel Lecture: Chemistry 1981-1990*, **1992**, 419-437.
[11] C. J. Pedersen, *Nobel Lecture: Chemistry 1981-1990*, **1992**, 495-511.
[12] N. S. Dighe, S. R Pattan, D. S. Musmade, S. S. Dengale, R. S. Kalkotwar, V. M. Gaware, M. B. Hole, *Res. J.Pharm. Biol. Chem. Sci.*, **2010**, *1*, 291.

1.1.2 From molecular to supramolecular chemistry

Molecular chemistry ''the chemistry of the covalent bond'' is concerned with understanding the structures, properties and transformations of individual molecules constructed using covalent bonds between atoms. Moreover the application of the principles of this classical chemistry fails to explain the structures, functions and properties of the molecular assemblies formed between several molecules through non-covalent intermolecular forces.[13] That inability opened the way to the introduction of supramolecular chemistry concepts to provide acceptable understanding to supermolecule characteristics.

Supramolecular chemistry may be defined as ``*chemistry beyond the molecules´´*, or ``*chemistry of non-covalent bond´´* where the term *supermolecule* was illustrated by Dr. J. Lehn as an organized complex entity that resulted from the association of two or more chemical species through non-covalent interaction.[14] The nature of molecular and supramolecular chemistry was easily explained as the relationship between the individual family and the whole society by Dr. J. Lehn.[15] Molecules are like individual families that are formed by persons (atoms). Each family has its special properties and the interaction between the members is controlled by molecular chemistry. However, the interaction between one family and others in the whole society to form bigger associations and alliances with different characteristics (supermolecule) are controlled by supramolecular chemistry.[16]

The water molecule is the first logic example to illustrate the difference between molecular and supramolecular chemistry. A water molecule in the vapor phase is formed by covalent bonds between hydrogen and oxygen atoms (see

[13] K. Ariga, T. Kunitake, *Supramolecular Chemistry-Fundamentals and application* © Springer Verlag Berlin Heidelberg Edition **2006**.

[14] J. M. Lehn, *Angew. Chem*., **1988**, *100*, 91–116.

[15] J. M. Lehn, "*Supramolecular chemistry can help to understand better how to make efficient drugs*". Universitat Autònoma de Barcelona, Spain. October **2012**. Lecture.

[16] J. M. Lehn, Supramolecular chemistry, Ed. VCH, **1995**.

Figure 1.1). However, in the liquid phase, water molecules are linked together through hydrogen bonding interactions forming a supramolecular entity.

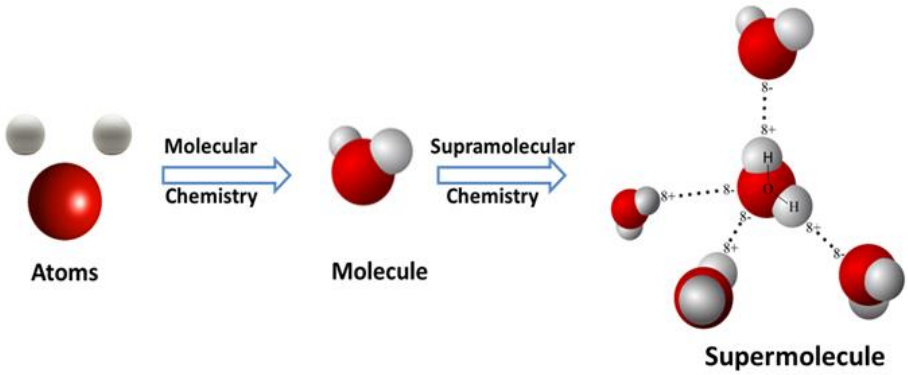

Figure 1.1. *Schematic representation illustrates the difference between molecular and supramolecular chemistry using water molecules.*

Cellulose is another natural example where intermolecular interaction appears. More in detail, each hydroxyl group of one saccharide unit can form hydrogen bonds with other -OH moieties in neighbor sugar molecules in the same polysaccharide chain (see Figure 1.2). Also hydrogen bonds between two saccharides in parallel polysaccharide chains can be formed (see again Figure 1.2). These hydrogen bonds reduce the distance between polysaccharide chains forming a coherent mono horizontal layer of polysaccharides like a sheet. Besides that, there is another type of non-covalent interaction in cellulose where the formed sheets stacked tightly into layers held together by Van der Waals forces to form a micro fibril.

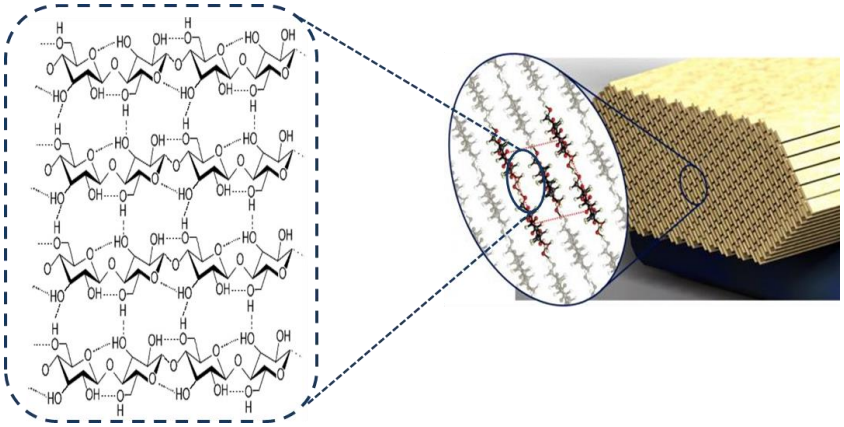

Figure 1.2. *Intermolecular interactions in cellulose. Left: side to side hydrogen bonds between hydroxyl groups of the polysaccharide chains in the same horizontal layer. Right: Van der Waals forces hold polysaccharide layers together.*

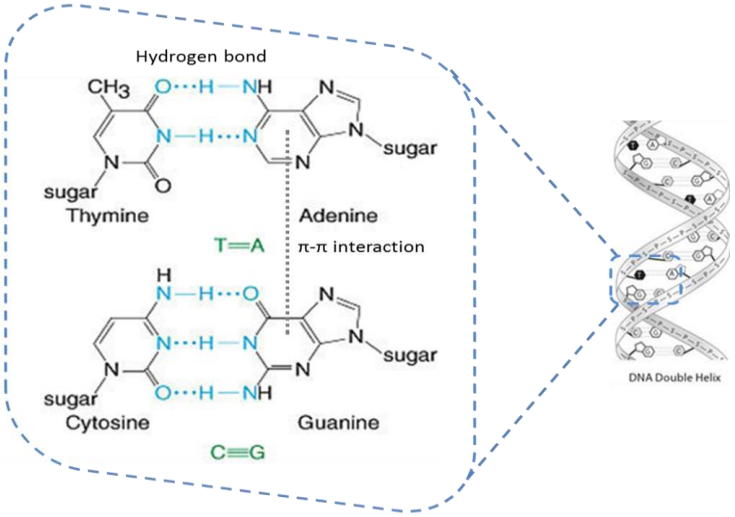

Figure 1.3. *Non-covalent interactions in DNA double helix: Hydrogen bond and π-π interaction.*

Another example of a biological supermolecule is DNA which shows the ability of molecules to form enormous entities through intermolecular interactions in order to adapt its structure to achieve an optimal manner of function. It is known that the helix shape of DNA is the best form which allows replication and recombination processes. This helix conformation (see Figure 1.3) is obtained by combining two different types of supramolecular interactions namely (i) hydrogen

bonds between the bases in different strands and (ii) π-π interactions between the aromatic rings of the nucleobases.

1.2 Molecular recognition (Host-Guest chemistry)

Molecular recognition can be defined as the specific binding of a *guest* molecule with a *host* compound forming a host-guest complex (supermolecule) through non-covalent interactions.[17] In order to form a stable complex, the host molecule must possess a high degree of complementarity (in terms of geometric and electronic features) with the guest. The host and guest concept clearly resembles to the classical *lock* and *key* principle proposed in 1894 by Dr. Emil Fisher. This was the first model of molecular recognition which describes the selective interaction between enzymes and substrates.[18] Enzymes (the lock) and their substrate (the key) should present a complementary in size and shape as shown in Figure 1.4. The lock and key analogy is an overly simplistic representation of a biological system but gives rise to many of the properties of enzymes, particularly in substrate binding and catalysis.

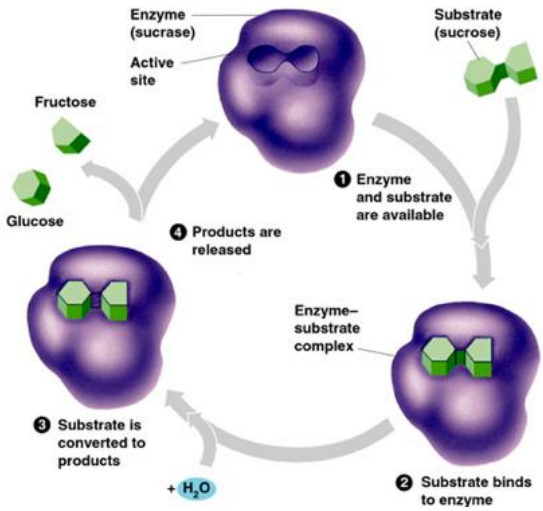

Figure 1.4. *Schematic representation of an enzymatic catalysis process based on the lock and key principle.*

[17] J. M. Lehn, *Noble Lecture*, **1987**.

[18] H. E. Fischer, *Nobel Lecture: Chemistry 1901-1921*, **1966**, 21-35.

A key point in the host-guest interaction is the selectivity, which is defined as the ability of the host to distinguish among different guests. This selectivity can arise from a number of different factors, such as *complementarity* between the guest and the host binding sites, *cooperativity* of the binding groups and *preorganization* of the host.[19]

- *Complementarity*: Both the host and guest must have mutual spatially and electronically complementary binding sites to form the supermolecule.

- *Cooperativity:* A host molecule with multiple binding sites that are covalently connected (*i.e*. acting as a 'team') forms a more stable host–guest complex than a similar system with sites that are not covalently connected (therefore acting separately from each other).

- *Preorganization:* A pre-organized host has a series of binding sites in a well-defined geometry within its structure and does not require a significant conformational change in order to bind to a specific guest in the most stable possible way.

In addition, the binding of a guest by a host or the interaction of two or more molecules by non-covalent bonds is an equilibrium process defined by a *binding constant*. The equilibrium that exists for a simple 1:1 host-guest interaction is:

$$H + G \rightleftharpoons HG$$

Where H is the host molecule, G the guest molecule and HG is the host-guest complex.

The association constant K_a is defined as: $K_a = \frac{[HG]}{[H][G]}$

Moreover, the selective binding of receptor (host) toward specific substrate (guest) is directly affected by the kinetic/thermodynamic stabilization of the

[19] J. W. Steed, J. L. Atwood, *Supramolecular Chemistry*, © **2009**, John Wiley & Sons, Ltd.

complex formed. At constant pressure and temperature, HG complex is favored kinetically/thermodynamically when K_a is high where in that case its free energy is lower than that of the individual molecules.[20]

1.3 Molecular self-assembly chemistry

Self-assembly is defined as ``the spontaneous association or aggregation of two or more molecules or ions with the reversible formation of a supermolecule''.[21] This generic definition has significantly broadened over time to incorporate many aspects of biochemistry and nanotechnology, both fields employing the basic principles of self-assembly. A relatively simple molecule with complementary functionalities may under certain conditions, interact with another one to form significantly more complex supramolecular species held together only by non-covalent interactions. In its strictest sense, the term self-assembly can be applied only to systems in which the assembly process is kinetically rapid, completely reversible and replicable. The reversible nature of assembly process gives rise to an important feature of self-assembling systems, their ability to correct 'mistakes' during assembly and gradually found their way towards the most thermodynamically stable supermolecule (enthalpically and entropically). Self-assembled systems can be classified according to the diversity of interactions that they contain into *single-interaction self-assembly* when only one specific interaction is present (e.g. only hydrogen bond interaction) and *multiple-interaction self-assembly* where more than one type of interactions is present (e.g. hydrogen bond and Van der Waal interactions).[22]

Examples of such self-assembly processes are repeatedly found in nature. For instance, the DNA double-helix requires two complementary strands to become

[20] P. W. Atkins, L. L. Jones, *Chemistry: Molecular, Matter and Change. Third Edition.* © **1997**, W H Freeman & Co (Sd).
[21] G. M. Whitesides, M. Boncheva, *Proc. Natl. Acad. Sci. U.S.A.*, **2002**, *99*, 4769-4774.
[22] I. M. Atkinson, L. F. Lindoy: *Self Assembly in Supramolecular Systems* © Royal Sociaty of chemistry. Edition. **2000**.

entwined via hydrogen bonds and π-π stacking in a self-assembly process (see Figure 1.3). The strands recognize each other and join together to form the most thermodynamically stable assembly product.[23]

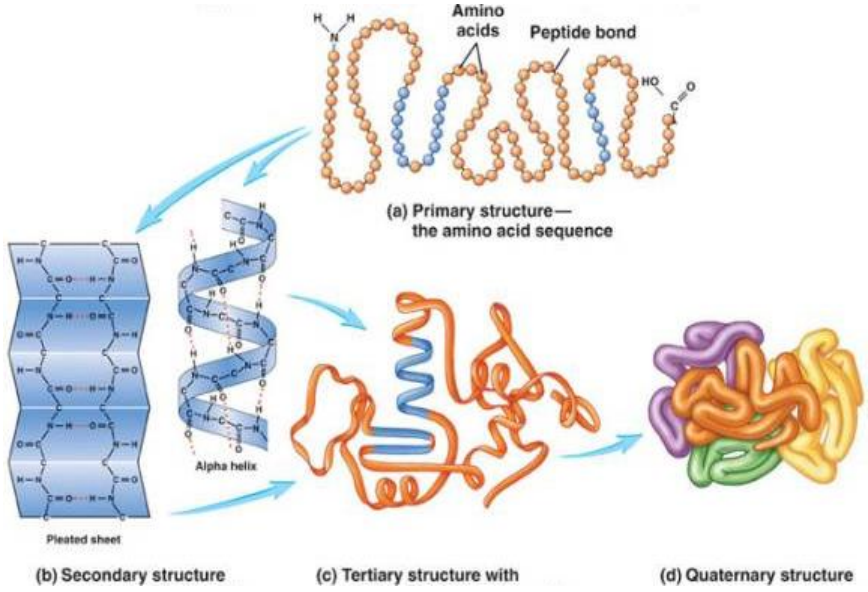

Figure 1.5. *Proteins are polypeptide assemblies formed sequentially from primary, secondary, tertiary and quaternary structures.*

Supramolecular chemistry and in particular self-assembly plays a major role in protein structure and behavior. Moreover, proteins are responsible for numerous functions throughout the body, acting as transporting agents, as the scaffold of biological catalysts (enzymes), as hormone receptors and in many more roles. Proteins are essentially linear molecules composed of typically 200-300 amino acid linked through peptide bonds. This covalent sequence is referred to as the primary structure of the protein. However, proteins do not exist in the body as simple linear covalent strands rather they are folded upon themselves (secondary and tertiary structures) and joined with other proteins in larger aggregates (quaternary structure). A number of different types of interactions play roles in determining the tertiary structure (e.g. hydrogen bonds, hydrophobic influences

[23] J. M. Lehn, *Proc. Natl. Acad. Sci. U.S.A.*, **2002**, *99*, 4763-4768.

and ionic attractions). While in the quaternary structure the individual proteins come together through non-covalent interactions to form larger assemblies comprised of several separate polypeptide chains (see Figure 1.5).

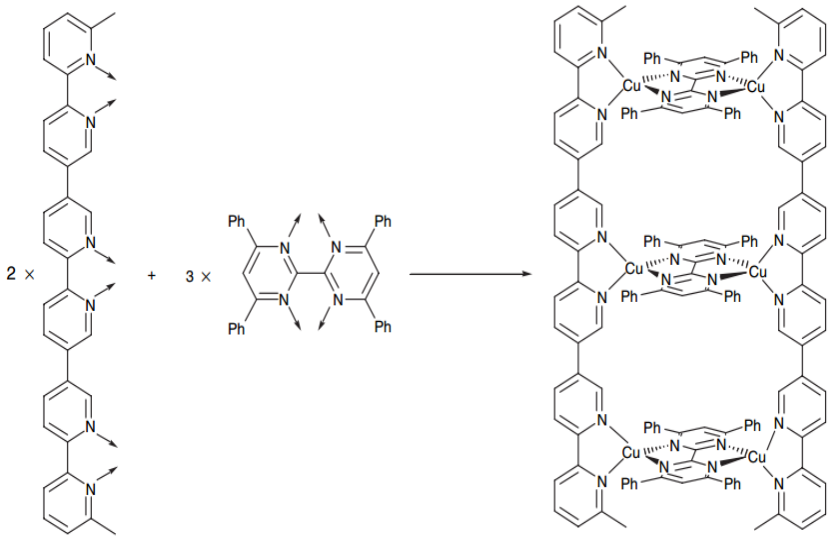

Figure 1.6. *Schematic representation of the structures of the cylindrical inorganic architectures contains internal cavities using Cu^{2+} as metal forming template.*

Synthetic self-assembly processes are well known and a huge amount of work devoted to the development of several supramolecular architectures has been published in the last years. One of the most widely used interactions in synthetic self-assembly processes are metal-ligand complexations due to their high degree of directionality as a result of predictable metal-ion coordination environments. An example of the use of metal-ligand interactions to prepare a self-assembly supermolecule is shown in Figure 1.6. Cylindrical inorganic architectures were generated in a single operation by the self-assembly of stoichiometric mixtures of trisbipyridine, hexaphenylhexaazatriphenylene and $[Cu(CH_3CN)_4]X$ ($X=PF_6^-$, $CF_3SO_3^-$). The resultant structures appear to have 'floors' held in place one above

the other effectively separating cavities that are potentially able to hold anions and solvent as guest species.[24]

[24] P. N. W. Baxter, J. M. Lehn, B. O. Kneisel, G. Baum, D. Fenske. *Chem. Eur. J.*, **1999**, *5*, 113-120.

2. Molecular Sensors

An ascending advanced application of supramolecular chemistry is the concept of molecular sensors. A molecular sensor, chemical sensor or chemosensor is a molecule composed by two subunits (a "binding site" and a "reporter") that can interact selectively with an analyte (guest) displaying a measurable signal (as a consequence of the interaction). Thus, the molecular event of the coordination between the chemosensor and the analyte is reflected in a macroscopic signal that allowed the detection of the later. More in detail, the IUPAC definition of chemosensor is ``a device that transforms chemical information ranging from the concentration of a specific sample component to total composition analysis into an analytically useful signal".[25]

2.1 Chemosensors design. The binding site and the signaling subunit

As cited above, a molecular chemosensor is usually composed of two main units namely the binding site and the signaling subunit. The binding site is the unit responsible of the selective interaction with one specific guest. This selective recognition of one molecule from different analytes can be achieved by an accurate design of the binding site in order to introduce a high degree of complementarity (matching size, shape, charge, etc.) with the target guest. On the other hand, the signaling subunit is a molecular entity able to transduce the interaction of the target analyte with the binding site into a measurable macroscopic signal generally related with the concentration of the former. Traditionally, changes in the optical properties (color or fluorescence) or a modification in the electrochemical features (redox potential) have been used as signal outputs.[26] The important advantages with respect to other analytical methods offered by the optical (chromo-fluorogenic) chemosensors are related to the possibility of use cheap and simple instrumentation, the need of very small quantity of sample and in some cases, the possibility of in-situ and on-time

[25] a) A. Hulanicki, S. Geab, F. Ingman, *Pure. Appl. Chem.,* **1991**, *63*, 1247-1250; b) U. E. Spichiger-Keller, "*Chemical Sensors for Medical and Biological Applications*", Wiley-VCH, **1998**.

[26] a) D. N. Reinhoudt, J. F. Stoddart, R. Ungaro, *Chem. Eur. J.*, **1998**, *4*, 1349-1351; b) P. J. Lusby, *Annu. Rep. Prog. Chem., Sect. A: Inorg. Chem.,* **2013**, *109*, 254-276.

measurements. Moreover, colorimetric sensors induced noticeable color changes observable to the naked eye and can be used for rapid qualitative determinations. On the other hand, fluorogenic chemosensors have a high degree of sensitivity and normally allow the achievement of lower detection limits when compared with colorimetric techniques. For the above mentioned facts, in this PhD thesis we focused our attention toward the development of optical chemosensors.

As the binding site plays a crucial role in the selective detection of the target analyte, the signal subunit is a very important part in the design of optical chemosensors in order to obtain probes with high sensitivity. There are different mechanisms operating in the signaling subunit that are responsible of the optical output generated upon binding of the target analyte with the binding site. Some of these mechanisms involve irreversible changes in the optical properties of whole chemosensor (due to irreversible reaction between the target analyte and the probe accompanied by the formation of new compounds with different optical properties),[27] changes occurred in the probe upon proton transfer processes[28] and changes in the excited state energy of the signaling unit upon coordination.[29] In addition, sensitivity of chemosensors is the result of the ability of both the binding site to interact at low concentrations with the target analyte and of the signaling subunit to report the event. Both selectivity and sensitivity are strongly influenced by environmental conditions and physical/chemical characteristics of the environment in which the molecular recognition takes place.

Three main approaches (see Figure 2.1) are used in the design of optical chemosensors, (i) the ‘‘binding site-signaling subunit’’ protocol, (ii) the ‘‘displacement’’ approach and (iii) the ‘‘chemodosimeter’’ paradigm. The choice of one protocol or another depends largely on important aspects of chemosensor design such as analyte affinity, binding selectivity, the medium in which the

[27] H. Lu, H, Q. Wang, Z. Li, G. Lai, J. Jiang, Z. Shen, *Org. Biomol. Chem*., **2011**, *9*, 4558–4562.
[28] A. Helal, H. S. Kim, *Tetrahedron.*, **2010**, *66*, 7097–7103.
[29] Z. R. Grabowski, K. Rotkiewicz, W. Rettig, *Chem. Rev.,* **2003,** *103*, 3899-4032.

sensing is performed, the optical signaling mechanism and the synthetic effort that it desired to made in the chemosensor preparation.

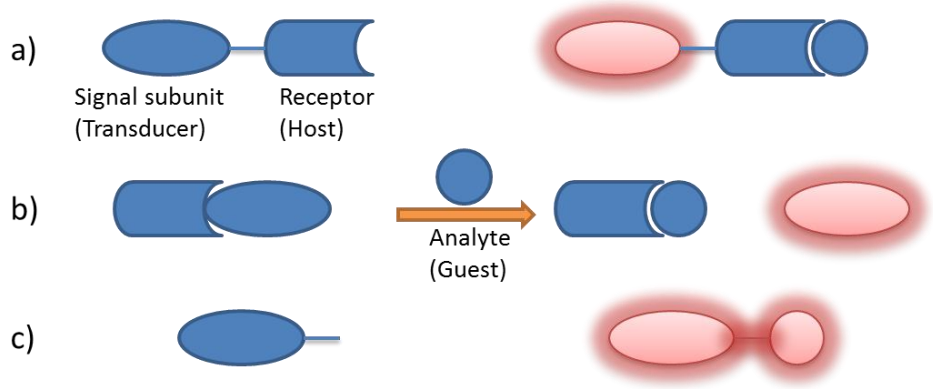

Figure 2.1. *Representation scheme of the three main approaches used in the development of optical chemosesors. (a) Binding site-signaling subunit (b) Displacment protocol and (c) Chemodosimeter.*

2.1.1 Binding site-signaling subunit protocol

On this approach, the binding site and the signaling unit (namely a chromophore or a fluorophore) are covalently linked. The non-covalent interaction of the target analyte with the binding site induced measurable chromo or fluorogenic changes in the signaling unit (see Figure 2.1 a).[30] This is perhaps the most widely used approach in the design of optical chemosensors for charged and neutral analytes. However, the most common drawback of the chemosensors constructed under this paradigm relies in the fact that the interaction between the target analyte and the binding site is of non-covalent nature (hydrogen bonding, proton transfer processes, etc.) and as a consequence, optical modulations are generally observed in organic solvents or organic solvents-water mixtures.

[30] V. Amendola, D. Esteban-Gómez, L. Fabbrizzi, M. Licchelli, *Acc. Chem. Res.*, **2006**, *39*, 343-353.

A particular example of binding site-signaling subunit chromogenic chemosensor was reported in 2011 by P. Molina and co-workers.[31] In this case receptor **1** (see Figure 2.2) containing 2-arylamino-1,3-diaza-[3]ferrocenophane, which acts as a binding site for anions, and a nitrobenzene group, as signal subunit, was prepared. Acetronitrile solutions of **1** presented an absorption centered at 350 nm that progressively decreased with the concomitant growth of a new band at 374 nm upon addition of AcO^-, BzO^- and F^- anions. This change was ascribed to the formation of a hydrogen bonded complex between probe **1** and AcO^-, BzO^- and F^- anions (see also Figure 2.2). However addition of OH^- induced the appearance of another low energy band at 481 nm ($\Delta\lambda$ = 131 nm) with the development of a deep orange-red color attributable to deprotonated receptor.

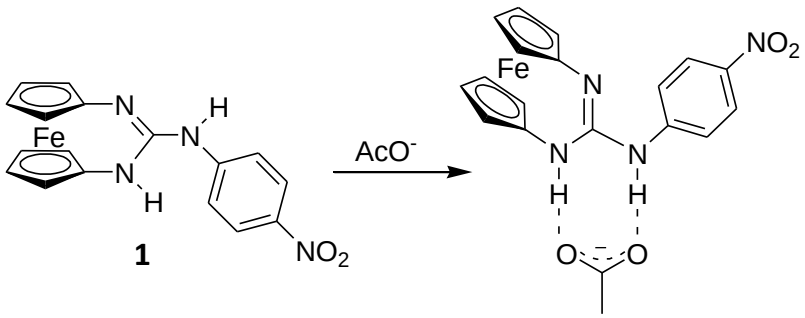

Figure 2.2. *Structure and binding mode of receptor **1**.*

Other probes constructed under the binding site-signaling subunit paradigm, used metallic centers as coordinating units. A recent example was reported by S. Yang and co-workeres.[32] Probe **2** (see Figure 2.3) used two Zn^{2+} complexes as binding sites and a 7-nitrobenz-2-oxa-1,3-diazole (NBD) heterocycle as signaling subunit. Aqueous solutions of probe **2** (HEPES, pH 7.4) showed an intense red color due to an absorption band centered at 501 nm. Among all anions tested ($H_2PO_4^-$, F^-, Cl^-, Br^-, AcO^-, NO_3^-, HCO_3^-, ClO_4^-, N_3^-, SO_4^{2-}, $S_2O_7^{2-}$, citrate, PO_4^{3-} AMP, ADP, ATP and pyrophosphate) only addition of pyrophosphate (ppi) induced the appearance of a new absorption at 526 nm (with a clear color change from red to

[31] A. Sola, R. A. Orenes, M. A. García, R. M. Claramunt, I. Alkorta, J. Elguero, A. Tarraga, P. Molina, *Inorg. Chem*., **2011**, *50*, 4212–4220.

[32] S. Yang, G. Feng, N. H. Williams, *Org. Biomol*. *Chem*., **2012**, *10*, 5606–5612.

purple) ascribed to the formation of a 1:1 probe-anion complex in which ppi coordinates with the Zn^{2+} cations through electrostatic interactions.

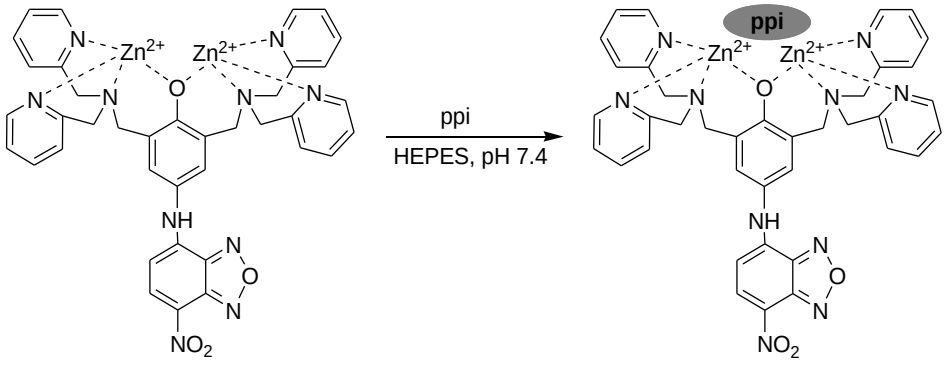

2

Figure 2.3. *Schematic representation of the binding mode of receptor **2** with ppi.*

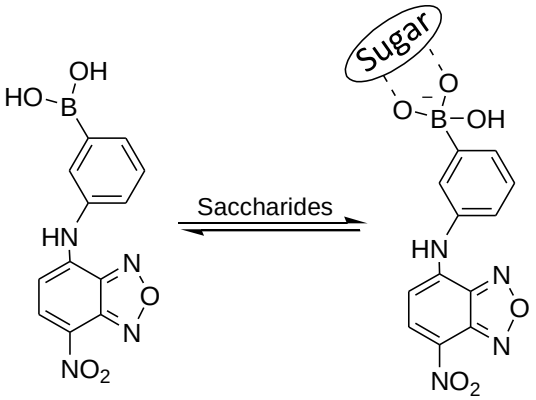

3

Figure 2.4. *Schematic representation of probe **3** and its coordination with saccharides.*

The binding-site-signaling-subunit approach was also applied to the preparation of optical sensors for the recognition of neutral species.[33] One example is probe **3** (see Figure 2.4), prepared by Badugu and co-workers for the chromogenic detection of glucose.[34] Chemosensor **3** is composed by a NBD chromophore and by a boronic acid as receptor for saccharides (through the formation of boronate esters). Specifically, **3** showed an absorbance band at

[33] G. J. Mohr., *Anal Bioanal Chem.,* **2006**, *386*, 1201–1214.

[34] R. Badugu, J. R. Lakowicz, C. D. Geddes, *Dyes Pigments.,* **2006**, *68*, 159–163.

around 490 nm in pH 7 phosphate buffer. Addition of fructose induced the shift of the visible band to 500 nm together with a remarkable color change from yellow to orange. The boronic acid subunit in probe **3** has an electron-withdrawing character that changed to electron-donor upon coordination with saccharides. As a consequence, the charge-transfer character of the probe changes upon coordination yielding color modulations. Sensitivity for fructose was in the 0.2–20 mM range while it was in the range of 1–100 mM for glucose.

2.1.2 Displacement approach

The displacement approach was used for the first time in the development of chromo-fluorogenic chemosensors by the research groups of Anslyn[35] and Fabbrizzi.[36] In this approach, the binding site and the signaling subunits are not covalently linked but forming a molecular complex (see Figure 2.1 b).[37] The key issue in this approach is related with the different optical properties (color and/or emission) presented by the signaling subunit when is coordinated with the binding site or free in the solution. Upon addition of the target analyte for which the binding site has a higher affinity, a displacement reaction occurs; *i.e*. the receptor binds to the analyte and release the signaling subunit to the solution.

One example of a displacement assay for the chromogenic recognition of ppi anion was recently described by Chen and co-workers.[38] For this purpose the authors prepared probe **4** (see Figure 2.5) by the complexation of a binuclear Cu^{2+} receptor with the dye pyrocatechol violet (PV). Aqueous solution of the sensing ensemble showed a blue color due to the presence of an intense absorption band centered at 630 nm. Of all the anions tested only ppi was able to induce the

[35] a) Z. Zong, E. V. Anslyn, *J. Am. Chem. Soc*., **2002**, *124*, 9014–9015; b) S. L. Wiskur, P. N. Floriano, E. V. Anslyn, J. T. McDevitt, *Angew. Chem. Int. Ed.,* **2003**, *42*, 2070 – 2072.

[36] a) L. Fabbrizzi, N. Marcotte, F. Stomeo, A. Taglietti, *Angew. Chem. Int. Ed*., **2002**, *41*, 3811–3814; b) M. A. Hortala, L. Fabbrizzi, N. Marcotte, F. Stomeo, A. Taglietti, *J. Am. Chem. Soc*., **2003**, *125*, 20–21.

[37] a) X. Lou, Y. Zhang, Q. Li, J. Qin, Z. Li, *Chem. Commun*., **2011**, *47*, 3189-3191; b) B. T. Nguyen, E. V. Anslyn, *Coord. Chem. Rev*., **2006**, *250*, 3118-3127.

[38] W. Yu, J. Qiang, J. Yin, S. Kambam, F. Wang, Y. Wang, X. Chen, *Org. Lett*., **2014**, *16*, 2220−2223.

disappearance of the band centered at 630 nm together with the simultaneous growing of an absorption at 444 nm (change in color from blue to yellow). The formed yellow color was ascribed to the release of the PV dye upon coordination of ppi with the two Cu^{2+} centers of the probe.

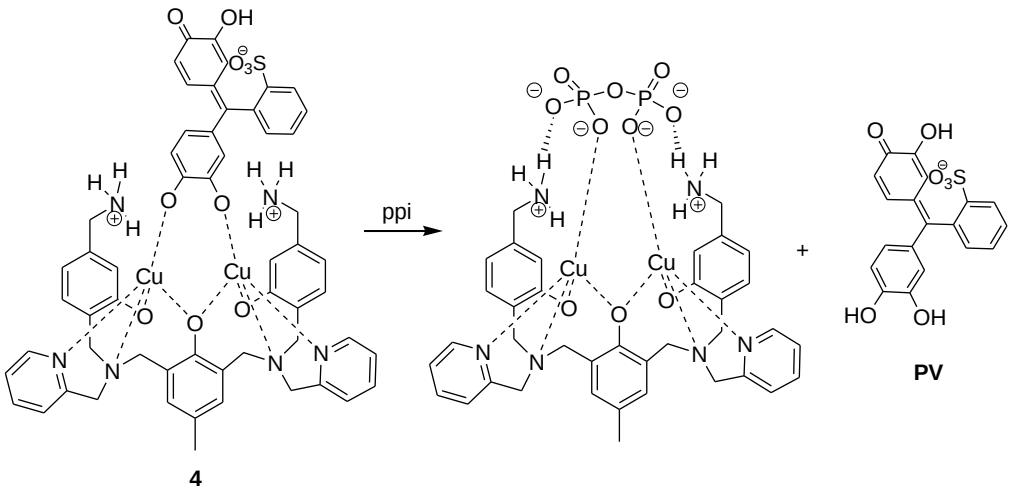

Figure 2.5. *Proposed sensing mechanism of probe* ***4*** *with ppi.*

Using this approach, novel fluorescent sensors for the recognition of biologically relevant HS^- anion were recently prepared (see Figure 2.6). At this respect, aqueous solutions (HEPES, pH 7.4) of complex **5** showed an absorption band centered at 491 nm and an emission at 516 nm.[39] When HS^- was added a considerable immediate 50-fold enhancement in emission intensity was observed, whereas almost no fluorescence change was seen with the addition of glutathione (GSH) even when in excess. That probe showed high selectivity for hydrogen sulfide (H_2S) over other thiols (*i.e.*, Cysteine (L-Cys), Homo-cysteine (DL-Hcy), Dithiothreitol (DTT)), inorganic sulphur containing compounds and reducing agents. Besides, reagent **5** did not show any fluorescence enhancement in the presence of reactive oxygen or inorganic sulfur compounds.

[39] K. Sasakura, K. Hanaoka, N. Shibuya, Y. Mikami, Y. Kimura, T. Komatsu, T. Ueno, T. Terai, H. Kimura, T. Nagano, *J. Am. Chem. Soc*., **2011**, *133*, 18003–18005.

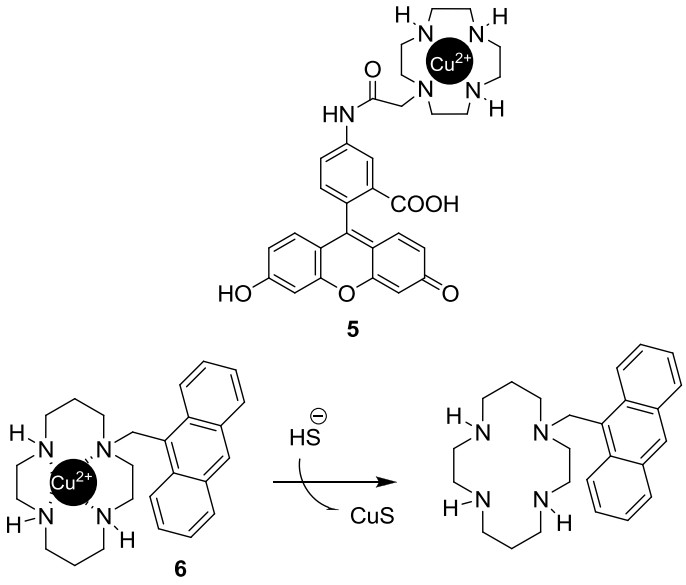

Figure 2.6. *Probes **5**, **6** and its reaction with HS^- in water.*

The displacement approach has also been used for the chromo-fluorogenic detection of neutral molecules. A representative example was the work published very recently by A. M. Costero and co-workers related with the chromo-fluorogenic sensing of demeton-S, a mimic of V-type nerve agents.[40] The authors prepared an Eu^{3+} complex (see probe **7** in Figure 2.7) that showed an absorption band at 553 nm in acetonitrile (solutions of pink color). In addition, probe **7** emits strongly at 572 nm. Upon addition of dementon-S (V-type nerve agent simulant), a progressive decrease in the absorption at 553 nm with the appearance of new band at 600.5 nm (color change from pink to blue) was observed. Also a remarkable quenching of the emission band at 572 was found. The changes in color and emission were ascribed to a demetallation of **7** due to the formation of a strong (Eu^{3+}-demeton-S) complex (see also Figure 2.7).

[40] A. Barba-Bon, A. M. Costero, S. Gil, F. Sancenón, R. Martínez-Máñez, *Chem. Commun*., **2014**, *50*, 13289–13291.

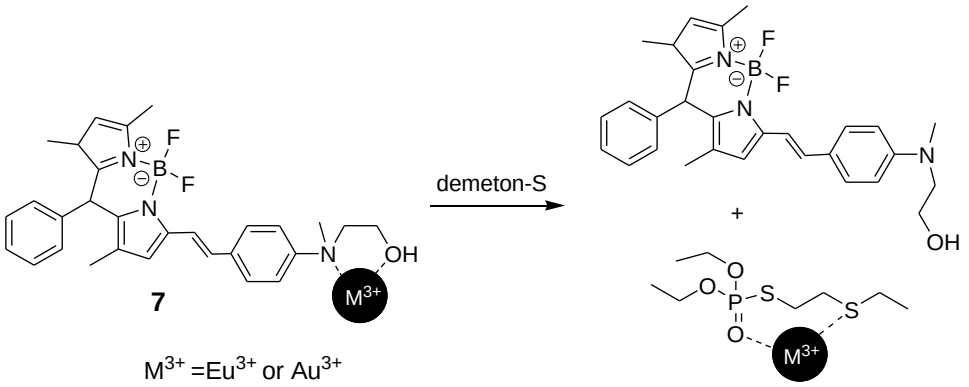

Figure 2.7. *Probe **7** and the sensing mechanism of the V-type nerve agent simulant demeton-S.*

2.1.3 Chemodosimeter paradigm

The chemodosimeter paradigm has been grown in importance in the last years and is today a well-established procedure for the design of optical chemosensor especially for the chromo-fluorogenic recognition of anions and neutral molecules (see Figure 2.1 c). This paradigm made use of specific, in most cases irreversible reactions induced by the target analyte. These reactions involved the rupture or formation of several covalent bonds followed by structure modulation with color and/or fluorescence changes. In addition to, the chemodosimeter approach has been applied for the selective detection of basic or nucleophilic anions such as F^-, CN^- and HS^- and very recently, for the recognition of neutral species. For example, over the last ten years, a large number of optical sensors for F^- detection based on this paradigm have been described. The mechanisms employed in these sensors are mainly based on the strong Lewis-acidic boron and fluoride interactions, hydrogen bonding and fluoride-induced Si-O bond cleavage.[41] This last mechanism is perhaps the most used and several chemosensors based on the hydrolysis of R_3-Si-O bonds induced by fluoride have been described. Silyl groups are widely used as protection groups for hydroxyl-containing substances and for this, have been actively used as key reactive elements in fluoride-selective chemodosimeters.

[41] Y. Zhou, J. F. Zhang, J, Yoon. *Chem. Rev.*, **2014**, *114*, 5511−5571.

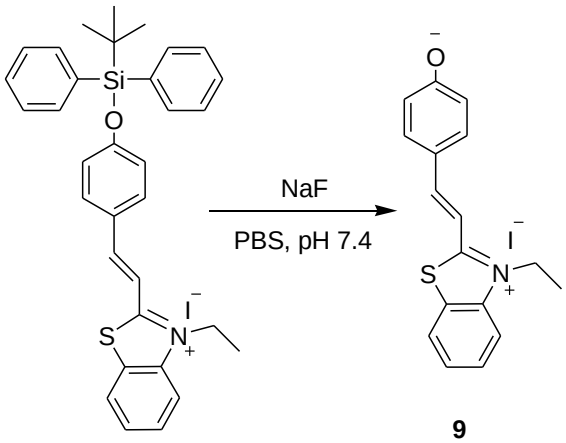

Figure 2.8. *Schematic representation of probe **8** for F^- detection and the fluorophore **9**.*

As an example of this mechanism, probe **8** was prepared and its optical behavior toward selected anions tested (see Figure 2.8).[42] Ethanol-water 3:7 v/v solutions of **8** showed an absorption centered at 407 nm that progressively decreased in intensity together with the appearance of a new band at 517 nm (color change from pale yellow to orange) upon addition of increasing quantities of F^- anion. The same changes were observed when fluorescence was measured and the emission at 500 nm vanished progressively with the addition of F^- concomitant with the growth of a new band at 558 nm. The optical changes were ascribed to F^--triggered cleavage of the Si-O bond in **8** with the subsequent formation of fluorophore **9**. This probe has a detection limit of 0.08 mM for fluoride and was used for bioimaging of F^- in live cells.

On account of the importance of HS^- in biological and environmental processes and the relation found between its abnormal levels and various diseases, there is recent interest in its detection. Very recently, several probes based in the chemodosimeter paradigm for the sensitive and selective of HS^- anion have been described. Most of the probes reported are based of the hydrogen sulfide-induced reduction of azides or nitro moieties, electronically connected with a fluorophore,

[42] B. Zhu, F. Yuan, R. Li, Y. Li, Q. Wei, Z. Ma, B. Du, X. Zhang. *Chem. Commun*., **2011**, *47*, 7098–7100.

to amines.[43] Other sulfide-selective fluorescent probes used Michael type addition reactions coupled with emission changes.[44] Also, cyclization processes that yielded fluorescent compounds have recently been used for the design of fluorescent probes for hydrogen sulfide anion.[45] Finally, hydrolysis reactions coupled with emission changes have been also used for the preparation of other hydrogen sulfide sensitive probes.[46]

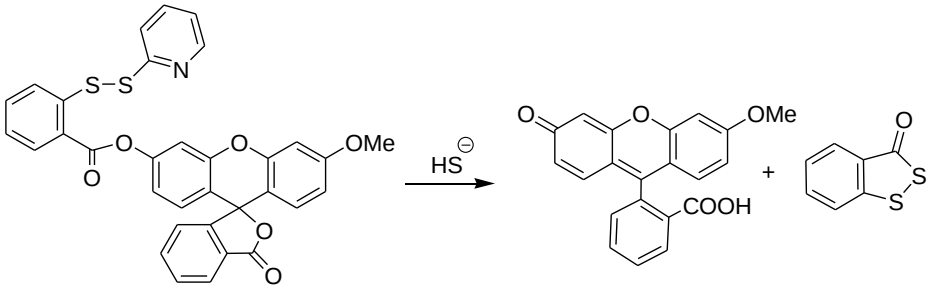

10

Figure 2.9. *Chemical structure of probe **10** and the reaction with HS^-.*

As an example, probe **10** (see Figure 2.9) was designed to detect HS^-. This probe contained an ester electrophilic center, capable of reacting with the nucleophilic HS^- anion, in a suitable position which underwent spontaneous cyclization leading to the release of a fluorophore.[47] Aqueous solutions (at pH 7.4) of probe **10** showed a very weak emission centered at 515 nm (when excited at 465 nm). Of all the anions tested (including biothiols such as Cys and GSH) only HS^- was able to induce a remarkable 77-fold enhancement of the emission intensity. Besides, the efficiency of this probe for HS^- detection was demonstrated both in plasma and cells.

[43] a) L. A. Montoya, M. D. Pluth, *Chem. Commun.,* **2012**, *48*, 4767–4769; b) A. R. Lippert, E. J. New, C. J. Chang, *J. Am. Chem. Soc.*, **2011**, *133*, 10078.

[44] Y. Chen, C. Zhu, Z.Yang, J. Chen, Y. He, Y. Jiao, W.He, L. Qiu, J. Cen, Z. Guo, *Angew. Chem., Int. Ed.*, **2013**, *52*, 1688.

[45] C. Liu, B. Peng, S. Li, C. -M, Park, A. R. Whorton, M. Xian. *Org. Lett.*, **2012**, *14*, 2184–2187.

[46] a) X.–F. Yang, L. Wang, H. Xu, M. Zhao, *Anal. Chim. Acta*., **2009**, *631*, 91–95; b) X. Cao, W. Lin, K. Zheng, L. He, *Chem. Commun*., **2012**, *48*, 10529–10531; c) T. Liu, Z. Xu, D. R. Spring, J. Cui, *Org. Lett*., **2013**, *15*, 2310-2313; d) Y. Liu, G. Feng, *Org. Biomol. Chem*., **2014**, *12*, 438–445.

[47] C. Liu, J. Pan, S. Li, Y. Zhao, L. Y. Wu, C. E. Berkman, A. R. Whorton, M. Xian, *Angew. Chem. Int. Ed*., **2011**, *50*, 10327–10329.

Nerve agents are a group of organophosphates that can irreversibly inactivate acetylcholinesterase of the human nerve system. The use of these lethal chemicals in terrorist attacks has increased the interest of the scientific community into the preparation of chromo-fluorogenic probes for the rapid and easy detection of these lethal chemicals.[48] Most of the described receptors used the chemodosimeter paradigm and are based in the electrophilic character of the phosphorus atom in the structure of the nerve agents.

As a representative example, Han gand co-workers prepared probe **11** for nerve agent simulant detection (see Figure 2.10).[49] This probe contains a rhodamine-deoxylactam group as signaling subunit and a nucleophilic hydroxyl group as reactive site. DMF solutions of probe **11** were colorless and upon addition of diethylchlorophosphate (DCP) turned red due to the appearance of a new absorption band centered at 560 nm. Also a very remarkable emission enhancement at 590 nm was observed upon addition of DCP. The authors proposed a mechanism which involved a nucleophilic addition of the hydroxyl group of **11** to the electrophilic phosphorus atom of DCP. Finally, another nucleofilic attack from the deoxylactam amine to the linked phosphate yielded a highly fluorescent and colored compound (see Figure 2.10).

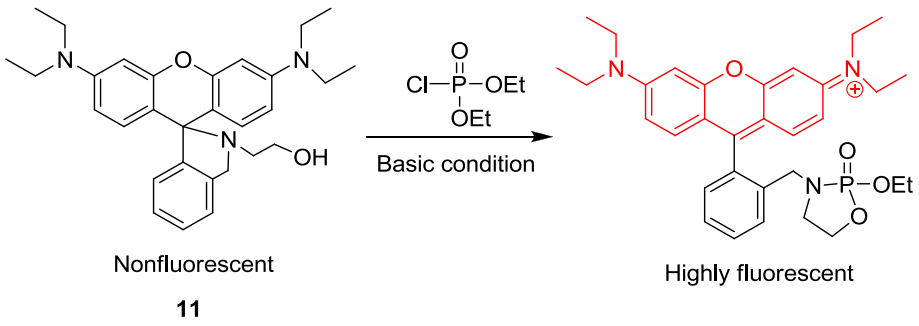

Figure 2.10. *Chemical structure of chemodosimeter **11** and its reaction with DCP.*

[48] S. Royo, R. Martínez-Mañez, F. Sancenón, A. M. Costero, M. Parra, S. Gil, *Chem. Commun*., **2007**, 4839–4847.

[49] X. Wu, Z. Wu, S. Han, *Chem. Commun*., **2011**, *47*, 11468–11470.

2.2 Objectives

The main objectives of this chapter were the preparation of molecular sensors, using the chemodosimeter paradigm for the chromo-fluorogenic sensing of F^-, nerve agent and HS^-. More in detail, the specific objectives are:

- Synthesis and characterization of chemical probes based in the chemodosimeter paradigm for the selective chromo-fluorogenic recognition of F^- anion.

- Synthesis and characterization of chemical probes based in the chemodosimeter paradigm for the selective chromo-fluorogenic recognition of nerve agent simulants.

- Synthesis and characterization of chemical probes based in the chemodosimeter paradigm for the selective chromo-fluorogenic recognition of HS^- anion.

- To evaluate the response of the prepared chemodosimeters in the presence or absence of these target analytes.

An instantaneous and highly selective chromo-fluorogenic chemodosimeter for fluoride anion detection in pure water

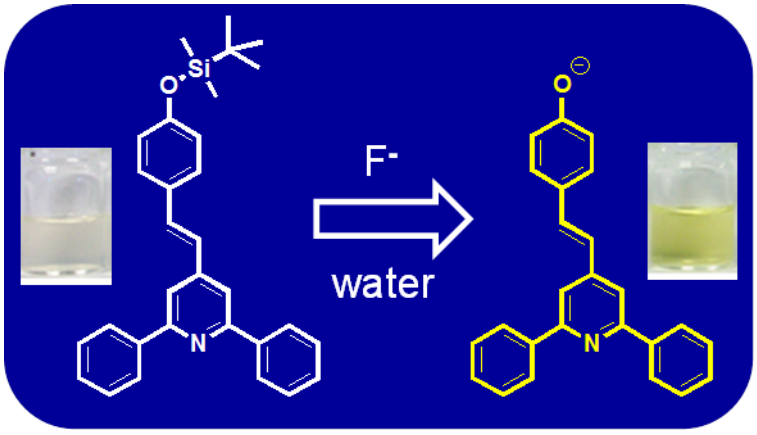

An instantaneous and highly selective chromo-fluorogenic chemodosimeter for fluoride anion detection in pure water

Sameh El Sayed,[a] Alessandro Agostini,[a] Luis E. Santos-Figueroa,[a] Ramón Martínez-Máñez[a] and Félix Sancenón[a]*

[a] Centro de Reconocimiento Molecular y Desarrollo Tecnológico (IDM), Unidad Mixta Universidad Politécnica de Valencia-Universidad de Valencia, Spain.

[a] Departamento de Química, Universidad Politécnica de Valencia, Camino de Vera s/n, 46022, Valencia.

[a] CIBER de Bioingeniería, Biomateriales y Nanotecnología (CIBER-BNN). E-mail: rmaez@qim.upv.es

Received: *22 February 2013*
First published on the web: *3 April 2013*

ChemistryOpen., ***2013****, 2, 58 – 62*

(Reproduced with permission of Wiley-VCH Verlag GmbH & Co. KGaA copyright © 2013)

The development of chromo-fluorogenic sensors for anions is a well-established and studied field in the supramolecular chemistry realm.[1] This is due to the important roles played by anions in biological processes, in deleterious effects (such as environmental pollutants), as toxic compounds and as carcinogenic species.[2]

Among inorganic anions, fluoride is widely used in the prevention of dental caries and in osteoporosis treatments.[3] In spite of these important applications, acute exposure to this anion can cause various diseases, such as nausea, abdominal pain, coma, hypocalcaemia, skeletal fluorosis and osteomalacia.[4] For all these reasons, the interest in developing chromo-fluorogenic probes for the selective detection of fluoride has grown in the last few years.[5]

Most of the examples reported for fluoride sensing are based on the use of the "binding site-signalling subunit" approach or on the "chemodosimeter" protocol.[6] In the probes for which the "binding site-signalling subunit" approach is used, an optical signalling unit is covalently bonded to a binding site, which usually consists in one H-bond donor moiety or more, such as urea or thiourea groups. The coordination or deprotonation of the acidic protons of the binding sites by fluoride induces changes in colour or fluorescence which enables anion detection.[7] In spite of these important features, the chemosensors constructed according to this paradigm present some drawbacks, such as lack of selectivity (other basic anions like cyanide, acetate and dihydrogenphosphate usually give nearly the same optical response) and are unable to display sensing features in competitive media such as water or mixed aqueous environments.

In order to overcome these limitations, the chemodosimeter approach has been recently applied for the chromo-fluorogenic sensing of fluoride anion.[5b] These probes use selective reactions induced by the target anion coupled with chromo-fluorogenic changes. Some of the reported chemodosimeters for fluoride recognition employ this anion's well-known ability to promote the hydrolysis of silyl ethers.[8] In particular, several examples of selective chemodosimeters for fluoride anion based on bodipy derivatives,[9] terphenyl derivatives,[10]

diphenylacetylenes,[11] naphthalimides,[12] benzothiazolium hemicyanine derivatives,[13] coumarins[14] and azo dyes functionalized with silyl ether moieties, have been recently described.[15] Regardless of the high selectivity of these probes to the fluoride anion most of them work in organic solvents (acetonitrile, acetone, tetrahydrofuran, dimethyl sulfoxide, dichloromethane) or organic/water mixture (acetonitrile/water or ethanol/water).

In fact, as far as we know, there are only two molecular based examples that display sensing features for fluoride in water. One example is based on a *N*-(3-(benzo[d]thiazol-2-yl)-4-(hydroxyphenyl) benzamide derivative that is functionalized with *t*-butyldiphenylsilyl ether.[16a] In this case, the chemodosimeter solutions showed an emission band at 418 nm that was progressively quenched and substituted for new fluorescence at 560 nm upon the addition of increasing quantities of fluoride anion. The observed fluorogenic response was ascribed to the hydrolysis of the *t*-butyldiphenilsilyl moiety which yielded a highly emissive compound. The second is a very recently published example based on a fluorescein derivative bearing a biocompatible hydrophilic poly(ethylene glycol) polymer and two *t*-butyldiphenylsilyl ether moieties.[16b] Aqueous solutions (buffered at pH 7.4) of this chemodosimeter showed a very weak emission band centered at 526 nm (excitation at 490 nm) that increased gradually upon addition of fluoride anion. Again, the observed response was due to the fluoride-induced *t*-butyldiphenylsilyl ether hydrolysis. Moreover it is worthy to mention that reported silyl ether-based probes for fluoride detection, showing sensing features in aqueous environments, usually require several minutes (typically in the 3-50 min range) in order to achieve the complete hydrolysis of the silyl ether group.

Bearing in mind the very few examples that the literature reports of the chromo-fluorogenic sensing of fluoride in pure water and after considering our interest in the development of new optical probes for anions, we designed the novel chemodosimeter **3** for fluoride sensing based on a pyridine derivative functionalized with a *t*-butyl-dimethylsilyl ether group. Compound **3** was able to sense fluoride instantaneously in pure water in the presence of a cationic surfactant. The cationic surfactant was selected as a simple method to solubilize

the probe in the inner hydrophobic core of the formed micelles, thus also favouring the inclusion of fluoride anion due to their positively charged shell.

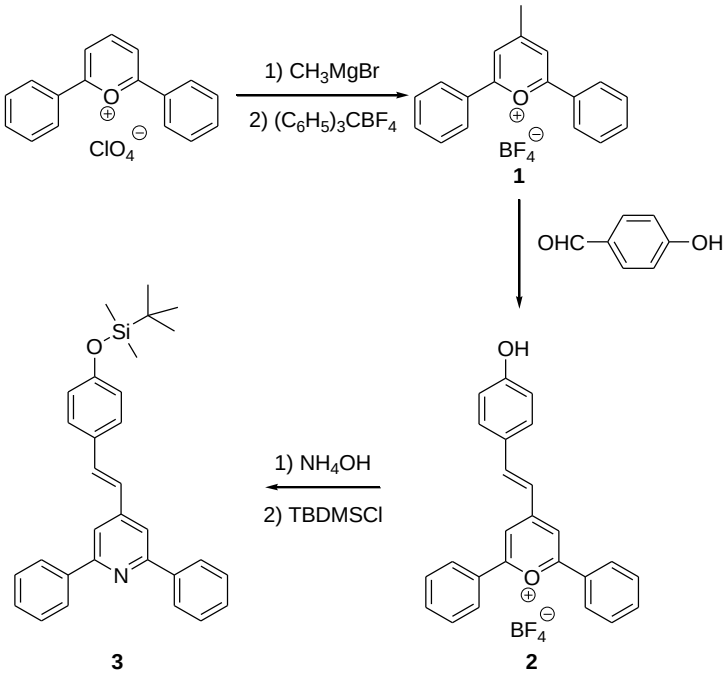

***Scheme 1**. Synthesis of probe **3**.*

The synthesis of chemodosimeter **3** was achieved by a three-step procedure (Scheme 1). In the first step, 2,6-diphenylpyrylium perchlorate was treated consecutively with methylmagnesium iodide and triphenylcarbenium tetrafluoroborate yielding 4-methyl-2,6-dipneylpyrylium tetrafluoroborate (**1**).[17] Then, compound **1** was condensed with *p*-hydroxybenzaldehyde to yield stilbene-pyrylium derivative **2**.[18] Finally, **2** was reacted with ammonium hydroxide (for transformation of the pyrylium ring into a pyridine) and with *t*-butyl-dimethylsilyl chloride (TBDMSCl, for transformation of the hydroxyl moiety into a silyl ether), to give the final chemodosimeter **3**. The ^{1}H NMR (in $CDCl_3$) spectra of **3** showed two singlets centred at 0.25 ppm (6H) and 1.02 ppm (9H) ascribed to the methyl and *t*-butyl groups of the silyl ether group. The most characteristic signals in the aromatic zone were one singlet centred at 7.75 ppm attributed to the two equivalent protons located in the 2,4,6-trisubstituted pyridine heterocycle and the two doublets with a 15 Hz coupling constant centred at 7.04 and 7.38 ppm

assignable to the hydrogen atoms of the *trans* double bond. HRMS-EI measurements confirmed the structure of the final product with an *m/z* value of 464.2403 (464.2331 calculated for $C_{31}H_{34}ONSi^{+}$).

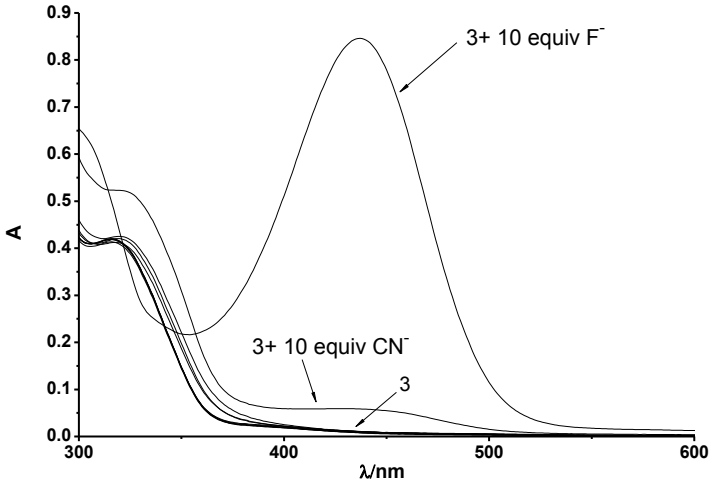

***Figure 1**. The UV-vis spectra of the acetonitrile solutions of chemodosimeter **3** (3.0 x 10^{-5} mol L^{-1}) in the presence of 10 equivalents of the selected anions.*

As a first step, the chromogenic behaviour of probe **3** in acetonitrile (3.0 x 10^{-5} mol L^{-1}) in the presence of 10 equivalentes of selected anions was studied (*i.e.*, F^-, Cl^-, Br^-, I^-, CN^-, SCN^-, AcO^-, BzO^-, CO_3^{2-}, NO_3^-, ClO_4^-, HSO_4^- and $H_2PO_4^-$). Only the addition of fluoride anion induced remarkable optical changes. In particular, the UV band at 325 nm underwent a hypsochromic shift while a new band appeared at 445 nm upon fluoride addition (Figure 1). Due to these changes, the solutions of probe **3** changed from colourless to yellow. The other anions tested induced negligible changes in the UV/Vis profile of **3**.

Encouraged by the selective response shown by **3** in acetonitrile, further assays in pure water were performed. UV/Vis studies in the presence of anions were carried out in this highly competitive medium. Probe **3** is weakly soluble in water but is readily solubilised in aqueous solutions at pH 7.4 containing the cationic surfactant cetyltrimethylammonium bromide (CTABr) at a concentration of 5 mM. The improved solubilisation of **3** in the prescence of CTABr is ascribed to the

inclusion of **3** into the hydrophobic core of the surfactant micelles. A cationic surfactant was selected to favour the approach of the anionic fluoride to the positively charged CTABr and enhance diffusion of anions into the micelles. The aqueous CTABr solutions of **3** (3.0×10^{-5} mol L^{-1}) were also colourless. Moreover, the addition of fluoride anion induced the appearance of a visible band together with a colour change from colourless to yellow. The other anions tested gave no response (*i.e.*, Cl^-, Br^-, I^-, CN^-, SCN^-, AcO^-, BzO^-, CO_3^{2-}, NO_3^-, ClO_4^-, HSO_4^- and $H_2PO_4^-$).

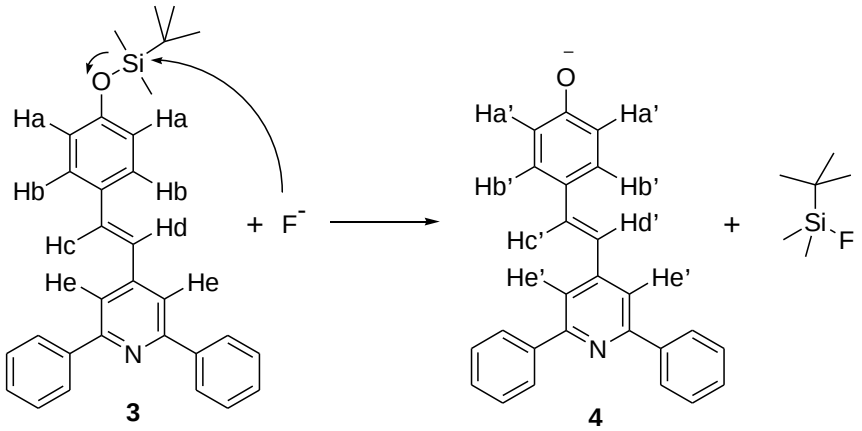

***Scheme 2**. Mechanism of the chromogenic response of **3** in the presence of fluoride anion.*

This fluoride-selective response arises from this known ability of the anion to hydrolyse silyl ether moieties. This hydrolysis induced the formation of a phenolate anion (see structure **4** in scheme 2) with a strong negatively charged donor oxygen atom which is responsible of the appearance of both the red shifted band at 445 nm and the colour changed observed. These results are in agreement with the well-established rule that an increase in the donor ability of a donor moiety in a pull-push chromophore results in a bathochromic shift.[19] Further studies demonstrated that sensing features of **3** in water containing CTABr and fluoride were observed when the pH is larger than 6.5 whereas lower pH values resulted in no colour changes. (data not shown)

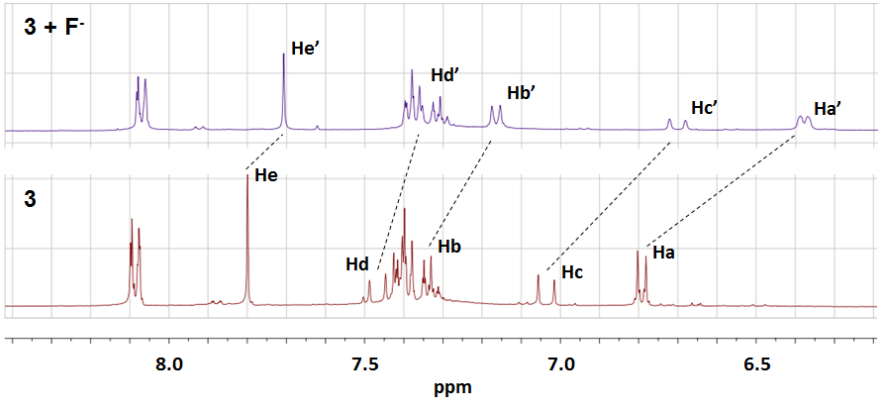

Figure 2. *^{1}H-NMR spectra of probe **3** in CD_3CN (bottom) and **3** with one equivalent of the fluoride anion (top).*

The sensing mechanism was confirmed by the ^{1}H-NMR studies carried out in deutrated acetonitrile. In this solvent, nearly all the signals of **3** underwent upfield shifts in the presence of fluoride (see Figure 2; see Scheme 2 for proton assignation). Moreover, the most remarkable shifts were observed for protons He, Ha and Hc. The singlet of the trisubstituted pyridine ring shifted from 7.80 (He) to 7.73 ppm (He'). In addition, the protons of the 1,4-disubstituted benzene ring located in an *ortho* position of the silyl ether moiety shifted from 6.79 (Ha) to 6.37 ppm (Ha'), whereas one of the protons of the double bond shifted from 7.04 (Hc) to 6.71 ppm (Hc'). These upfield shifts are in agreement with the formation of phenolate anion **4** (see Scheme 2) by fluoride-induced silyl ether hydrolysis as a key step in the chromogenic response observed.

Having assessed the selective chromogenic behaviour of probe **3** in water in the presence of anions, fluorogenic studies were also carried out. The solutions of chemodosimeter **3** (3.0×10^{-5} mol L^{-1}) at pH 7.4 contaning 5 mM CTABr were not fluorescent upon excitation at 445 nm (ϕ = 0.0024). However, the addition of fluoride induced the appearance of an intense emission band centred at 540 nm (ϕ = 0.042), whereas the other anions tested (*i.e.*, Cl^-, Br^-, I^-, CN^-, SCN^-, AcO^-, BzO^-, CO_3^{2-}, NO_3^-, ClO_4^-, HSO_4^- and $H_2PO_4^-$) induced negligible changes in the emission profile of **3** (see Figure 3).

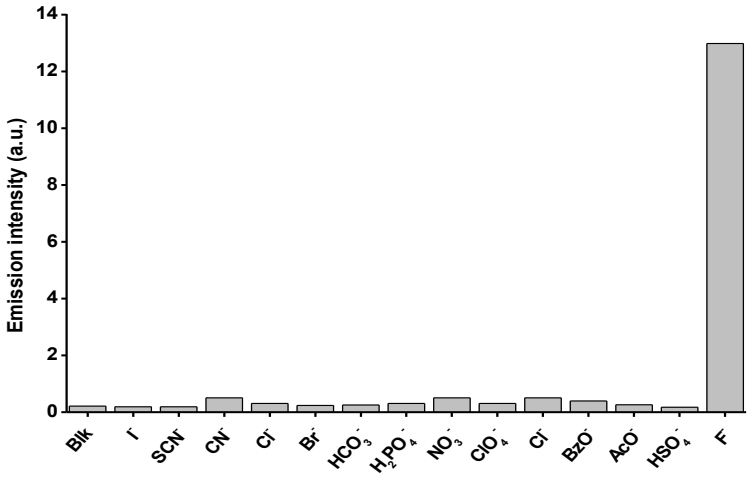

***Figure 3**. Emission intensity at 540 nm (λ_{ex}=445 nm) of chemodosimeter **3** (3.0 x 10^{-5} mol L^{-1}) in H_2O at pH 7.4 contaning 5 mM CTABr in the abscence (blank) and in the presence of selected anions (10 equivalente).*

To further characterise the fluorogenic behaviour of dosimeter **3**, changes in the emission intensity band at 540 nm were studied in the presence of increasing amounts of the fluoride anion. Figure 4 shows a typical titration profile. From this calibration curve, a detection limit of 1.4 ppm of fluoride was calculated using a conventional fluorimeter. This detection limit is below the recommended value of fluoride content in drinking water (1.8 ppm).

An additional remarkable feature of probe **3** was the fact that the hydrolysis reaction in the micellar medium was instantaneous. In this sense, it is worth mentioning to that other silyl ether-based chemodosimeters for fluoride detection showing sensing features in aqueous environments (usually mixed organic/water media), usually require several minutes, typically in the rang of 3-50 min, to achieve the complete hydrolysis of the silyl ether group, whereas probe **3** displayed changes instantaneously.[14-16]

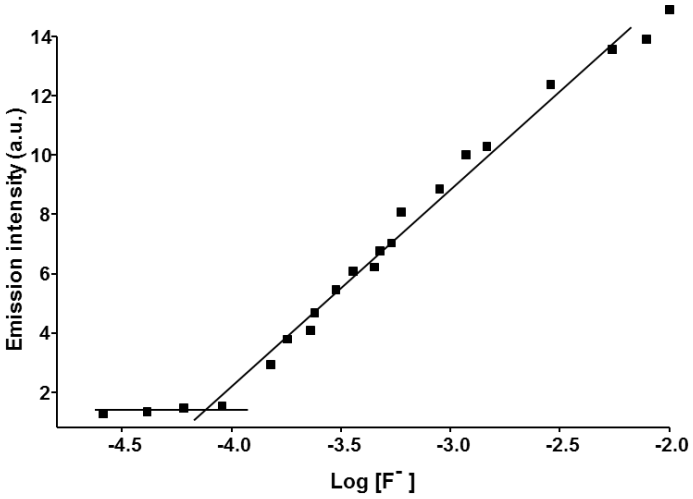

***Figure 4**. Calibration curve for fluoride using chemodosimeter **3** (3.0 x 10^{-5} mol L^{-1}) in water (pH 7.4) containing 5 mM CTABr.*

In summary, we report herein the design of a chromo-fluorogenic pyridine-based silyl ether-containing probe for the selective recognition of fluoride anions in water/CTABr solutions. Addition of fluoride anion induces a change in colour from colourless to yellow and the appearance of a strong emission band. Both changes are ascribed to a fluoride-induced hydrolysis of the silyl ether moiety which yields a phenolate anion. Probe **3** is highly selective and one of the very few systems for fluoride that displays sensing features in pure water. Moreover the optical changes are instantaneous and as far as we know, our system is the fastest reagent for fluoride signaling in a aqueous environment using silyl ether-based probes.

Experimental Section

General:

UV/Vis spectra were recorded with a JASCO V-650 Spectrophotometer (Easton, MD, USA). Fluorescence measurements were carried out in a JASCO FP-8500

Spectrophotometer. ^{1}H and ^{13}C-NMR spectra were acquired in a 400 MHZ BRUKER ADVANCE III, whereas mass spectra were carried out in a TRIPLETOF T5600 spectrometer (AB Sciex, Framingham, MA, USA).

Trietylorthoformate (98%), CH_3I (99%), *t*-butyldimethylsilylchloride (98%), 4-hydroxybenzaldehyde (98%), acetophenone (99%), anhyd. CH_3CN (99.8%), magnesium, tetraphenylphosphonium tetrafluoroborate and hexadecyltrimethylammonium bromide (CTABr) were purchased from Sigma-Aldrich. Analytical-grade solvents, aq. NH_4OH (32%, *w/v*), perchloric acid (60%, *v/v*) and anhyd magnesium sulfate were purchased from Scharlau (Barcelona, Spain).

Synthesis of 2,6-diphenylpyrylium perchlorate:

Acetophenone (4 mL, 34.3 mmol) and triethylorthoformate (10 mL, 60.1 mmol) were placed in a round bottomed flask (250 mL) under Ar atmosphere at 0 ^{o}C. After 15 minutes of stirring, perchloric acid (60% *v/v*; 7.4 mL, 86.5 mmol) was added dropwise over 30 min. The reaction was allowed to react at RT for 1 h. By addition of Et_2O (15 mL), the final 2,6-diphenylpyrylium perchlorate derivative (10.1 g, 30.4 mmol, 88.6% yield) was precipitated as a yellow solid (10.1 g, 30.4 mmol, 88.6 % yield). NMR data of the synthesized product agreed with those described in the literature.[20]

Synthesis of 4-methyl-2,6-diphenylpyrylium tetrafluoroborate (1):

Magnesium (1 g, 41.1 mmol) was dissolved in anhydrous diethyl ether (20 mL) and the solution formed was added dropwise to a round bottomed flask containing CH_3I (5 mL, 80.3 mmol) dissolved in anhyd. Et_2O (30 mL). The mixture was stirred at RT for 1 h, and was added dropwise to a round-bottomed flask

containing 2,6-diphenylpyrylium perchlorate (2 g, 8.6 mmol) in anhyd. Et_2O (50 mL) under Ar atmosphere. The crude reaction was stirred at RT for 10 h and poured onto H_2O (20 mL). After, the organic layer was washed with saturated aq. NH_4Cl (2 x 30 mL), and water H_2O (2 x 20 ml), dried with anhyd. $MgSO_4$ and filterated, the solvent was evaporated in vacuo, the sticky residue was dissolved in CH_3CN (50 mL) and triphenylcarbenium tetrafluoroborate (3 g, 9.1 mmol) was added. The crude solution was stirred for 3 h at RT. After, the solvent was evaporated in vacuo, the residue dissolved in minimum volume of acetone and the final product **1** was precipitated with *n*-hexane to give a redish-brown solid (1.9 g, 5.7 mmol, 66% yield).

^{1}H-NMR (400 MHz/DMSO-D_6): δ =2.84 (s, 3H), 7.78 (t, J=6.5 Hz, 4H), 7.85 (t, J=6.5 Hz, 2H), 8.42 (d, J=6.5 Hz, 4H), 8.83 ppm (s, 2H).

Synthesis of 4-((E)-2-(2,6-diphenylpyryliumtetrafluroborate-4-yl)vinyl)phenol (2):

4-Hydroxybenzaldehyde (184 mg, 1.5 mmol) was added to a solution of compound **1** (500 mg, 1.5 mmol) in EtOH (50 mL). The reaction was carried out at reflux for 12 h. The solvent was evaporated in vacuo and the final residue dissolved in a minimum volume of acetone. Precipitation with *n*-hexane gave compound **2** as a reddish solid (463.6 mg, 1.13 mmol, 75% yield).

^{1}H-NMR (400 MHz/DMSO-D_6): δ=7.00 (d, J=6.6 Hz, 2H), 7.45 (d, J=15.0 Hz, 1H), 7.79 (m, 8H), 8.38 (d, J=6.5 Hz, 4H), 8.67 (d, J=15.0 Hz, 1H), 8.74 ppm (s, 1H).

Synthesis of chemodosimeter 3:

Aq. NH_4OH (32% v/v; 5 mL) was added to a solution of compound **2** (750 mg, 2.14 mmol) in EtOH (30 mL), and the solution was stirred at RT for 1 h. The solvent was evaporated in vacuo to give a blue solid (700 mg, 2 mmol, 93% yield). This blue solid (700 mg, 2 mmol) was dissolved in anhyd. CH_3CN (20 mL) and after *t*-

butyldimethylsilylchloride (424 mg, 2.2 mmol) and *N*-methylimidazole (493 mg, 6.6 mmol) were added, the mixture was stirred at RT for 1 h. The solvent was evaporated in vacuo and the crude was dissolved in Et_2O (20 mL), washed with a concd. $Na_2S_2O_3$ (1 x 30 mL), dried with Na_2SO_4, filtered and purified by column chromatography (alumina; hexane/acetone 9:1 *v/v*). The chemodosimeter **3** was obtained as yellowish brown solid (490.6 mg, 1.12 mmol, 56% yield).

^{1}H-NMR ($CDCl_3$, 400 MHz): δ 0.25 (s, 6H), 1.02 (s, 9H), 6.89 (d, 2H), 7.04 (d, 1H), 7.38 (d, 1H), 7.48 (m, 8H), 7.75 (s, 2H), 8.19 (d, 4H) ppm.

^{13}C NMR (100 MHz, $CDCl_3$): δ -4.2, 18.4, 25.8, 116.1, 122.9, 128.9, 133.0, 135.0, 135.4, 135.6, 136.3, 141.1, 151.8, 161.2, 176.0, 177.4 ppm.

HRMS-EI *m/z*: calcd for $C_{31}H_{34}ONSi^+$ 464.2331; found: 464.2403.

Acknowledgements

Financial support from the Spanish Government (project MAT2012-38429-C04-01) and the Generalitat Valencia (project PROMETEO/2009/016) is gratefully acknowledged. S.E. is grateful to the Generalitat Valenciana for his Santiago Grisolia fellowship.

Keywords: • chemodosimeter • colour change fluoride • hydrolysis •silyl ether

References

1. M. E. Moragues, R. Martínez-Máñez, F. Sancenón, *Chem. Soc. Rev.*, **2011**, *40*, 2593.
2. P. D. Beer, P. A. Gale, *Angew. Chem. Int. Ed.*, **2001**, *40*, 486; *Angew. Chem.*, **2001**, *113*, 502.
3. a) M. Kleerekoper, *Endocrinol. Metab. Clin. North Am.*, **1998**, *27*, 441. b) R. H. Dreisbuch, *Handbook of Poisoning*, Lange Medical Publishers, Los Altos, CA, **1980**.
4. WHO (World Health Organization), Geneva, **2002**.
5. a) T. D. Hudnall, C. –W. Chiu, F. P. Gabbaï, *Acc. Chem. Res.*, **2009**, *42*, 388; b) K. Kaur, R. Saini, A. Kumar, V. Luxami, N. Kaur, P. Singh, S.Kumar, *Coord. Chem. Rev.*, **2012**, *256*, 1992; c) Z. Xu, N. J. Singh, S. K. Kim, D. R. Spring, K. S. Kim, J. Yoon, *Chem. Eur. J.*, **2011**, *11*, 1163;

d) Z. Guo, N. R. Song, J. H. Moon, M. Kim, E. J. Jun, J. Choi, J. Y. Lee, C. W. Bielawski, J. L. Sessler, J. Yoon, *J. Am. Chem. Soc.*, **2012**, *134*, 17846.

6. R. Martínez-Máñez, F. Sancenón, *Chem. Rev.*, **2003**, *103*, 4419.
7. a) V. Amendola, D. Estebán-Gómez, L. Fabbrizzi, M. Licchelli, *Acc. Chem. Res.*, **2006**, *39*, 343; b) P. A. Gale, S. E. García-Garrido, J. Garric, *Chem. Soc. Rev.*, **2008**, *37*, 151; c) J. Yoon, S. K. Kim, N. J. Singh, K. S. Kim, *Chem. Soc. Rev.*, **2006**, *35*, 355.
8. a) T. –H. Kim, T. M. Swager, *Angew. Chem. Int. Ed.*, **2003**, *42*, 4803; *Angew. Chem.*, **2003**, *115*, 4951; b) S. Yamaguchi, S. Akiyama, K. Tamao, *J. Am. Chem. Soc.*, **2000**, *122*, 6793.
9. a) X. Cao, W. Lin, Q. Yu, J. Wang, *Org. Lett.*, **2011**, *13*, 6098; b) O. A. Bozdemir, F. Sozmen, O. Buyukcakir, R. Gulyev, Y. Cakmak, E. U. Akkaya, *Org. Lett.*, **2010**, *12*, 1400.
10. a) V. Bhalla, H. Singh, M. Kumar, *Org. Lett.*, **2010**, *12*, 628; b) V. Bhalla, R. Tejpal, M. Kumar, *Tetrahedron*, **2011**, *67*, 1266.
11. A. K. Atta, I. H. Ahn, A. Y. Hong, J. Heo, C. K. Kim, D. G. Cho, *Tetrahedron Lett.*, **2012**, *53*, 575.
12. J. F. Zhang, C. S. Lim, S. Bhuniya, B. R. Cho, J. S. Kim, *Org. Lett.*, **2011**, *13*, 1190.
13. B. Zhu, F. Yuan, R. Li, Q. Wei, Z. Ma, B. Du, X. Zhang, *Chem. Commun.*, **2011**, *47*, 7098.
14. P. Sokkalingam, C. -H. Lee, *J. Org. Chem.*, **2011**, *76*, 3820.
15. A. Agostini, M. Milani, R. Martínez-Máñez, M. Licchelli, J. Soto, F. Sancenón, *Chem. Asian J.*, **2012**, *7*, 2040.
16. a) R. Hu, J. Feng, D. Hu, S. Wang, S. Li, Y. Li, G. Yang, *Angew. Chem. Int. Ed.*, **2010**, *49*, 4915; *Angew. Chem.*, **2010**, *122*, 5035; b) F. Zheng, F. Zeng, C. Yu, X. Hou, S. Wu, *Chem. Eur. J.*, **2013**, *19*, 936.
17. K. L. Hoffmann, G. Maas, M. Regitz, *J. Org. Chem.*, **1987**, *52*, 3851.
18. J. L. Bricks, J. L. Slominskii, M. A. Kudinova, A. I. Tolmachev, K. Rurack, U. Resch-Genger, W. Rettig, *J. Photochem. Photobiol. A*, **2000**, *132*, 193.
19. a) B. Valeur, I. Leray, *Coord. Chem. Rev.*, **2000**, *205*, 3. b) K. Rurack, *Spectrochim. Acta, Part A.*, **2001**, *57*, 2161.
20. D. Markovitsi, C. Jallabert, H. Strzelecka, M. Veber, *J. Chem. Soc., Faradat Trans.*, **1990**, *86*, 2819.

A chromogenic probe for the selective recognition of Sarin and Soman mimic DFP

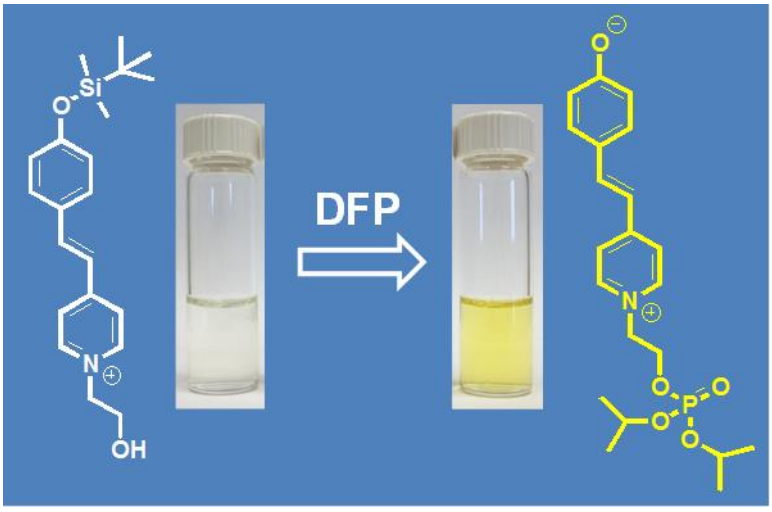

A chromogenic probe for the selective recognition of Sarin and Soman mimic DFP

Sameh El Sayed,[a,b,c] Lluís Pascual,[a,b,c] Alessandro Agostini,[a,b,c] Ramón Martínez-Máñez,[a,b,c] Félix Sancenón,[a,b,c] Ana M. Costero,*[a,d] Margarita Parra[a,d] and Salvador Gil[a,d]*

[a] Centro de Reconocimiento Molecular y Desarrollo Tecnológico (IDM), Unidad Mixta Universidad Politécnica de Valencia-Universidad de Valencia, Spain.
[b] Departamento de Química, Universidad Politécnica de Valencia, Camino de Vera s/n, 46022, Valencia, Spain.
E-mail: rmaez@qim.upv.es
[c] CIBER de Bioingeniería, Biomateriales y Nanomedicina (CIBER-BBN).
[d] Departamento de Química Orgánica, Universitat de València, Dr. Moliner 50, 46100, Burjassot, Valencia, Spain.

Received: *7 May 2014*
First published on the web: *9 July 2014*

ChemistryOpen., ***2014****, 3, 142 – 145*

(Reproduced with permission of Wiley-VCH Verlag GmbH & Co. KGaA copyright © 2014)

*The synthesis, characterization and sensing features of a novel probe **1** for the selective chromogenic recognition of diisopropylfluorophosphate (DFP), a sarin and soman mimic in 99:1 (v/v) water/acetonitrile and in the gas phase is reported. Colour modulation is based on the combined reaction of phosphorylation of **1** and fluoride-induced hydrolysis of a silyl ether moiety. As fluoride is a specific reaction product of the reaction between DFP and the -OH group, the probe shows a selective colour modulation in the presence of this chemical. Other nerve agent simulants, certain anions, oxidant species and other organophosphorous compounds were unable to induce colour changes in **1**. This is one of the very few examples of a selective detection, in solution and in the gas phase of a Sarin and Soman simulant versus other reactive derivatives such as the Tabun mimic diethylcyanophosphate (DCNP).*

The use of chemical warfare agents (CWA) in terrorist attacks has led to increasing interest in the study of these lethal chemicals.[1] Among CWA, nerve agents are especially dangerous because are capable of interfering with the action of the nervous system. More in detail, their primary mode of action is the inhibition of acetylcholinesterase enzyme resulting in acetylcholine accumulation in the synaptic junctions hindering muscles from relaxing and causing serious toxicity.[2] From a chemical point of view, nerve agents are classified into the organophosphonates family.

The easy fabrication of nerve gases and their indiscriminate use by certain nations and by terrorist groups have increased the efforts of the scientific community toward the detection and remediation of these deadly chemicals.[3] Currently, the most used methods for monitoring the presence of nerve agents are based on the use of biosensors,[4] ion mobility spectroscopy,[5] electrochemical methods,[6] micro-cantilevers,[7] photonic crystals[8] and optical-fiber arrays.[9] Recently, as an alternative to these instrumental methods the development of fluorogenic and chromogenic probes has gained increasing interest.[3b,10] Chromogenic systems are especially appealing because there are few techniques

as simple as visual detection and they allow rapid and sensitive detection to the naked eye in situ or at site without any sample pretreatment. However in this field there are relatively few examples of selective probes for the detection of nerve gases.[11] Usually in these studies nerve gas simulants such as diethylcyanophosphate (DCNP), diisopropylfluorophosphate (DFP) and diethylchlorophosphate (DCP) are used (see Figure 1). These compounds show similar reactivity than real nerve agents Sarin, Soman and Tabun but lack their severe toxicity (see Figure 1).

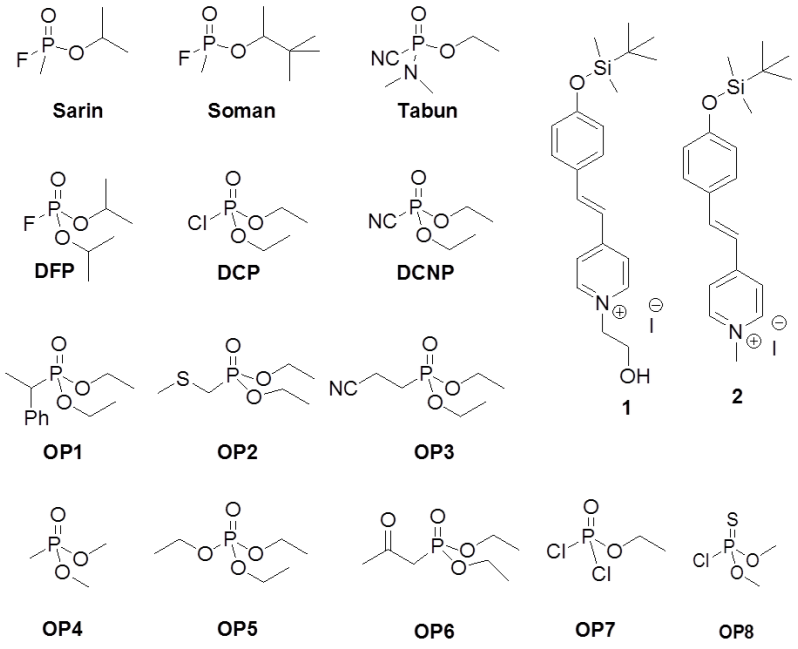

Figure 1. *Chemical structures of nerve agents Sarin, Soman, Tabun, their simulants (DFP, DCP and DCNP), selected organophosphates (**OP1** to **OP8**) and compounds **1** and **2**.*

Most of these reported probes make use of the electrophilic reactivity of nerve gases with suitable nucleophiles.[12] However, these reactions are in most cases unspecific and usually the probes display the same optical response to all nerve agents.[13] In this context, it has been indicated that the design of rapid methods for the individual signalling of nerve agents is of importance. At this respect, even though the emergency response protocol is similar for Sarin, Soman and Tabun,

there are evidences that some antidotes are effective only for certain nerve gases indicating the importance of distinguishing one specific agent within this family of deadly compounds.[14] In this field there are very few examples of probes capable to selectively discriminate between DCNP[11a] and DFP[11b] as model compounds for Tabun and Sarin/Soman, respectively.

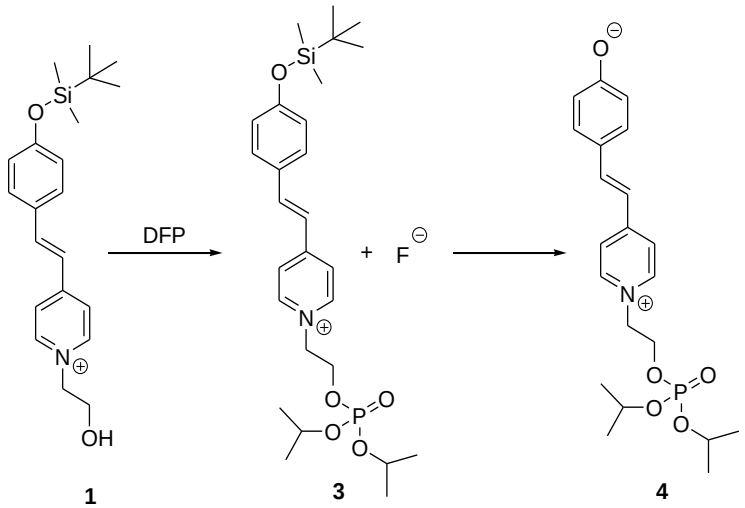

Scheme 1. *Mechanism of the chromogenic response with DFP.*

Following our interest in the design of chromogenic probes for the potential discrimination of nerve agents[15] we report herein probe **1** (see Figure 1) which is able to display a highly selective chromogenic response both in solution and in gas phase in the presence of DFP (a Sarin and Soman mimic) versus other simulants and organophosphates. Probe **1** (see Supporting Information for details of its synthesis) contains two reactive subunits, that is a nucleophilic hydroxyl moiety and a silyl ether group. The underlying sensing idea is that phosphorylation of the hydroxyl moiety of probe **1** by DFP would yield the phosphate derivative **3** and the release of a fluoride anion that would hydrolyse the silyl ether[16] moiety generating a coloured phenolate derivative (see **4** in Scheme 1). Both reactions, and therefore colour modulation are expected to occur only in the presence of the Sarin and Soman simulant DFP.

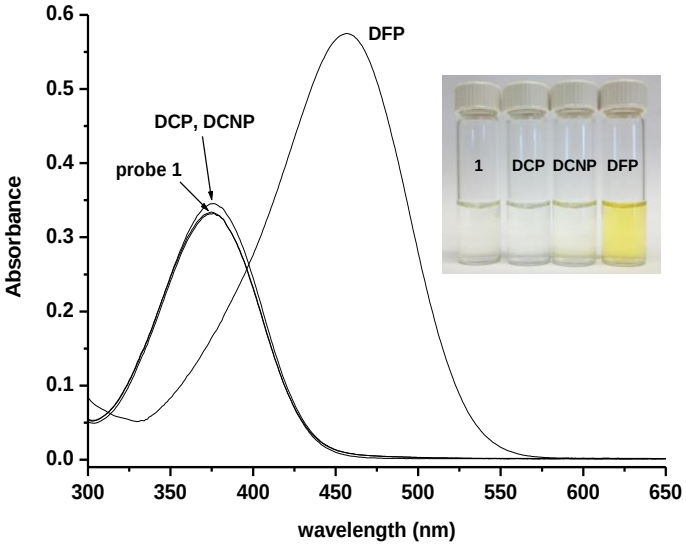

Figure 2. *UV-visible spectra of probe **1** (1.0 x 10^{-5} mol L^{-1}) in 99:1 (v/v) H_2O/CH_3CN at pH 8.0 in the presence of 10 equiv. DFP, DCP and DCNP. The inset shows a photograph of the colour changes observed upon addition of DFP, DCP and DCNP to solutions of probe **1**.*

In a first step, the response of **1** was tested with nerve agent simulants in 99:1 (v/v) water/acetonitrile solutions buffered at pH 8.0. Probe **1** is colourless and shows an intense absorption band centred at 374 nm. Upon addition of 10 equivalents of DFP, a remarkable change was observed with the appearance of a new band at 465 nm which resulted in a colour modulation from colourless to yellow (see Figure 2). Addition of DCP and DCNP induced negligible changes neither in the colour nor in the band at 374 nm. Moreover from further titration experiments of **1** with DFP a remarkable limit of detection (LOD) of 5.4 ppm in 99:1 (v/v) water/acetonitrile solutions was determined (see Supporting Information for details).

The chromogenic response of probe **1** was also tested against certain anions (F^-, Cl^-, Br^-, I^-, HCO_3^-, $H_2PO_4^-$, OH^-, CN^-, N_3^-, NO_3^-, SO_4^{2-} and citrate), oxidant species (H_2O_2 and $S_2O_3^{2-}$) and other organophosphorous compounds (**OP1** to **OP8** see Figure 1) in 99:1 (v/v) water/acetonitrile. The results observed in the presence of nerve agent simulants, F^- anion and organophosphates are shown in Figure 3 (for the response of other selected anions and oxidant species see Supporting

Information). Of all chemicals tested, only fluoride anion (in addition to DFP) was able to induce a chromogenic response. Competitive studies were also carried out and in all cases mixtures of DFP with other anions, oxidants or organophosphorous derivatives resulted in a chromogenic signal similar to that obtained for DFP alone (see Supporting Information).

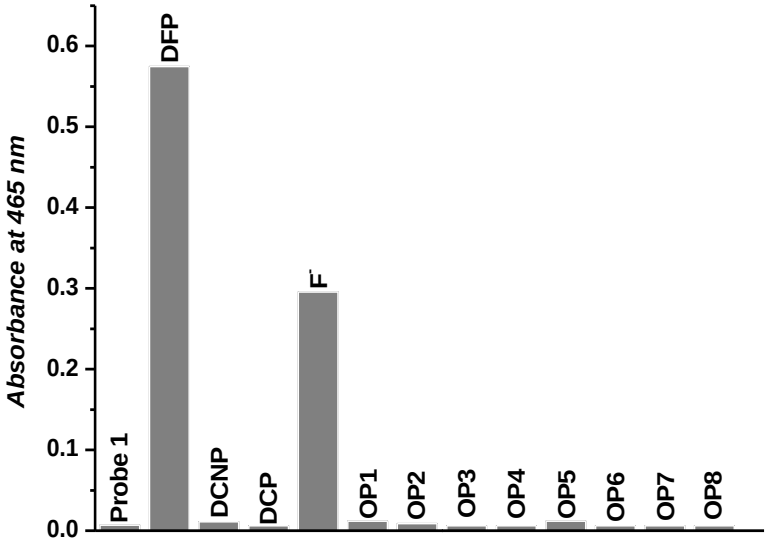

Figure 3. *Absorbance at 465 nm of probe **1** (1.0 x 10^{-5} mol L^{-1}) in 99:1 (v/v) H_2O/CH_3CN at pH 8.0 solutions in the presence of 10 equiv. DFP, DCP, DCNP,F^- or organophosphates (**OP1**-**OP8**).*

The mechanism of the chromogenic response was assessed by ^1H, ^{31}P NMR and MS studies. In the ^1H spectrum of **1**, there was a characteristic triplet centered at 3.83 ppm which corresponds to the methylene group directly connected with the hydroxyl moiety that was shifted downfield to 4.34 ppm upon addition of DFP. Moreover, the ^{31}P-NMR spectrum of DFP (in $[D_6]$DMSO) showed a sharp doublet at 11.0 ppm (J_{PF}= 967 Hz) that progressively disappeared upon addition of increasing quantities of probe **1**, together with the growth of a new singlet at -1.54 ppm ascribed to the formation of a phosphate moiety. In addition, MS studies confirmed the formation of phenolate **4** upon reaction between probe **1** and DFP (*m/z* calculated for [**4**+H^+]: 533.08; found: 533.30). These facts clearly pointed to a DFP phosphorylation of the hydroxyl moiety and the subsequent

fluoride-induced hydrolysis of the silyl ether group as the mechanism of the chromogenic response observed.

Additionaly, the central role played by the hydroxyl moiety in **1** was assessed by testing the analogous derivative **2** (see Figure 1) under similar conditions. 99:1 (v/v) water/acetonitrile solutions (pH 8.0) of probe **2** were colourless and showed an absorption band at 350 nm. However, addition of DFP, DCNP and DCP induced negligible changes in the band indicating that the presence of the hydroxyl moiety in probe **1** is crucial to observe a final chromogenic response.

In order to focus our research to a more potential application we moved a step further and developed studies using probe **1** to design test strips for the colorimetric detection of DFP in solution and in gas phase. To check this possibility, a polyethylene oxide film containing 0.1% of **1** and 1% of Cs_2CO_3 was prepared. In a typical assay, the polymer containing probe **1** was either exposed to 99:1 (v/v) water/acetonitrile solutions of DFP, DCP and DCNP or placed in a container containing the simulants as gases at different concentrations. A similar selective colour change in the presence of DFP in aqueous solution was observed when using the polyethylene oxide membranes containing **1**. Moreover Figure 4 shows that there is a selective response to DFP to the naked eye in air at concentrations of about 10 ppm; whereas the other simulants DCP and DCNP did not induce colour changes even at concentrations of 50 ppm in air. Further, it was also confirmed that these membranes containing probe **1** were not affected by the presence of vapours of other potential interferents such as the organophosphorous **OP1**-**OP8** derivatives.

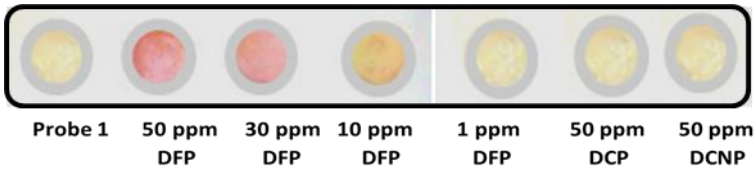

Figure 4. *Polyethylene oxide membranes containing probe **1** after exposure to vapours of DCP, DCNP and DFP at different concentrations.*

To summarize, we report herein the synthesis, characterization and sensing features of a new probe **1** for the selective chromogenic recognition DFP (a Sarin and Soman mimic) in 99:1 (v/v) water/acetonitrile and in gas phase. Colour modulation was due to the combined reaction of phosphorylation of **1** and fluoride-induced hydrolysis of a silyl ether moiety. As fluoride is a specific reaction product of the reaction between DFP and the –OH group, the probe shows a selective colour modulation in the presence of this chemical. Other nerve agent simulants, certain anions, oxidant species and other organophosphorous compounds were unable to induce colour changes in **1**. This is one of the very few examples of a selective detection in solution and in gas phase of a Sarin and Soman simulant versus other reactive derivatives such as DCNP (a Tabun mimic).

Acknowledgements

Financial support from the Spanish Government (Project MAT2012-38429-C04) is gratefully acknowledged. S.E. is grateful to the Generalitat Valenciana for his Santiago Grisolia fellowship. Ll.P. thanks the Universitat Politècnica de València for his doctoral fellowship.

Keywords: •chromogenic probe • diisopropylfluorophosphate •nerve agents • Sarin • Soman

References

1. a) L. M. Eubanks, T. J. Dickerson, K. D. Janda, *Chem. Soc. Rev.*, **2007**, *36*, 458; b) H. H. Hill Jr., S. J. Martin, *Pure Appl. Chem.*, **2002**, *74*, 2281.
2. S. M. Somani, Chemical Warfare Agents, Academic Press, San Diego, **1992**.
3. a) B. M. Smith, *Chem. Soc. Rev.*, **2008**, *37*, 470; b) M. Burnworth, S. J. Rowan, C. Werder, *Chem. Eur. J.*, **2007**, *13*, 7828; c) D. Ajami, J. Rebek, *Org. Biomol. Chem.*, **2013**, *11*, 3936.
4. a) A. J. Russell, J. A. Berberich, G. F. Drevon, R. R. Koepsel, *Annu. Rev. Biomed. Eng.*, **2003**, *5*, 1; b) H. Wang, J. Wang, D. Choi, Z. Tang, H. Wu, Y. Lin, *Biosens. Bioelectron.*, **2009**, *24*, 2377; c) A. Mulchandani, I. Kaneva, W. Chen, *Anal. Chem.*, **1998**, *70*, 5042.

5. E. Steiner, S. J. Klopsch, W. A. English, B. H. Clowers, H. H. Hill, *Anal. Chem.*, **2005**, *77*, 4792.
6. a) M. A. K. Khan, Y. T. Long, G. Schatte, H. B. Kraatz, *Anal. Chem.*, **2007**, *79*, 2877; b) O. V. Shulga, C. Palmer, *Anal. Bioanal. Chem.*, **2006**, *385*, 1116; c) J. C. Chen, J. L. Shih, C. H. Liu, M. Y. Kuo, J. M. Zen, *Anal. Chem.*, **2006**, *78*, 3752; d) G. Liu, Y. Lin, *Anal. Chem.*, **2006**, *78*, 835.
7. a) G. Zuo, X. Li, P. Li, T. Yang, Y. Wang, Z. Chen, S. Feng, *Anal. Chim. Acta*, **2006**, *580*, 123; b) C. Karnati, H. Du, H. F. Ji, X. Xu, Y. Lvov, A. Mulchandani, P. Mulchandani, W. Chen, *Biosens. Bioelectron.*, **2007**, *22*, 2636; c) Q. Zhao, Q. Zhu, W. Y. Shih, W. H. Shih, *Sens. Actuators B*, **2006**, *117*, 74.
8. a) W. He, Z. Liu, X. Du, Y. Jiang, D. Xiao, *Talanta*, **2008**, *76*, 698; b) J. P. Walker, K. W. Kimble, S. A. Asher, *Anal. Bioanal. Chem.*, **2007**, *389*, 2115; c) J. P. Walker, S. A. Asher, *Anal. Chem.*, **2005**, *77*, 1596.
9. M. J. Aernecke, D. R. Walt, *Sens. Actuators B*, **2009**, *142*, 464.
10. a) S. Royo, R. Martínez-Máñez, F. Sancenón, A. M. Costero, M. Parra, S. Gil, *Chem. Commun.*, **2007**, 4839; b) D. Ajami, J. Rebek Jr., *Org. Biomol. Chem.*, **2013**, *11*, 3936; c) H. Lee, H. –J. Kim, *Tetrahedron*, **2014**, *70*, 2966.
11. a) S. Royo, A. M. Costero, M. Parra, S. Gil, R. Martínez-Máñez, F. Sancenón, *Chem. Eur. J.*, **2011**, *17*, 6931; b) R. Gotor, A. M. Costero, S.Gil, M. Parra, R. Martínez-Máñez, F. Sancenón, *Chem. Eur. J.*, **2011**, *17*, 11994; c) B. D. de Greñu, D. Moreno, T. Torroba, A. Berg, J. Gunnars, T. Nilsson, R. Nyman, M. Persson, J. Pettersson, I. Eklind, P. Wästerby, *J. Am. Chem. Soc.*, **2014**, *136*, 4125; d) K. Chulvi, P. Gaviña, A. M. Costero, S. Gil, M. Parra, R. Gotor, S. Royo, R. Martínez-Máñez, F. Sancenón, J. L. Vivancos, *Chem. Commun.*, **2012**, *48*, 10105.
12. Nerve Agents, A FOA Briefing Book on Chemical Weapons, **1992**, (from www.fas.org/cw/cwagents) (last accessed: July 2007).
13. a) K. A. Van Houten, D. C. Heath, R. S. Pilato, *J. Am. Chem. Soc.*, **1998**, *120*, 12359; b) S. –W. Zhang, T. M. Swager, *J. Am. Chem. Soc.*, **2003**, *125*, 3420; c) T. J. Dale, J. Rebek Jr., *J. Am. Chem. Soc.*, **2006**, *128*, 4500; d) K. J. Wallace, J. Morey, V. M. Lynch, E. V. Anslyn, *New J. Chem.*, **2005**, *29*, 1469.
14. a) M. Jokanovic, *Curr. Top. Med. Chem.*, **2012**, *12*, 1775; b) O. Soukup, G. Tobin, U. K. Kumar, J. Binder, J. Proska, D. Jun, J. Fusek, K. Kuca, *Curr. Med. Chem.*, **2010**, *17*, 1708; c) F. Worek, H. Thiermann, L. Szinicz, P. Eyer, *Biochem. Pharmacol.*, **2004**, *68*, 2237; d) F. Brandhuber, M. Zengerie, L. Porwol, A. Bierwisch, M. Koller, G. Reiter, F. Worek, S. Kubik, *Chem. Commun.*, **2013**, *49*, 3425.

15. a) I. Candel, A. Bernardos, E. Climent, M.D. Marcos, R. Martínez-Máñez, F. Sancenón, J. Soto, A. Costero, S. Gil, M. Parra, *Chem. Commun*. **2011**, *47*, 8313; b) E. Climent, A. Martí, S. Royo, R. Martínez-Máñez, M.D. Marcos, F. Sancenón, J. Soto, A.M. Costero, S. Gil, M. Parra, *Angew. Chem. Int. Ed*., **2010**, *49*, 5945; *Angew. Chem.*, **2010**, *122*, 6081; c) A. M. Costero, S. Gil, M. Parra, P. M. E. Mancini, R. Martínez-Máñez, F. Sancenón, S. Royo, *Chem. Commun.*, **2008**, 6002; d) A. M. Costero, M. Parra, S- Gil, R. Gotor, P. M. E. Mancini, R. Martínez-Máñez, F. Sancenón, S. Royo, *Chem. As. J.*, **2010**, *5*, 1573; e) A. M. Costero, M. Parra, S. Gil, R. Gotor, R. Martínez-Máñez, F. Sancenón, S. Royo, *Eur. J. Org. Chem.*, **2012**, 4937; f) S. Royo, R. Gotor, A. M. Costero, M. Parra, S. Gil, R. Martínez-Máñez, F. Sancenón, *New J. Chem.*, **2012**, *36*, 1485; g) R. Gotor, S. Royo, A. M. Costero, M. Parra, S. Gil, R. Martínez-Máñez, F. Sancenón, *Tetrahedron*, **2012**, *68*, 8612.

16. See for instance: a) V. Bhalla, H. Singh, M. Kumar, *Org. Lett*., **2010**, *12*, 628; b) J. F. Zhang, C. S. Lim, S. Bhuniya, B. R. Cho, J. S. Kim, *Org. Lett*., **2011**, *13*, 1190; c) B. Zhu, F. Yuan, R. Li, Q. Wei, Z. Ma, B. Du, X. Zhang, *Chem. Commun*., **2011**, *47*, 7098; d) P. Sokkalingam, C. H. Lee, *J. Org. Chem*., 2011, **76**, 3820; e) S. El Sayed, A. Agostini, L.. E. Santos-Figueroa, R. Martínez-Máñez, F. Sancenón, *ChemistryOpen.*, **2013**, *2*, 58; f) A. Agostini, M. Milani, R. Martínez-Máñez, M. Licchelli, J. Soto, F. Sancenón, *Chem. As. J.*, **2012**, *7*, 2040.

SUPPORTING INFORMATION

A Chromogenic Probe for the Selective Recognition of Sarin and Soman Mimic DFP

Sameh El Sayed, Lluís Pascual, Alessandro Agostini, Ramón Martínez-Máñez, Félix Sancenón, Ana M. Costero, Margarita Parra and Salvador Gil

Chemicals:

The chemicals 4-picoline, 4-hydroxy benzaldehyde, acetic anhydride, *t*-butyldimethylsilyl chloride (TBDMSCl), *N*-methylimidazole, 2-iodoethanol, iodomethane, DFP, DCNP and DCP were provided by Sigma-Aldrich. Analytical-grade solvents and anhydrous magnesium sulfate were purchased from Scharlau (Barcelona, Spain). For the spectroscopy studies hydrogen peroxide and tetrabutylammonium or sodium salts of hydrogen sulfide, fluoride, chloride, bromide, iodide, hydroxide, acetate, cyanide, azide, nitrate, hydrogen carbonate, sulfate, thiosulfate and hydrogen phosphate were used.

General techniques:

UV-visible spectra were recorded with a JASCO V-650 Spectrophotometer. Fluorescence measurements were carried out in a Jasco FP-8500 Spectrophotometer. ^{1}H, ^{13}C and ^{31}P-NMR spectra were acquired in a Bruke Advance III (400 MHZ). Mass spectra were carried out in a Tripletof T5600 (ABSciex, USA) spectrometer.

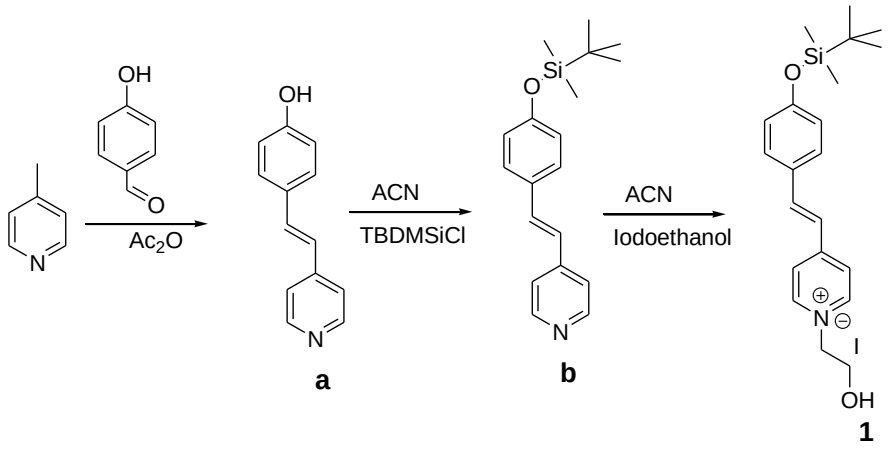

Scheme SI-1. *Synthesis of probe **1**.*

Synthesis of probes 1 and 2:

*Synthesis of **a**:* 4-Hydroxybenzaldehyde (500 mg, 4.1 mmol) and 4-picoline (382 mg, 4.1 mmol) were dissolved in acetic anhydride (3 mL) and the final crude refluxed for 24 h. Afterwards, the acetic anhydride was evaporated under reduced pressure and the dark brown residue obtained dissolved in water-ethanol 1:1 v/v (200 mL). The pH of the solution was adjusted to 8 (by the addition of KOH) and refluxed for 6 h. The obtained suspension was cooled to RT and then the pH adjusted to 6. Pale yellow crystals of compound **a** (730 mg, 3.7 mmol, 85% yield) appeared that were filtered off, washed with water and dried.
^{1}H NMR (400 MHz, DMSO-D6) δ: 9.81 (br s, 1H) 8.49 (d, *J* = 6 Hz, 2H), 7.46 (m, 4H), 7.41 (d, *J* = 16 Hz, 1H), 7.00 (d, *J* = 16 Hz, 1H), 6.80 (d, *J* = 8 Hz, 2H).

*Synthesis of **b**:* Compound **a** (200 mg, 1.02 mmol) and *N*-methylimidazole (250 mg, 3.06 mmol) were dissolved in anhydrous acetonitrile (50 mL) and strirred at RT for 30 min in an inert atmosphere (Ar gas). Then, a solution of *t*-butyldimethylsilyl chloride (153 mg, 1.02 mmol) in anhydrous acetonitrile (20 mL) was added dropwise to the crude containing compound **a** and *N*-methylimidazole. After stirring the crude at RT overnight the acetonitrile was evaporated and the yellow residue purified by column chromatography using hexane-acetone 9:1 v/v as eluent. Product **b** was obtained as yellow solid (184 mg, 0.6 mmol, 55% yield).

^{1}H NMR (400 MHz, $CDCl_3$) δ: 8.54 (d, *J* = 6 Hz, 2H), 7.42 (d, *J* = 8 Hz, 2H), 7.33 (d, *J* = 6 Hz, 2H), 7.20 (d, *J* = 16 Hz , 2H), 6.88 (d, *J* = 16 Hz, 2H), 6.84 (d, *J* = 8 Hz, 2H), 1.00 (s, 9H), 0.22 (s, 6H).

*Synthesis of **1**:* Compound **b** (50 mg, 0.16 mmol) and 2-iodoethanol (30.4 mg, 0.17 mmol) were dissolved in anhydrous acetonitrile (20 mL) and the resultant crude refluxed under Ar inert atmosphere for 24 h. Afterward, acetonitrile was evaporated and the obtained solid was purified by column chromatography using hexane-acetone 1:1 v/v as eluent. The final probe **1** was isolated as red solid (74 mg, 0.15 mmol, 92% yield).
^{1}H NMR (400 MHz, DMSO) δ: 8.68 (d, *J* = 6 Hz, 2H), 8.05 (d, *J* = 6 Hz, 2H), 7.87 (d, *J* = 16.1 Hz, 1H), 7.56 (d, *J* = 8 Hz, 2H), 7.16 (d, *J* = 16.1 Hz, 1H), 6.75 (d, *J* = 8 Hz, 2H), 4.46 (t, 2H), 3.83 (t, 2H), 0.84 (s, 9H), -0.04 (s, 6H). ^{13}C NMR (101 MHz, DMSO) δ: 160.1, 153.5, 144.3, 141.3, 131.0, 126.2, 123.4, 119.8, 116.2, 62.0, 60.2, 26.0, 18.0, -3.0. HRMS-EI *m/z*: calcd for $C_{21}H_{30}INO_2Si$ 483.1085; found: 483.2123 (M).

*Synthesis of **2**:* Compound **b** (25 mg, 0.08 mmol) and iodomethane (12.5 mg, 0.09 mmol) were dissolved in anhydrous acetonitrile (20 mL) and the crude refluxed under Ar inert atmosphere for 24 h. Afterward, acetonitrile was evaporated and the obtained solid was purified by column chromatography using hexane-acetone 1:1 v/v as eluent. Probe **2** was isolated as reddish solid (35 mg, 0.07 mmol, 94% yield).
^{1}H NMR (400 MHz, DMSO) δ: 8.51 (d, J = 6 Hz, 2H), 7.61-7.41 (m, 5H), 7.09 (d, J = 16.1 Hz, 1H), 6.89 (d, J = 8 Hz, 2H), 4.23 (s, 3H), 0.96 (s, 9H), 0.21 (s, 6H).

Polyethylene oxide membrane preparation:

A mixture of Cs_2CO_3 (27.2 mg) and polyethylene oxide (2 g, Mv 400.000 Dalton) were slowly added to a solution of probe **1** (4 mg) in dichloromethane (40 mL). The mixture was stirred until polymer dissolution. Then, the solvent was partially evaporated until a high viscous mixture was formed. This mixture was poured on a glass plate (40 cm^2) and kept in a dry atmosphere during 6 hours.

Limit of detection for DFP:

Addition of increasing quantities of DFP to water-acetonitrile 99:1 v/v solutions (pH 8.0) of probe **1** (1.0 x 10^{-5} mol L^{-1}) induced the progressive growth of the absorption band centered at 465 nm (see figure SI-1). From the titration profile representing the absorbance of the 465 nm band vs. the quantity of DFP added, a limit of detection of 5.4 ppm was determined (see figure SI-2).

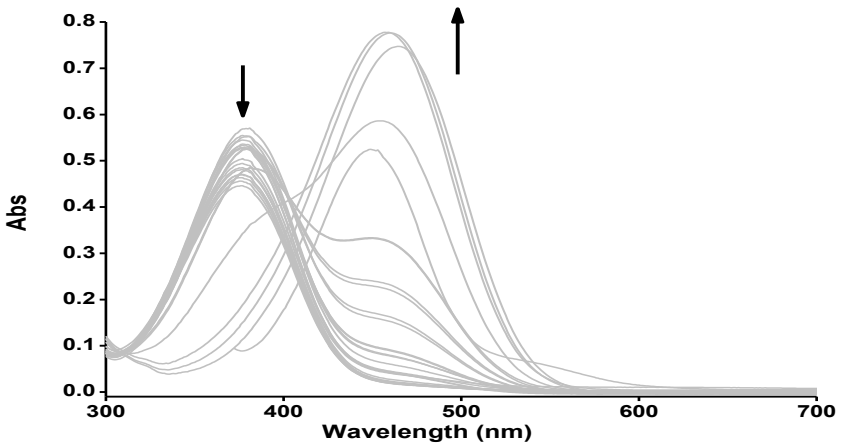

Figure SI-1. *UV-visible changes of water-acetonitrile 99:1 v/v solutions (pH 8.0) of probe* ***1*** *(1.0 x 10^{-5} mol L^{-1}) upon addition of increasing quantities of DFP (from 0 to 20 eq).*

UV-visible selectivity studies:

The UV-visible behavior of probe **1** in the presence of nerve agent simulants, anions, oxidants and organophosphates has been studied. The chromogenic response of probe **1** was also tested against certain anions (F^-, Cl^-, Br^-, I^-, HCO_3^-, HPO_4^{2-}, OH^-, CN^-, N_3^-, NO_3^-, SO_4^{2-} and citrate), oxidant species (H_2O_2 and $S_2O_3^{2-}$) and other organophosphorous compounds (**OP1** to **OP8** in Scheme 1 in the manuscript) in water:acetonitrile 99:1 v/v. The results are shown in Figure SI-3. Of all chemicals tested, DFP and fluoride anion were able to induce a chromogenic response. Figure SI-4 showed the absorbance at 465 nm of probe **1** alone, probe **1** in the presence of 10 eq. of DFP and probe **1** in the presence of 10 eq. of DFP and

10 eq. of selected interferents. As seen neither of the tested chemical species were able to change the chromogenic response of probe **1** toward DFP.

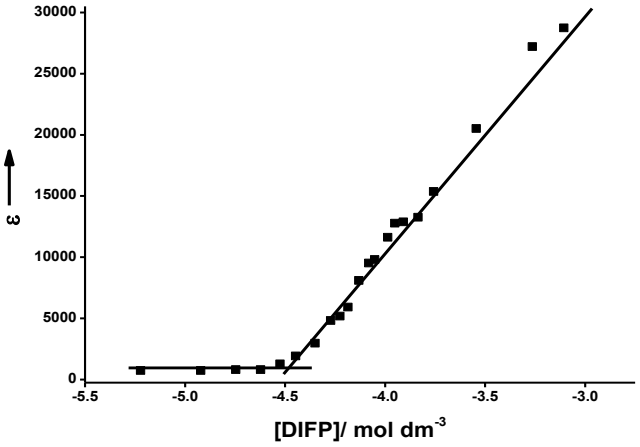

Figure SI-2. *Absorbance at 465 nm of water-acetonitrile 99:1 v/v solutions (pH 8.0) of probe **1** (1.0 x 10^{-5} mol L^{-1}) upon addition of increasing quantities of DFP.*

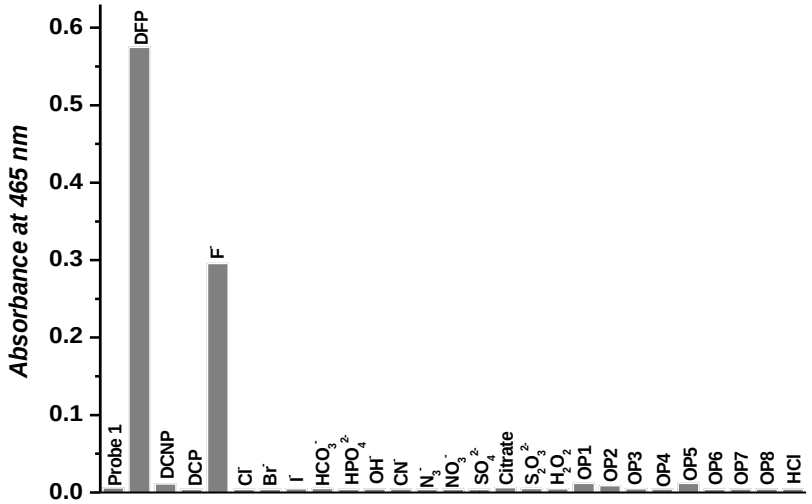

Figure SI-3. *Absorbance at 465 nm of water-acetonitrile 99:1 v/v at pH 8.0 solutions of probe **1** in the presence of 10 eq. of nerve agent simulants, anions, oxidants, organophosphates and HCl.*

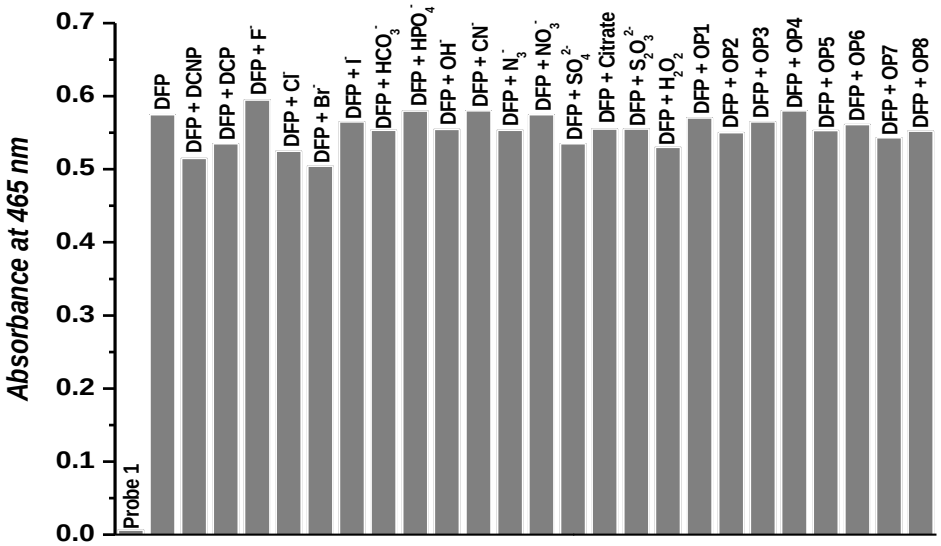

Figure SI-4. *Absorbance at 465 nm of probe **1** alone, probe **1** in the presence of 10 eq. of DFP and probe **1** in the presence of 10 eq. of DFP and 10 eq. of selected interferents in water-acetonitrile 99:1 v/v at pH 8.0 solutions.*

Mechanism of the observed chromogenic response:

The mechanism of the chromo-fluorogenic response was assessed by ^{1}H and ^{31}P NMR measurements (see figure SI-5).

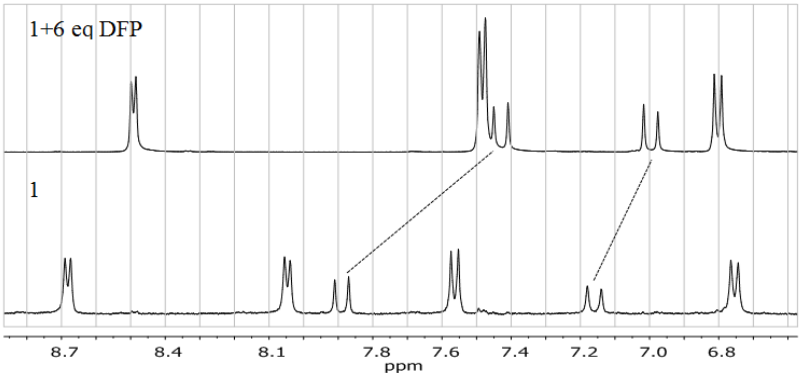

Figure SI-5. *^{1}H-NMR spectra (aromatic zone) of probe **1** (in DMSO-D6) alone and in the presence of 6 eq. of DFP.*

A new fluorescent "turn-on" chemodosimeter for the detection of hydrogen sulfide in water and living cells

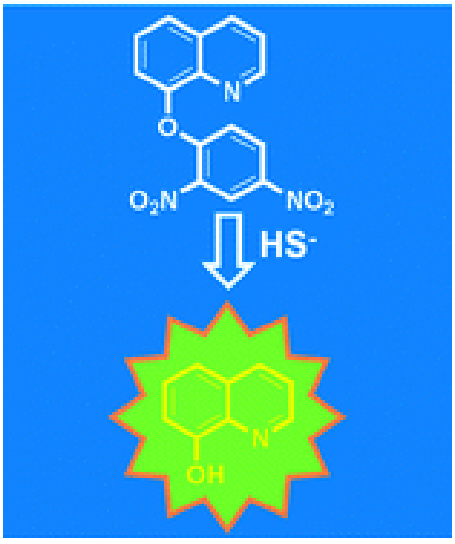

A new fluorescent "turn-on" chemodosimeter for the detection of hydrogen sulfide in water and living cells

Sameh El Sayed,[a,b,c] Cristina de la Torre, [a,b,c] Luis E. Santos-Figueroa,[a,b,c] Enrique Pérez-Payá, [d] Ramón Martínez-Máñez,[a,b,c] Félix Sancenón, [a,b,c] Ana M. Costero,*[a,e] Margarita Parra[a,e] and Salvador Gil[a,e]*

[a] Centro de Reconocimiento Molecular y Desarrollo Tecnológico (IDM), Unidad Mixta Universidad Politécnica de Valencia-Universidad de Valencia, Spain.
[b] Departamento de Química, Universidad Politécnica de Valencia, Camino de Vera s/n, 46022, Valencia, Spain. E-mail: rmaez@qim.upv.es
[c] CIBER de Bioingeniería, Biomateriales y Nanomedicina (CIBER-BBN).
[d] Laboratorio de Péptidos y Proteinas, Centro de Investigación Principe Felipe, Autopista El Saler, Valencia, Spain.
[e]Departamento de Química Orgánica, Universitat de València, Dr. Moliner 50, 46100, Burjassot, Valencia.E-mail: ana.costero@uv.es

Received: *14 October 2013*
First published on the web: *24 October 2013*

RSC Adv., ***2013****, 3, 25690-25693*

(Reproduced with permission of Royal Society of Chemistry 2013)

A new fluorescent turn-on probe for the selective detection of hydrogen sulfide in water and living cells based on a 8-hydroxyquinoline fluorophore functionalized with a 2,6-dinitrophenyl ether moiety has been developed.

Hydrogen sulfide has traditionally been considered a highly toxic gas. However, recent studies have demonstrated that H_2S is an endogenously generated gaseous signaling molecule with very potent cytoprotective properties similar to those found for the two well-known endogenous nitric oxide (NO) and carbon monoxide (CO) gasotransmitters.[1] Hydrogen sulfide may interact with downstream proteins by the post-translational cysteine sulfhydration[2] and binding to iron centers,[3] which regulate various physiological processes, including ischemia reperfusion injury,[4] vasodilation,[5] apoptosis,[6] angiogenesis,[7] neuromodulation,[8] inflammation,[9] and insulin signaling.[10] The exact hydrogen sulfide mechanisms of action are still being actively investigated. Some chemical and biochemical catabolic reactions of H_2S have been reported; for example, hydrogen sulfide can react readily with methemoglobin to form sulfhemoglobin, which acts as the metabolic sink for sulfide. As a potential reductant, hydrogen sulfide is likely to be consumed by endogenous oxidant species, such as hydrogen peroxide, superoxide, peroxynitrite, etc. This process is potentially significant because it provides a possible mechanism by which sulfide changes the functions of a wide range of cellular proteins and enzymes. Moreover, abnormal levels of hydrogen sulfide are associated with various diseases, such as Alzheimer's[11] and Down syndrome.[12]

Based on these concepts and given the important roles that hydrogen sulfide plays in biological processes, growing interest has been shown in the development of reliable selective and sensitive detection systems for this chemical. Current techniques for sulfide detection, such as colorimetric,[13-15] electrochemical assays,[16] gas chromatography,[17] and metal-induced sulfide precipitation,[18] are often not suitable for monitoring sulfide levels in biological living environments. As an alternative to these methods, the design of fluorogenic probes has recently become an important focal point. In particular, reduction reactions of azide or nitro groups to amines coupled with emission changes,[19-22]

and demetallation of macrocyclic Cu(II) complexes,[23,24] have been used for the development of highly sensitive probes for sulfide detection.

Another alternative to the above-mentioned protocols, the thiolysis of 2,4-dinitrophenyl ethers, has also been used as a mechanism in the preparation of HS^- turn-on fluorescent probes. In particular, Lin and co-workers synthesized a NIR fluorescent chemodosimeter for the detection of HS^- in solutions and living cells. This probe is based on a BODIPY dye functionalized with a 2,4-dinitrophenyl ether moiety that is non fluorescent in PBS-ethanol 9:1 v/v mixtures. Addition of HS^--induces the hydrolysis of the ether with subsequent emission enhancement.[25] Very recently, Xu and co-workers synthesized a 1,8-naphthalimide probe also containing a 2,4-dinitrophenyl ether group which was utilized for the fluorescent detection of HS^- anion in PBS-acetonitrile 9:1 v/v solutions.[26]

Despite these interesting results, there is still room to improve the behavior of probes based on the HS^--induced hydrolysis of 2,4-dinitrophenyl ethers. For instance, the examples reported by Lin and Xu, displayed sensing features in media with a relatively large percentage (10%) of a non aqueous solvent and displayed an interesting turn-on fluorescence enhancement of *ca*. 42- and 18-fold (upon the addition of 10 eq. of HS^- anion) which could, however, still be improved.

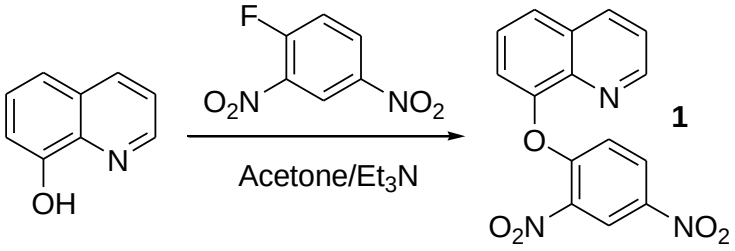

Scheme 1. *Synthesis of chemodosimeter* ***1****.*

Bearing in mind our interest in developing molecular chemosensors for anions of environmental and biological interest,[27] we report herein the synthesis and sensing features of fluorescent probe **1** (see Scheme 1) for hydrogen sulfide detection in water and living cells. Probe **1** was readily prepared, with a good yield

and in a one-step procedure, by a nucleophilic aromatic substitution of 1-fluoro-2,4-dinitrobenzene with 8-hydroxyquinoline (see Supporting Information for synthetic details and characterization).

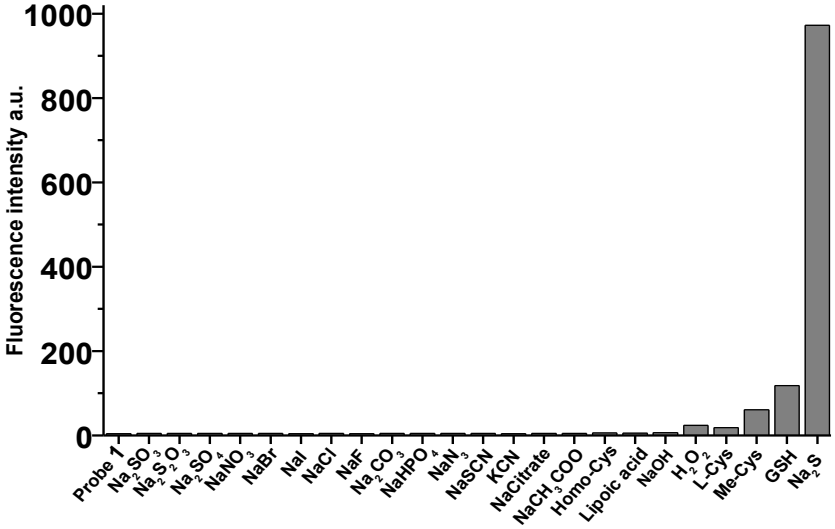

Figure 1. *Fluorescent intensity at 514 nm (excitation at 450 nm) of chemodosimeter **1** (5.0 x 10^{-5} M) in HEPES (7 mM, pH 7.4)-DMSO 99:1 v/v upon the addition of 10 equivalents of selected anions, biothiols, oxidants and reducing agents after 50 min of the addition.*

The emission behavior of probe **1** in the presence of 10 equivalents of selected anions (HS^-, OH^-, F^-, Cl^-, Br^-, I^-, N_3^-, CN^-, SCN^-, AcO^-, CO_3^{2-}, PO_4^{2-}), oxidants (H_2O_2), bio-thiols (Cys, Me-Cys, Hcy, GSH, lipoic acid) and reducing agents (SO_4^{2-}, SO_3^{2-}, $S_2O_3^{2-}$) was evaluated. HEPES (7 mM, pH 7.4)-DMSO 99:1 v/v solutions of **1** are essentially non fluorescent (upon excitation at 450 nm). Of all the chemicals tested, only the addition of HS^- induced the appearance of a strong emission band at 514 nm (λ_{ex} = 450 nm) with an impressive 345-fold enhancement upon the addition of 10 equivalents of the anion (see Figure 1). Besides, time-dependent studies have shown that a maximum change in emission was observed after *ca*. 50 min upon the addition of HS^- (see Supporting Information). Moreover, fluorescence studies at different pHs in water-DMSO 99:1 v/v solutions of **1** in the absence and presence of 5 μM of HS^- anion have demonstrated that the probe can be used in a wide range of pH values (from 2 to 9) with no significant reduction in its sensing behavior (see Supporting Information).

After assessing the highly selective turn-on response of probe **1** to hydrogen sulfide, the sensitivity of the probe was assessed by studies on the emission modulation of **1** in HEPES-DMSO 99:1 v/v upon the addition of HS^-. Increasing the HS^- concentration (up to 100 eq.) resulted in the progressive growth of fluorescence intensity (see Figure 2). From typical titration profiles (see Supporting Information), a remarkable limit of detection (LOD) of 60 nM was determined. **1** showed remarkably low sensitivity below the hydrogen sulfide concentration required to elicit physiological responses (10-1000 μM).[28]

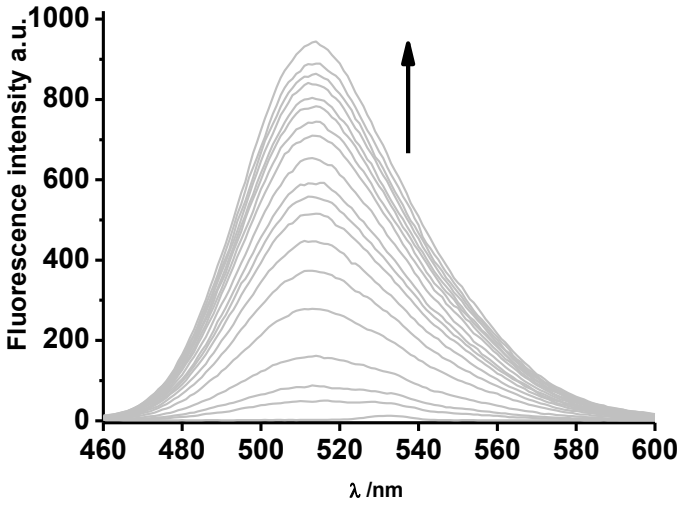

Figure 2. *Emission spectra of probe **1** (5.0 x 10^{-5} M) in HEPES (7 mM, pH 7.4)-DMSO 99:1 v/v (excitation at 450 nm) upon the addition of increasing quantities of HS^- anion (from 0 to 10 equivalents) and after 50 minutes of the addition.*

The selectivity toward HS^- was ascribed to the HS^--induced hydrolysis of the 2,4-dinitrophenyl ether moiety, which yielded the highly fluorescent 8-hydroxyquinoline group.[29] This sensing mechanism was confirmed by isolating the reaction product between **1** and the HS^- anion, which was unequivocally characterized as 8-hydroxyquinoline.

The selective emission enhancement of **1** in the presence of HS^- and the poor response observed upon the addition of bio-thiols (GSH, Cys and Hcy) strongly

suggest that the probe can be used for HS^- imaging in living cells. Based on these observations, the cytotoxicity of **1** was first evaluated. HeLa cells were treated with **1** at different concentrations over a 24-hour period and cell viability was determined by a WST-1 assay. The obtained results are shown in Figure 3. As seen, probe **1** is essentially non toxic in the range of concentrations tested (5-50 μM).

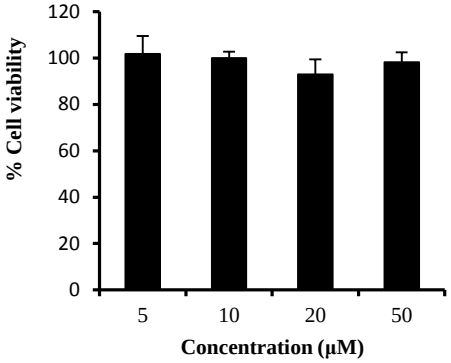

Figure 3. *Cell viability test of different concentrations of probe **1** at 24 h in HeLa cells by a WST-1 assay.*

In a second step, and in order to verify the feasibility of the developed probe to detect HS^- in highly competitive environments, we prospectively used **1** for the fluorescence imaging of sulfide in living cells. In a typical experiment, HeLa cells were incubated in DMEM supplemented with 10% fetal bovine serum. To conduct fluorescence microscopy studies, HeLa cells were seeded in 24 mm glass coverslips in 6-well plates and were allowed to settle for 24 h. Cells were treated with **1** in DMSO (1%) at a final concentration of 30 μM. After 20 minutes, the medium was removed and solutions of different concentrations of NaHS in PBS were added (0, 100, 200 and 500 μM) and cells were incubated for another 10-minute period. The results are shown in Figure 4. The control experiment (HeLa cells without probe **1**) and the cells incubated with **1** showed no fluorescence, whereas a marked enhancement in intracellular emission was observed in the HS^--treated cells, clearly indicating the possible use of **1** to detect hydrogen sulfide in complex media.

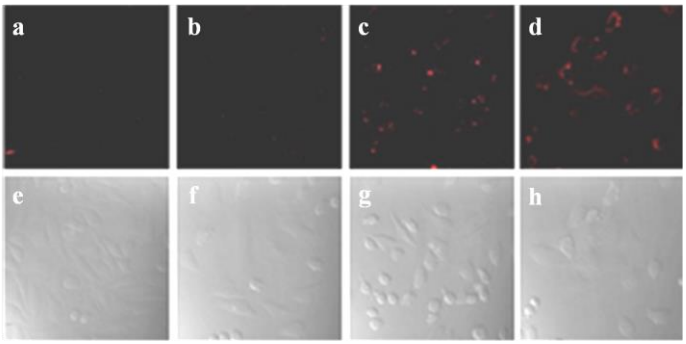

Figure 4. *Detection of HS^- levels in living cells using probe **1**. HeLa cells were incubated with **1** (30 μM) for 30 min at 37 ^oC in DMEM. Transmitted light and fluorescence images were captured for (a) Hela cells, (b) Hela cells incubated with **1**, and Hela cells incubated with **1** in the presence of HS^- at concentrations of (c) 200 μM and (d) 500 μM. The range of excitation was 330-380 nm and emission was monitored for wavelengths exceeding 420 nm.*

In summary, here we report the synthesis and sensing features of new fluorescent probe **1**. Probe **1** is easy to prepare and is able to selectively detect the HS^- anion in HEPES-DMSO 99:1 v/v solutions via remarkable turn-on emission at 514 nm. The observed fluorescence enhancement is ascribed to a selective HS^--induced hydrolysis of a 2,4-dinitrophenyl moiety in **1,** which gives a free 8-hydroxyquinoline fluorophore. The probe can selectively and sensitively detect HS^- anion in water over other anions, biothiols and common oxidants. Moreover, real-time fluorescence imaging measurements have confirmed that probe **1** can be used to detect intracellular HS^- at micromolar concentrations. Similar designs using other available dyes for the straightforward signaling of HS^- in cells are currently being investigated in our laboratory.

Aknowledgements

Financial support from the Spanish Government (Project MAT2012-38429-C04-01) and the Generalitat Valencia (Project PROMETEO/2009/016) is gratefully acknowledged. S.E. is grateful to the Generalitat Valenciana for his Santiago Grisolia fellow. L.E.S.F. also thanks the Carolina Foundation and UPNFM-Honduras for his doctoral grant.

References

1. a) L. Li, P. Rose, P. K. Moore, *Annu. Rev. Pharmacol. Toxicol*., **2011**, *51*, 169; b) C. Szabo, *Nat. Rev. Drug Discover.,* **2007**, *6*, 917; c) K. R. Olson, *Am. J. Physiol. Regul. Integr. Comp. Physiol*., **2011***, 301*, R297; d) M. Lavu, S. Bhushan, D. Lefer, *J. Clin. Sci*., **2011**, *120*, 219; e) M. Whiteman, P. K. Moore, *J. Cell. Mol. Med*., **2009**, *13*, 488.
2. A. K. Mustafa, M. M. Gadalla, N. Sen, S. Kim, W. Mu, S. K. Gazi, R. K. Barrow, G. Yang, R. Wang, S. H. Snyder, *Sci. Signaling.,* **2009**, *2*, ra72.
3. E. Blackstone, M. Morrison, M. B. Roth, *Science.,* **2005**, *308*, 518.
4. J. W. Elrod, J. W. Calvert, J. Morrison, J. E. Doeller, D. W. Kraus, L. Tao, X. Jiao, R. Scalia, L. Kiss, C. Szabo, H. Kimura, C. -W. Chow, D. J. Lefer, *Proc. Natl. Acad*. *Sci. USA.,* **2007**, *104*, 15560.
5. G. Yang, L. Wu, B. Jiang, B. Yang, J. Qi, K. Cao, Q. Meng, A. K. Mustafa, W. Mu, S. Zhang, S. H. Snyder, R. Wang, *Science.,* **2008**, *322*, 587.
6. G. Yang, L. Wu, R. Wang*, FASEB J*., **2006**, *20*, 553.
7. A. Papapetropoulos, A. Pyriochou, Z. Altaany, G.Yang, A. Marazioti, Z. Zhou, M. G. Jeschke, L. K. Branski, D. N. Herndon, R. Wang, C. Szabó , *Proc. Natl. Acad. Sci. USA.,* **2009**, *106*, 21972.
8. K. Abe, H. Kimura, *J. Neurosci*., **1996**, *16*, 1066.
9. L. Li, M. Bhatia, Y. Z. Zhu, Y. C. Zhu, R. D. Ramnath, Z. J. Wang, F. B. Anuar, M. Whiteman, M. Salto-Tellez, P. K. Moore, *FASEB J*., **2005**, *19*, 1196.
10. W. Yang, G. D. Yang, X. M. Jia, L. Y. Wu, R. Wang, *J. Physiol*., **2005**, *569*, 519.
11. K. Eto, T. Asada, K. Arima, T. Makifuchi, H. Kimura, *Biochem. Biophys. Res. Commun.,* **2002**, *293*, 1485.
12. P. Kamoun, M. -C. Belardinelli, A. Chabli, K. Lallouchi, B. Chadefaux-Vekemans, *Am. J. Med. Genet*. *A.,* **2003**, *116*, 310.
13. D. Jimenez, R. Martinez-Mañez, F. Sancenon, J. V. Ros-Lis, A. Benito, J. Soto, *J. Am*. *Chem*. *Soc*., **2003**, *125*, 9000.
14. M. M. F. Choi, *Analyst*., **1998**, *123*, 1631.
15. M. G. Choi, S. Cha, H. Lee, H. L. Jeon, S. K. Chang, *Chem. Commun*., **2009**, 7390.
16. N. S. Lawrence, J. Davis, L. Jiang, T. G. J. Jones, S. N. Davies, R. G. Compton*, Electroanalysis.,* **2000**, *12*, 1453.
17. J. Furne, A. Saeed, M. D. Levitt, *Am. J. Physiol*., **2008**, *295*, R1479.
18. M. Ishigami, K. Hiraki, K. Umemura, Y. Ogasawara, K. Ishii, H. Kimura, *Antioxid. Redox Signaling.,* **2009**, *11*, 205.
19. A. R. Lippert, E. J. New, C. J. Chang, *J. Am. Chem. Soc*., **2011**, *133*, 10078.
20. H. Peng, Y. Cheng, C. Dai, A. L. King, L. B. Predmore, D. J. Lefer, B. Wang, *Angew. Chem*. *Int. Ed*., **2011**, *50*, 9672.
21. F. Yu, P. Li, P. Song, B. Wang, J. Zhao, K. Han, *Chem. Commun*., **2012**, *48*, 2852.

22. a) C. Liu, J. Pan, S. Li, Y. Zhao, L. Y. Wu, C. E. Berkman, A. R. Whorton, M. Xian, *Angew. Chem. Int. Ed*., **2011**, *50*, 10327; b) C. Liu, B. Peng, S. Li, C. -M. Park, A. R. Whorton, M. Xian, *Org. Lett*., **2012**, *14*, 2184.
23. K. Sasakura, K. Hanaoka, N. Shibuya, Y. Mikami, Y. Kimura, T. Komatsu, T. Ueno, T. Terai, H. Kimura, T. Nagano, *J. Am. Chem. Soc*., **2011**, *133*, 18003.
24. M. –Q. Wang, K. Li, J. –T. Hou, M. –Y. Wu, Z. Huang, X. –Q. Yu, *J. Org. Chem.*, **2012**, *77*, 8350.
25. X. Cao, W. Lin, K. Zheng, L. He, *Chem. Commun.,* **2012**, *48*, 10529.
26. T. Liu, Z. Xu, D. R. Spring, J. Cui, *Org. Lett.,* **2013**, *15*, 2310.
27. a) L. E. Santos-Figueroa, M. E. Moragues, E. Climent, A. Agostini, R. Martínez-Máñez, F. Sancenón, *Chem. Soc. Rev.,* **2013**, *42*, 3489; b) M. E. Moragues, R. Martínez-Máñez, F. Sancenón, *Chem. Soc. Rev.,* **2011**, *40*, 2953; c) R. Martínez-Máñez, F. Sancenón, *Chem. Rev.,* **2003**, *103*, 4419; d) A. Agostini, M. Milani, R. Martínez-Máñez, M. Licchelli, J. Soto, F. Sancenón, *Chem. As. J.,* **2012**, *7*, 2040; e) E. Climent, P. Calero, M. D. Marcos, R. Martínez-Máñez, F. Sancenón, J. Soto, *Chem. Eur. J.,* **2009***, 15*, 1816.
28. a) C. Szabó, *Nat. Rev. Drug Discov.,* **2007**, *6*, 917; b) M. Hoffman, A. Rajapakse, X. Shen, K. S. Gates, *Chem. Res. Toxicol.,* **2012**, *25*, 1609.
29. a) S. Shaltiel, *Biochem. Biophys. Res. Commun.,* **1967**, *29*, 178; b) R. Philosof-Oppenheimer, I. Pechtz, M. Fridkin, *Int. J. Pept. Protein Res.,* **1995**, *45*, 116.

SUPPORTING INFORMATION

A new fluorescent “turn-on” chemodosimeter for the detection of hydrogen sulfide in water and in living cells

Sameh El Sayed, Cristina de la Torre, Luis E. Santos-Figueroa, Enrique Pérez-Payá, Ramón Martínez-Máñez, Félix Sancenón, Ana M. Costero, Margarita Parra and Salvador Gil

Reagents:

The chemicals 8-hydroxyquinoline and 1-fluoro-2,4-dinitrobenzene were purchased from Sigma-Aldrich. Triethylamine (98%) was purchased from J.T.Baker. Analytical-grade solvents, sodium hydroxide and hydrochloric acid (37%) were purchased from Scharlau (Barcelona, Spain). For cell culture experiments, DMEM with L-glutamine, piruvate and Fetal Bovine Serum (FBS) trypan blue solution (0.4%) cell culture grade and trypsin were purchased from Roche Applied Science. DMSO for cell culture and PBS were purchased from Sigma-Aldrich. The cell proliferation reagent WST-1 was purchased from Roche Applied Science.

Methods:

UV-visible spectra were recorded with a Jasco V-650 Spectrophotometer. Fluorescence measurements were carried out in a Jasco FP-8500

Spectrophotometer. ^{1}H and ^{13}C-NMR spectra were acquired in a Bruker Advance III (400 MHZ). Mass spectra were obtained from a Tripletof T5600 (ABSciex, USA) spectrometer. Cell viability measurements were carried out with a Wallac 1420 Workstation.

Synthesis of 8-(2,4-dinitrohydroxy)quinoline (1):

8-Hydroxyquinoline (0.725 g, 5 mmol) and triethylamine (0.5 ml, 3.6 mmol) were dissolved in acetone (5 mL). To this solution at room temperature, 1-fluoro-2,4-dinitrobenzene (0.930 g, 5 mmol) dissolved in acetone (5 mL) was added. The reaction mixture was refluxed for 30 minutes. After evaporation of acetone, 5% HCl (10 mL) was added and the precipitate was filtered, washed with water then suspended in 5% NaOH (15 mL) and stirred for 15 minutes. The solid was filtered and washed with water and finally purified by silica gel chromatography using hexane-acetone 1:1 v/v as eluent. The final product was isolated as a yellow solid (1.3 g, 4.4 mmol, 85% yield).

^{1}H NMR (400 MHz, $CDCl_3$) δ: 8.93 (d, *J* = 2.8 Hz, 1H), 8.79 (dd, *J* = 4.2, 1.7 Hz, 1H), 8.25 (dd, *J* = 8.4, 1.7 Hz, 1H), 8.18 (dd, *J* = 9.3, 2.8 Hz, 1H), 7.83 (dd, *J* = 7.9, 1.7 Hz, 1H), 7.65 – 7.56 (m, 2H), 7.47 (dd, *J* = 8.4, 4.2 Hz, 1H), 6.79 (d, *J* = 9.3 Hz, 1H). ^{13}C NMR (101 MHz, $CDCl_3$) δ: 157.45 (s), 151.00 (s), 149.39 (s), 141.36 (s), 140.56 (s), 138.88 (s), 136.37 (s), 130.31 (s), 128.66 (s), 126.81 (d, *J* = 3.1 Hz), 122.40 (d, *J* = 11.1 Hz), 120.94 (s).

HRMS-EI *m/z*: calcd for $C_{15}H_9N_3O_5$ 311.0542; found: 312.0615 ($M+H^+$).

Characterization of chemodosimeter 1:

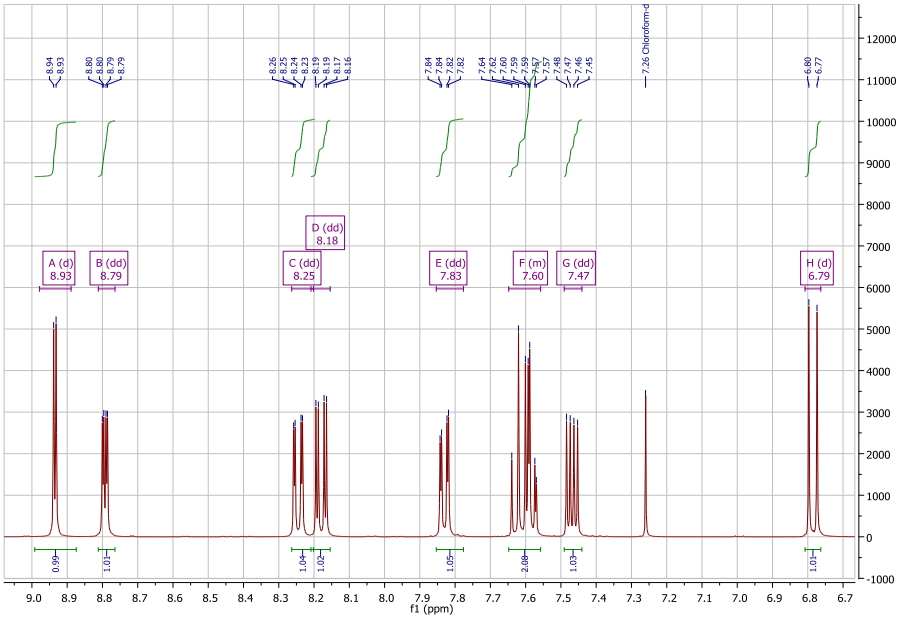

Figure SI-1. *^{1}H-NMR spectrum of probe **1** in $CDCl_3$.*

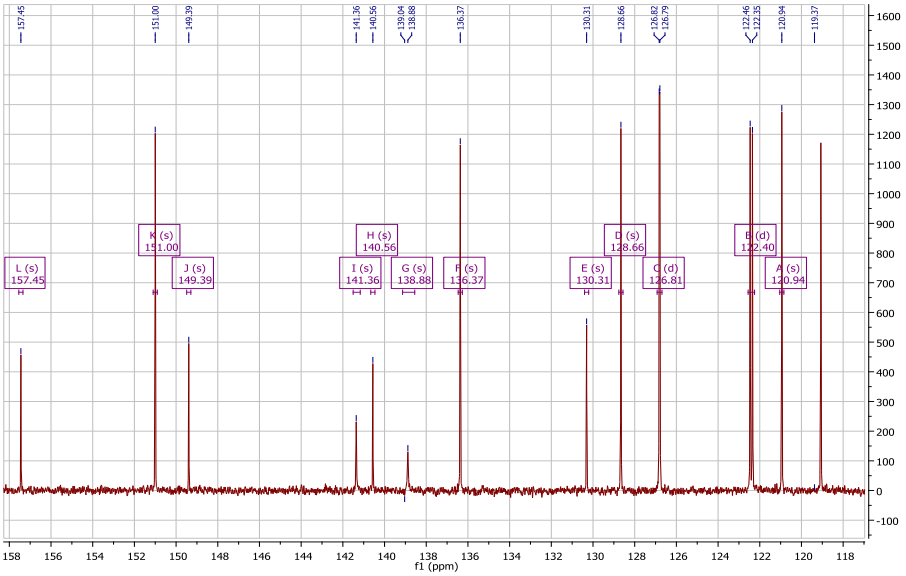

Figure SI-2. *^{13}C-NMR spectrum of probe **1** in $CDCl_3$.*

Fluorescence measurements of 1 in the presence of HS^-:

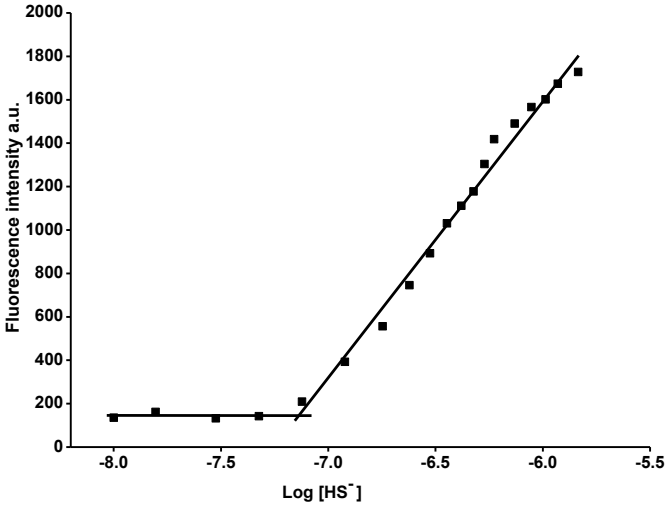

Figure SI-3. *Emission intensity at 514 nm (excitation at 450 nm) of HEPES (7 mM, pH 7.4)-DMSO 99:1 v/v solutions of probe **1** (5.0 μM) upon addition of increasing quantities of HS^- anion after 50 min of the reaction.*

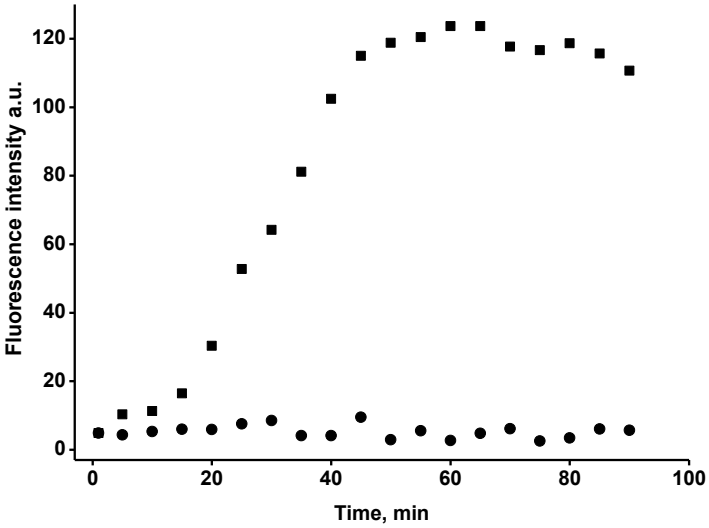

Figure SI-4. *Time-dependent emission intensity at 514 nm (upon excitation at 450 nm) of HEPES (7 mM, pH 7.4)-DMSO 99:1 v/v solutions of chemodosimeter **1** (5.0 μM) in absence (●) and in the presence of 10 equivalents of HS^- anion (■).*

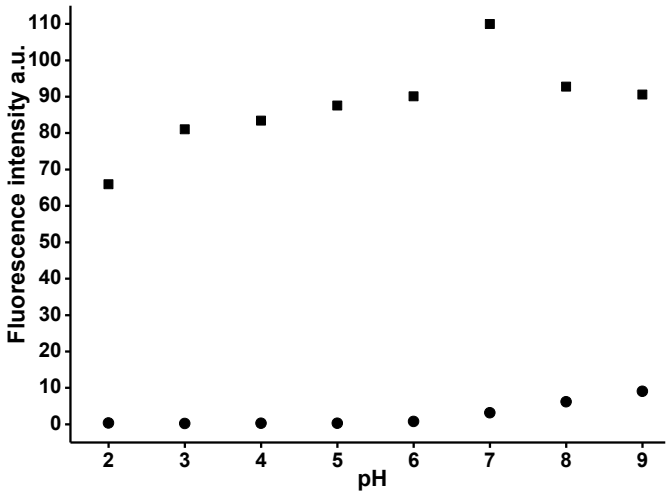

Figure SI-5. *Fluorescence intensity at 514 nm (upon excitation at 450 nm) of H_2O: DMSO (99:1 v/v) solutions of chemodosimeter **1** (5.0 μM) at different pH values in absence (●) and in the presence of 10 equivalents of HS^- anion (■).*

Hydrolysis of probe 1 with HS^- anion:

Probe **1** (50 mg, 0.16 mmol) was dissolved in ethanol (5 mL) and then an excess of Na_2S (200 mg, 0.83 mmol) was added. The reaction was stirred at room temperature for 3 h. After that, ethanol was eliminated in a rotary evaporator and the crude obtained was purified by silica column chromatography with hexane-acetone 1:1 v/v as eluent. The ^1H and ^{13}C of the final product (21.8 mg, 0.15 mmol, 94% yield) was coincident with that of 8-hydroxyquinoline.

Cell culture conditions:

HeLa human cervix adenocarcinoma cells were purchased from the German Resource Centre for Biological Materials (DSMZ) and were grown in DMEM supplemented with 10% FBS. Cells were maintained at 37 °C in an atmosphere of 5% carbon dioxide and 95% air and underwent passage twice a week.

WST-1 cell viability assay

HeLa cells were seeded in a 96-well plate at a density of 2.5 x 10^3 cells/well in 100 µL of DMEM and were incubated 24 hours in a CO_2 incubator at 37 °C. Then, probe **1** or 1,3-dinitrobenzene in DMSO were added to cells in sextuplicate at final concentrations of 5, 10, 20 and 50 µM. After 23 hours, 7 µL of WST-1 were added to each well and then incubated for 1 hour more. Before reading the plate, it was shaked for one minute to ensure homogeneous distribution of colour. Then the absorbance was measured at a wavelength of 450 nm. The results are depicted in figure SI-6.

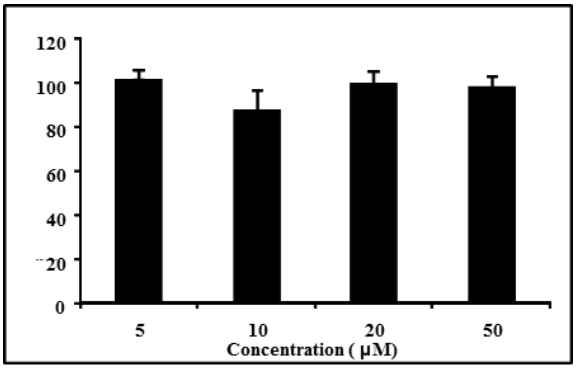

Figure SI-6. *Cell viability studies with **1**. HeLa cells were treated with chemodosimeter **1** at concentrations of 5, 10, 20 and 50 µM for 24 hours. Cell viability was quantified by means of WST-1 assay. Three independent experiments were performed and data are reported as (mean ± SE).*

Live Confocal Microscopy:

HeLa cells were seeded in a 24 mm Ø glass coverslips in six-well plates at a seeding density of 1 x 10^5 cells /well. After 24 hours, cells were treated with chemodosimeter **1** for 30 minutes at a final concentration of 10 µM. Then the medium was changed and the well was washed with PBS. After that, a solution of Na_2S in PBS was added at a final concentration of 0, 200 and 500 µM for 1 hour. Then, coverslips were washed twice to eliminate compounds and, were visualized

under a confocal microscope employing Leica TCS SP2 AOBS (Leica Microsystems Heidelberg GmbH, Mannheim, Germany) inverted laser scanning confocal microscope using oil objectives: 63X Plan-Apochromat-Lambda Blue 1.4 N.A. Confocal microscopy studies were performed by Confocal Microscopy Service. The images were acquired with an excitation wavelength of 450 nm (argon laser) and a emission wavelength of 470-570 nm. Two-dimensional pseudo colour images (255 colour levels) were gathered with a size of 1024 x 1024 pixels and Airy 1 pinhole diameter. All confocal images were acquired using the same settings and the distribution of fluorescence was analyzed using the Image J Software. Three independent experiments were performed obtaining similar results.

2,4-dinitrophenyl ether-containing chemodosimeters for the selective and sensitive "in vitro" and "in vivo" detection of hydrogen sulfide

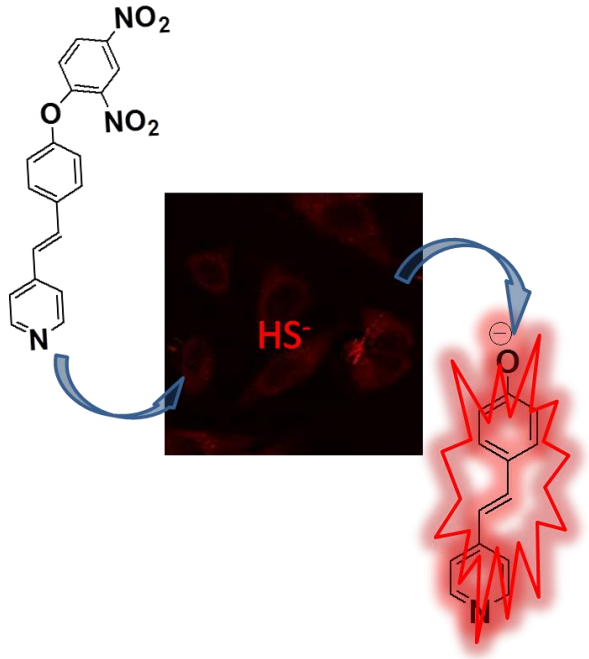

2,4-dinitrophenyl ether-containing chemodosimeters for the selective and sensitive "in vitro" and "in vivo" detection of hydrogen sulfide

Sameh El Sayed,[a,b,c] Cristina de la Torre,[a,b,c] Luis E. Santos-Figueroa,[a,b,c] Ramón Martínez-Máñez,[a,b,c] Félix Sancenón,[a,b,c] Mar Orzáez,[d] Ana M. Costero,*[a,e] Margarita Parra,[a,e] and Salvador Gil[a,e]*

[a] Centro de Reconocimiento Molecular y Desarrollo Tecnológico (IDM), Unidad Mixta Universitat Politècnica de València – Universitat de València. E-mail: rmaez@qim.upv.es

[b] Departamento de Química, Universitat Politècnica de València, Camino de Vera s/n, 46022, Valencia, Spain.

[c] CIBER de Bioingeniería, Biomateriales y Nanomedicina (CIBER-BBN).

[d] Laboratorio de Péptidos y Proteinas, Centro de Investigación Príncipe Felipe, Autopista El Saler, Valencia, Spain.

[e] Departamento de Química Orgánica, Universitat de València, Dr. Moliner 50, 46100, Burjassot, Valencia, Spain.

Received: *15 August 2014*

First published on the web: *4 January 2014*

Supramol. Chem., ***2014****, 4, 244-254*

(Reproduced with permission of Taylor & Francis Copyright © 2015)

Abstract

*Four probes (i.e. **D1**-**D4**) for the selective and sensitive fluorogenic detection of HS^- have been prepared and characterized. HEPES (10 mM, pH 7.4)-DMSO 99:1 v/v solutions of **D1**-**D4** are essentially non-fluorescent. Changes in the emission using **D1**-**D4** in the presence of anions (F^-, Cl^-, Br^-, I^-, N_3^-, CN^-, SCN^-, AcO^-, CO_3^{2-}, PO_4^{2-}, SO_4^{2-}, HS^- and OH^-), biothiols (GSH, Cys, Hcy, Me-Cys and lipoic acid), reducing agents (SO_3^{2-} and $S_2O_3^{2-}$) and oxidants (H_2O_2) demonstrated that only HS^- is able to induce the appearance of intense emission bands in the 400-520 nm range in the four probes. The selectivity observed was ascribed to a unique hydrogen sulfide-induced hydrolysis of the 2,4-dinitrophenyl ether moiety that yielded the corresponding free highly fluorescent alcohols. The potential detection of intracellular HS^- was also studied.*

Keywords: Hydrogen sulfide • fluorescence • dinitrophenyl ether • in vivo detection • chemodosimeter

Introduction

Hydrogen sulfide (H_2S), a colourless and flammable gas with high solubility in water and in organic solvents, is well-known for its unpleasant “rotten eggs” smell. Hydrogen sulfide has been traditionally studied for its toxicity,[1] its presence as a corrosive industrial refuse and emission in the energy industry,[2] as parameter for geological activity,[3] as quality control of foods and as an important compound related with the presence of microbial activity in anaerobic environments.[4] Moreover, this simple molecule has been recently recognized to play a relevant role in living systems. For instance hydrogen sulfide has been documented to be the third gaseous transmitter (the other two being nitric oxide and carbon monoxide).[5-7] The production of H_2S in mammalian systems has been attributed to at least three endogenous enzymes, *i.e*. cystathionine b-synthase (CBS), cystathionine g-lyase (CSE), and 3-mercaptopyruvate sulfurtransferase (MPST).[8-11] These enzymes use cysteine or cysteine derivatives as substrates and convert

them into hydrogen sulfide in different organs and tissues. In addition to these enzymatic pathways, there are also a range of simple chemical events that may liberate hydrogen sulfide from the intracellular pool of “labile” sulfur such as the so-called “sulfane pool” (compounds containing sulfur atoms bound only to other sulfur atoms).[12] The production of endogenous hydrogen sulfide and exogenous administration of hydrogen sulfide has been demonstrated to exert protective effects in many pathologies. For example, hydrogen sulfide has been shown to relax vascular smooth muscle, induce vasodilation of isolated blood vessels, and reduce blood pressure.[13] Hydrogen sulfide has proved also to inhibit leukocyte adherence in mesenteric microcirculation in vascular inflammation in rats, suggesting that hydrogen sulfide is a potent anti-inflammatory molecule.[14] Additionally, it has become evident that hydrogen sulfide is a potent antioxidant and, under chronic conditions, can up-regulate antioxidant defense.[15]

However hydrogen sulfide exact mechanism of action and production in living systems is still under active investigation. For example it is known that hydrogen sulfide can react readily with methemoglobin to form sulfhemoglobin, which act as the metabolic sink for H_2S. As a potential reductant, hydrogen sulfide is likely to be consumed by endogenous oxidant species such as hydrogen peroxide, superoxide, peroxynitrite, etc. This process is significant and it provides a mechanism by which the concentration of hydrogen sulfide changes. Besides, abnormal levels of hydrogen sulfide have been associated with various diseases such as chronic kidney disease, liver cirrhosis,[16] Alzheimer,[17] and Down syndrome.[18]

Due to the important roles that hydrogen sulfide plays in environmental and in biological processes the development of selective detection systems for this compound has recently become a focus of importance. In particular it was a major challenge to clarify the complex contributions of H_2S in certain diseases by finding methods for selective tracking of this small molecule within living systems. Current techniques for hydrogen sulfide detection, such as colorimetry,[19-21] electrochemical assays,[22] gas chromatography[23] and metal-induced sulfide

precipitation[24] show some shortcomings typically involving destruction of the sample and/or poor selectivity.

In addition to the above mentioned classical methodologies, fluorescence is an attractive highly sensitive technique for studying biomolecule distribution in living cells. For instance very recently, fluorescent probes for monitoring redox cycles in *vivo* have been described.[25] In this area, several fluorescent probes designed taking into account supramolecular chemistry concepts for the selective recognition of H_2S or HS^- have been described.[26] Most of the fluorescent probes reported are based of the hydrogen sulfide-induced reduction of azides or nitro moieties, electronically connected with a fluorophore to amines.[27-36] This reduction induced perturbations in the electronic structure of the signaling unit that is reflected in emission changes. Another important group of probes are constructed under a displacement paradigm and are based on non-fluorescent Cu(II) complexes.[37-46] In these systems the hydrogen sulfide-induced demetallation of the probes induced marked emission enhancements. Other sulfide-selective fluorescent probes used Michael type addition reactions coupled with emission changes.[47-50] Also, cyclization processes that yielded fluorescent compounds have recently been used for the design of fluorescent probes for sulfide anion.[51-53] In other examples, hydrolysis reactions coupled with emission changes have been also used for the preparation of other hydrogen sulfide sensitive probes.[54-56] Finally, selenium containing BODIPY dyes have also been used for the reversible detection of sulfide in solution and in living cells.[57,58] Among probes that used hydrolysis reactions, as far as we know only three probes containing 2,4-dinitrophenyl ethers have been described and used for the selective and sensitive recognition of HS^- anion. In particular, Lin and co-workers prepared a NIR dye functionalized with a 2,4-dinitrophenyl ether moiety.[59] PBS (pH 7.0)-ethanol 9:1 v/v solutions containing CTABr and this probe were non-fluorescent whereas addition of increasing quantities of HS^- anion induced a progressive appearance of an emission band. This emission enhancement was ascribed to a thiolysis of the 2,4-dinitrophenyl ether moiety. The same sensing mechanism was used by Spring and co-workers that prepared a 1,8-naphthalimide fluorophore equipped with a 2,4-dinitrophenyl ether group.[60] Finally, Liu and Feng prepared an ESIPT (excited

state intramolecular proton transfer) probe functionalized with a 2,4-dinitrophenyl ether moiety for the rapid chromo-fluorogenic recognition of hydrogen sulfide.[61] The above described facts demonstrate that the design of new fluorogenic probes for hydrogen sulfide is a timely field of interest. Such simple systems may be used to control H_2S concentrations in target industrial processes, for in *situ* environmental, geological monitoring and detection of hydrogen sulfide levels in living systems. Nevertheless, in spite of these possible applications, there are still relatively few examples of optical probes for the selective and sensitive detection of hydrogen sulfide (*vide ante*).

Bearing in mind the above mentioned concepts and following our interest in the development of new approaches for optical sensing,[62] we show herein a family of chemodosimeters (**D1**-**D4**) composed by selected fluorophores functionalized with 2,4-dinitrophenyl ether moieties for the detection of hydrogen sulfide. The synthesis and sensing features of probe **D3** were recently published by us in a short communication.[63] These dosimeters were easily synthesized through nucleophilic aromatic substitution reactions with 1-fluro-2,4-dintrobenzene with different fluorophores. The four probes displayed sensing features in buffered aqueous solution containing 1% of DMSO and gave marked emission enhancements only in the presence of HS^- anion, whereas other bio-thiols were unable to induce emission changes. The probes showed excellent sensitivities with limits of the detection in the 0.05-0.30 μM range, and some of the chemosensors were used for the fluorescence detection of both exogenous and endogenous HS^- in living cells.

Results and discussion

Synthesis and characterizations of the probes:

The path of synthesis and the structures of probes **D1**-**D4** are shown in Scheme 1. **D1**-**D4** are 2,4-dinitrophenyl ether derivatives which are easily obtained in good yield (65 to 88%) through an aromatic nucleophilic substitution reaction between

1-fluoro-2,4-dinitrobenzene (**1**) and alcohols **1c**, **2a**, **3a** and **4b**. Compounds **2a** and **3a** are commercially available. Alcohol **1c** was prepared through the base-catalysed condensation between 4-hydroxybenzaldehyde (**1a**) and 4-picoline (**1b**), whereas alcohol **4b** was obtained through methylation of fluorescein (**4a**) with methyliodide.

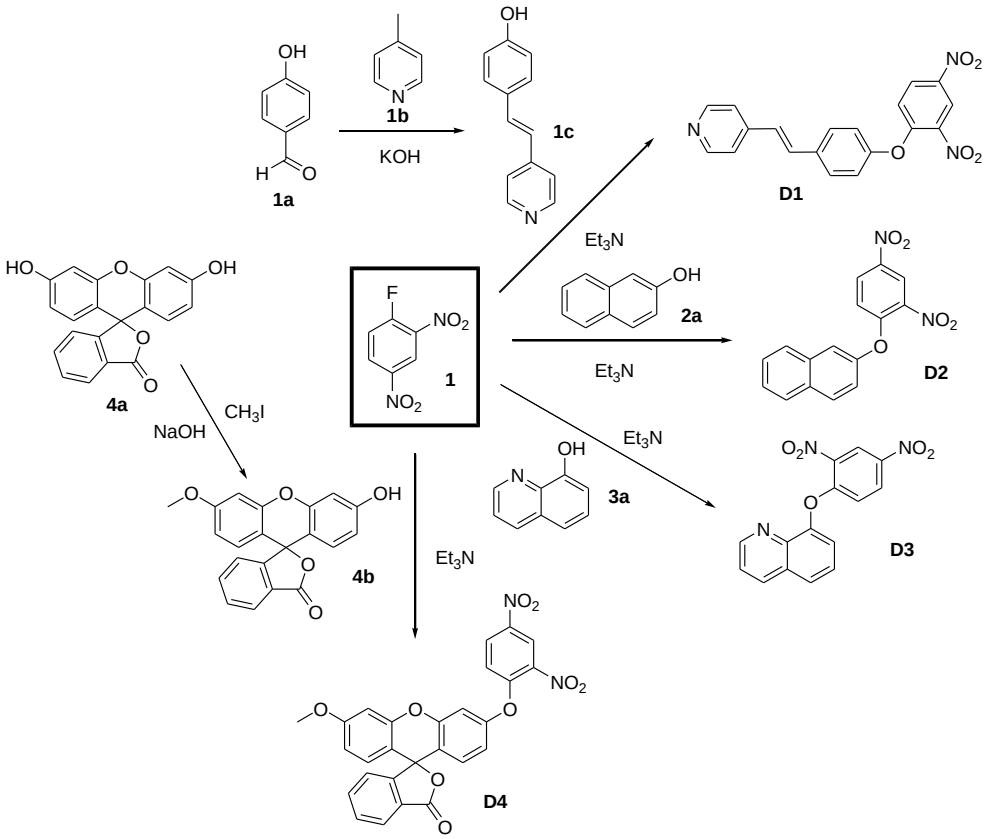

Scheme 1. *Synthesis and chemical structure of chemodosimeters **D1**-**D4**.*

All new probes were characterized by ^{1}H, ^{13}C-NMR and HRMS. At this respect, the more indicative signals in the ^{1}H-MNR spectra of dosimeter **D1** in DMSO-D_6 were the doublets centred at 7.81 and 7.32 ppm attributed to the protons of the *trans* double bond. Moreover the protons of the 2,4-dinitrophenyl ether moiety appeared at 8.91 (1H, d), 8.47 (1H, dd) and 7.57 (1H, d) ppm. On changing to chemodosimeter **D2**, the most characteristic signals in the ^{1}H-NMR ($CDCl_3$) spectrum were also those of the 2,4-dinitrophenyl ether moiety centred at 8.97,

8.41 and 7.39 ppm. Nearly the same pattern was observed for **D3** in which the dinitrophenyl ether protons were located at 8.93 (1H, d), 8.18 (1H, dd) and 7.83 (1H, d) ppm. Dealing with fluorescein derivative **D4**, the signals ascribed to the dinitrophenyl ether appeared at nearly the same chemical shift than those observed for **D1**-**D3**, whereas the methoxy moiety appeared as singlet at 3.76 ppm (in DMSO-D_6).

Sensing features of the probes:

The four synthesized probes contain a chromo-fluorogenic subunit functionalized with a sulfide-sensitive 2,4-dinitrophenyl ether moiety. It is well known that the dinitrophenyl group has been often used for tyrosine protection in peptide synthesis.[64] The removal of this protective group is carried out using thiols under basic conditions. In our prepared probes the dinitrophenyl ether was electronically coupled with the fluorophore and the rupture of the ether bond was expected to induce changes in the emission spectra of the fluorogenic subunit. This simple sensing mechanism was used very recently in the preparation of selective and sensitive chemodosimeters for HS^- anion in water and in cellular media (*vide ante*).[59-61] The high selectivity obtained for HS^- versus thiols (*vide infra*) relies on the fact that H_2S is a small molecule with a pK_a of 6.9, while typical cellular free thiols (*i.e*. GSH and Cys) have pK_a values of *ca*. 8.5.[65] Taking into account these differences at physiological pH, the thiolysis of 2,4-dinitrophenyl ethers is chemoselective for HS^- over GSH, Cys and other biologically-relevant thiols.

In a first step we tested the fluorescent response of the probes **D1**-**D4** (5 μM) in HEPES (10 mM, pH 7.4)-DMSO 99:1 v/v solution upon addition of an excess (10 equivalents) of selected anions (F^-, Cl^-, Br^-, I^-, N_3^-, CN^-, SCN^-, AcO^-, CO_3^{2-}, PO_4^{2-}, SO_4^{2-}, HS^- and OH^-), biothiols (GSH, Cys, Hcy, Me-Cys and lipoic acid), reducing agents (SO_3^{2-} and $S_2O_3^{2-}$) and oxidants (H_2O_2). As it can be seen in Figure 1 the four dosimeters were practically non-fluorescent, however addition of HS^- induced a very remarkable fluorescent "*turn-on*" response, whereas addition of the other

chemicals tested induced negligible changes in the emission behaviour. Besides, the fluorescent behavior of the four probes in the presence of GSH 6 mM (GSH concentrations in cells are in the 1-10 mM range) was also tested. As could be seen in Figure 2 GSH was unable to induce a remarkable fluorescent enhancement of the four probes even at mM concentrations.

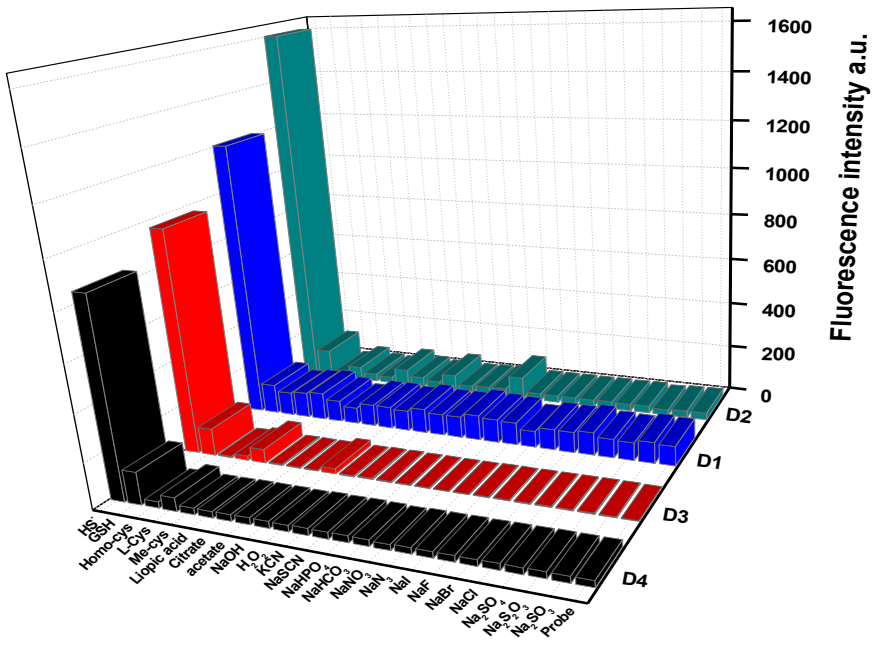

Figure 1. *Emission intensity of **D1** (at 515 nm upon excitation at 390 nm), **D2** (at 415 nm upon excitation at 350 nm), **D3** (at 516 nm upon excitation at 450 nm) and **D4** (at 515 nm upon excitation at 450 nm) dosimeters (5 μM) in HEPES (10 mM, pH 7.4)-DMSO 99:1 v/v solutions upon addition of 10 equivalents of anions, bio-thiols, reducing agents and oxidants (after 60, 70, 50 and 30 minutes of the addition for **D1**, **D2**, **D3** and **D4** respectively). The temperature was set at 25 °C.*

More in detail, addition of 10 equivalents of HS^- anion to HEPES (10 mM, pH 7.4)-DMSO 99:1 v/v solution of dosimeter **D1** induced the appearance of an emission band at 515 nm (λ_{ex} = 390 nm) that reached its maximum intensity after 60 minutes (15-fold enhancement) (see Figure 3). For **D2**, addition of HS^- induced a 46-fold enhancement of the emission intensity at 415 nm (λ_{ex} = 350 nm) after 70 minutes (Figure 4).

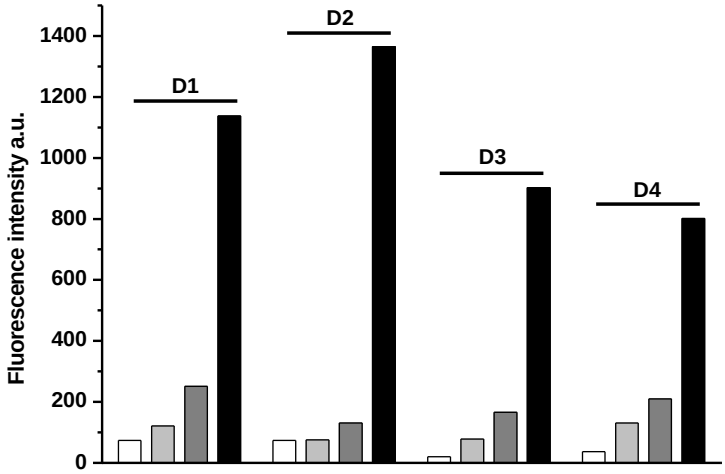

Figure 2. *Emission intensity of **D1** (at 515 nm upon excitation at 390 nm), **D2** (at 415 nm upon excitation at 350 nm), **D3** (at 516 nm upon excitation at 450 nm) and **D4** (at 515 nm upon excitation at 450 nm) dosimeters (5 µM) in HEPES (10 mM, pH 7.4)-DMSO 99:1 v/v solutions alone (white bars) and upon addition of 50 µM GSH (light grey bars), 6 mM GSH (dark grey bars) and 50 mM HS^- (black bars). The temperature was set at 25 °C.*

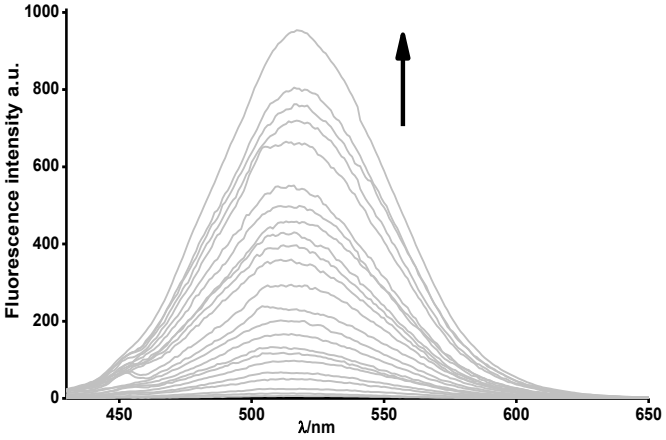

Figure 3. *Fluorescene enhancement of dosimeter **D1** (5 µM) in HEPES (10 mM, pH 7.4)-DMSO 99:1 v/v solution upon addition of increasing quantities of HS^- anion (from 0 to 10 equivalents) after 60 minutes of the addition (λ_{ex} = 390 nm). The temperature was set at 25 °C.*

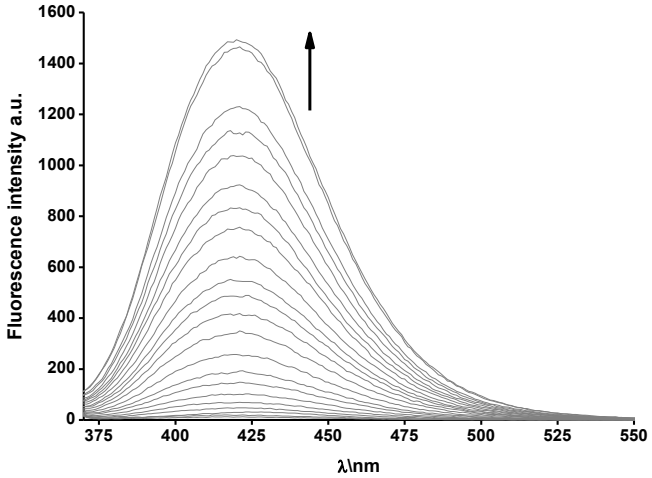

Figure 4. *Fluorescene enhancement of dosimeter **D2** (5 μM) in HEPES (10 mM, pH 7.4)-DMSO 99:1 v/v solution upon addition of increasing quantities of HS^- anion (from 0 to 10 equivalents) after 70 minutes of the addition (λ_{ex} = 350 nm). The temperature was set at 25 °C.*

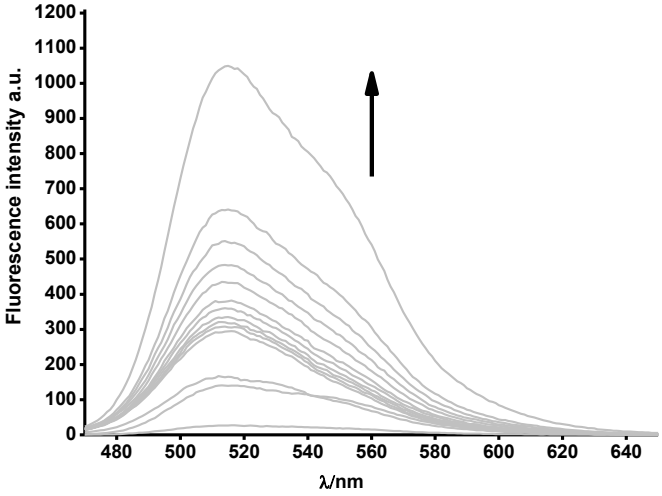

Figure 5. *Fluorescene enhancement of dosimeter **D4** (5 μM) in HEPES (10 mM, pH 7.4)-DMSO 99:1 v/v solution upon addition of increasing quantities of HS^- anion (from 0 to 10 equivalents) after 30 minutes of the addition (λ_{ex} = 450 nm). The temperature was set at 25 °C.*

Nearly the same enhancement (32-fold) in the intensity at 515 nm (λ_{ex} = 450 nm) was obtained upon addition of HS^- anion to probe **D4** (Figure 5). In this case the response was faster (when compared with **D1** and **D2**) as the maximum

enhancement was observed after 30 minutes upon HS^- addition. Besides, dosimeter **D3** gives the larger response, in this case the addition of HS^- anion induced a remarkable 344-fold enhancement in the emission band at 516 nm (λ_{ex} = 450 nm) after 50 minutes (see Figure 6). The subtle differences in response time and in emission enhancement upon addition of HS^- anion to the four dosimeters could be ascribed to the different electronic properties of the probes although in all cases a clear highly selective *turn-on* response was observed.

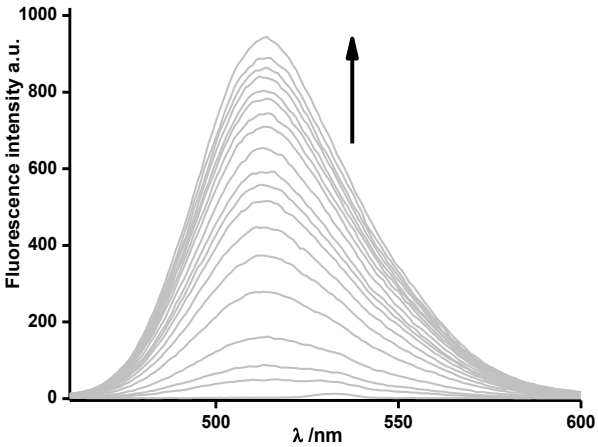

Figure 6. *Fluorescene enhancement of dosimeter **D3** (5 μM) in HEPES (10 mM, pH 7.4)-DMSO 99:1 v/v solution upon addition of increasing quantities of HS^- anion (from 0 to 10 equivalents) after 50 minutes of the addition (λ_{ex} = 450 nm). The temperature was set at 25 ºC.*

After assessing the highly selective turn-on response of **D1**-**D4** to hydrogen sulfide, the sensitivity of the probes was studied from titration profiles with HS^- obtained in HEPES-DMSO 99:1 v/v solutions. From these studies a limit of detection (LOD) of 0.20 μM for HS^- was determined for **D1**. Nearly the same response and sensitivity was obtained with probe **D2** (LOD = 0.29 μM). A more sensitive response was found on changing to dosimeters **D3** and **D4**. In these cases the titration profiles obtained allowed to calculate LOD of 0.06 and 0.05 μM for **D3** and **D4**, respectively. In all cases the probes displayed LODs below the hydrogen sulfide concentration required to elicit physiological responses (10-1000 μM).[66]

The selective emission enhancements observed for **D1**-**D4** in the presence of

HS^- is ascribed in all cases to an HS^--induced hydrolysis of the 2,4-dintrophenyl ether groups that results in the release of the highly fluorescent alcohols **1c**, **2a**, **3a** and **4b**. In order to corroborate this hypothesis probes **D1**-**D4** were dissolved in ethanol and an excess of Na_2S was added. The reactions were stirred at room temperature for 3 h and then the solvent was eliminated in a rotary evaporator. The crudes obtained were purified by silica column chromatography and ^1H and ^{13}C confirmed the presence of the alcohols **1c**, **2a**, **3a** and **4b** (for **D1**, **D2**, **D3** and **D4** respectively) as main products of the reaction.

Table 1. *Mechanism used in the development of fluorogenic probes for hydrogen sulfide.*

Mechanism	Time	Limit of detection	References
hydrolysis of 2,4-dinitrophenylether (**D1**-**D4**)	30-70 minutes	0.05-0.29 μM	this paper
hydrolysis of 2,4-dinitrophenylether	5-20 minutes	0.05-0.48 μM	59-61
demetallation of Cu(II) complexes	Few seconds-5 minutes	0.01-16 μM	37-46
Michael addition reactions	2-60 minutes	0.12-1 μM	47-50
other hydrolysis reactions	30-60 minutes	0.05-9 μM	54-56
reduction reactions	3-120 minutes	0.01-5 μM	27-36
oxidation of Se-containing fluorophores	5 minutes	not reported	57,58
cyclization reactions	2-50 minutes	0.1-100 μM	51-53

The sensing features of **D1**-**D4** probes were quite similar to those reported for analogous fluorophores functionalized with 2,4-dinitrophenylethers (see Table 1). In particular, reaction times when using hydrolysis of 2,4-dinitrophenylether as sensing mechanism are in the range of minutes whereas the detection limits are in the 0.05-0.29 μM interval. Table 1 also shows the typical sensing parameters for probes for hydrogen sulfide when using different sensing mechanisms. From the data in the table it is apparent that the best response, in terms of reaction time, are obtained with probes in which the sensing mechanism is related with demetallation of Cu(II) complexes (from few seconds to minutes). As seen also in Table 1, lower limits of detection for hydrogen sulfide are obtained when

demetallation processes and reduction reactions are used as transduction mechanisms.

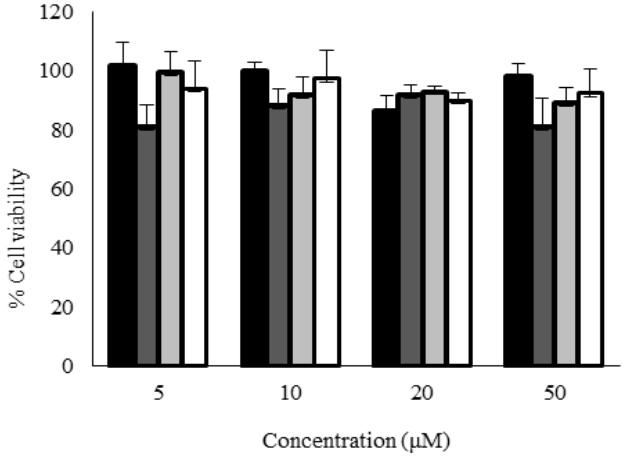

Figure 7. *Cell viability assays. Hela cells were treated with dosimeters* ***D1*** *(black),* ***D2*** *(dark grey),* ***D3*** *(grey) and* ***D4*** *(white) at concentrations of 5, 10, 20, 50 μM during 24h.*

Cell viability assays:

The selective emission enhancement of **D1**-**D4** in the presence of HS^- and the poor response observed upon the addition of bio-thiols (GSH, Cys and Hcy) strongly suggest that these probes could be used for HS^- imaging in living cells. Based on these observations, the cytotoxicity of **D1**-**D4** was first evaluated. For this purpose HeLa cells were treated with probes **D1**-**D4** at different concentrations (5, 10, 20 and 50 μM) over a 24-hour period and cell viability was determined by using a WST-1 assay. The obtained results are shown in Figure 7. As seen, the four dosimeters were essentially non-toxic in the range of concentrations tested.

Detection of HS^- in HeLa cells:

Once assessed the biocompatibility of the prepared probes and with the aim to test the dosimeters in highly competitive environments, we prospectively used probes **D1**-**D4** for the fluorescence imaging of sulfide in living cells. Of the four probes tested, only **D1** and **D3** gave remarkable results due to the low solubility of

D2 and **D4** at the concentrations required in the confocal microscopy studies.

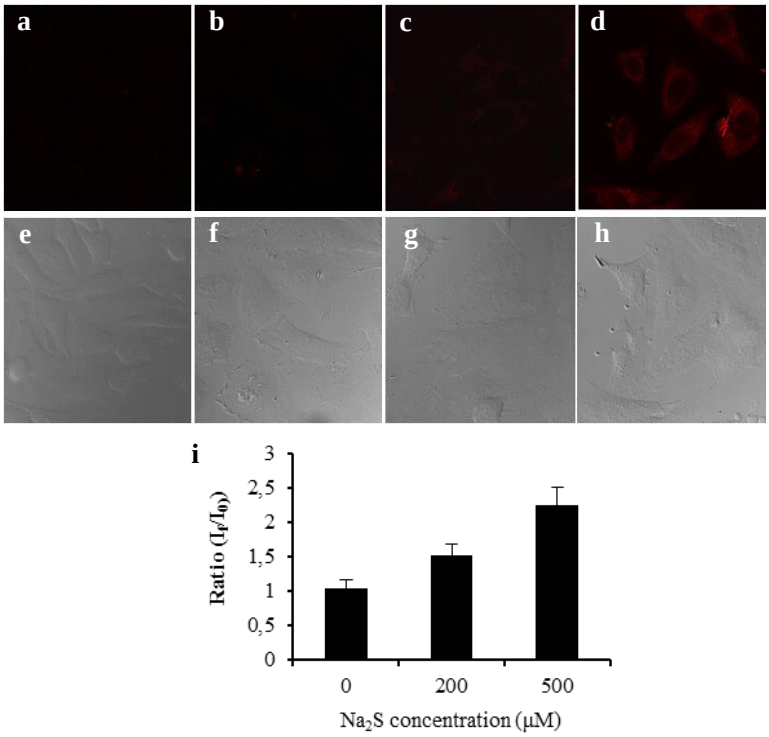

Figure 8. *Detection of HS^- levels in living cells using dosimeter **D1**. (a, e) Transmitted light and fluorescence images of untreated HeLa cells. (b, f) Hela cells incubated with **D1** for 90 minutes. (c, g) HeLa cells incubated with **D1** for 30 minutes at 37 °C and then with 200 μM Na_2S for 60 minutes. (d, h) Hela cells incubated during 30 min with **D1** and 500 μM Na_2S for other 60 minutes. (i) Average I_f/I_0 intensity ratios after addition of 200 and 500 μM of Na_2S in PBS buffer. The excitation and emission wavelength were 450-470 nm and 510-530 nm. Representative fluorescence images from replicate experiments (n = 3) are shown. Error bars are (SD).*

In a typical experiment, HeLa cells were incubated in DMEM supplemented with 10% fetal bovine serum. To conduct fluorescence microscopy studies, HeLa cells were seeded in 24 mm glass coverslips in 6-well plates and were allowed to settle for 24 h. Cells were treated with the probes in PBS-DMSO 99:1 v/v at final concentrations of 10 and 30 μM, for **D1** and **D3** respectively. After 30 minutes, the medium was removed and solutions of different concentrations of NaHS in PBS were added (0, 100, 200 and 500 μM) and cells were incubated for another 10-minute period.

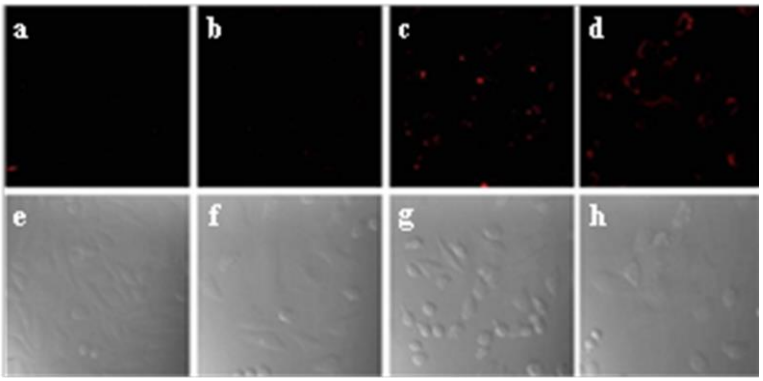

Figure 9. *Detection of HS^- levels in living cells using probe **D3**. HeLa cells were incubated with **D3** (30 μM) for 30 min at 37°C in DMEM. Transmitted light and fluorescence images were captured for (a) Hela cells, (b) Hela cells incubated with **D3**, and Hela cells incubated with **D3** in the presence of HS^- at concentrations of (c) 200 μM and (d) 500 μM. The range of excitation was 330-380 nm and emission was monitored for wavelengths exceeding 420 nm.*

The results are shown in Figures 8 (for **D1**) and 9 (for **D3**). The control experiment (HeLa cells without dosimeters) and the cells incubated with **D1** and **D3** showed no fluorescence, whereas a clear and marked enhancement in intracellular emission was found in the HS^--treated cells. The emission enhancement observed was clearly dependent of the amount of NaHS added. The enhancement in the intracellular fluorescence intensity with **D1** was quantified by a standard image analysis and the results are shown in Figure 8. A similar response (not shown) was observed for **D3**.

Conclusions

In summary, here we reported the synthesis and sensing features of four compounds (**D1**-**D4**) as fluorescent turn-on probes for hydrogen sulfide. These chemodosimeters were based in a different fluorophores (*i.e*. styryl pyridine, naphthalene, quinoline and fluoresceine for **D1**, **D2**, **D3** and **D4**, respectively) functionalized with a 2,4-dinitrophenyl ether moiety. This chemical modification made the final probes poorly emissive. Probes **D1**-**D4** were easy to prepare and were able to selectively detect the HS^- anion in HEPES (10 mM, pH 7.4)-DMSO 99:1 v/v solutions via a remarkable *turn-on* emission. The emission enhancements

observed were due to a selective sulfide-induced hydrolysis of the 2,4-dinitrophenyl ether moiety that released the free fluorophores. **D1**-**D4** can selectively and sensitively detect HS^- anion in water over other anions, biothiols and common oxidants. The titration profiles obtained upon addition of increasing quantities of HS^- anion to aqueous solutions of the four dosimeters allowed us to determine LODs of 0.20, 0.29, 0.06 and 0.05 μM for **D1**, **D2**, **D3** and **D4** respectively. Besides the four dosimeters showed remarkably low sensitivities below the hydrogen sulfide concentration required to elicit physiological responses. From cell viability assays it was found that the four probes were essentially non-toxic. Moreover, real-time fluorescence imaging measurements confirmed that probes **D1** and **D3** can be used to detect intracellular HS^- at micromolar concentrations.

Experimental section

Materials and methods:

UV-visible spectra were recorded with a JASCO V-650 Spectrophotometer. Fluorescence measurements were carried out in a JASCO FP-8500 Spectrophotometer. ^{1}H and ^{13}C-NMR spectra were acquired in a BRUKER ADVANCE III (400 MHZ), where mass spectra were carried out in a TRIPLETOF T5600 (ABSciex, USA) spectrometer. The chemicals 4-picoline, 2-hydroxynaphthalene, 8-hydroxyquinoline, fluorescein, iodomethane, 1-fluoro-2,4-dinitrobenzene, 4-hydroxybenzaldehyde (98%), acetic anhydride (98%) and sodium bicarbonate were purchased from Sigma-Aldrich. Triethylamine (98%) was purchased from J. T. Baker. Analytical-grade solvents, potassium hydroxide, sodium sulfate and hydrochloric acid (37%) were purchased from Scharlau (Barcelona, Spain).

Synthesis of 4-((E)-2-(pyridin-4-yl)vinyl)phenol (1c):

4-hydroxybenzaldehyde (**1a**, 500 mg, 4.1 mmol) and 4-picoline (**1b**, 0.4 mL, 4.1 mmol) were refluxed in acetic anhydride (5 mL) for 24 h. After cooling to room

temperature a precipitate appeared. This was collected and recrystallized from ethanol. Then, the solid was dissolved in ethanol-water (20 mL, 1:1 v/v) containing potassium hydroxide (400 mg, 7.1 mmol) and refluxed for 6 h. Afterwards the crude reaction was neutralized with diluted hydrochloric acid. The product **1c** precipitated and was isolated as a yellow solid after filtration (749 mg, 3.8 mmol, 85% yield).

^{1}H NMR (400 MHz, DMSO) δ 12.10 (s, 1H), 10.79 (d, J = 5.6 Hz, 2H), 9.75 (dd, J = 21.4, 11.6 Hz, 5H), 9.29 (d, J = 16.4 Hz, 1H), 9.10 (d, J = 8.5 Hz, 2H).

Synthesis of 4-(4-(2,4-dinitrophenoxy)styryl)pyridine (D1):

1c (200 mg, 1.17 mmol) was dissolved in acetone (5 mL) and then triethyl amine (0.5 ml, 3.6 mmol) was added. After that, 1-fluoro-2,4-dinitrobenzene (217.7 mg, 1.17 mmol) dissolved in acetone (5 mL) was added to the crude reaction and the mixture refluxed for 30 min. Then, acetone was evaporates and the residue taken up in 5% hydrochloric acid (10 mL). A precipitate appeared that was filtered, washed with water and then suspended in 5% sodium hydroxide (15 mL) and stirred for 15 min. After that, the solid was filtered, washed with water and purified by silica column chromatography using hexane-acetone 1:1 v/v as eluent. Dosimeter **D1** was isolated as yellow solid (310 mg, 0.85 mmol, 74% yield).

^{1}H NMR (400 MHz, DMSO) δ 8.91 (d, J = 2.8 Hz, 1H), 8.56 (d, J = 6.0 Hz, 2H), 8.47 (dd, J = 9.3, 2.8 Hz, 1H), 7.81 (d, J = 8.7 Hz, 2H), 7.57 (dd, J = 4.9, 3.4 Hz, 3H), 7.34 – 7.25 (m, 4H).

^{13}C NMR (101 MHz, $CDCl_3$) δ 154.7, 153.9, 150.1, 144.2, 141.6, 139.6, 134.3, 131.8, 129.7, 129.4, 126.6, 122.0, 121.0, 120.7, 119.7.

HRMS-EI m/z: calcd for $C_{19}H_{13}N_3O_5$ 363.0855; found: 364.0944 ($M+H^+$).

Synthesis of 2-(2,4-dinitrophenoxy)naphthalene (D2):

Dosimeter **D2** was prepared by the same experimental procedure used for **D1**. The final product was isolated as pale yellow solid (725 mg, 2.33 mmol, 88 %

yield).

^{1}H NMR (400 MHz, $CDCl_3$) δ 8.97 (d, J = 2.7 Hz, 1H), 8.41 (dd, J = 9.3, 2.7 Hz, 1H), 8.09 (d, J = 8.9 Hz, 1H), 8.04 – 8.00 (m, 1H), 7.96 – 7.92 (m, 1H), 7.67 (ddd, J = 9.4, 4.2, 2.3 Hz, 3H), 7.40 – 7.37 (m, 1H), 7.18 (s, 1H).

^{13}C NMR (101 MHz, $CDCl_3$) δ 156.3, 151.2, 141.6, 139.6, 134.2, 131.7, 131.2, 128.9, 128.1, 127.6, 126.5, 122.2, 119.7, 118.8, 117.6.

HRMS-EI m/z: calcd for $C_{16}H_{10}N_2O_5$ 310.0590; found: 310.0817 (M^+).

Synthesis of 8-(2,4-dinitrohydroxy)quinoline (D3):

Dosimeter **D3** was prepared by the same experimental procedure used for **D1**. The final product was isolated as pale yellow solid (703 mg, 2.25 mmol, 85 % yield).

^{1}H NMR (400 MHz, $CDCl_3$) δ 8.93 (d, J = 2.8 Hz, 1H), 8.79 (dd, J = 4.2, 1.7 Hz, 1H), 8.25 (dd, J = 8.4, 1.7 Hz, 1H), 8.18 (dd, J = 9.3, 2.8 Hz, 1H), 7.83 (dd, J = 7.9, 1.7 Hz, 1H), 7.65 – 7.56 (m, 2H), 7.47 (dd, J = 8.4, 4.2 Hz, 1H), 6.79 (d, J = 9.3 Hz, 1H).

^{13}C NMR (101 MHz, $CDCl_3$) δ 157.4, 151.0, 149.4, 141.4, 140.6, 138.9, 136.4, 130.3, 128.7, 126.8, 122.4, 120.9.

HRMS-EI m/z: calcd for $C_{15}H_{10}N_3O_5$ 311.0542; found: 312.0628 ($M+H^+$).

Synthesis of 3-hydroxy-6-methoxy-3H-spiro[isobenzofuran-1,9-xanthen]-3-one (4b):

Fluorescein (**4a**, 2 g, 6.18 mmol) was suspended in methanol (50 mL) and NaOH (160 mg, 4 mmol) was then added. The final mixture was stirred until complete dissolution of fluorescein. After evaporation of methanol, the disodium salt (2.0 g, 5.32 mmol) was suspended in DMF (50 mL) containing methyl iodide (332 µL, 5.32 mmol) and the reaction was then stirred at room temperature for 48 h. After this time, the crude was diluted with 5% $NaHCO_3$ (50 mL) and extracted with diethyl ether (2 x 25 mL). The organic phase was washed with brine (20 mL), dried over Na_2SO_4 and evaporated to give an orange precipitate. This solid was dissolved in methanol (30 mL), 2M NaOH (10 mL) was added and the mixture stirred at room temperature for 2 h. After evaporation of methanol, the crude

was diluted with water (20 mL) and impurities extracted with diethyl ether (2 x 10 mL). The aqueous phase was acidified (pH 2.0) by the addition of concentrated HCl and then extracted with diethyl ether (3 x 15 mL), washed with brine (25 mL) and dried over Na_2SO_4. After evaporation of the diethyl ether a brown solid was obtained. The final product was purified by silica column chromatography using diethyl ether-hexane 2:1 v/v as eluent. Compound **4b** was isolated as brown solid (831.2 mg, 2.4 mmol, 45% yield).

Synthesis of 3-(2,4-dinitrophenoxy)-6-methoxy-3H-spiro[isobenzofuran-1,9-xanthen]-3-one (D4):

Dosimeter **D4** was prepared by the same experimental procedure used for **D1**. The final product was isolated as brown solid (162 mg, 0.315 mmol, 65 % yield).
^{1}H NMR (400 MHz, DMSO) δ 8.84 (d, J = 2.8 Hz, 1H), 8.58 (d, J = 3.1 Hz, 1H), 8.45 (dd, J = 9.2, 2.6 Hz, 1H), 8.01 (d, J = 7.6 Hz, 1H), 7.90 – 7.77 (m, 1H), 7.73 (t, J = 7.3 Hz, 1H), 7.37 (d, J = 9.2 Hz, 1H), 7.22 (dd, J = 9.8, 5.1 Hz, 1H), 6.92 (ddd, J = 20.1, 13.2, 5.6 Hz, 1H), 6.74 (dd, J = 8.9, 2.5 Hz, 1H), 6.67 (d, J = 8.8 Hz, 1H), 6.45 (d, J = 9.7 Hz, 1H), 3.76 (s, 1H).
^{13}C NMR (101 MHz, DMSO) δ 158.3, 155.0, 144.7, 141.2, 140.9, 139.1, 138.7, 138.5, 136.6, 129.7, 127.9, 126.6, 126.0, 125.8, 125.6, 124.8, 123.0, 121.7, 120.3, 117.8, 114.8, 115.8, 113.0, 110.1, 107.8, 56.1, 18.6.
HRMS-EI m/z: calcd for $C_{27}H_{16}N_2O_9$ 512.0856; found: 513.0935 ($M+H^+$).

Cell culture conditions:

The HeLa human cervix adenocarcinoma cells were purchased from the German Resource Centre for Biological Materials (DSMZ) and were grown in DEM supplemented with 10% FBS. Cells were maintained at 37 °C in an atmosphere of 5% CO_2 and 95% air ad underwent passage twice in a week.

WST-1 cell viability assays:

Cells were cultured in sterile 96 –well plates at a seeding density of 2.5 x 10^3 cells/well for HeLa and were allowed to settle for 24 h. Dosimeters **D1**, **D2**, **D3** and **D4** were added to the cells at final concentrations of 10, 20, 30 and 50 µM. After 23 h, WST-1 (7 µL of a 50 mg/ml solution) was added to each well. Cells were further incubated for 1 h (a total of 24 h of incubation was therefore studied). Then shacked thoroughly for 1 min. on a shaker and the absorbance was measured at 450 nm against a background control as blank using a microplate ELISA reader. The reference wavelength is 690 nm.

Live confocal microscopy:

Hela cells were seeded in 24 mm glass coverslips in 6-well plates at a seeding density of 10^{-5} cells/well. After 24 hours, cells were treated with **D1** and **D3** at a final concentration of 10 and 30 µM, respectively. After 30 minutes, the medium was removed to eliminate compounds and washed with PBS. Then a solution of Na_2S in PBS was added at a final concentrations of 0, 100, 200, 500 µM and cells were incubated during 1h at 37 ºC. After that, slides were washed twice with PBS to remove traces of the dosimeters. Then slides were visualized under a confocal. Confocal microscopy studies were performed by Confocal Microscopy Service. The images were acquired with a Leica TCS SP2 AOBS (Leica Microsystems Heidelberg GmbH, Mannheim, Germany) inverted laser scanning confocal microscope using oil objectives: 63X Plan-Apochromat-Lambda Blue 1.4 N.A. The excitation wavelengths were 450 nm (argon laser) for both dosimeters. Two-dimensional pseudo colour images (255 colour levels) were gathered with a size of 1024 x 1024 pixels and Airy 1 pinhole diameter. All confocal images were acquired using the same settings and the distribution of fluorescence was analyzed using the Image J Software. Identical experiments were done three times to obtain reproducible results.

Acknowledgements

Financial support from the Spanish Government (project MAT2012-38429-C04-01) and the Generalitat Valencia (project PROMETEO/2009/016) is gratefully acknowledged. S. E. also thanks the Generalitat Valenciana for his Santiago Grisolia fellowship.

References

1. Guidotti, T. L. *Int. J. Toxicol.,* **2010**, *29*, 569.
2. H. Ma, X. Cheng, G. Li, S. Chen, Z. Quan, S. Zhao, L. Niu, *Corros. Sci.,* **2000**, *42*, 1669.
3. M. Bates, N. N. Garrett, P. Shoemack, *Arch. Environ. Health.,* **2002**, *57*, 405.
4. a) D. S. Mottram, *Food Chem.,* **1998**, *62*, 415; b) P. M. Schweizer-Berberich, S. Vaihinger, W. Göpel, *Sensors Act. B Chem.,* **1994**, *18*, 282; c) P. J. A. Vos, R. S. Gray, *Am. J. Enol. Viti.,* **1979**, *30*, 187.
5. L. Li, P. Rose, P. K. More, *Annu. Rev. Pharmacol Toxicol.,* **2011**, *51*, 169.
6. C. Szabo, *Nat. Rev. Drug Discovery.,* **2007**, *6*, 917.
7. E. Lowicka, J. Beltowski, *Pharmacol. Rep.,* **2007**, *59*, 4.
8. H. Kimura, *Amino Acids.,* **2011**, *41*, 113.
9. M. H. Stipanuk, I. Ueki, *J. Inherited Metab. Dis.,* **2011**, *34,* 17.
10. M. Whiteman, P. K. Moore, *Cell. J. Mol. Med.,* **2009**, *13*, 488.
11. C. W. Leffler, H. Parfenova, J. H. Jaggar, R. Wang, *J. Appl. Physiol.,* **2006**, *100*, 1065.
12. C. Jacob, A. Anwar, T. Burkholz, *Planta Med.,* **2008**, *74*, 1580.
13. G. Yang, L. Wu, B. Jiang, W. Yang, J. Qi, K. Cao, Q. Meng, A. K. Mustafa, W. Mu, S. Zhang, S. H. Snyder, R. Wang, *Science*., **2008**, *322*, 587.
14. C. Szabo, *Critical Care.,* **2009**, *13*, P365.
15. a) D. Lefer, *Proc. J. Natl. Acad. Sci. USA.,* **2007**, *104*, 17907; b) G. Szabó, G. Veres, T. Radovits, D. Gero, K. Módis, C. Miesel-Gröschel, F. Horkay, M. Karck, C. Szabo, *Nitric Oxide.,* **2011**, *25*, 201.
16. S. Fiorucci, E. Antonelli, A. Mencarelli, S. Orlandi, B. Renga, G. Rizzo, E. Distrutti, V. Shah, A. Morelli, *Hepatology.,* **2005**, *42*, 539.
17. K. Eto, T. Asada, K. Arima, T. Makifuchi, H. Kimura, *Biochem. Biophys. Res. Commun.,* **2002**, *293*, 1485.
18. P. Kamoun, M. -C. Belardinelli, A. Chabli, K. Lallouchi, B. Chadefaux-Vekemans, *Am. J. Med. Genet.,* **2003**, *116A*, 310.
19. E. Fisher, *Chem. Ber.,* **1883**, *16*, 2234.
20. M. M. F. Choi, *Analyst.,* **1998**, *123*, 1631.
21. M. G. Choi, S. Cha, H. Lee, H. L. Jeon, S. K. Chang, *Chem. Commun.,* **2009**, 7390.

22. N. S. Lawrence, J. Davis, L. Jiang, T. G. Jones, S. N. Davies, R. G. Compton, *Electroanalysis.,* **2000**, *12*, 1453.
23. J. Furne, A. Saeed, M. D. Levitt, *Am. J. Physiol.,* **2008**, *295*, R1479.
24. M. Ishigami, K. Hiraki, K. Umemura, Y. Ogasawara, K. Ishii, H. Kimura, *Antioxid. Redox Signaling.,* **2009**, *11*, 205.
25. a) F. Yu, P. Li, G. Li, G. Zhano, T. Chu, K. Han, *J. Am. Chem. Soc.,* **2011**, *133*, 11030; b) F. Yu, P. Li, B. Wang, K. Han, *J. Am. Chem. Soc,.* **2013**, *135*, 7674.
26. a) R. Martínez-Máñez, F. Sancenón, *Chem. Rev.,* **2003**, *103*, 4419; b) M. E. Moragues, R. Martínez-Máñez, F. Sancenón, *Chem. Soc. Rev.,* **2011**, *40*, 2593; c) L. E. Santos-Figueroa, M. E. Moragues, E. Climent, A. Agostini, R. Martínez-Máñez, F. Sancenón, *Chem. Soc. Rev.,* **2013**, *42*, 3489; d) C. Coll, A. Bernardos, R. Martínez-Máñez, F. Sancenón, *Acc. Chem. Res.,* **2013**, *46*, 339.
27. A. R. Lippert, E. J. New, C. J. Chang, *J. Am. Chem. Soc.,* **2011**, *133*, 10078.
28. H. Peng, Y. Cheng, C. Dai, A. L. King, L. B. Predmore, D. J. Lefer, B. Wang, *Angew. Chem. Int. Ed.,* **2011**, *50*, 9672.
29. F. Yu, P. Li, P. Song, B. Wang, J. Zhao, K. Han, *Chem. Commun.,* **2012**, *48*, 2852.
30. W. Xuan, R. Pan, Y. Cao, K. Liu, W. Wang, *Chem. Commun.,* **2012**, *48*, 10669.
31. L. Montoya, A. M. D. Pluth, *Chem. Commun.,* **2012**, *48*, 4767.
32. S. K. Das, C. S. Lim, S. Y. Yang, J. H. Han, B. R. Cho, *Chem. Commun.,* **2012**, *48*, 8395.
33. W. Sun, J. Fan, C. Hu, J. Cao, H. Zhang, X. Xiong, J. Wang, S. Cui, S. Sun, X. Peng, *Chem. Commun.,* **2013**, *49*, 3890.
34. T. Saha, D. Kand, P. Talukdar, *Org. Biomol. Chem.,* **2013**, *11*, 8166.
35. G. Zhou, H. Wang, Y. Ma, X. Chen, *Tetrahedron.,* **2013**, *69*, 867.
36. C. Yu, X. Li, F. Zeng, F. Zheng, S. Wu, *Chem. Commun.,* **2013**, *49*, 403.
37. K. Sasakura, K. Hanaoka, N. Shibuya, Y. Mikami, Y. Kimura, T. Komatsu, T. Ueno, T. Terai, H. Kimura, T. Nagano, *J. Am. Chem. Soc.,* **2011**, *133*, 18003.
38. L.E. Santos-Figueroa, C. de la Torre, S. El Sayed, F. Sancenón, R. Martínez-Máñez, A. M. Costero, S. Gil, M. Parra, *Eur. J. Inorg. Chem.* **2014**, 41.
39. M. –Q. Wang, K. Li, J. –T. Hou, M. –Y. Wu, M. Z. Huang, X. –Q. Yu, X. *J. Org. Chem.,* **2012**, *77*, 8350.
40. C. Gao, X. Liu, X. Jin, J. Wu, Y. Xie, W. Liu, X. Yao, Y. Tang, *Sensors Act. B Chem.,* **2013**, *185*, 125.
41. X. Hou, F. Zeng, F. Du, S. Wu, *Nanotechnology.,* **2013**, *24*, 335502.
42. J. Wang, L. Long, D. Xie, Y. Zhan, *J. Lumin.,* **2013**, *139*, 40.
43. X. Qu, C. Li, H. Chen, J. Mack, Z. Guo, Z. Shen, *Chem. Commun.,* **2013**, *49*, 7510.
44. X. Wu, H. Li, Y. Kan, B. Yin, *Dalton Trans.,* **2013**, *42*, 16302.
45. C. Kar, M. D. Adhikari, A. Ramesh, G. Das, *Inorg. Chem.,* **2013**, *52*, 743.
46. F. Zheng, M. Wen, F. Zeng, S. Wu, *Sensors Act. B Chem.,* **2013**, *185*, 1012.
47. C. Liu, B. Peng, S. Li, C. –M. Park, A. R. Whorton, M. Xian, *Org. Lett.,* **2012**, *14*, 2184.

48. C. Liu, J. Pan, S. Li, Y. Zhao, L. Y. Wu, C. E. Berkman, A. R. Whorton, M. Xian, *Angew. Chem. Int. Ed.,* **2011**, *50*, 10327.
49. Z. Xu, L. Xu, J. Zhou, Y. Xu, W. Zhu, X. Qian, *Chem. Commun.,* **2012**, *48*, 10871.
50. J. Liu, Y. –Q. Sun, J. Zhang, T. Yang, J. Cao, L. Zhang, W. Guo, *Chem. Eur. J.,* **2013**, *19*, 4717.
51. Z. Wu, Z. Li, L. Yang, J. Han, S. Han, *Chem. Commun.,* **2012**, *48*, 10120.
52. X. Li, S. Zhang, J. Cao, N. Xie, T. Liu, B. Yang, Q. He, Y. Hu, *Chem. Commun.,* **2013**, *49*, 8656.
53. J. Zhang, Y. –Q. Sun, J. Liu, Y. Shi, W. Guo, *Chem. Commun.,* **2013**, *49*, 11305.
54. C. Wei, Q. Zhu, W. Liu, W. Chen, Z. Xi, L. Yi, *Org. Biomol. Chem.,* **2013**, *11*, 479.
55. C. Wei, L. Wei, Z. Xi, L. Yi, *Tetrahedron Lett.,* **2013**, *54*, 6937.
56. X. –F. Yang, L. Wang, H. Xu, M. Zhao, *Anal. Chim. Acta.,* **2009**, *631*, 91.
57. B. Wang, P. Li, F. Yu, P. Song, X. Sun, S. Yang, Z. Lou, K. Han, *Chem. Commun.,* **2013**, *49*, 1014.
58. B. Wang, P. Li, F. Yu, J. Chen, Z. Qu, K. Han, *Chem. Commun.,* **2013**, *49*, 5790.
59. X. Cao, W. Lin, K. Zheng, L. He, *Chem. Commun.,* **2012**, *48*, 10529.
60. T. Liu, Z. Xu, D. R. Spring, J. Cui, *Org. Lett.,* **2013**, *15*, 2310.
61. a) Y. Liu, G. Feng, *Org. Biomol. Chem.,* **2014**, *12*, 438; b) G. –Y. Li, Y. –H. Li, H. Zhang, G. –H. Cui, *Commun. Comput. Chem.,* **2013**, *1*, 88.
62. a) E. Climent, A. Agostini, M. E. Moragues, R. Martínez-Máñez, F. Sancenón, T. Pardo, M. D. Marcos, *Chem. Eur. J.* **2013**, *19*, 17301; b) S. El Sayed, Li. Pascual, A. Agostini, R. Martínez-Máñez, F. Sancenón, A. M. Costero, M. Parra, S. Gil, *ChemistryOpen*., **2014**, *3*, 145; c) S. El Sayed, A. Agostini, L. E. Santos-Figueroa, R. Martínez-Máñez, F. Sancenón, *ChemistryOpe*n., **2013**, *2*, 58; d) E. Climent, C. Giménez, M. D. Marcos, R. Martínez-Máñez, F. Sancenón, J. Soto, *Chem. Commun.,* **2011**, *47*, 6873; e) M. E. Moragues, J. Esteban, J. V. Ros-Lis, R. Martínez-Máñez, M. D. Marcos, M. Martínez, J. Soto, F. Sancenón, *J. Am. Chem. Soc.* **2011**, *133*, 15762; f) E. Climent, A. Martí, S. Royo, R. Martínez-Máñez, M. D. Marcos, F. Sancenón, J. Soto, A. M. Costero, S. Gil, S.; M. Parra, *Angew. Chem. Int. Ed.,* **2010**, *49*, 5945; g) E. Climent, M. D. Marcos, R. Martínez-Máñez, F. Sancenón, J. Soto, K. Rurack, P. Amorós, *Angew. Chem. Int. Ed.,* **2009**, *48*, 8519.
63. S. El Sayed, C. de la Torre, L. E. Santos-Figueroa, E. Pérez-Payá, R. Martínez-Máñez, F. Sancenón, A. M. Costero, M. Parra, S. Gil, *RSC Adv.,* **2013**, *3*, 25690.
64. a) S. Shaltiel, *Biochem. Biophys. Res. Commun.,* **1967**, *29*, 178; b) R. Philosof-Oppenheimer, I. Pechtz, M. Fridkin, *Int. J. Pept. Protein Res.,* **1995**, *45*, 116.
65. J. C. Mathai, A. Missner, P. Kügler, S. M. Saparov, M. L. Zeidel, J. K. Lee, P. Pohl, *Proc. Natl. Acad. Sci. USA.,* **2009**, *106*, 16633.
66. M. Hoffman, A. Rajapakse, X. Shen, K. S. Gates, *Chem. Res. Toxicol.,* **2012**, *25*, 1609.

SUPPORTING INFORMATION

2,4-dinitrophenyl ether-containing chemodosimeters for the selective and sensitive "*in vitro*" and "*in vivo*" detection of hydrogen sulfide

Sameh El Sayed, Cristina de la Torre, Luis E. Santos-Figueroa, Ramón Martínez-Máñez, Félix Sancenón, Mar Orzáez, Ana M. Costero, Margarita Parra, and Salvador Gil

Characterization of compound 1c:

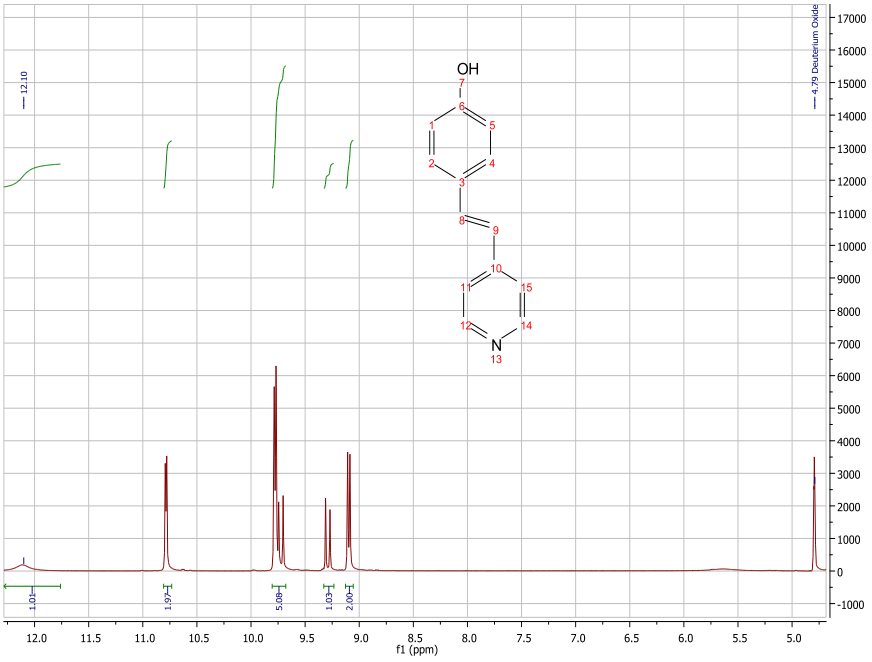

Figure SI-1. *^{1}H-NMR spectrum of **1c** in DMSO-D6.*

Characterization of probe D1

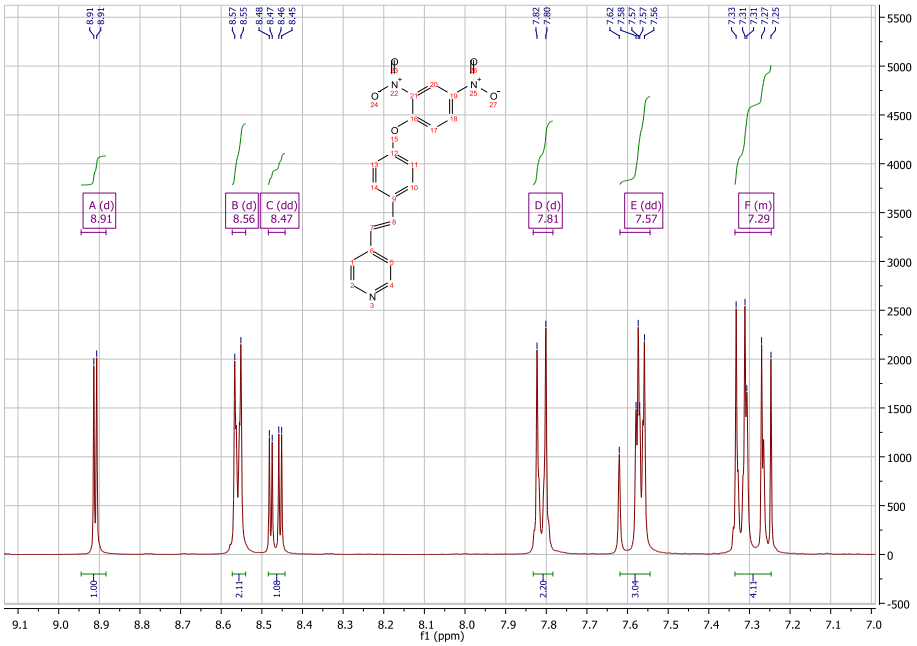

Figure SI-2. *^{1}H-NMR spectrum of probe **D1** in DMSO-D6.*

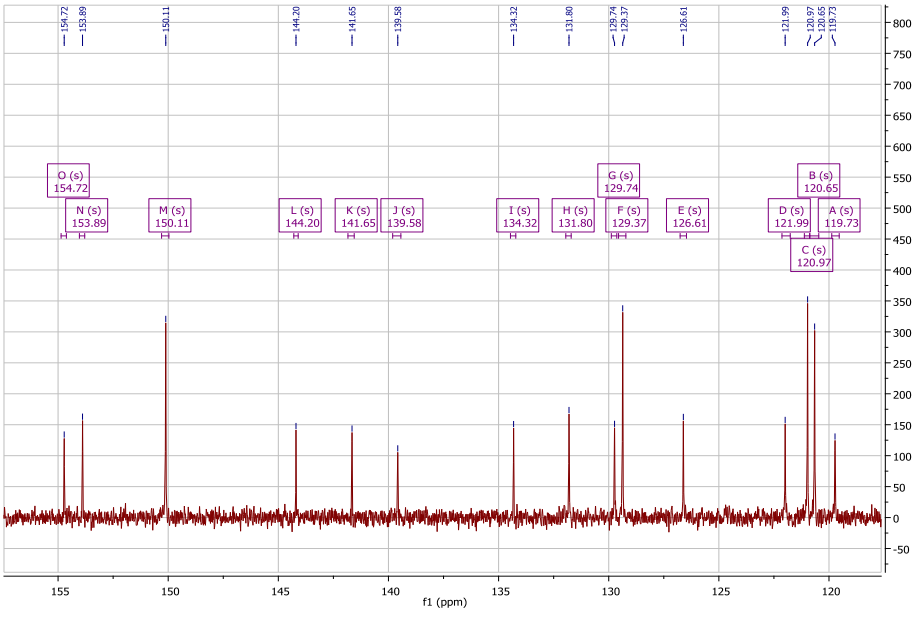

Figure SI-3. *^{13}C-NMR spectrum of probe **D1** in DMSO-D6.*

Characterization of probe D2:

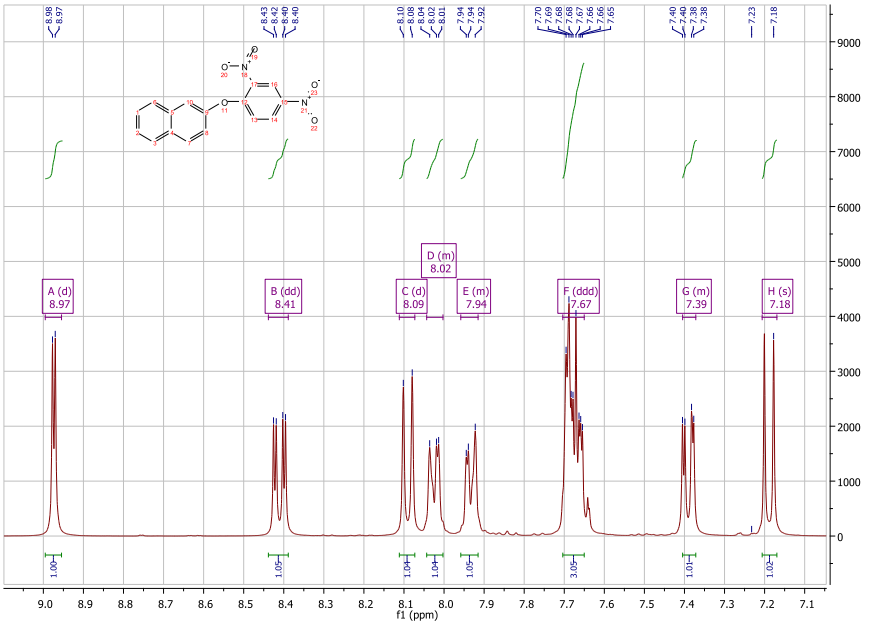

Figure SI-4. *^{1}H-NMR spectrum of probe **D2** in $CDCl_3$.*

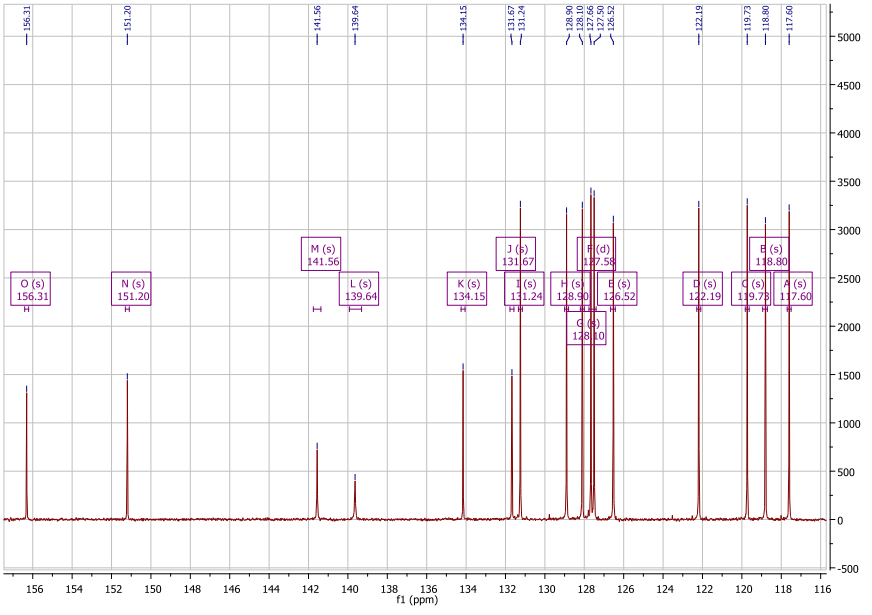

Figure SI-5. *^{13}C-NMR spectrum of probe **D2** in $CDCl_3$.*

Characterization of probe D3:

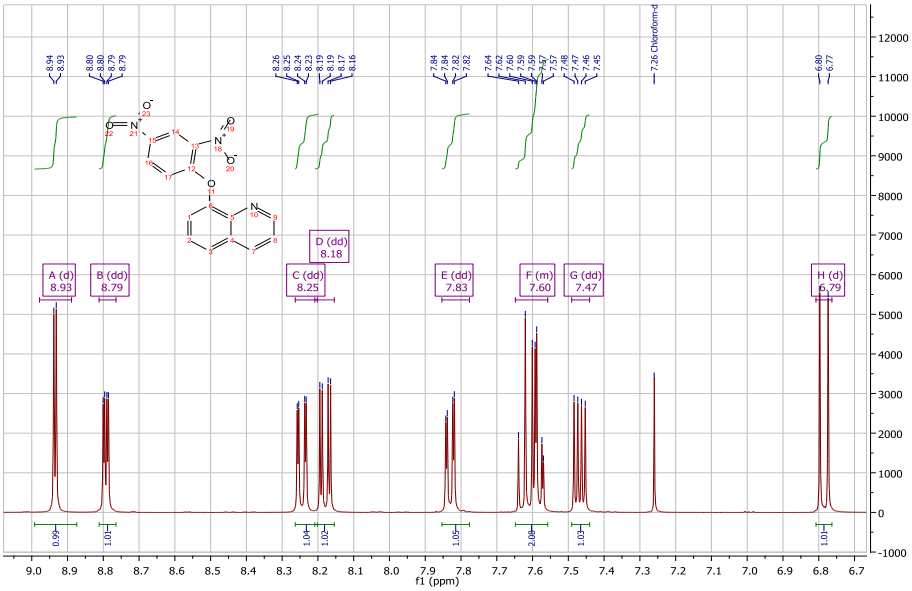

Figure SI-6. *^{1}H-NMR spectrum of probe **D3** in $CDCl_3$.*

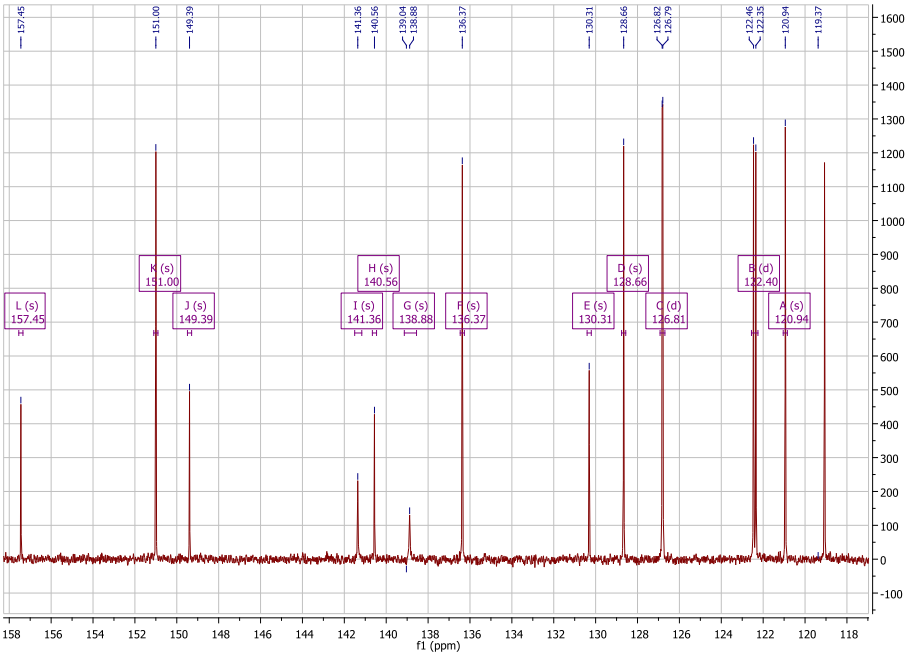

Figure SI-7. ^{13}C-NMR spectrum of probe **D3** in $CDCl_3$.

Characterization of compound 4b:

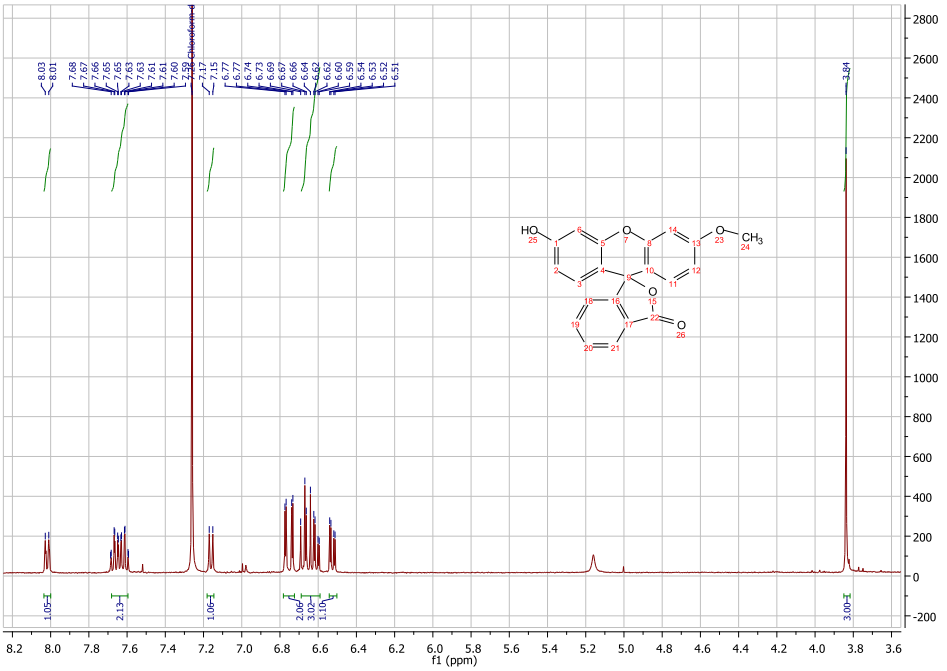

Figure SI-8. *^{1}H-NMR spectrum of **4b** in $CDCl_3$.*

Characterization of probe D4:

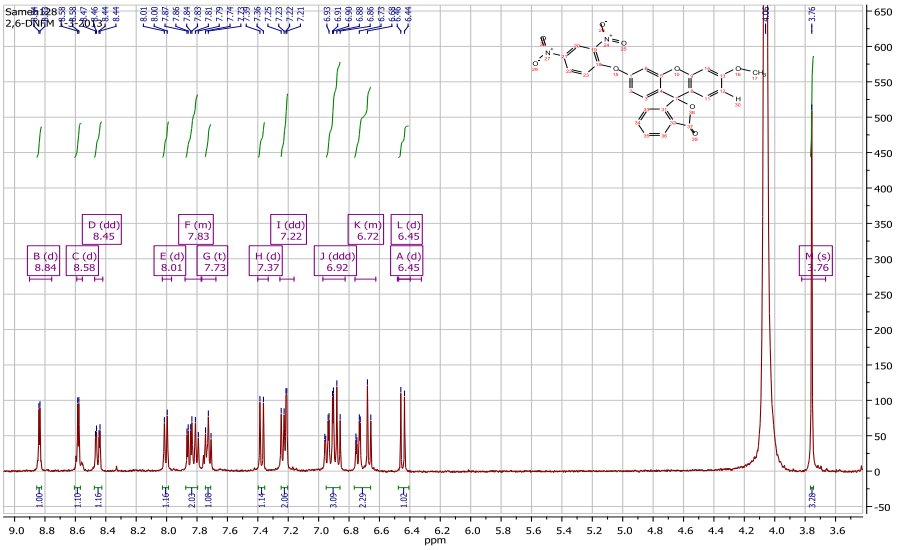

Figure SI-9. *^{1}H-NMR spectrum of probe **D4** in DMSO-D6.*

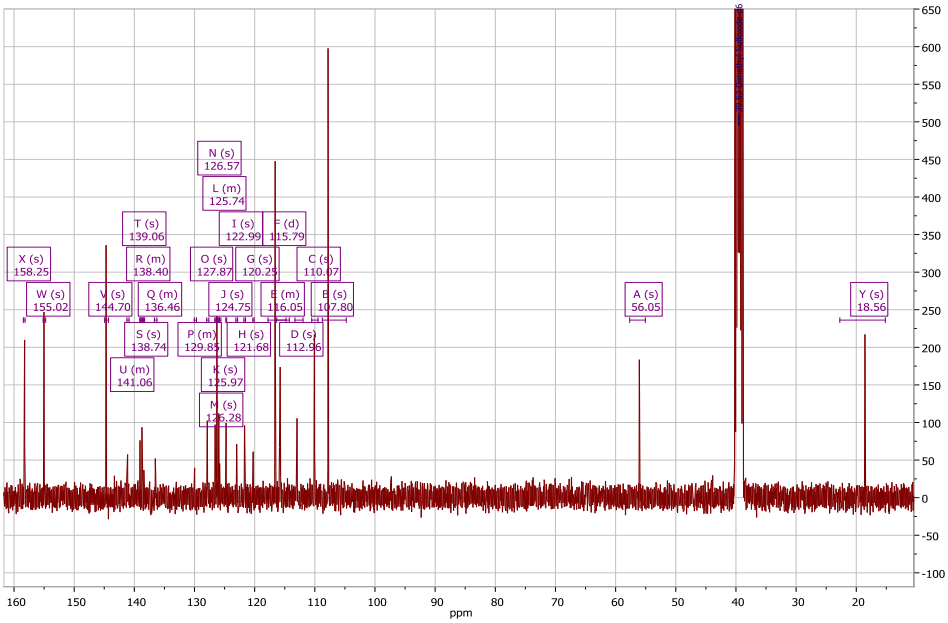

Figure SI-10. *^{13}C-NMR spectrum of probe **D4** in DMSO-D6.*

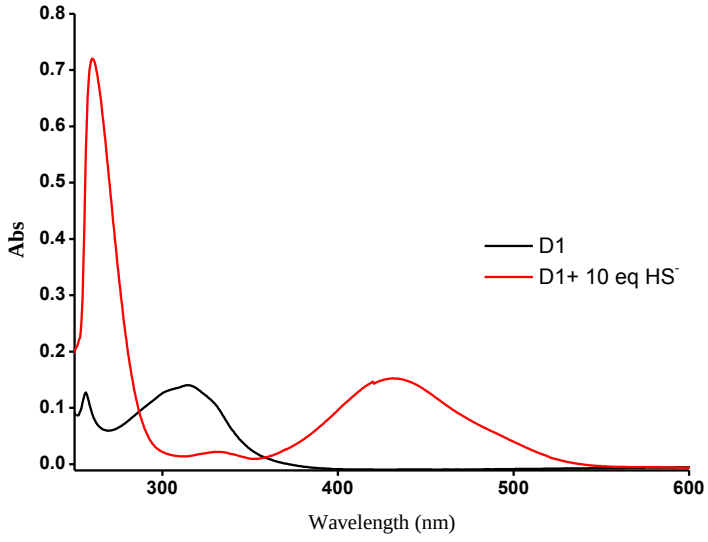

Figure SI-11. *UV-visible spectra of probe **D1** (5 µM) in DMSO alone and upon addition of 10 eq. of HS^- anion.*

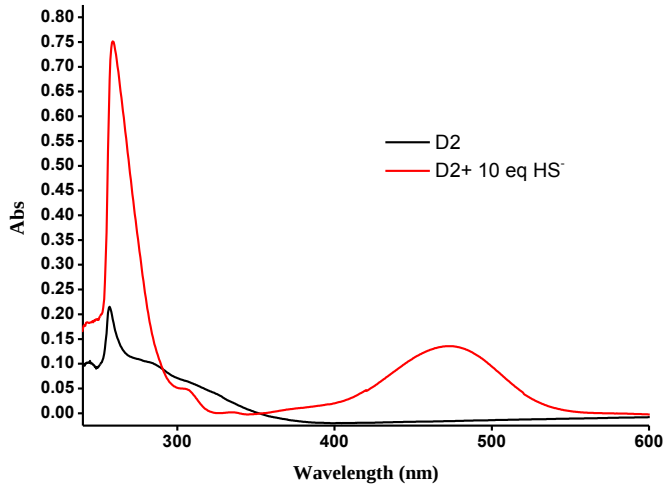

Figure SI-12. *UV-visible spectra of probe* ***D2*** *(5 µM) in DMSO alone and upon addition of 10 eq. of* HS^- *anion.*

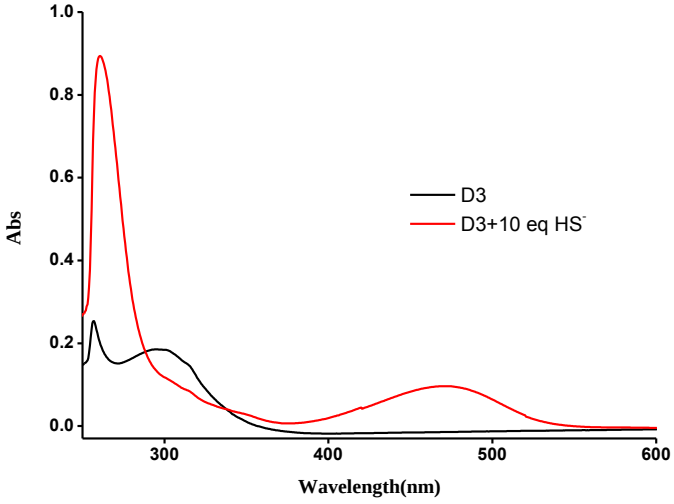

Figure SI-13. *UV-visible spectra of probe* ***D3*** *(5 µM) in DMSO alone and upon addition of 10 eq. of* HS^- *anion.*

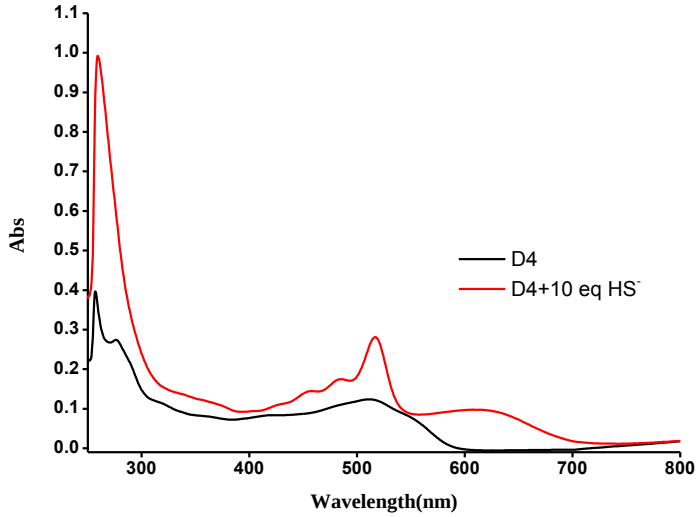

Figure SI-14. *UV-visible spectra of probe* ***D4*** *(5 µM) in DMSO alone and upon addition of 10 eq. of* HS^- *anion.*

Azide and sulfonylazide functionalized fluorophores for the selective and sensitive detection of hydrogen sulfide

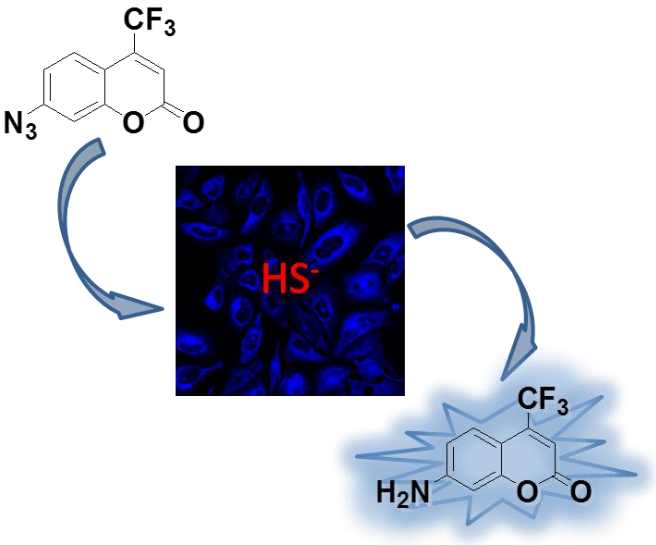

Azide and sulfonylazide functionalized fluorophores for the selective and sensitive detection of hydrogen sulfide

Sameh El Sayed,[a,b,c] Cristina de la Torre,[a,b,c] Luis E. Santos-Figueroa,[a,b,c] Cristina Marín-Hernández,[a,b,c] Ramón Martínez-Máñez,[a,b,c] Félix Sancenón,[a,b,c] Ana M. Costero,[a,d] Salvador Gil[a,d] and Margarita Parra[a,d]*

[a] Centro de Reconocimiento Molecular y Desarrollo Tecnológico (IDM). Centro Mixto de la Universitat Politècnia de València y de la Universitat de València.

[b] Departamento de Química. Universitat Politècnica de València. Camino de Vera s/n, 46022, Valencia, Spai. E-mail: rmaez@qim.upv.es

[c] CIBER de Bioingeniería, Biomateriales y Nanotecnología (CIBER-BNN).

[d] Departamento de Química Orgánica. Facultad de Ciencias Químicas. Universitat de València. Dr. Moliner 50, 46100, Burjassot, Valencia, Spain.

First published on the web: *2 May 2014*

Sens. Actuators, B., ***2015****, 207, 987-994.*

(Reproduced with permission of Elsevier B.V copyrights 2015.)

Abstract

*Three fluorescent probes (**1**-**3**) for the selective and sensitive detection of hydrogen sulfide have been synthesized and characterized. Probe **1** is a coumarin derivative functionalized with an azide moiety whereas **2** contain the azide reactive group into a naphthalene fluorophore backbone. Probe **3** is composed also by a naphthalene fluorophore but in this case, functionalized with a sulfonylazide reactive moiety. Probes **1** and **3** are non-fluorescent whereas **2** is weakly emissive in HEPES (10 mM, pH 7.4)-DMSO 99:1 v/v. The emission behavior of the three probes was tested against selected anions, bio-thiols and oxidant molecules. Of all the chemical species tested, only HS^- is able to induce an enhancement in the emission intensity (50, 11 and 20-fold for **1**, **2** and **3** respectively). The observed emission in the presence of hydrogen sulfide is ascribed, in the case of probes **1** and **2**, to an azide-amine reduction induced by HS^- anion, whereas for probe **3** the sensing mechanism is related with a sulfonylazide-sulfonamide conversion. The three probes are very sensitive to HS^- anion with limits of detection of 0.17, 0.20 and 0.40 mM for **1**, **2** and **3** respectively. Cell viability studies demonstrated that **1**-**3** probes are essentially non-toxic at concentrations 10-50 μM and are well suited for in vivo studies. Finally, probe **1** was used for the detection on intracellular HS^- anion in HeLa cells by means of confocal microscopy.*

Keywords: hydrogen sulfide • fluorescence • azide • sulfonylazide • in vivo detection

Introduction

Hydrogen sulfide (H_2S), along with CO and NO, has been recognized as one of the three known endogenous gasotransmitters involved in many physiological processes of biological systems,[1] such as cardiovascular, central nervous, respiratory, gastrointestinal and endocrine systems. Previously, NO has been successfully detected with suitable fluorophores for their fast and real-time

determination in cells.[2] For quite a long time, it was difficult to accurately and selectively detect H_2S without interruption by other reactive sulfur species, such as thiols, sulfenic acids and sulfites. H_2S may interact with downstream proteins by post-translational cysteine sulfhydration[3] and binding to iron centers[4] which regulates various physiological processes including ischemia reperfusion injury[5] vasodilation,[6] apoptosis,[7] angiogenesis,[8] neuromodulation,[9] inflammation[10] and insulin signaling.[11] Hydrogen sulfide's exact mechanisms of action are still under active investigation. Some chemical and biochemical catabolic reactions of H_2S have been reported. For example, H_2S can react readily with methemoglobin to form sulfhemoglobin, which act as the metabolic sink for H_2S. As a potential reductant, H_2S is likely to be consumed by endogenous oxidant species such as hydrogen peroxide, superoxide, peroxynitrite, etc. This process is potentially significant because it provides a possible mechanism by which H_2S changes the functions of a wide range of cellular proteins and enzymes. However, abnormal levels of H_2S are associated with various diseases such as Alzheimer[12] and Down syndrome.[13] H_2S is highly diffusible and reactive, so it is difficult to follow. Colorimetric,[14] electrochemical,[15] and chromatographic assays[16] are available to measure H_2S in blood plasma and homogenized tissues, but they often require sample processing and do not provide much spatial and temporal information on H_2S concentrations and distribution in living cells and organisms.

By contrast, fluorescence imaging provides a tractive technique for biomolecules studding in living cells. As known, H_2S is a reductant as well as nucleophilic specie, which can specially react with some fluorogenic signaling subunits containing selected functional groups. Recently, several research groups have made great efforts toward the preparation of fluorogenic probes for the detection of hydrogen sulfide in blood and in cells.[17] These probes are constructed bearing in mind the reactivity of the HS^- anion. In particular, reduction, hydrolysis, nucleophilic additions and demetallation processes has been used as triggers for obtaining a fluorescent response for this anion.

For instance, very recently, several examples of non-emissive Cu(II) complexes were used for the fluorogenic recognition of hydrogen sulfide.[18] This anion is able

to induce demetallation with the subsequent regeneration of fluorescent receptors. Michael-type additions[19] and hydrolysis of disulfide bonds[20] and 2,4-dinitropneylethers[21] has also been extensively used in the development of fluorescent probes for hydrogen sulfide. However, probably, the type of reactions most used for the design of fluorogenic probes for hydrogen sulfide are reductions. In this context reductions of nitro, hydroxylamine and azide functional groups hy hydrogen sulfide have been selected due to their short reaction times, high yields and because usually can be carried out in water or in mixed aqueous environments.[22] Among these reactions, the azide-amine reductions are perhaps the most used and several examples of probes based on this reaction have been developed. At this respect, in a pioneering work, Chang and co-workers prepared two weakly emissive rhodamine derivatives bearing azide moieties that yielded the correspondent fluorescent amines upon addition of HS^- anion.[22a] The authors also demonstrated that both probes are able to detect intracellular HS^- anions in HEK293T cells using confocal microscopy. Wang and co-workers used a similar approach and prepared a dansyl sulfonylazide derivative that yielded a highly emissive dansyl sulfonamide upon reaction with HS^-.[22b] Cho and co-workers extended the fluorescent recognition of HS^- anion to the use of two-photon probes.[22c] Authors prepared a 7-(benzo[*d*]thiazol-2-yl)-9,9-(2-methoxyethoxy)ethyl-9*H*-fluorene functionalized with an azide moiety. This probe has been used for the detection of HS^- in vitro, in HeLa cells and in a rat hippocampal slice at a depth of 90-190 μm by using two-photon microscopy. A reduction reaction coupled with an intramolecular substitution was used by Han and co-workers for the preparation of a highly selective HS^- fluorescent probe.[22d] In particular, 7-*o*-2'-(azidomethyl)benzoyl-4-methylcoumarin was prepared and the reduction of the azide to amine (induced by HS^-) triggered the generation of fluorescent 7-hydroxy-4-methylcoumarin fragment. Finally, also fluorescent proteins were recently modified with azide moieties and used for the fluorogenic detection of HS^- in HeLa cells.[22e]

Taking into account the above mentioned examples and bearing in mind our interest in the preparation of chemodosimeters for the chromo-fluorogenic detection of anions with environmental or biological significance,[23] here we

present the synthesis, characterization and sensing features of three new molecular probes (**1**-**3**) for HS^- detection. Probes **1** and **2** are azide derivatives of coumarin and naphthalene fluorophores whereas **3** is 2-sulfonylazidonaphthalene. The three probes are nearly non-fluorescent in aqueous environments and, upon addition of HS^- anion, an emission was developed. The selectivity of the three probes is remarkable and other anions, bio-thiols and oxidants are unable to induce emission changes in **1**-**3**. The probes showed remarkable limits of detection in the 0.1-0.4 μM range and can be used for the fluorescence detection of both exogenous and endogenous HS^- in cells.

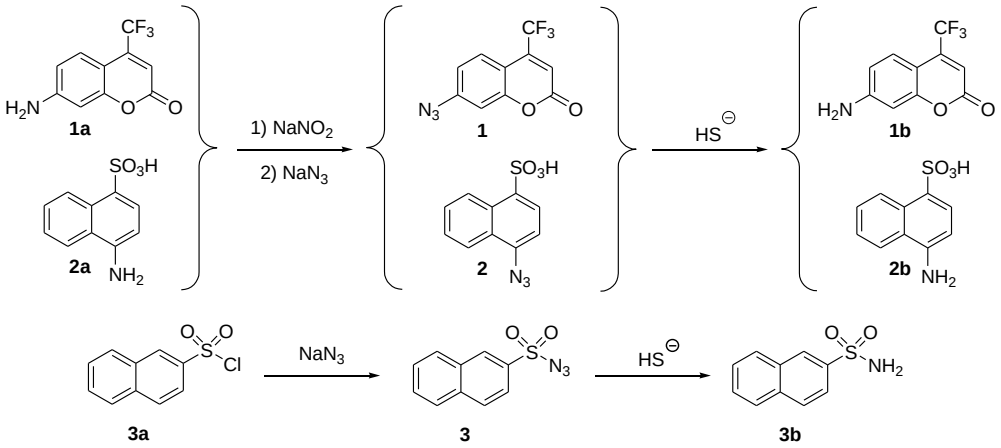

***Scheme 1**. Synthesis and chemical structure of probes **1**-**3**.*

Results and Discussion

The fluorogenic probes:

Three fluorogenic probes, **1**, **2** and **3** have been prepared by conventional synthetic procedures (see Scheme 1). Probes **1** and **2** were obtained through an aromatic nucleophilic substitution from 7-amino-4-(trifluoromethyl)coumarin (**1a**) and 4-amino-1-naphthalenesulfonic acid (**1b**) respectively. In a first step, **1a** and **2a** were reacted with sodium nitrite in acidic media yielding the corresponding diazonium salts. These salts were not isolated and were converted to **1** and **2** by

reaction with sodium azide. Probe **3** was easily obtained by direct reaction of 2-naphthalenesulfonyl chloride (**3a**) with sodium azide. The final probes were characterized by ^{1}H, ^{13}C-NMR and HRMS (see experimental section for details). ^{1}H-NMR spectra of probe **1** is characterized by the presence of one singlet centered at 7.00 ppm ascribed to the ethylene proton neighboring to the carbonyl group of the lactonic ring. Also, one characteristic signal is the sharp doublet centered at 7.34 ppm attributed to the proton located between the azide moiety and the oxygen atom of the lactone ring. Moreover, the IR spectra of **1** showed the typical strong band of the azide stretching at 2117 cm^{-1}. Dealing with probe **2**, the most characteristic signals in the ^{1}H-NMR spectra are two doublets centered at 8.03 and 8.85 ppm that are ascribed to the protons located near the azide and sulfonic acid moieties respectively. Also for probe **2** the stretching band of the azide moiety is observed at 2128 cm^{-1}. Finally, the more characteristic signals of probe **3** are a singlet centered at 8.55 ppm and two doublets centered at 7.97 and 7.90 ppm that were ascribed to the aromatic ring containing the sulfonyl azide moiety (stretching at 2131 cm^{-1}).

Hydrogen sulfide recognition:

The three synthesized probes are composed by a fluorophore directly linked with an azide moiety (probes **1** and **2**) or functionalized with a sulfonyl azide functional group (probe **3**). It is well documented the ability of hydrogen sulfide to reduce azide groups to amines.[24] In addition when azides are coupled with a fluorophore, the difference in the electronic properties of this moiety and the amino group is expected to trigger the emission properties of the fluorophore with the subsequent recognition of hydrogen sulfide anion. In fact this simple sensing mechanism has been used very recently in the preparation of selective and sensitive probes for HS^{-} anion in water and in cellular media.[22] For these probes the selectivity observed is high due to the fact that reduction of an azide to the correspondent amine by hydrogen sulfide is faster than that observed when GSH and Cys are used. This is a consequence of the small size and lower pK_a (6.9) of the hydrogen sulfide when compared to GSH and Cys (pK_a values about 8.5).[25]

In a first step, the sensing features of the three synthesized probes **1**-**3** was evaluated in the presence of selected anions (F^-, Cl^-, Br^-, I^-, N_3^-, OH^-, CN^-, SCN^-, AcO^-, citrate, NO_3^-, HCO_3^-, $H_2PO_4^-$, SO_4^{2-} and HS^-), reducing agents (SO_3^{2-} and $S_2O_3^{2-}$), oxidants (H_2O_2) and thiol-containing biomolecules (lipoic acid, Cys, Me-Cys, Hcy and GSH) in HEPES (10 mM, pH 7.4)-DMSO 99:1 v/v. Probes **1** and **3** are nearly non-fluorescent whereas **2** showed a very weak emission band centered at 420. As a general trend, Figure 1 shows how addition of HS^- to **1**-**3** induced a significant fluorescent "*turn-on*" response, whereas addition of the other anions, oxidants and biothiols induced negligible changes in the emission.

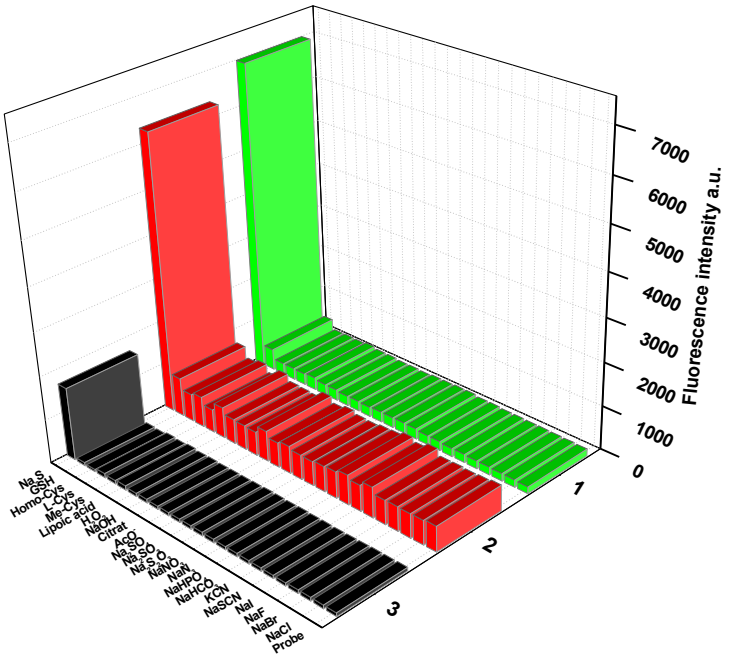

Figure 1*. Emission intensity of probes (5 μM)* ***1*** *(at 496 nm upon excitation at 420 nm),* ***2*** *(at 420 nm upon excitation at 350 nm) and* ***3*** *(at 350 nm upon excitation at 295 nm) in HEPES (10 mM, pH 7.4)-DMSO 99:1 v/v solutions upon addition of 10 equivalents of anions, bio-thiols, reducing agents and oxidants (after 50 minutes of the addition).*

More in detail, addition of 10 equivalents of HS^- anion to HEPES (10 mM, pH 7.4)-DMSO 99:1 v/v solution of probe **1** (5 μM) induced the appearance of an emission band centered at 496 nm (λ_{ex} = 420 nm) that reached their maximum intensity after 50 minutes upon addition of 10 equivalents of HS^-. The intensity enhancement for probe **1** is *ca*. 50-fold. Nearly the same results were obtained

when probe **2** is used. In particular, HEPES (10 mM, pH 7.4)-DMSO 99:1 v/v solution of probe **2** (5 μM) showed a very weak emission band centered at 420 nm upon excitation at 350 nm. Again, of all the anions, oxidants and biothiols tested, only addition of HS^- anion induced a remarkable 11-fold enhancement (after 50 minutes of the addition) of the emission band. Finally, HEPES (10 mM, pH 7.4)-DMSO 99:1 v/v solution of probe **3** (5 μM) are non-emissive but the typical broad unstructured band of the naphthalene fluorophore at *ca*. 350 nm (λ_{ex} = 295 nm) emerged upon addition of HS^- anion (20-fold enhancement after 50 minutes of the addition).

Once assessed the selectivity of the three probes toward HS^-, in a second step, sensitivity studies were carried out. Addition of increasing quantities of HS^- anion to HEPES (10 mM, pH 7.4)-DMSO 99:1 v/v solution of probe **1** (5 μM) induced a progressive enhancement in the emission centered at 496 nm (see Figure 2). From the titration profile a limit of detection (LOD) of 0.17 μM for HS^- was determined. Similar titration experiments with **2** allowed to determine a LOD of 0.20 μM (see Figure 3), whereas LOD calculated for **3** was 0.40 μM. The low limits of detection determined for the three probes suggested that these could be used to detect HS^- in cells as the LOD are below the hydrogen sulfide concentration required to elicit physiological responses (10-1000 μM).[26]

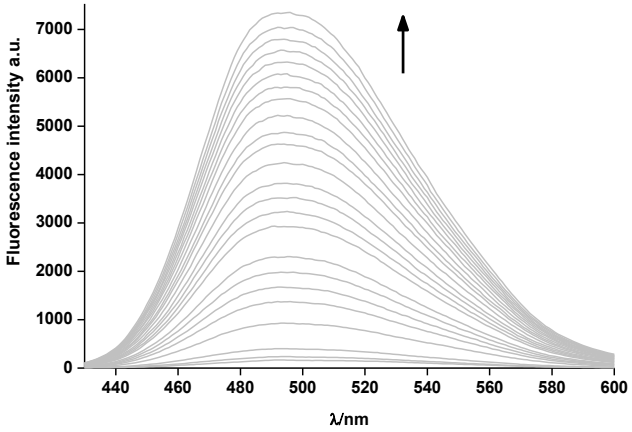

***Figure 2**. Fluorescene enhancement of probe **1** (5 μM) in HEPES (10 mM, pH 7.4)-DMSO 99:1 v/v solution upon addition of increasing quantities of HS^- anion (from 0 to 10 equivalents) after 50 minutes of the addition (excitation at 420 nm).*

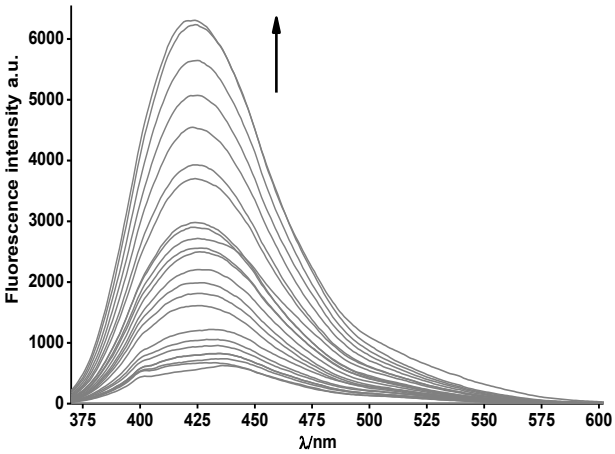

***Figure 3**. Fluorescene enhancement of probe **2** (5 µM) in HEPES (10 mM, pH 7.4)-DMSO 99:1 v/v solution upon addition of increasing quantities of HS^- anion (from 0 to 10 equivalents) after 50 minutes of the addition (excitation at 350 nm).*

The selective emission enhancements observed for **1**-**3** probes was ascribed to an HS^- induced reduction of the azide moieties presented in the chemical structure of the three dosimeters (see Scheme 1). The stoichiometry of the reaction between probes **1**-**3** and HS^- anion is 1:1 was confirmed by the corresponding Job's plots. As an example, Figure 4 showed the Job's plot obtained for probe **2** and HS^- anion.

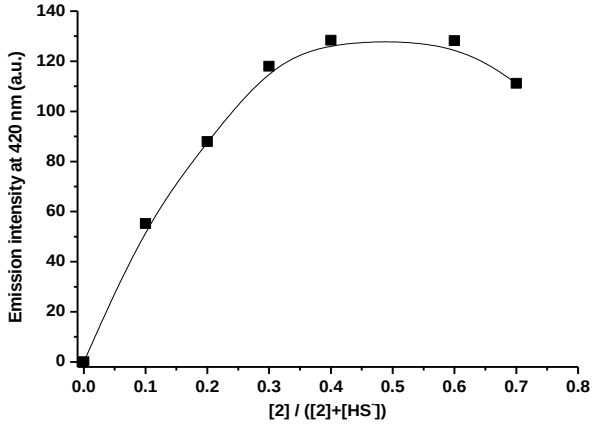

***Figure 4**. Job´s plot for the reaction between probe **2** and HS^- anion determined by fluorescence (emission at 420 nm registered after 50 minutes of the addition, excitation at 350 nm) in HEPES (10 mM, pH 7.4)-DMSO 99:1 v/v solution and with [2]+[HS^-] = 10 µM.*

These hydrolysis reactions yielded the correspondent highly fluorescent amines **1b** and **2b** (in the case of probes **1** and **2**) and sulfonamide **3b** (in the case of probe **3**). The hydrogen sulfide-induced azide-amine reduction as a mechanism of the fluorescence response observed has been corroborated by the isolation of **1b**, **2b** and **3b** after the reaction of the probes with Na_2S. In a typical experiment, probes **1-3** were dissolved in ethanol and then an excess of Na_2S was added. The mixtures were stirred at room temperature for 1 h. Then the ethanol was eliminated in a rotary evaporator and the crudes obtained were purified by silica column chromatography. The ^{1}H and ^{13}C of the final products were coincident with that of **1b**, **2b** and **3b** amines. Besides, the hydrogen sulfide-induced azide-amine reduction was corroborated by ^{1}H-NMR titration measurements. At this respect, DMSO-D6 solutions of probe **1** showed the protons of the aromatic ring containing the azide moiety centered at 7.71 (Ha), 7.34 (Hc) and 7.23 (Hb) (see Figure 5 for proton assignation). Addition of increasing quantities of HS^- anion induced a progressive upfield shift of the three protons (see also Figure 5) that would be clearly ascribed to the reduction of the electron withdrawing azide group to an electron donor amine moiety.

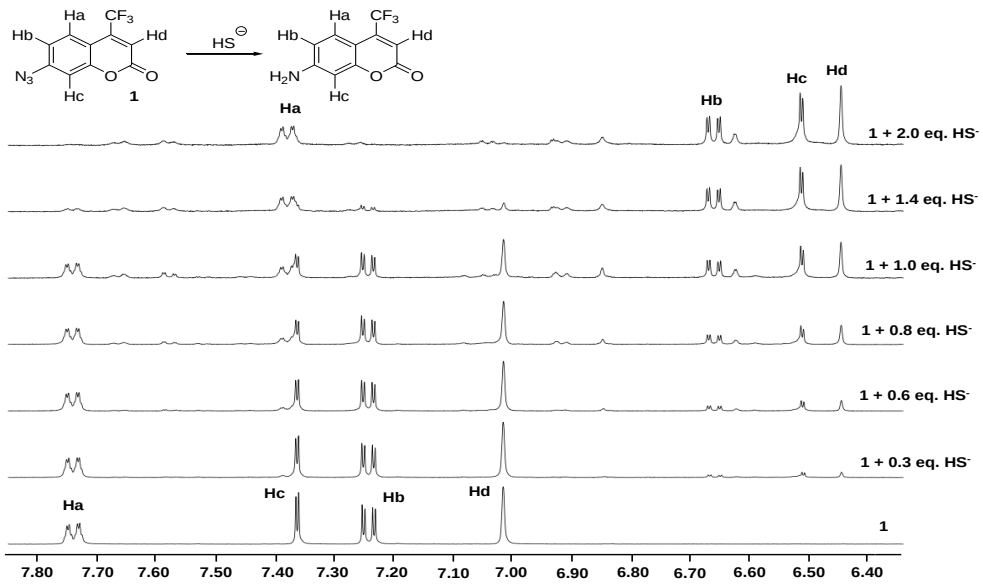

***Figure 5**. ^{1}H-NMR spectra of probe **1** in DMSO-D6 alone and in the presence of 0.3, 0.6, 0.8, 1, 1.4 and 2 equivalents of HS^- anion.*

The time dependent fluorescence enhancement of the three probes (5 μM) upon addition of HS^- anion (50 μM) was studied. The obtained results are depicted in Figure 6. As could be seen, for the three probes, the emission intensity increased gradually with time until *ca*. 50 minutes. At this time nearly constant emission intensity was observed indicative of the complete reduction of the azide moiety.

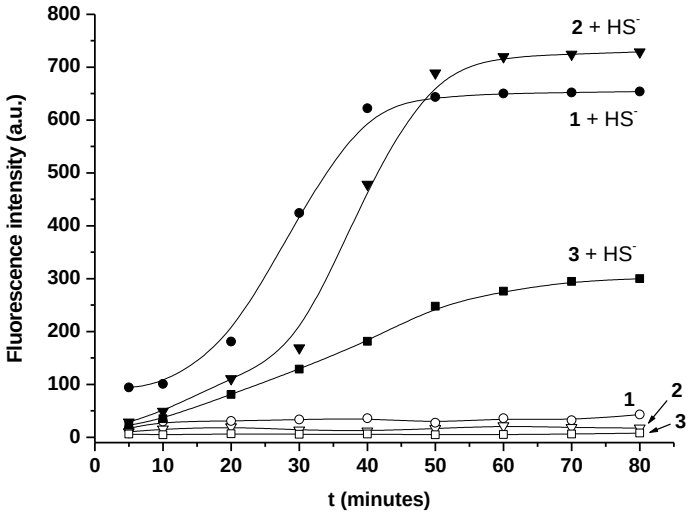

Figure 6. *Emission intensity changes of the three probes (5 μM) at different times in the absence and in the presence of HS^- anion (10 equivalents). Emission at 496, 420 and 350 nm for probe **1** (●), **2** (▼) and **3** (■) respectively in prescence of 10 equivalents of HS^- anion. The picture also show the changes of probes in the absence of HS^- (**1** (○), **2** (▽) and **3** (□)).*

Also, the emission behavior of the three probes in the absence and in the presence of HS^- anion at different pH was also studied. The weak (for **2**) or negligible (for **1** and **3**) emission remained unchanged in the 3-9 pH range. In the presence of HS^- anion (50 μM), the emission intensity of the probes (5 μM) did not change in the 3-5 pH range, whereas the maximum intensity was observed at pH from 7 to 9 (see Figure 7). This is an expected result bearing in mind the fact that below pH 7.0 hydrogen sulfide is in the H_2S form (the pK_a is 6.9) which is unable to promote the azide-amine reduction.

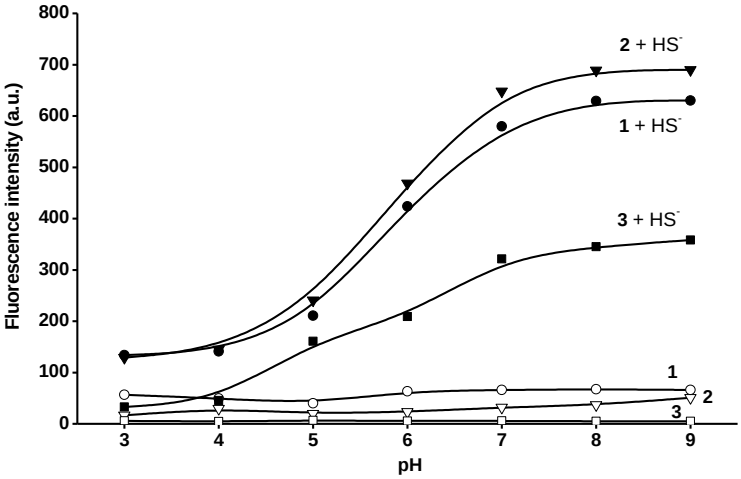

***Figure 7**. Emission intensity changes of the three probes (5 μM) at different pH values in the absence and in the presence of HS^- anion (10 equivalents) after 50 minutes of the addition. Emission at 496, 420 and 350 nm for probe **1** (●), **2** (▼) and **3** (■) respectively in the prescence of 10 equivalents of HS^- anion. The picture also show the changes of probes in the absence of HS^- (**1** (○), **2** (▽) and **3** (□)).*

Cell viability studies:

The selective and sensitive emission enhancements observed for the three probes in the presence of HS^- anion and the absence of any modulation of the fluorescence upon addition of GSH, Cys and Hcy strongly suggest that **1**-**3** can be used for HS^- detection and imaging in living cells. Based on these observations, the cytotoxicity of **1**-**3** was first evaluated. For this purpose HeLa cells were treated with the three probes at different concentrations (10, 20, 30 and 50 μM) over a 24-hour period and cell viability was determined by a WST-1 assay. The obtained results are shown in Figure 8. As seen, the three probes are essentially non-toxic in the range of concentrations tested.

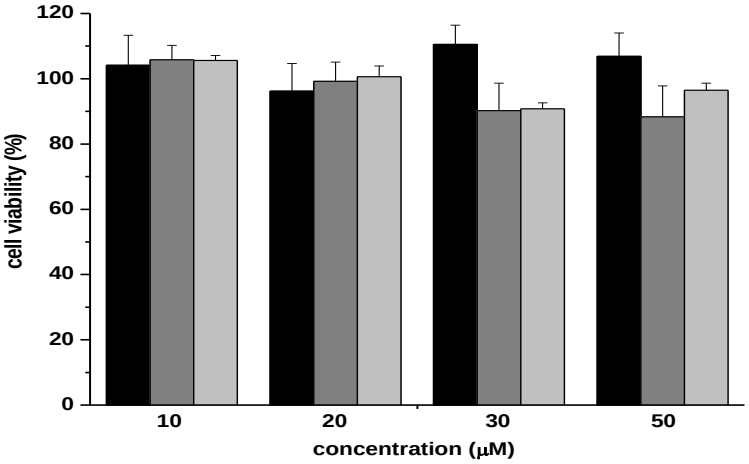

***Figure 8**. Cell viability assays. HeLa cells were treated with probes **1** (black), **2** (grey) and **3** (light grey) at concentrations between 10 and 50 μM for 24h. Then cell viability was quantified by means of WST-1 assay.*

Detection of HS^- in HeLa cells:

Once assessed the biocompatibility of the prepared probes and with the aim to test the probes in highly competitive environments, we prospectively used probe **1** for the fluorescence imaging of sulfide in living cells.

In a typical experiment, HeLa cells were incubated in DMEM supplemented with 10% fetal bovine serum. To conduct fluorescence microscopy studies, HeLa cells were seeded in 24 mm glass coverslips in 6-well plates and were allowed to settle for 24 h. Cells were treated with probe **1**, in PBS-DMSO 99:1 v/v, at final concentrations of 50 μM. After 30 minutes, the medium was removed and solutions of different concentrations of NaHS in PBS were added (0, 100, 200 and 500 μM) and cells were incubated for another 30-minute period. The result is shown in Figure 9. The control experiment (HeLa cells without dosimeters) and the cells incubated with **1** showed no fluorescence, whereas a marked enhancement in intracellular emission was observed in the HS^--treated cells. The emission enhancement observed is clearly dependent of the amount of NaHS added. The enhancement in the intracellular fluorescence intensity with **1** was

quantified by a standard image analysis and the results are shown in Figure 10. All, the above mentioned facts clearly indicated the possible use of probe **1** to detect hydrogen sulfide in complex media.

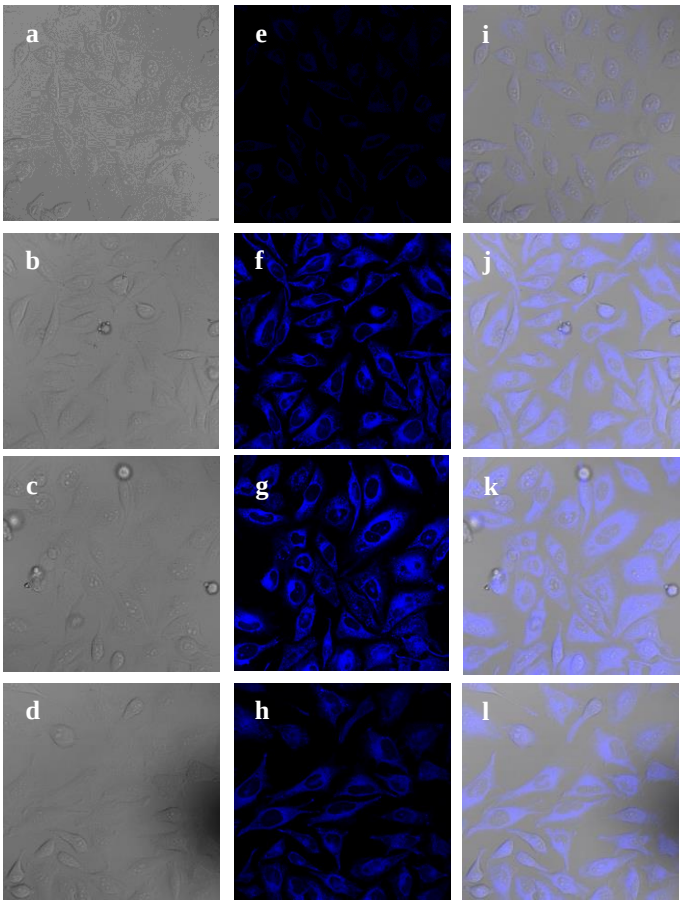

Figure 9. *Confocal microscopy images of H_2S detection in HeLa cells using probe **1** (a-d). Bright field images of the cells, (e,i) HeLa cells incubated with probe **1** for 30 minutes at 37 °C, (f,j) HeLa cells incubated with probe **1** for 30 minutes at 37 °C and 30 minutes incubated with 100 µM NaHS, (g,k) with 200 µM NaHS and (h,l) 500 µM NaHS. The excitation and emission wavelength were 420-440 nm and 490-530 nm.*

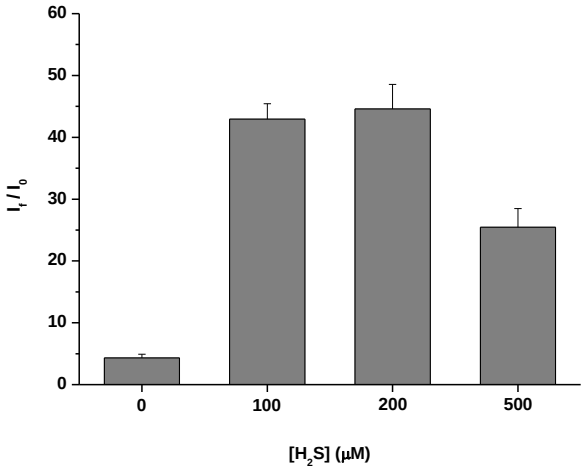

***Figure 10**. Average I_f/I_0 intensity ratios of probe **1** (50 μM) in HeLa cells after addition of 0, 100, 200 and 500 μM of Na_2S in PBS buffer. Representative fluorescence images from replicate experiments (n = 3) are shown. Error bars are (SD).*

Conclusions

In summary, we have synthesized three chemodosimeters (**1**-**3**) as fluorescence *turn-on* H_2S probes. HEPES (10 mM, pH 7.4)-DMSO 99:1 v/v solutions of the three probes are practically non-fluorescent and only the addition of HS^- anion induced remarkable emission enhancements. The emission enhancements observed are due to a selective sulfide-induced reduction of azide and sulfonylazide to amine (yielding **1b** and **2b**) and sulfonamide (yielding **3b**) moieties. Probes **1**-**3** can selectively and sensitively detect HS^- anion in water over other anions, biothiols and common oxidants. The titration profiles obtained upon addition of increasing quantities of HS^- anion to aqueous solutions of the three dosimeters allowed us to determine limits of detection of 0.17, 0.20 and 0.40 μM for **1**, **2** and **3**, respectively. Besides the three probes showed remarkably low sensitivities below the hydrogen sulfide concentration required to elicit physiological responses (10-1000 μM). Cell viability assays showed that **1**-**3** probes are essentially non-toxic in the 10-50 μM range. Moreover, real-time fluorescence imaging measurements have confirmed that probe **1** can be used to detect intracellular HS^- at micromolar concentrations.

Experimental Section

Materials and methods:

UV-visible spectra were recorded with a JASCO V-650 Spectrophotometer. Fluorescence measurements were carried out in a JASCO FP-8500 Spectrophotometer. ^{1}H and ^{13}C-NMR spectra were acquired in a BRUKER ADVANCE III (400 MHZ), where mass spectra were carried out in a TRIPLETOF T5600 (ABSciex, USA) spectrometer, IR in BRUKER TENSOR 27.

The chemicals 7-amino-4-(trifluoromethyl)coumarin, 4-amino-1-naphthalenesulfonic acid, 2-naphthalenesulfonyl chloride, sodium bicarbonate, sodium azide and sodium nitrite were purchased from Sigma-Aldrich. Hydrochloric acid (37%) and sulfuric acid (95%) were purchased from Scharlau (Barcelona, Spain).

Synthesis of probes 1 and 2:

7-Amino-4-(trifluoromethyl)coumarin (**1a**) or 4-amino-1-naphthalenesulfonic acid (**1b**) (0.22 mmol) were dissolved in 3.6 M H_2SO_4 (500 µL) and then cooled to 2 °C with an ice bath. After that, an aqueous solution of $NaNO_2$ (0.66 M, 1 mL, 0.66 mmol) was added dropwise over 10 minutes period. Then, NaN_3 aqueous solution (1.2 mL, 1.32 mmol) was added dropwise during 10 minutes and the reaction crude was stirred at 2 °C for an additional 40 minutes. Finally, the crude reaction was quenched by addition of concentrated NH_4OH (0.5 mL) and the final products (**1** and **2**) precipitated as white solids. The final probes were crystalized from ethanol (**1**: 53.6 mg, 0.21 mmol, 95% yield; **2**: 30.2 mg, 0.12 mmol, 55% yield).

1: ^{1}H NMR (400 MHz, DMSO) δ 7.71 (dd, *J* = 8.7, *J* = 1.0, 1H), 7.34 (d, *J* = 2.3 Hz, 1H), 7.23 (dd, *J* = 8.7, 2.3 Hz, 1H), 7.00 (br s, 1H).

^{13}C NMR (101 MHz, DMSO) δ 158.3, 155.0, 144.7, 126.3, 116.6, 115.7, 113.0, 112.9, 110.1, 107.6.

HRMS-EI *m/z*: calcd for $C_{10}H_4F_3N_3O_2$ 255.0256; found: 256.0123 ($M+H^+$).

2: ^{1}H NMR (400 MHz, DMSO) δ 8.85 (dd, *J* = 7.8, 1.5 Hz, 1H), 8.07 – 7.94 (m, 2H), 7.64 – 7.49 (m, 2H), 7.37 (d, *J* = 7.8 Hz, 1H).

^{13}C NMR (101 MHz, DMSO) δ 158.3, 155.0, 144.7, 126.3, 116.6, 115.8, 113.0, 110.1, 107.8.

HRMS-EI *m/z*: calcd for $C_{10}H_7N_3O_3S$ 249.0208; found: 250.0118 ($M+H^+$).

Synthesis of probe 3:

2-naphthalenesulfonyl chloride (**3a**, 1 g, 4.4 mmol) was dissolved in acetone (20 mL) and then an aqueous solution of NaN_3 (860 mg, 13.2 mmol, 4 mL) was added dropwise during 15 minutes. Afterwards, the crude reaction was stirred at room temperature for 24 hours. Then, acetone was eliminated using a reotary evaporator and the formed solid washed with water and with an aqueous solution of $Na_2S_2O_5$ (670 mg, 2.9 mmol, 65% yield).

^{1}H NMR (400 MHz, $CDCl_3$) δ 8.55 (d, *J* = 1.5 Hz, 1H), 8.04 (t, *J* = 9.0 Hz, 2H), 7.97 (d, *J* = 8.4 Hz, 1H), 7.90 (dd, *J* = 8.7, 2.0 Hz, 1H), 7.76 – 7.64 (m, 2H).

^{13}C NMR (101 MHz, $CDCl_3$) δ 135.8, 135.4, 132.1, 130.4, 130.1, 129.71, 128.3, 122.0.

HRMS-EI *m/z*: calcd for $C_{10}H_7N_3O_2S$ 233.0259; found: 234.0243 ($M+H^+$).

Cell culture conditions:

The HeLa human cervix adenocarcinoma cells were purchased from the German Resource Centre for Biological Materials (DSMZ) and were grown in DEM supplemented with 10% FBS. Cells were maintained at 37 °C in an atmosphere of 5% CO_2 and 95% air ad underwent passage twice in a week.

WST-1 cell viability assays:

Cells were cultured in sterile 96–well microtiter plates at a seeding density of 2.5 x 10^3 cells/well for HeLa and were allowed to settle for 24 h. Probes **1**, **2** and **3** were added to the cells at final concentrations of 10, 20, 30 and 50 μM. After 23 hours, WST-1 (7 μL of a 50 mg/ml solution) was added to each well. Cells were

further incubated for 1 hours (a total of 24 h of incubation was therefore studied). Then shaked thoroughly for 1 minute on a shaker and the absorbance was measured at 450 nm against a background control as blank using a microplate ELISA reader. The reference wavelength is 690 nm.

Live confocal microscopy:

Hela cells were seeded in 24 mm glass coverslips in 6-well microtiter plates at a seeding density of 10^{-5} cells/well. After 24 hours, cells were treated with probe **1** at a final concentration of 50 μM. After 30 minutes, the medium was removed to eliminate probe **1** and washed with PBS. Then a solution of Na_2S in PBS was added at a final concentrations of 0, 100, 200, 500 μM and cells were incubated during 30 minutes at 37 °C. After that, slides were washed twice with PBS to remove traces of the probe. Then slides were visualized under a confocal.

Confocal microscopy studies were performed by Confocal Microscopy Service. The images were acquired with a Leica TCS SP2 AOBS (Leica Microsystems Heidelberg GmbH, Mannheim, Germany) inverted laser scanning confocal microscope using oil objectives: 63X Plan-Apochromat-Lambda Blue 1.4 N.A. The excitation wavelength was 488 nm (argon laser). Two-dimensional pseudo colour images (255 colour levels) were gathered with a size of 1024 x 1024 pixels and Airy 1 pinhole diameter. All confocal images were acquired using the same settings and the distribution of fluorescence was analyzed using the Image J Software. Identical experiments were done three times to obtain reproducible results.

Acknowledgements

Financial support from the Spanish Government (Project MAT2012-38429-C04-01) and the Generalitat Valencia (Project PROMETEO/2009/016) is gratefully acknowledged. S.E. is grateful to the Generalitat Valenciana for his Santiago Grisolia fellow. C. T. also thanks the Ministerio de Ciencia e Innovación for her FPU

grant. L.E.S.F. thanks the Carolina Foundation and UPNFM-Honduras for his doctoral grant.

References

1. a) C. Szabo, *Nat. Rev. Drug. Discov.,* **2007**, *6*, 917–935; b) S. Fiorucci, E. Antonelli, A. Mencarelli, S. Orlandi, B. Renga, G. Rizzo, E. Distrutti, V. Shah, A. Morelli, *Hepatology.,* **2005**, *42*, 539–548.
2. a) L. E. McQuade, S. J. Lippard, *Curr. Opin. Chem. Biol.,* **2010**, *14*, 43–49; b) E. W. Miller, C. J. Chang, *Curr. Opin. Chem. Biol.,* **2007**, *11*, 620–625; c) N. Boens, V. Leen, W. Dehaen, *Chem. Soc. Rev.,* **2012**, *41*, 1130–1172.
3. A. K. Mustafa, M. M. Gadalla, N. Sen, S. Kim, W. Mu, S. K. Gazi, R. K. Barrow, G. Yang, R. Wang, S. H. Snyder, *Sci. Signaling.,* **2009**, *2*, ra72.
4. E. Blackstone, M. Morrison, M. B. Roth, *Science.,* **2005**, *308*, 518-519.
5. J. W. Elrod, J. W. Calvert, J. Morrison, J. E. Doeller, D. W. Kraus, L. Tao, X. Jiao, R. Scalia, L. Kiss, C. Szabo, H. Kimura, C.-W. Chow, D. J. Lefer, *Proc. Natl. Acad. Sci. U. S. A.*, **2007**, *104*, 15560-15565.
6. G. Yang, L. Wu, B. Jiang, B. Yang, J. Qi, K. Cao, Q. Meng, A. K. Mustafa, W. Mu, S. Zhang, S. H. Snyder, R. Wang, *Science.,* **2008**, *322*, 587-590.
7. G. Yang, L. Wu, R. Wang*, FASEB J.*, **2006**, *20*, 553-555.
8. A. Papapetropoulos, A. Pyriochou, Z. Altaany, G.Yang,A.Marazioti, Z. Zhou, M. G. Jeschke, L. K. Branski, D. N. Herndon, R. Wang, C. Szabó , *Proc. Natl. Acad. Sci. U. S. A.*, **2009**, *106*, 21972-21977.
9. K. Abe, H. Kimura, *J. Neurosci.*, **1996**, *16*, 1066-1071.
10. L. Li, M. Bhatia, Y. Z. Zhu, Y. C. Zhu, R. D. Ramnath, Z. J. Wang, F. B. Anuar, M. Whiteman, M. Salto-Tellez, P. K. Moore, *FASEB J.*, **2005**, *19*, 1196-1198.
11. W. Yang, G. D. Yang, X. M. Jia, L. Y. Wu, R. Wang, *J. Physiol.*, **2005**, *569*, 519-531.
12. K. Eto, T. Asada, K. Arima, T. Makifuchi, H. Kimura, *Biochem. Biophys. Res. Commun.,* **2002**, *293*, 1485-1488.
13. P. Kamoun, M.-C. Belardinelli, A. Chabli, K. Lallouchi, B. Chadefaux-Vekemans, *Am. J. Med. Genet. A.,* **2003**, *116A*, 310-311.
14. R. R. Moest, *Anal. Chem.,* **1975**, *47*, 1204-1205.
15. A. V. Kroll, V. Smorchkov, A. Y. Nazarenko, *Sensors Act. B Chem.,* **1994**, *21*, 97-100.
16. T. W. Mitchell, J. C. Savage, D. H. Gould, *J. Appl. Toxicol.,* **1993**, *13*, 389-394.
17. a) R. Martínez-Máñez, F. Sancenón, *Chem. Rev.,* **2003**, *103*, 4419-4476; b) M. E. Moragues, R. Martínez-Máñez, F. Sancenón, *Chem. Soc. Rev.,* **2011**, *40*, 2593-2643; c) L. E. Santos-Figueroa, M. E. Moragues, E. Climent, A. Agostini, R. Martínez-Máñez, F. Sancenón, *Chem. Soc. Rev.,* **2013**, *42*, 3489-3613; d) C. Coll, A. Bernardos, R. Martínez-Máñez, F. Sancenón, *Acc. Chem. Res.,* **2013**, *46*, 339-349.

18. a) K. Sasakura, K. Hanaoka, N. Shibuya, Y. Mikami, Y. Kimura, T. Komatsu, T. Ueno, T. Terai, H. Kimura, T. Nagano, *J. Am. Chem. Soc*., **2011**, *133*, 18003-18005; b) L. E. Santos-Figueroa, C. de la Torre, S. El Sayed, F. Sancenón, R. Martínez-Máñez, A. M. Costero, S. Gil, M. Parra, *Eur. J. Inorg. Chem.,* **2014**, 41-45; c) M. –Q. Wang, K. Li, J. –T. Hou, M. –Y. Wu, Z. Huang, X. –Q. Yu, *J. Org. Chem.,* **2012**, *77*, 8350-8354; d) C. Gao, X. Liu, X. Jin, J. Wu, Y. Xie, W. Liu, X. Yao, Y. Tang, *Sensors Act. B Chem.,* **2013**, *185*, 125-131; e) X. Hou, F. Zeng, F. Du, S. Wu, *Nanotechnology.,* **2013**, *24*, 335502; f) J. Wang, L. Long, D. Xie, Y. Zhan, *J. Lumin.,* **2013**, *139*, 40-46; g) X. Qu, C. Li, H. Chen, J. Mack, Z. Guo, Z. Shen, *Chem. Commun.,* **2013**, *49*, 7510-7512; h) X. Wu, H. Li, Y. Kan, B. Yin, *Dalton Trans.,* **2013**, *42*, 16302-16310; i) C. Kar, M. D. Adhikari, A. Ramesh, G. Das, *Inorg. Chem.,* **2013**, *52*, 743-752; j) F. Zheng, M. Wen, F. Zeng, S. Wu, *Sensors Act. B Chem.,* **2013**, *185*, 1012-1018.

19. a) C. Liu, B. Peng, S. Li, C. –M. Park, A. R. Whorton, M. Xian, *Org. Lett.,* **2012**, *14*, 2184-2187; b) C. Liu, J. Pan, S. Li, Y. Zhao, L. Y. Wu, C. E. Berkman, A. R. Whorton, M. Xian, *Angew. Chem. Int. Ed.,* **2011**, *50*, 10327-10329; c) Z. Xu, L. Xu, J. Zhou, Y. Xu, W. Zhu, X. Qian, *Chem. Commun.,* **2012**, *48*, 10871-10873; d) J. Liu, Y. -Q. Sun, J. Zhang, T. Yang, J. Cao, L. Zhang, W. Guo, *Chem. Eur. J.,* **2013**, *19*, 4717-4722.

20. a) C. Wei, Q. Zhu, W. Liu, W. Chen, Z. Xi, L. Yi, *Org. Biomol. Chem.,* **2013**, *11*, 479-485; b) C. Wei, L. Wei, Z. Xi, L. Yi, *Tetrahedron Lett.,* **2013**, *54*, 6937-6939; c) X. –F. Yang, L. Wang, H. Xu, M. Zhao, *Anal. Chim. Acta.,* **2009**, *631*, 91-95.

21. a) X. Cao, W. Lin, K. Zheng, L. He, *Chem. Commun.,* **2012**, *48*, 10529–10531; b) T. Liu, Z. Xu, D. R. Spring, J. Cui, *Org. Lett.*, **2013**, *15*, 2310-2313; c) Y. Liu, G. Feng, *Org. Biomol. Chem.,* **2014**, *12*, 438-445; d) S. El Sayed, C. de la Torre, L. E. Santos-Figueroa, R. Martínez-Máñez, F. Sancenón, A. M. Costero, M. Parra, S. Gil, *RSC Adv.,* **2013**, *3*, 25690-25693.

22. a) A. R. Lippert, E. J. New, C. J. Chang, *J. Am. Chem. Soc*., **2011**, *133*, 10078-10080; b) H. Peng, Y. Cheng, C. Dai, A. L. King, L. B. Predmore, D. J. Lefer, B. Wang, *Angew. Chem. Int. Ed*., **2011**, *50*, 9672-9675; c) S. K. Das, C. S. Lim, S. Y. Yang, J. H. Han, B. R. Cho, *Chem. Commun.,* **2012**, *48*, 8395-8397; d) Z. Wu, Z. Li, L. Yang, J. Han, S. Han, *Chem. Commun.,* **2012**, *48*, 10120-10122; e) S. Chen, Z. –J. Chen, W. Ren, H. –W. Ai, *J. Am. Chem. Soc.,* **2012**, *134*, 9589-9592; f) F. Yu, P. Li, P. Song, B. Wang, J. Zhao, K. Han, *Chem. Commun*., **2012**, *48*, 2852-2854; g) W. Xuan, R. Pan, Y. Cao, K. Liu, W. Wang, *Chem. Commun.,* **2012**, *48*, 10669-10671; h) L. A. Montoya, M. D. Pluth, *Chem. Commun.,* **2012**, *48*, 4767-4769; i) W. Sun, J. Fan, C. Hu, J. Cao, H. Zhang, X. Xiong, J. Wang, S. Cui, S. Sun, X. Peng, *Chem. Commun.,* **2013**, *49*, 3890-3892; j) T. Saha, D. Kand, P. Talukdar, *Org. Biomol. Chem.,* **2013**, *11*, 8166-8170; k) G. Zhou, H. Wang, Y. Ma, X. Chen, *Tetrahedron.,* **2013**, *69*, 867-870; l) C. Yu, X. Li, F. Zeng, F. Zheng, S. Wu, *Chem. Commun.,* **2013**, *49*, 403-405.

23. a) L. E. Santos-Figueroa, C. Giméñez, A. Agostini, M. D. Marcos, F. Sancenón, R. Martínez-Máñez, P. Amorós, *Angew. Chem. Int. Ed.,* **2013**, *52*, 13712-13716; b) E. Climent, A. Agostini, M. E. Moragues, R. Martínez-Máñez, F. Sancenón, T. Pardo, M. D. Marcos, *Chem. Eur. J.,* **2013**, *19*, 17301-17304; c) A. Agostini, M. Milani, R. Martínez-Máñez, M. Licchelli, J. Soto, F. Sancenón, *Chem. Asian. J.,* **2012**, *7*, 2040-2044; d) E. Climent, C. Giménez, M. D.

Marcos, R. Martínez-Máñez, F. Sancenón, J. Soto, *Chem. Commun.,* **2011**, *47*, 6873-6875; e) M. E. Moragues, J. Esteban, J. V. Ros-Lis, R. Martínez-Máñez, M. D. Marcos, M. Martínez, J. Soto, F. Sancenón, *J. Am. Chem. Soc.,* **2011**, *133*, 15762-15772; f) E. Climent, A. Martí, S. Royo, R. Martínez-Máñez, M. D. Marcos, F. Sancenón, J. Soto, A. M. Costero, S. Gil, M. Parra, *Angew. Chem. Int. Ed.,* **2010**, *49*, 5945-5948; g) E. Climent, M. D. Marcos, R. Martínez-Máñez, F. Sancenón, J. Soto, K. Rurack, P. Amorós, *Angew. Chem. Int. Ed.,* **2009**, *48*, 8519-8522.

24. a) F. Kazemi, A. R. Kiasat, S. Sayyahi, *Phosphorus, Sulfur Silicon Relat. Elem.,* **2004**, *179*, 1813-1817; L. Pang, D. Wang, J. Zhou, L. Zhang, X. Ye, *Org. Biomol. Chem.,* **2009**, *7*, 4252-4266.
25. J. C. Mathai, A. Missner, P. Kügler, S. M. Saparov, M. L. Zeidel, J. K. Lee, P. Pohl, *Proc. Natl. Acad. Sci. USA.,* **2009**, *106*, 16633-16638.
26. M. Hoffman, A. Rajapakse, X. Shen, K. S. Gates, *Chem. Res. Toxicol.,* **2012**, *25*, 1609-1615.

3. Organic-Inorganic Hybrid Materials in sensing protocols

The sections below are devoted to the use of functionalized organic-inorganic hybrid mesoporous silica materials in sensing protocols. The synthesis, characterization techniques and main features of silica-based materials will be reported.

3.1 Organic-inorganic Hybrid materials

Organic-inorganic hybrid materials are easily obtained by the covalent anchoring of organic compounds into 2D and 3D solid supports. The anchoring of organic molecules (such as receptors) on the surface of nanoscopic inorganic materials (support) can lead to hybrid organic-inorganic solids which present different properties often better than those of the isolated components.[50] The main advantages of anchoring receptors through the formation of covalent bond on inorganic supports are the following:

- Modulation of properties of the hybrid material by multi functionalization in successive steps.

- Improvement of the recognition process due to the restriction of the receptor movement upon anchoring onto the solid surface.

- Reversibility of the sensing system. If the coordination processes are reversible, the material could be reused several times.

- The possible control of size, shape and surface area can provide interesting changes on physical and chemical properties of the inorganic surface,[51] improving selectivity and sensitivity.[52]

[50] *The supramolecular chemistry of organic-inorganic hybrid materials*, *Ed.* K. Rurack, R. Martínez-Máñez, **2010**, Wiley.

[51] C. Sánchez, *J. Mater. Chem.*, **2005**, *15*, 3557.

[52] a) A. Verma, V. M. Rotello, *Chem. Commun.*, **2005**, *3*, 303; b) U. Drechsler, B. Erdogan, V. M. Rotello, *Chem. Eur. J.*, **2004**, *10*, 5570; c) A. B. Descalzo, R. Martínez-Máñez, F. Sancenón, K.

3.2 Mesoporous materials

According to the International Union of Pure and Applied Chemistry (IUPAC) pore sizes are classified into three main categories, namely *micro*-pores (<2 nm), *meso*-pores (2-50 nm) and *macro*-pores (>50 nm).[53] As a result to their large internal surface area, microporous and mesoporous materials are attracting research attention for applications in catalysis,[54] filtration and separation,[55] gas adsorption and storage,[56] enzyme immobilization,[57] drug delivery,[58] and chemical/biochemical sensing.[59]

Moreover, MCM mesoporous silica materials (where MCM stands for **M**obil **C**omposition of **M**atter), discovered in 1992 by Mobil Oil Company were the first mesoporous solid synthetized.[60] These materials showed a regular ordered pore arrangement and a very narrow pore-size distribution. It was demonstrated that by using different synthesis conditions (solvent, pH, temperature, concentration) different phases was possible to obtained such as the silica solid MCM-41 (with a hexagonal arrangement of the mesopores), MCM-48 (with a cubic arrangement of mesopores) and MCM-50 (with a lamellar structure) (see Figure 3.1). Besides, these materials are chemically inert, possess high thermal stability, have large specific surface areas (between 500 and 1000 $m^2 g^{-1}$), homogeneous pore size and a high pore volumes (in the order of 1 $cm^3 g^{-1}$).

Hoffmann, K. Rurack, *Angew. Chem. Int. Ed.*, **2006**, *45*, 5924; d) F. Mancin, E. Rampazzo, P. Tecilla, U. Tonellato, *Chem. Eur. J.*, **2006**, *12*, 1844; e) I. Willner, B. Basnar, B. Willner, *Adv. Funct. Mater.*, **2007**, *17*, 702.

[53] G. Zhao, *J. Mater. Chem*., **2006**, *16*, 623-625.

[54] D. E. De Vos, M. Dams, B. F. Sels, P. A. Jacobs*, Chem. Rev*., **2002**, 102, 3615.

[55] X. Liu, Y. Du, Z. Guo, S. Gunasekaran, C. -B. Ching, Y. Chen, S. S. J. Leong, Y. Yang, *Microporous Mesoporous Mater*., **2009**, *122*, 114.

[56] C. Ispas, I. Sokolov, S. Andreescu, Anal. *Bioanal Chem*., **2009**, *393*, 543.

[57] M. Vallet-Regi, M. Colilla, I. J. Izquierdo-Barba, *Biomed. Nanotechnol*., **2008**, *4*, 1.

[58] a) M. Vallet-Regi, F. Balas, D. Arcos, *Angew. Chem., Int. Ed*., **2007**, *46*, 7548; b) K. A. Kilian, T. Bocking, K. Gaus, J. King-Lacroix, M. Gal, J. J. Gooding, *Chem. Commun*., **2007**, 1936.

[59] a) K. A. Kilian, T. Boecking, K. Gaus, M. Gal, J. J. Gooding, *ACS Nano*., **2007**, *1*, 355; b) A. Jane, R. Dronov, A. Hodges, N. H. Voelcker, *Trends Biotechnol*., **2009**, *27*, 230.

[60] a) K. S. W. Sing, D. H. Everett, R. H. W. Haul, L. Moscou, R. A. Pierotti, J. Rouquerol, T. Siemieniewska, *Pure Appl. Chem.*, **1985**, *57*, 603; b) F. Hoffmann, M. Cornelius, J. Morell, M. Froba, Angew. *Chem. Int. Ed*., **2006**, *45*, 3216.

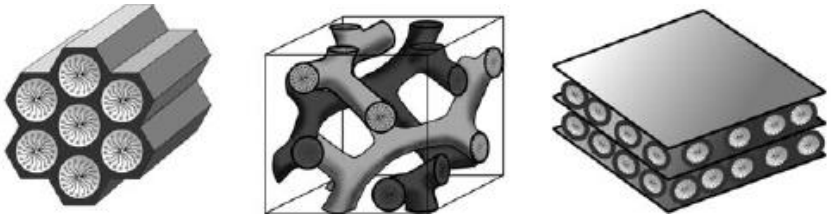

MCM-41 ***MCM-48*** ***MCM-50***

Figure 3.1. *Scheme of structures of mesoporous M41S phase materials. (Reprinted with permission from F. Hoffmann et al., Angew. Chem. Int. Ed., 2006, 45, 3216.Copyright © 2006 Wiley-VCH Verlag GmbH & Co. KGaA, Weinheim).*

3.2.1 Synthesis of mesoporous materials

Two main components are necessary to build up a system that presents a high ordered porous structure with homogeneous pore dimensions:

- a *template* whose function is to direct the construction of a high ordered (crystalline) porous net.

- a *polymeric precursor* which has to self-organize around the template and upon polymerization, build up the final rigid structure.

Structure-directing agents (SDAs) templates, as supramolecular ionic surfactants (long-chain alkyltrimethylammonium halides), were used in the synthesis of mesoporous materials. In the form of a lyotropic liquid-crystalline phase, SDAs lead to the assembly of an ordered mesostructured composite during the condensation of the silica precursors under basic conditions. M41S silica materials are usually synthesized in alkaline media with the cationic surfactant cetyltrimethylammonium bromide (CTABr) as the structure-directing agent. As explained above, MCM-41 is one of the best known and most widely studied mesoporous support and its synthesis is schematically represented in Figure 3.2.

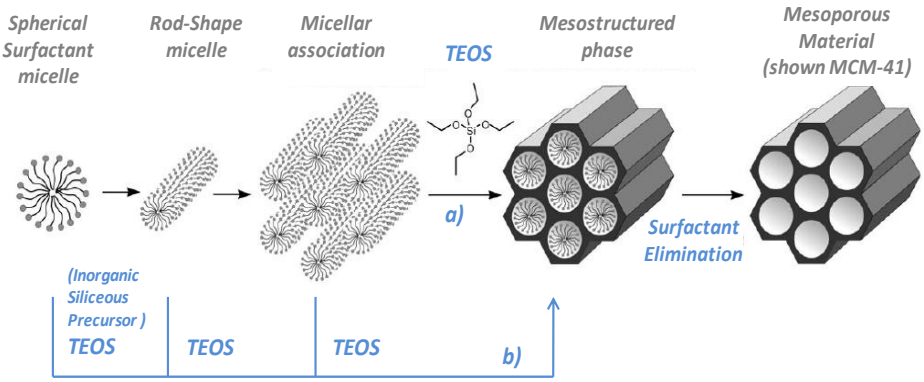

Figure 3.2. *Synthesis pathways of MCM-41 by structure-directing agents: a) true liquid-crystal template mechanism and b) cooperative liquid-crystal mechanism. (Reprinted and adapted with permission from F. Hoffmann et al., Angew. Chem. Int. Ed., 2006, 45, 3216.Copyright © 2006 Wiley-VCH Verlag GmbH & Co. KGaA, Weinheim).*

The first step in the synthesis of MCM-41 material is the preparation of the template to obtain the final hexagonal mesoporous phase (see Figure 3.2). Thus, as reported above, in the correct conditions of temperature, pH and concentration the surfactant firstly self-organizes into micelles and secondly micelles give origin to hexagonal shaped supra micellar aggregates. When the polymeric precursor tetraethyl orthosilicate (TEOS) added to the solution at basic pH, it polymerizes around the template giving rise to the final mesoporous scaffold with its pores full of surfactant. Depending on various reaction parameters (temperature, polymeric precursor, concentration and reaction time) nano or micro-particles can be specifically obtained.

The second step is the removal of surfactant by aerobic high temperature calcination (500-600 °C) or by extraction with adequate solvents. These procedures allowed to obtain the final mesoporous inorganic scaffold which presents cylindrical unidirectional empty channels of approximately 3 nm of diameter (when CTABr is used as surfactant) arranged in a hexagonal distribution. The principal advantage of this synthetic method is that the high grade of homogeneity of the initial elements (surfactant and polymer) is transmitted to the

final material, showing a system of pores not only homogeneously in size but also in form and regularity. Making small changes in the synthetic procedure, it is possible to modify final important features in the solid such as pore size (from 2 up to 50 nm) only by change the surfactant used as directing agent.[61]

3.2.2 Functionalization of inorganic silica scaffolds. Preparation of organic-inorganic mesoporous hybrid materials

The functionalization of the inorganic silica-based mesoporous scaffold can be easily carried out, bearing in mind that this support presents a high concentration of silanol (Si-OH) groups in its surface. These silanols can easily react with trialkoxysilane derivatives $(R'O)_3$-Si-R to generate organic–inorganic nanocomposites. By changing the chemical nature of R moiety different hybrid materials with selected properties and for different purpose can be prepared. In addition, these R groups can contain one or more reactive atoms, which can be later chemically modified. Two main procedures for the preparation of the organic-inorganic mesoporous hybrid materials have been described (see Figure 3.3).[62]

- ***Co-condensation***

  In this approach, trialkoxy organosilanes of the type $(R'O)_3SiR$ with structure-directing agents were incorporated simultaneously in the first step of the synthesis. This method leads to materials with organic residues anchored covalently to the pore walls (see also Figure 3.3). By using this procedure a homogeneous distribution of the organic moieties along the material particles and between the inner and outer surface is obtained. However, this method presented some drawbacks such as (a) the degree of mesoscopic order of the products decreases with increasing concentration of $(R'O)_3$-Si-R in the reaction mixture, (b) the proportion of terminal organic groups that are incorporated

[61] S. A. Bagshaw, E. Prouzet, T. J. Pinnavaia, *Science.*, **1995**, *269*, 1242.
[62] A. Vinu, K. Z. Hossain, K. Ariga, *Nanosci. Nanotech.*, **2005**, *5*, 347.

into the pore-wall network is generally lower than that corresponding to the starting concentration of the reaction mixture (homo condensation reactions between silanes groups are increased), (c) the homogeneous distribution of different organic functionalities in the framework cannot be ensured, (d) the incorporated organic groups can lead to a reduction in the pore diameter, pore volume, and specific surface areas. In this method, care must be taken in order to preserve the organic functionality during removal of the surfactant. This is achieved by changing the calcination procedures for an extraction method.[63,64]

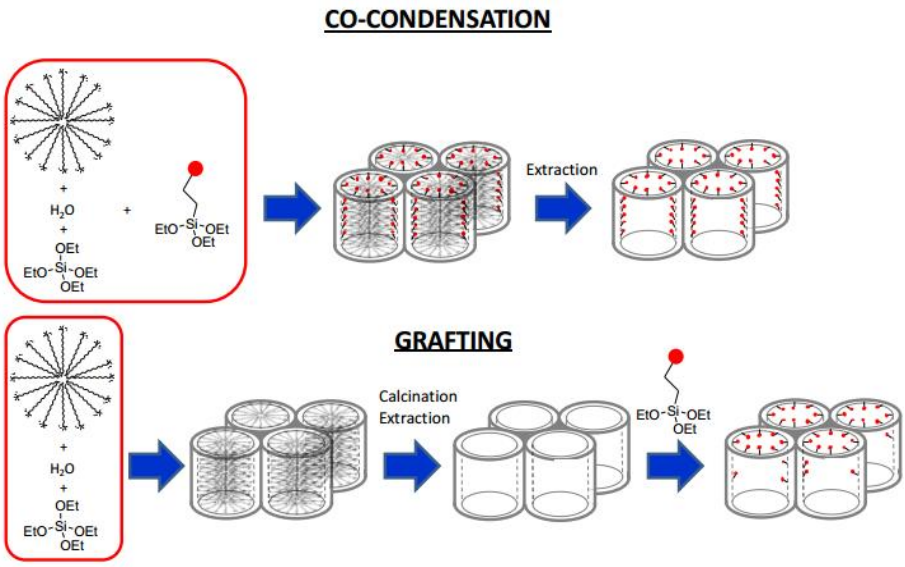

Figure 3.3. *A Schematic representations of the functionalization routes of siliceous mesoporous materials. Adapted from E. Climent PhD Thesis.*[65]

- ***Grafting***

Grafting refers to the subsequent modification of the surface of mesostructured silica phases, after the removal of surfactant, with organic groups (see Figure 3.3). This process is carried out primarily by reaction of

[63] S. Huh, J. W. Wiench, J.-C. Yoo, M. Pruski, V. S.-Y. Lin, *Chem. Mater.*, **2003**, *15*, 4247.
[64] J. Kecht, A. Schlossbauer, T. Bein, *Chem. Mater.*, **2008**, *20*, 7207.
[65] E. Climent, *Desing of new hybrid materials: Study of its application in new detection formats and in controlled release*, **2013**, ISBN: 978-84-9048-015.

organosilanes of the type $(R'O)_3$-Si-R, or less frequently chlorosilanes $ClSiR_3$, with the free silanol groups of the pore surfaces. By this modification method, the mesostructure of the starting silica phase is usually retained. However, when bulky organic moieties are used for functionalization certain pore blocking can be observed. Also a superficial modification is usually obtained using this functionalization method.[66,67]

3.2.3 Characterization of mesoporous materials.

MCM-41 material has a hexagonal packing of unidimensional cylindrical pores. In particular some different features should be considered: (a) the integrity of the mesoporous structure, (b) the organic matter content in the final material and (c) the particles average diameter and particle's shape. Different techniques for characterization of this type of structure are powder X-ray diffraction (PXRD), transmission electron microscopy (TEM), adsorption analysis and nuclear magnetic resonance spectroscopy (NMR).[68]

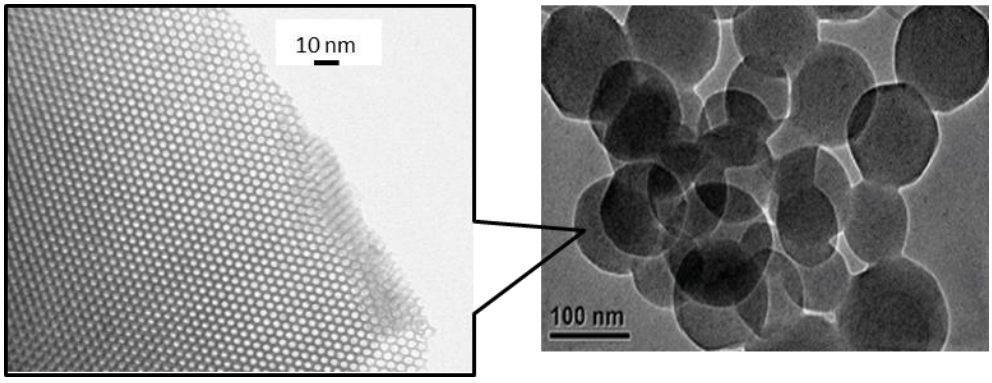

Figure 3.4. *TEM micrographs of MCM-41 at 10 and 100 nm.*

The typical MCM-41 PXRD pattern shows three to five reflections between $2\Theta = 2^{o}$ and 5^{o}, corresponding to the ordered hexagonal array of parallel silica tubes

[66] F. Juan, E. Ruiz-Hitzky, *Adv. Mater.,* **2000**, *12*, 430.

[67] F. Hoffmann, M. Cornelius, J. Morell, M. Fröba., *Angew. Chem. Int. Ed*., **2006**, *45*, 3216.

[68] U. Ciesla, M. Grün, T. Isajeva, A. A. Kurganov, A. V. Neimark, P. I. Ravikovitch, S. Schacht, F. Schüth, K. K. Unger., *Access in Nanoporous Materials;* T. J. Pinnavaia, M. F. Thorpe, Eds, *Plenum Press*, New York, **1995**.

and can be indexed assuming a hexagonal unit cell as (100), (110), (200), (210) and (300). Besides PXRD pattern, TEM can indicate the hexagonal arrangement where parallel lines observed in the micrographs are related to the hexagonal repeat between tubes and a uniform pores (size around 2-4 nm). (see Figure 3.4).[69]

The organic content of the final hybrid material can be determined by thermogravimetric (TGA) and elemental analysis (EA). For example when a mesoporous silica-based scaffold is firstly loaded with certain compound and subsequentaly functionalized on the surface with different trialkoxysilane derivatives, TGA and EA techniques can not be enough to fully characterize the final material.Therefore it can be useful to combine these characterization methods with UV-visible or chromatographic measurements to calculate the quantity of the loaded compound. From the difference between the total organic matter obtained by TGA, EA and the loaded cargo (calculated by UV-visible) the amount of the organic compounds anchored on the external surface can be obtained. Moreover the demonstration of effective loading and grafting procedures can be assessed by nitrogen adsorption desorption measurements.[70] This technique allows to determine the specific surface area of the material, at this respect a comparison between a calcined MCM-41 (very high specific surface area) and a loaded and functionalized MCM-41 scaffold (low specific surface area) is indicative of a correct pore filling.[71] Besides, the wall thickness of the pore wall can be calculated by difference between the lattice parameter ($a=2d_{(100)}/\sqrt{3}$) determined by X-Ray diffraction and the pore size obtained from the adsorption isotherm.[72]

The remarkable features of mesopouros silica materials such as chemical inertness, thermal stability, high surface area, high load capacity, uniform and

[69] A. Chenite, Y. LePage, A. Sayari, *Chem. Mater.*, **1995**, *7*, 1015.
[70] C. –Y. Chen, H. –X. Li, M. E. Davis, *Microporous Mater.*, **1993**, *2*, 17.
[71] a) E. P. Barrett, L. G. Joyner, P. P. Halenda. *J. Am. Chem. Soc.*, **1951**, *73*, 373; b) M. Kruk, M. Jaroniec, *Chem. Mater.*, **2001**, *13*, 3169.
[72] A. Corma, Q. Kan, M. T. Navarro, J. Perez-Pariente, F. Rey, *Chem. Mater.*, **1997**, *9*, 2123.

tuned pores system and biocompatibility[73] boosted the use of these materials in several technological and scientific applications. Significant are the applications of these inorganic supports in catalytic processes[74] and in transport of molecules to specific locations.[75] However, one of the most promising uses deals with the controlled release of certain chemicals (stored inside the porous network) upon the application of a certain stimuli (controlled release).[76]

3.2.4 Gated materials

Uncapped mesoporous materials have been extensively used as vehicles to store and subsequently release certain organic molecules. This application is a direct consequence of the presence of a uniform pore network that grants a high load capacity of large amounts of chemicals. In these materials the delivery process is regulated by a simple diffusion process and in general, it is very difficult to control the amount of delivered cargo. In the last years the use of mesoporous gated materials has suffered a remarkable increase. Molecular gates can be defied as supramolecular-based devices attached into the external surfaces of certain inorganic supports in which mass transport can be triggered by target external stimulus that can control the state of the gate (open or closed) at will.[77] In gated materials, the chemical properties of the anchored molecule (polarity, conformation, size, charge, shape) can be modified on command upon the application of an external stimuli resulting in cargo release (see Figure 3.5).

[73] a) M. Vallet-Regi, A. Rámila, R. P. del Real, J. Pérez-Pariente, *J. Chem. Mater.* **2001**, *13*, 308; b) B. Muñoz, A. Rámila, J. Pérez-Pariente, I. Díaz, M. Vallet-Regi, *Chem. Mater.,* **2003**, *15*, 500.

[74] K. Moller T. Bein, *Chem. Mater*., **1998**, *10*, 2950–2963.

[75] a) J. M. Rosenholm, E. Peuhu, L. T. Bate-Eya, J. E. Eriksson, C. Sahlgren, M. Linden, *Small*, **2010**, *6*, 1234; b) M. Liong, J. Lu, M. Kovochich, T. Xia, S. G. Ruehm, A. E. Nel, F. Tamanoi, J. I. Zink, *ACS Nano.*, **2008**, *2*, 889.

[76] K.K. Cotí, M. E. Belowich, M. Liong, M. W. Ambrogio, Y. A. Lau, H. A. Khatib, J. I. Zink, N. M. Khashab, J. F. Stoddart, *Nanoscale.,* **2009**, *1*, 16.

[77] a) N. K. Mal, M. Fujiwara, Y. Tanaka, *Nature*., **2003**, 421, 350; b) I. –l. Slowing, J. L. Vivero-Escoto, B. G. Trewyn, V. S. –Y. Lin, *J. Mater. Chem*., **2010**, *20*, 7924.

Several molecular and supramolecular systems have been developed which are able to trigger the entrapped cargo using several external stimuli such as pH,[78] changes in redox potential,[79] temperature[80] and the presence of certain ions, molecules or biomolecules.[81]

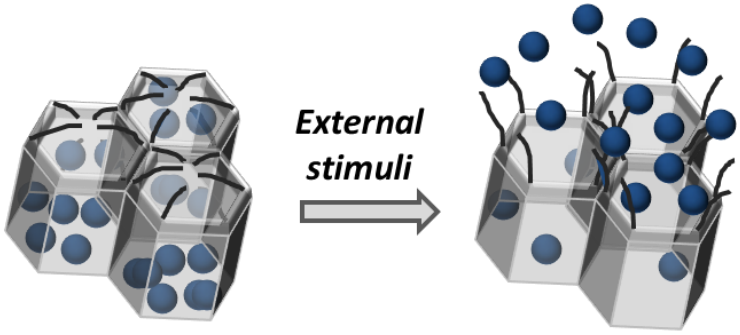

Figure 3.5. *A schematic representation of a gated material. The scheme represents a mesoporous support loaded with certain guest molecules and with a suitable molecular ensemble anchored in the pore outlets (molecular gate). The application of an external stimulus allows the release of the entrapped cargo due to changes in the capping ensemble.*

3.2.5. Gated materials in sensing protocols

Silica mesoporous materials bearing gate-like ensembles can be used for on-command delivery applications in the presence of different physical or (bio)-chemical stimuli. However in the last years, the possibility of designing gated

[78] a) Q. Yang, S. Wang, P. Fan, L. Wang, Y. Di, K. Lin, F. –S. Xiao, *Chem. Mater*., **2005**, *17*, 5999; b) S. Angelos, Y. –W. Yang, K. Patel, J. F. Stoddart, J. I. Zink, *Angew. Chem. Int. Ed.*, **2008**, *47*, 2222; c) Y. Klichko, N. M. Khashab, Y. –W. Yang, S. Angelos, J. F. Stoddart, J. I. Zink, *Micropor. Mesopor. Mater.*, **2010**, *132*, 435; d) J. Liu, X. Du, *J. Mat. Chem.*, **2010**, *20*, 3642.

[79] a) R. Liu, X. Zhao, T. Wu, P. Feng, *J. Am. Chem. Soc.*, **2008**, *130*, 14418; b) R. Mortera, J. Vivero-Escoto, I. I. Slowing, E. Garrone, B. Onida, V. S.-Y. Lin, *Chem. Commun.,* **2009**, 3219; c) Y. N. Cui, H. Q. Dong, X. J. Cai, D. P. Wang, D. P. Li, *ACS Appl. Mater. Interfaces.,* **2012**, *4*, 3177.

[80] a) C. Liu, J. Guo, W. Yang, J. Hu, C. Wang, S. Fu, *J. Mat. Chem.*, **2009**, *19*, 4764; b) J. Lai, X. Mu, Y. Xu, X. Wu, C. Wu, C. Li, J. Chen, Y. Zhao, *Chem. Commun.,* **2010**, *46*, 7370; c) C. R. Thomas, D. P. Ferris, J. –H. Lee, E. Choi, M. H. Cho, E. S. Kim, J. F. Stoddart, J. –S. Shin, J. Cheon, J. I. Zink, *J. Am. Chem. Soc.*, **2010**, *132*, 10623.

[81] a) C. Coll, R. Casasús, E. Aznar, M. D. Marcos, R. Martínez-Máñez, F. Sancenón, J. Soto, P. Amorós, *Chem. Commun.*, **2007**, 1957; b) T. D. Nguyen, K.C.-F. Leung, M. Liong, Y. Liu, J. F. Stoddart, J. I. Zink, *Adv. Funct. Mater*., **2007**, *17*, 2101; c) E. Aznar, C. Coll, M. D. Marcos, R. Martínez-Máñez, F. Sancenón, J. Soto, P. Amorós, J. Cano, E. Ruiz, *Chem. Eur. J.*, **2009**, *15*, 6877; d) Y. Zhao, B. G. Trewyn, I. I. Slowing, V. S.-Y. Lin, *J. Am. Chem. Soc.,* **2009**, *131*, 8398; e) R. Klajn, J. F. Stoddart, B. A. Grzybowski, *Chem. Soc. Rev*., **2010**, *39*, 2203; f) C. Coll, L. Mondragón, R. Martínez-Máñez, F. Sancenón, M. D. Marcos, J. Soto, P. Amorós, E. Pérez-Payá, *Angew. Chem. Int. Ed*., **2011**, *50*, 2138.

materials capable of responding specifically to a certain target molecule as a suitable method for developing new protocols for sensing applications has been described.[82]

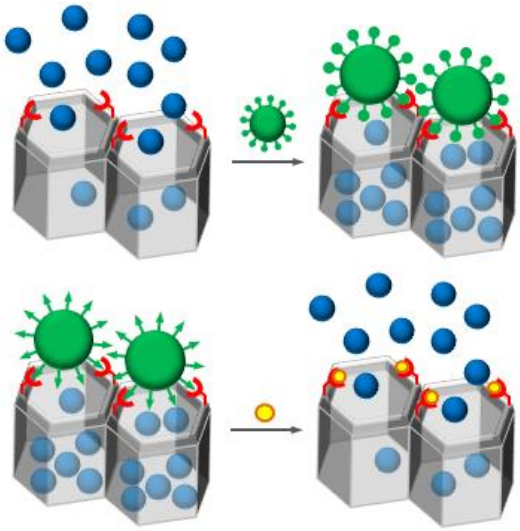

Figure 3.6. *Scheme of the recognition paradigm using nanoscopic gate-like scaffoldings. Up: inhibition of dye release due to the coordination of the selected analyte with the anchored binding sites. Down: uncapping pores by an analyte-induced displacement reaction. Adapted from Acc. Chem. Res.,* ***2013****, 46, 339. Copyright © 2013, American Chemical Society.*

The underlying idea is that the coordination or reaction of the target analyte with the binding sites could modulate the transport of the dye from pores to the solution and would result in a chromo-fluorogenic signal. Two possible situations can be envisioned (see Figure 3.6). In one pores remain open and the indicator can diffuse into the solution, whereas in the presence of a target analyte this molecule or ion can bind to receptors and close the gate. In a second approach, the starting material is capped and the presence of a target analyte induces pore opening and dye delivery. One of the advantages of both approaches is the presence of amplification features. At this respect, the presence of few analyte molecules induced the inhibition or the release of a relatively high amount of dye entrapped in the inner of the pores with the subsequent signal amplification.

[82] a) C. Coll, A. Bernardos, R. Martínez-Máñez, F. Sancenón, *Acc. Chem. Res*., **2013**, *46*, 339; b) M. W. Ambrogio, C. R. Thomas, Y.-L. Zhao, J. I. Zink and J. F. Stoddart, *Acc. Chem. Res*., **2011**, *44*, 903.

The first example of a gated mesoporous material used in sensing protocols was prepared by Martínez-Máñez and coworkers in 2006.[83] This consisted in an MCM-41 mesoporous material loaded with the $[Ru(bpy)_3]^{2+}$ indicator and polyamine moieties which act as receptors (see Figure 3.7). At pH 7.8 water suspensions of the solid showed an intense yellow color because polyamines are unprotonated, the molecular gate is open and the ruthenium complex is released into the solution. However, the presence of ATP and ADP allowed to selectively inhibit the indicator release by the formation of strong complexes with tethered polyamines through hydrogen bonding and electrostatic interactions. Other anions such as chloride, sulfate or GMP are too small or form complexes that are too weak to effectively close pores and they cannot stop the $[Ru(bpy)_3]^{2+}$ dye from leaching.

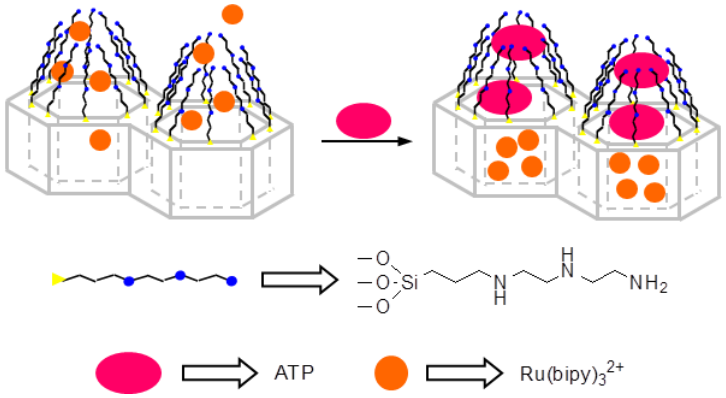

Figure 3.7. *Schematic representation of ATP recognition by inhibiting dye release with nanoscopic supramolecular gate like systems on mesoporous MCM-41.*

A gated material for the selective detection of methylmercury has also been prepared (see Figure 3.8).[84] The sensing gated support consists of a mesoporous support loaded with safranine O and capped with 2,4-bis(4-dialkylaminophenyl)-3-hydroxy-4-alkylsulfanylcyclobut-2-one (APC) groups (formed by the reaction of a squaraine dye and surface grafted thiols). Acetonitrile-toluene 4:1 v/v suspensions

[83] R. Casasús, E. Aznar, M. D. Marcos, R. Martínez-Máñez, F. Sancenón, J. Soto, P. Amorós, *Angew. Chem. Int. Ed.*, **2006**, *45*, 6661.

[84] E, Climent, M. D. Marcos, R. Martínez-Mañez, F. Sancenón, J. Soto, K. Rurack, P. Amoros, *Angew. Chem. Int. Ed.*, **2009**, *48*, 8519.

of gated solid remained capped due to the presence of the bulky APC groups. However, addition of methylmercury induces the uncapping of pores with the subsequent release of entrapped safranine O. This uncapping process is a direct consequence of the reaction of methylmercury with the thiol group (on APC moieties) resulting in the coordination of the cation to thiols and in the release of the squaraine. An inherent feature of such capped systems is the potential achievement of signal amplification. In this particular system for instance, the reaction of one equivalent of methylmercury with the APC groups leads to the delivery of one squaraine and of around 200 safranine O molecules.

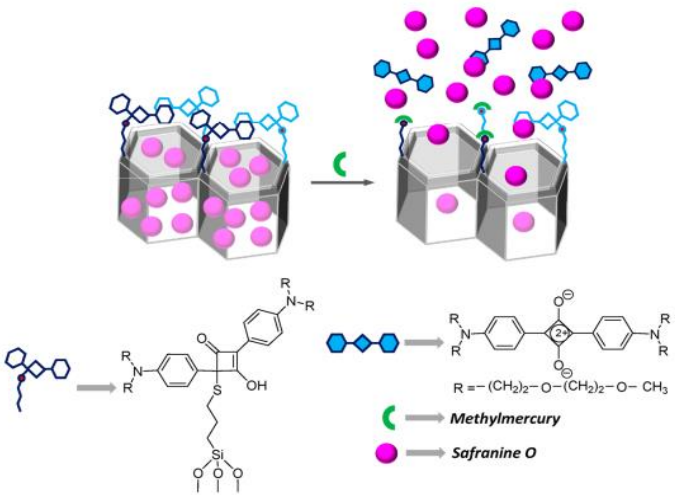

Figure 3.8. *Chromo-fluorogenic detection of methylmercury using mesoporous support loaded with safranine O and entrapped by APC groups.*

Antigen-antibody interactions have been also used as triggers for the detection of sulfathiazole.[85] For this purpose, the mesoporous support was loaded with $[Ru(bipy)_3]^{2+}$ and the derivative 4-(4-amino-benzenesulfonylamino)-benzoic acid was anchored onto the outer surface. Finally, the pores were capped with a polyclonal antibody for sulfathiazole (see Figure 3.9). Delivery of the entrapped complex from the capped material in the presence of a family of sulfonamides

[85] E. Climent, A. Bernardos, R. Martínez-Mañez, A. Maquieira, M. D. Marcos, N. Pastor-Navarro, R. Puchades, F. Sancenòn, J. Soto, P. Amorós, *J. Am. Chem. Soc.*, **2009**, *131*, 14075.

was studied in buffered aqueous solutions. A remarkable and highly selective uncapping of pores and the subsequent dye delivery is seen for sulfathiazole.

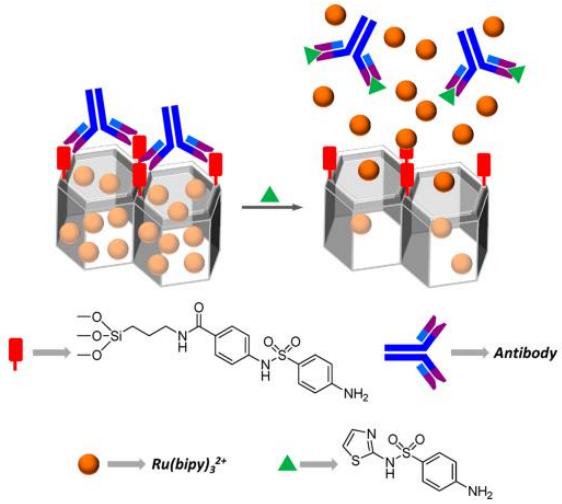

Figure 3.9. *Schematic representation of gated material capped with antibody and structures of hapten and the antigen sulfathiazole.*

Aptamer capped mesoporous silica nanoparticles that were uncapped in the presence of ATP were prepared by Wang and co-workers.[86] For this purpose, mesoporous silica nanoparticles were selected as inorganic scaffold. The as synthesized nanoparticles were functionalized with 3-cloropropyltrimethoxysilane and then the structure directing agent extracted with HCl-ethanol. Then, the chloride atom on the outer surface was transformed into an azide moiety by the reaction with NaN_3. On the other hand, ATP aptamer (5'-CAC CTG GGG GAG TAT TGC GGA GGA AGG TT-3') was hybridized with two different ssDNA (5'-alkyne-TTC CTC CGC A-3' and 5'-alkyne-ATA CTC CC-3') yielding a sandwich type DNA structure. The pores of the inorganic scaffold functionalized with azide moieties were loaded with $[Ru(bipy)_3]^{2+}$ and then capped through a click chemistry reaction with the sandwidh type DNA structure containing the ATP aptamer sequence. The grafting of the sandwich type DNA sequence completely blocks the pores inhibiting dye release (see Figure 3.10). However, upon addition of ATP a massive

[86] X. He, Y. Zhao, D. He, K. Wang, F. Xu, J. Tang, *Langmuir*., **2012**, *28*, 12909−12915.

dye release is observed. This cargo release is a consequence of the competitive displacement of the ATP aptamer from the sandwich type DNA after coordination with the added ATP. The release of $[Ru(bipy)_3]Cl_2$ fluorophore is only observed when ATP is present and for instance GTP, CTP and UTP were unable to displace ATP aptamer from the hybrid nanoparticles.

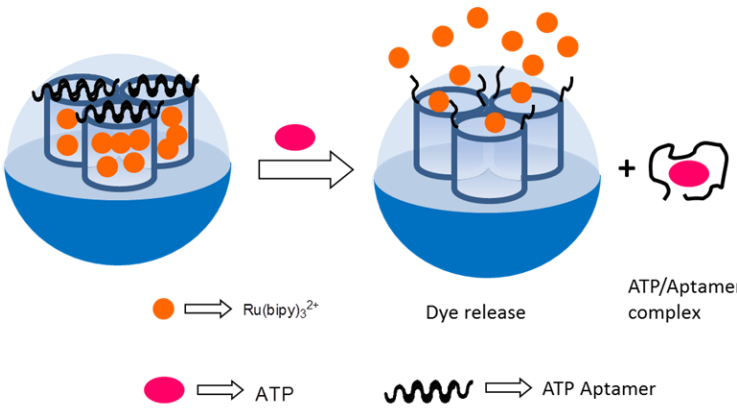

Figure 3.10. *Schematic representation of aptamer-based ATP responsive MSN System.*

Gated materials have also been used for the detection of neutral molecules such as nitroaromatic explosives.[87] For this purpose, MCM-41 was selected as inorganic scaffold and then the pores were loaded with $Ru(bipy)_3^{2+}$ dye. Then, the external surface was functionalized with a pyrene derivative using a click chemistry reaction (see Figure 3.11). The presence of a dense pyrene network around the pore outlets inhibited dye delivery. Upon addition of nitroaromatic explosives (Tetryl and TNT) a massive dye release was observed due to pore opening as a consequence of the formation of strong pyrene (electron donor)-nitroaromatic explosives (electron acceptor) charge transfer interactions. This material was used for the detection of explosives in soil samples with fine results.

[87] Y. Salinas, A. Agostini, É. Pérez-Esteve, R Martínez-Máñez, F. Sancenón, M. D. Marcos, J. Soto, A. M. Costero, S, Gil, M. Parra, P. Amorós, *J. Mater. Chem. A.,* **2013***, 1*, 3561.

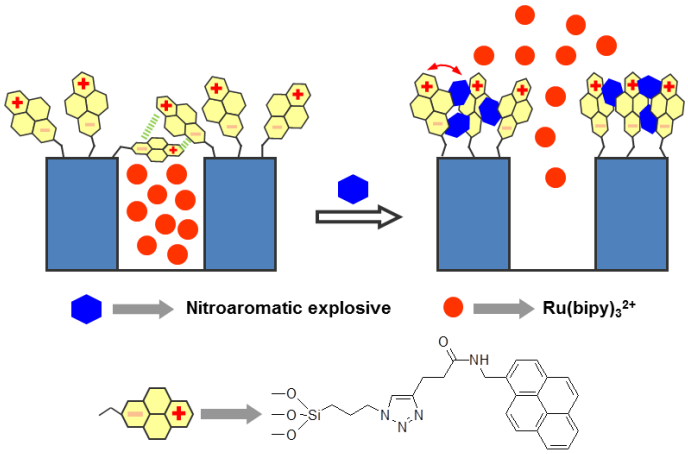

Figure 3.11. *Schematic representation of a gated material for the detection of nitroaromatic explosives. Adapted from J. Mater. Chem. A.,* ***2013****, 1, 3561. Copyright ©Royal Society of Chemistry.*

3.3 Objectives

In this chapter we focus on the designing of mesopourous hybrid materials for the selective colorimetric detection of glutathione and hydrogen sulfide. Particularly, our aim was:

- Synthesis and characterization of a hybrid organic-inorganic gated mesoporous material for the chromo-fluorogenic detection of glutathione.
- Synthesis and characterization of a hybrid organic-inorganic gated mesoporous material for the chromo-fluorogenic detection of HS^-.
- To evaluate the response of the prepared hybrid materials in the presence or absence of selected analytes.

Highly selective and sensitive detection of glutathione using mesoporous silica nanoparticles capped with disulfide-containing oligo(ethylene glycol) chains

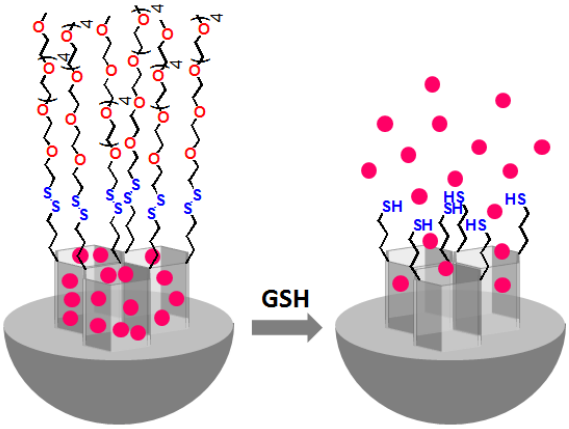

Highly selective and sensitive detection of glutathione using mesoporous silica nanoparticles capped with disulfide-containing oligo(ethylene glycol) chains

Sameh El Sayed,[a,b,c] Cristina Giménez,[a,b,c] Elena Aznar,[a,c] Ramón Martínez-Máñez,[a,b,c] Félix Sancenón [a,b,c] and Maurizio Licchelli *[d]*

[a] Centro de Reconocimiento Molecular y Desarrollo Tecnológico (IDM), Unidad Mixta Universidad Politécnica de Valencia-Universidad de Valencia, Spain.
[b] Departamento de Química, Universidad Politécnica de Valencia, Camino de Vera s/n, 46022, Valencia, Spain.
E-mail: rmaez@qim.upv.es
[c] CIBER de Bioingeniería, Biomateriales y Nanomedicina (CIBER-BBN).
[d] Dipartimento di Chimica, Università di Pavia, via Taramelli 12, 27100 Pavia, Italy. E-mail: maurizio.licchelli@unipv.it

Received: 30 September 2014,
First published on the web: 26 November 2014

Org. Biomol. Chem., ***2015***, *13, 1017–1021*

(Reproduced with permission of Royal Society of Chemistry 2015)

Mesoporous silica nanoparticles loaded with safranin O and capped with disulfide-containing oligo(ethylene glycol) chains were used for the selective and sensitive fluorimetric detection of glutathione.

Biothiols such as cysteine (Cys), homocysteine (Hcy), and glutathione (GSH) are of vital importance in cellular processes, especially in preventing the damage to cellular components caused by reactive oxygen species.[1] Biothiols are controlled by the equilibrium between thiols and disulfides and their relative levels in cells are closely related to aging and many diseases, such as cancer,[2] AIDS,[3] cystic fibrosis,[4] and neurodegenerative pathologies.[5] In particular, GSH is a fundamental small peptide having many biological functions such as maintenance of intra-cellular redox activity, xenobiotic metabolism, intra-cellular signal transduction and gene regulation.[6] Besides, several diseases have been associated with a decrease in plasma of GSH concentrations. For instance, low levels of GSH are involved in leucocyte loss,[7] psoriasis,[8] liver damage,[9] cancer[2] and AIDS.[3]

In this context, different analytical methods are currently available for GSH determination including HPLC,[10] capillary electrophoresis,[11] mass spectrometry,[12] etc. Moreover recently, the preparation of chromo-fluorogenic probes for the detection of thiol-cotaining bio-molecules has increased in interest. In most cases, these probes are designed following the chemodosimeter approach, which makes use of the high nucleophilic reactivity of the thiol functional group.[13] However, many of these probes only display sensing features in organic or mixed water-organic solvents and it is not unusual to observe a similar response for closely related species such as Cys, Hcy and GSH.[14] Besides, very recently, simple molecular probes for the selective recognition of GSH in aqueous environments have also been described.[15] As an alternative to molecular probes for GSH detection, the development of nano sensing systems has emerged in the last years. In particular, gold nanoparticles,[16] gold nanoclusters[17] and quantum dots[18] have been used for the optical sensing of GSH. From a different point of view there is an increasing interest in the design of responsive nanoscopic hybrid gated materials containing caps and showing the ability to release entrapped guests

upon application of external stimuli.[19] These devices usually contain a silica mesoporous support, in which the cargo is stored and molecular or supramolecular entities attached on the external surface that act as "gates" allowing the controlled release of entrapped molecules at will. Both components, *i.e.* gate and cargo have been carefully selected to achieve a wide range of control functions in most cases for drug delivery applications. Moreover, we have recently suggested that the use of gated materials can also be applied to the development of optical probes.[20] The underlying idea here is that the coordination or reaction of the target analyte with the binding sites could modulate dye delivery from pores to the solution resulting in a chromo-fluorogenic signal. One advantage of this approach is the potential existence of amplification features; in particular, the presence of few analyte molecules may induce the release of a relatively high amount of entrapped dye molecules. For these reasons, very recently, the application of gated materials in sensing protocols has deserved great attention.[21]

Given our interest in the application of capped mesoporous materials in sensing and recognition protocols,[22] we report herein the design of a simple capped system for the selective optical detection of GSH. Our proposed paradigm is briefly represented in Scheme 1. MCM-41 mesoporous silica nanoparticles (MSN) of *ca*. 100 nm were selected as support. MSN were loaded with a suitable dye (safranine O), and then the external surface was functionalized with disulfide-containing oligo(ethylene glycol) groups which act as molecular gates (solid **S1**). The signalling paradigm relies on the selective reduction of the disulfide bond by GSH which was expected to result in pore opening and dye release. In this context it should be noted that although disulfide-containing gated materials have been used for drug delivery in cells there are not as far as we know, specifically designed capped systems for GSH detection.[23] However, taking into account the possible use of different thiol-selective gate-like systems and choice of a wide range of indicator dyes, this tailor-made strategy displays enormous potential and is yet to be explored.

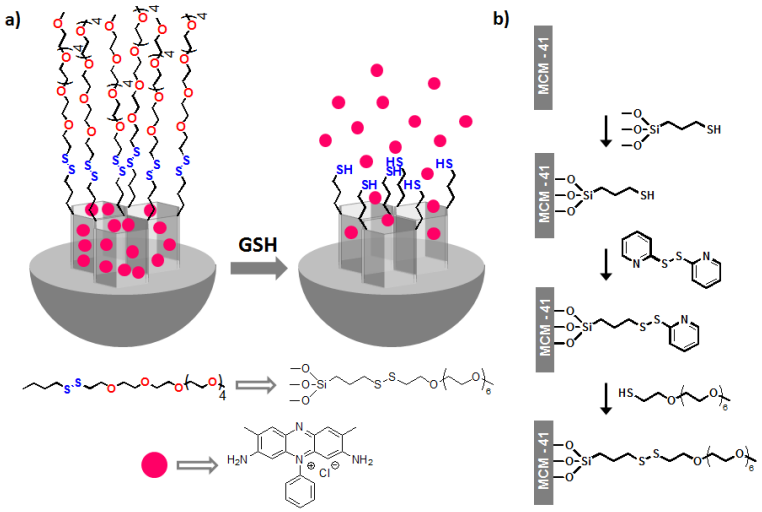

Scheme 1. *(a) Schematic representation of the sensing mechanism of solid **S1** in the presence of GSH. (b) Sequence of reactions used to anchor the molecular gate onto the outer surface of the loaded inorganic support.*

MCM-41 mesoporous nanoparticles were synthesized according to reported procedures.[24] Then, the pores of calcined MCM-41 were loaded with safranine O by stirring overnight at room temperature a suspension of the nanoparticles in an acetonitrile solution of the dye. Afterward, an excess of (3-mercaptopropyl) trimethoxysilane was added and the thiol-functionalised solid was further reacted with 2,2'-dipyridyl disulfide. Finally the preparation of **S1** was achieved by reaction of with *O*-(2-mercaptoethyl)-*O*'-methyl-hexa(ethylene glycol). The mixture was stirred for 12 h and the final support **S1** was isolated by centrifugation, washed with abundant water and dried (see Supporting Information for details).

The MCM-41 scaffold and the final sensing mesoporous solid **S1** were characterized using standard techniques. The main structural properties obtained from these studies such as particle diameter, BET specific surface area, pore volumes and pore sizes are listed in Table 1 (see Supporting Information for additional information). Powder X-ray diffraction (PXRD) and transmission electron microscopy (TEM) carried out on the MCM-41 nanoparticles showed clearly the presence of a mesoporous structure that remained in the final solid **S1** despite the loading process with the dye and further functionalization with

oligo(ethylene glycol) chains (see Figure 1 for TEM images). Moreover, contents of safranin O and the disulfide-containing oligo(ethylene glycol) groups in **S1** were determined by elemental and thermogravimetric analyses gaving values of 0.30 mmol g^{-1} and 0.86 mmol g^{-1}, respectively.

***Table 1**. Main structural properties calculated from TEM, PXRD and N_2 adsorption analysis.*

Sample	Diameter particle[a] (nm)	S_{BET} ($m^2\ g^{-1}$)	Pore Volume[b] ($cm^3\ g^{-1}$)	Pore size[a] (nm)
MCM-41	94.0 ± 5.0	1045.7	0.90	2.76
S1	92.0 ± 8.0	491.1	0.28	-

[a] Measured by TEM. [b] BJH model.

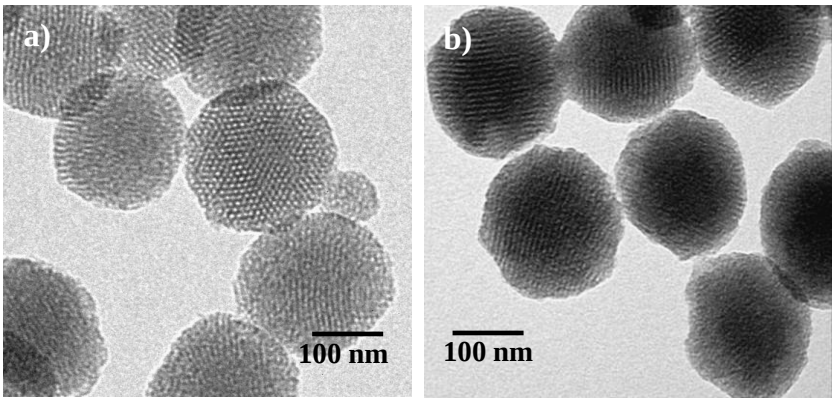

***Figure 1.** TEM images of (a) calcined MCM-41 and (b) **S1** solid.*

In a first step the response of **S1** in the presence of the bio-relevant thiol GSH was studied. In a typical experiment, 1 mg of solid **S1** was suspended in 2 ml of water at pH 7.0 in the presence of GSH (1 mM). At certain times fractions were collected, centrifuged to eliminate the solid and the emission in the solution of safranin O at 575 nm (λ_{ex} = 520 nm) measured. Moreover cargo delivery from **S1** in the absence of GSH was also studied. Safranin O release kinetics are depicted in Figure 2. As shown in the absence of GSH, **S1** showed nearly a "zero release" indicating tight pore closure. In contrast, the presence of GSH induced the opening of the pores and the subsequent release of the dye. Delivery was quite fast and for instance after 10 min *ca*. 90% (referred to the total amount of dye released after 4 h) of the cargo was released.

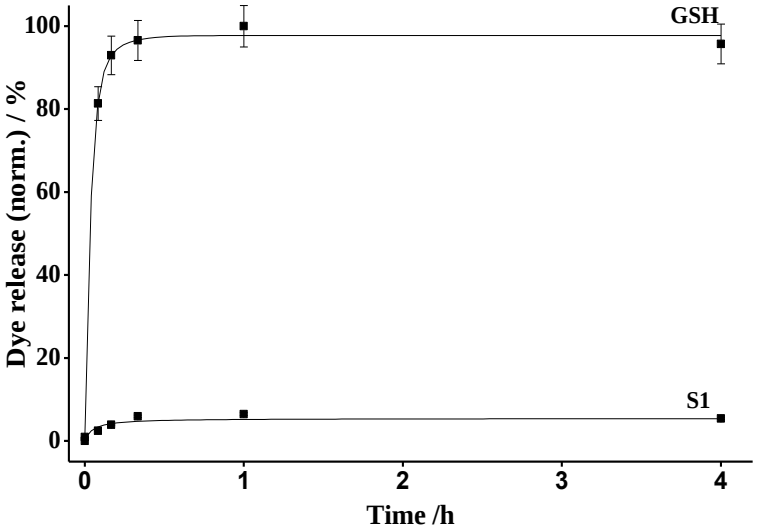

Figure 2. *Kinetics of the release of safranin O from solid **S1** in the absence and in the presence GSH (1 mM).*

Following a similar approach dye delivery from **S1** was studied as a function of the amount of GSH (see Figure 3). A correlation between the concentration of GSH and dye delivered was observed in agreement with an uncapping protocol involving reduction of the disulfide bond in the capping molecules in **S1**. A saturation of the delivery was observed for concentrations of GSH of about 10 µM. Moreover the limit of detection (LOD) of GSH following this procedure was determined to a concentration as low as 0.1 µM. As stated above one main characteristic of analyte-induced uncapping in gated mesoporous supports is the inherent feature of signal amplification in which only few analyte molecules (*i.e.* GSH) reacting at the pore openings are necessary to release a significant number of signalling units (*i.e*. safranine) entrapped in the nanoparticles. In the present case, for an intermediate point in Figure 3, the presence of one GSH molecule results in the delivery of *ca*. 100 safranine molecules.

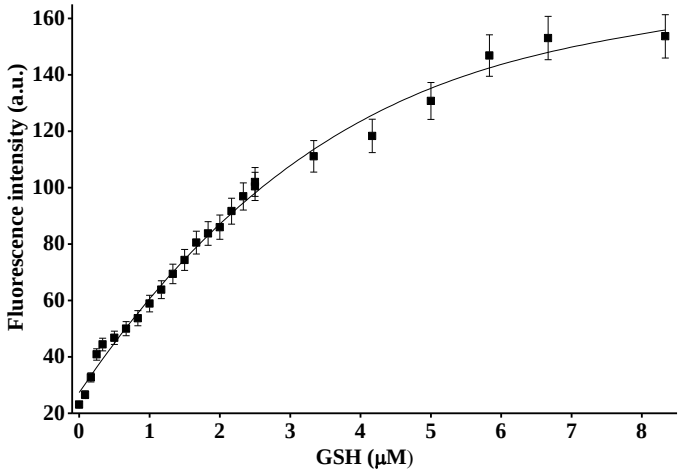

Figure 3. *Release of safranin O from solid **S1** in the presence of different amounts of GSH in water at pH 7.0 after 1h upon addition.*

In order to verify the selectivity of the method, similar experiments with solid **S1** were performed in the presence of 10 mM of selected anions (HS^-, F^-, Br^-, Cl^-, I^-, CN^-, OH^-, HPO_4^-, AcO^-, Citrate, N_3^-, NO_3^-, SO_3^{2-}, SO_4^{2-} and $S_2O_4^{2-}$), oxidants (H_2O_2), amino acids (Hcy, Cys, Me-Cys, Ala, Arg, Asn, Asp, Glu, Gln, Gly, His, Thr, Trp, Tyr and Val) and GSH. Dye delivery from **S1** after 30 min upon guest addition is shown in Figure 4. The results show that solid **S1** is highly selective to the presence of GSH, whereas other relevant bio-thiols (*i.e*. Hcy, Cys and Me-Cys) and HS^- induced a rather poor cargo delivery. This opens the way to the possible use of **S1** material for GSH detection in highly competitive media.

The uncapping mechanism was tentatively attributed to a selective reduction by GSH of the disulphide bond in **S1**. In order to further asses the mechanism, release experiments in the presence of 2-mercaptoethanol (ME) and dithiothreitol (DTT), which are reagents typically used to reduce disulfides to thiols, were carried out. The redox potentials for ME and DTT are -0.253 V and -0.33 V respectively, whereas that for GSH is -0.262 V. As a result it was expected that **S1** would be opened in the presence of DTT (with is a stronger reducing agent than GSH) whereas ME (with a slightly lower reduction potential than GSH) should uncap the pores in a much lower extent. This hypothesis was confirmed

experimentally and the results are shown in Figure 4, pointing to a reduction of the disulfide bond in the oligo(ethylene glycol) chain as the uncapping mechanism.

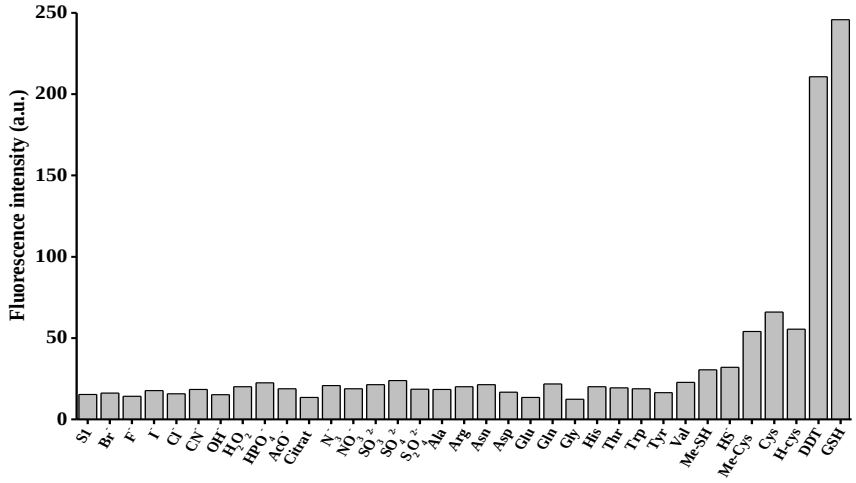

Figure 4. *Emission intensity of safranin O at 575 nm (excitation at 520 nm) released from solid* ***S1*** *(water at pH 7.0) in the presence of selected anions, amino acids and reducing agents (10 mM) after 30 min upon addition.*

Encouraged by these findings we attempted to detect GSH in a more complex system and selected human serum as a more realistic environment. Typical amounts of GSH in serum are in the 3-8 μM range, whereas other aminothiols such as Cys and Hcy are at concentrations of *ca*. 140-300 μM and 8-30 μM, respectively.[25] The LOD of **S1** for GSH is 0.1 μM, hence the probe is expected to sense GSH in typical concentrations in serum samples. Moreover **S1** displays a poor response to Cys and Hcy (see Figure 4) and therefore probe **S1** was expected to be selective for GSH. A human serum containing a concentration of GSH of 5.99 μM was used for the studies. The serum was spiked with additional known amounts of GSH (2.5, 4, 6, and 10 μM) and the total GSH concentration was determined using **S1** following the method of standard addition. Results are shown in Table 2. As seen in the table, **S1** was satisfactorily applied to the detection of GSH in a highly competitive environment such as human serum with rather high recovery ratios ranging from 92 to 107 %.

***Table 2**. Determination of total GSH in spiked human serum samples using solid **S1**.*

Sample	GSH spiked (μM)	GSH determined (μM)	Recovery (%)
1	5.99 + 2.5	8.12 ± 0.54	95
2	5.99 + 4.0	10.75 ± 0.84	107
3	5.99 + 6.0	10.98 ± 1.03	92
4	5.99 + 10.0	15.53 ± 1.86	97

In summary, we have reported herein the design of mesoporous silica nanoparticles capped with a disulfide-containing derivative and loaded with safranin O as a suitable system for the selective chromo-fluorogenic detection to GSH in pure water. The observed emission enhancement was ascribed to the GSH-induced selective uncapping of **S1** *via* the reduction of the disulfide bond that allowed the release of the dye entrapped in the porous network of the inorganic scaffold. The observed response was highly selective toward GSH whereas similar sulfur-containing derivatives such as Cys, Hcy and HS^-, were unable to uncap the gated material to a significant extent. **S1** can detect GSH down to concentrations of 0.1 μM. Besides, **S1** was used to detect GSH in human serum. Despite there are some reports on the use of disulfide-containing gated materials for drug delivery applications, this is, as far as we know, the first report in which capped nanoparticles have been used for the selective and sensitive detection of biothiols (in particular GSH). Moreover, the possibility of selecting different disulfide derivatives as caps, porous supports, cargos (such as fluorophores, dyes or redox active species for electrochemical sensing) and the inherent signal amplification features observed in capped materials make this approach attractive in the design of new probes for bio-thiols.

Acknowledgements

Financial support from the Spanish Government (Project MAT2012-38429-C04-01) and the Generalitat Valencia (Project PROMETEOII/2014/047) is gratefully acknowledged. S.E. is grateful to the Generalitat Valenciana for his Santiago

Grisolia fellow. Also, C.G. is grateful to the Spanish Ministry of Science and Innovation for her grant.

References

1. a) C. V. Smith, D. P. Jones, T. M. Guenthner, L. H. Lash, B. H. Lauterburg, *Toxicol. Appl. Pharmacol.,* **1996**, *140*, 1; b) F. Q. Schafer, G. R. Buettner, *Free Radical Biol. Med.,* **2001**, *30*, 1191.
2. W. W. Huber, W. Parzefall, *Curr. Opin. Pharm.,* **2007**, *7*, 404.
3. a) D. J. Naisbitt, J. F. Vilar, A. C. Stafford, E. G. L. Wilkins, M. Pimohamned, B. K. Park, *AIDS Res. Hum. Retroviruses.,* **2000**, *16*, 1929; b) M. M. Monick, L. Samavati, N. S. Butler, M. Mohning, L. S. Powers, T. Yarovinsky, D. R. Spitz, G. W. Hunninghake, *J. Immunol.,* **2003**, *171*, 5107.
4. P. L. Zeitlin, *Mol. Pharmacol.,* **2006**, *70*, 1155.
5. A. Rozycka, P. P. Jagodzinski, M. Lanen, W. Kozubski, J. Dorzsewska, *Curr. Genom.,* **2013**, *14*, 34.
6. H. Sies, *Free Radic. Biol. Med.,* **1999**, *27*, 916.
7. A. Theodoratos, J. W. Tu, J. Cappello, A. C. Blackburn, K. Matthaei, P. G. Board, *Biochem. Pharm.,* **2009**, *77*, 1358.
8. I. Kokcam, M. Nazroglu, *Clin. Chim. Acta.,* **1999**, *289*, 23.
9. D. Botta, C. C. White, P. Vilet-Gregg, I. Mohar, S. Shi, M. B. McGrath, L. A. McConnachie, T. J. Kavanagh, *Drug Metab. Rev.,* **2008**, *40*, 465.
10. H. Nakamura, Z. Tamura, *Anal. Chem.,* **1981**, *53*, 2190.
11. N. Maeso, D. García-Martínez, F. J. Rupérez, A. Cifuentes, C. Barbas, *J. Chromatogr. B.,* **2005**, *822*, 61.
12. Y. –F. Huang, H. –T. Chang, *Anal. Chem.,* **2007**, *79,* 4852.
13. See for example: a) H. S. Jung, K. C. Ko, G. –H. Kim, A. –R. Lee, Y. C. Na, C. Kang, J. Y. Lee, J. S. Kim, *Org. Lett.,* **2011**, *13*, 1498; b) H. Kwon, K. Lee, H. J. Kim, *Chem. Commun.,* **2011***, 47*, 1773; c) F. –J. Huo, Y. –Q. Sun, J. Su, J. –B. Chao, H. –J. Zhi, C. –X. Yin, *Org. Lett.,* **2009**, *11*, 4918; d) C. Yin, F. Huo, J. Zhang, R. Martínez-Máñez, Y. Yang, H. Lv, S. Li, *Chem. Soc. Rev*., **2013**, *42*, 6032; e) Y. Yang, F. Huo, C. Yin, A. Zheng, J. Chao, Y. Li, Z. Nie, R. Martínez-Máñez, D. Liu, *Biosensors and Bioelectronics*., **2013**, *47*, 300.
14. For recent examples see: a) J. Zhang, J. Tian, Y. He, Y. Zhao, S. Zhao, *Chem. Commun.,* **2014**, *50,* 2049; b) F. Kong, R. Liu, R. Chu, X. Wang, K. Xu, B. Tang, *Chem. Commun.,* **2013**, *49*, 9176; c) R. Peng, L. Lin, X. Wu, X. Liu, X. Feng, *J. Org. Chem.,* **2013**, *78,* 11602; d) L. Long, L. Zhou, L. Wang, S. Meng, A. Gong, F. Du, C. Zhang, *Org. Biomol. Chem.,* **2013**, *11*, 8214.
15. a) Z. Yao, X. Feng, C. Li, G. Shi, *Chem. Commun.,* **2009**, 5886; b) N. Shao, J. Jin, H. Wang, J. Zheng, R. Yang, W. Chan, Z. Abliz, *J. Am. Chem. Soc.,* **2010**, *132*, 725; c) L. –Y. Niu, Y. –S. Guan, Y. –Z. Chen, L. –Z. Wu, C. –H. Tung, Q. –Z. Yang, *J. Am. Chem. Soc.,* **2012**, *134*, 18928; d) Y. Guo, X. Yang, L. Hakuna, A. Barve, J. O. Escobedo, M. Lowry, R. M. Strongin, *Sensors.,* **2012**, *12*, 5940; e) J. Liu, Y. –Q. Sun, Y. Huo, H. Zhang, L. Wang, P. Zhang, D. Song, Y. Shi, W. Guo, *J. Am. Chem. Soc.,* 2014, **136**, 574; f) J. Yin, Y. Kwon, D. Kim, D. Lee, G. Kim, Y. Hu, J. –

H. Ryu, J. Yoon, *J. Am. Chem. Soc.,* **2014**, *136*, 5351; g) A. Agostini, I. Campos, M. Milani, S. Elsayed, Ll. Pascual, R. Martínez-Máñez, M. Licchelli, F. Sancenón, *Org. Biomol. Chem.,* **2014**, *12*, 1871.

16. a) Y. Li, P. Wu, H. Xu, H. Zhang, X. Zhong, *Analyst.,* **2011**, *136*, 196; b) Z. Chen, Z. Wang, J. Chen, S. Wang, X. Huang, *Analyst.,* **2012**, *137*, 3132; c) B. Hu, X. Cao, P. Zhang, *New J. Chem.,* **2013**, *37*, 3853; d) J. Li, S. Yang, W. Zhou, C. Liu, Y. Jia, J. Zheng, Y. Li, J. Li, R. Yang, *Chem. Commun.,* **2013**, *49*, 7932.
17. D. Tian, Z. Qian, Y. Xia, C. Zhu, *Langmuir.,* **2012**, *28*, 3945.
18. J. Liu, C. Bao, X. Zhong, C. Zhao, L. Zhu, *Chem. Commun.,* **2010**, *46*, 2971.
19. a) E. Aznar, R. Martínez-Máñez, F. Sancenón, *Expert Opin. Drug Deliver.,* **2009**, *6*, 643; b) M. W. Ambrogio, C. R. Thomas, Y. –L. Zhao, J. I. Zink, J. F. Stoddart, *Acc. Chem. Res.,* **2011**, *44*, 903.
20. C. Coll, A. Bernardos, R. Martínez-Máñez, F. Sancenón, *Acc. Chem. Res.,* **2013**, *46*, 339.
21. See for example: a) Y. Zhang, Q. Yuan, T. Chen, X. Zhang, Y. Chen, W. Tan, *Anal. Chem.,* **2012**, *84*, 1936; b) V. C. Özalp, T. Schäfer, *Chem. Eur. J.,* **2011**, *17*, 9893; c) E. Climent, R. Martínez-Máñez, A. Maquieira, F. Sancenón, M. D. Marcos, E. M. Brun, J. Soto, P.Amorós, *ChemOpen.,* **2012**, *1*, 251; d) C. –L. Zhu, C. –H. Lu, X. –Y. Song, H. –H. Yang, X. –R. Wang, *J. Am. Chem. Soc.,* **2011**, *133*, 1278; e) I. Candel, A. Bernardos, E. Climent, M. D. Marcos, R. Martínez-Máñez, F. Sancenón, J. Soto, A. Costero, S. Gil, M. Parra, *Chem. Commun.,* **2011**, *47*, 8313; f) Y. Salinas, R. Martínez-Máñez, J. O. Jeppesen, L. H. Petersen, F. Sancenón, M. D. Marcos, J. Soto, C. Guillem, P. Amorós, *ACS Appl. Mater. Inter.,* **2013**, *5*, 1538.
22. See for example: a) E. Climent, M. D. Marcos, R. Martínez-Máñez, F. Sancenón, J. Soto, K. Rurack, P. Amoros, *Angew. Chem. Int. Ed.,* **2009**, *48*, 8519; b) E. Climent, R. Martínez-Máñez, F. Sancenón, M. D. Marcos, J. Soto, A. Maquieira. P. Amorós, *Angew. Chem. Int. Ed.,* **2010**, *49*, 7281; c) E. Climent, A. Bernardos, R. Martínez-Máñez, A. Maquieira, M. D. Marcos, N. Pastor-Navarro, R. Puchades, F. Sancenón, J. Soto, P. Amorós, *J. Am. Chem. Soc.,* **2009**, *131*, 14075.
23. See for example: a) H. Kim, S. Kim, C. Park, H. Lee, H. J. Park, C. Kim, *Adv. Mater.,* **2010**, *22*, 4280; b) R. Liu, X. Zhao, T. Wu, P. Feng, *J. Am. Chem. Soc.,* **2008**, *130*, 14418.
24. S. Cabrera, J. El Haskouri, C. Guillem, J. Latorre, A. Beltrán, D. Beltrán, M. D. Marcos, P. Amorós, *Solid State Sci.,* **2000**, *2*, 420.
25. A. A. Mangoni, A. Zinellu, C. Carru, J. R. Attia, M. McEvoy, *J. Transl. Med.,* **2013**, *11*, 99.

SUPPORTING INFORMATION

Highly selective and sensitive detection of glutathione using mesoporous silica nanoparticles capped with disulfide-containing oligo(ethylene glycol) chains

Sameh El Sayed, Cristina Giménez, Elena Aznar, Ramón Martínez-Máñez, Félix Sancenón and Maurizio Licchelli

Reagents:

The chemicals tetraethylorthosilicate (TEOS), *n*-cetyltrimethylammonium bromide (CTABr), sodium hydroxide (NaOH), Safranine O, (3-mercaptopropyl) trimethoxysilane, 2,2'-dipyridyl disulfide, *O*-(2-Mercaptoethyl)-*O*'-methyl-hexa(ethylene glycol), GSH and selected amino acids (Cys, Hcy, Ala, Arg, Asn, Asp, Glu, Gln, Gly, His, Thr, Trp, Tyr and Val) were provided by Sigma-Aldrich. Human serum from male AB plasma, USA origin were provided by Sigma-Aldrich. Analytical-grade solvents were from Scharlab (Barcelona, Spain). All reagents were used as received.

Methods:

X-ray measurements were performed on a Brücher AXS D8 Advance diffractometer using Cu-Kα radiation. Thermo gravimetric analysis were carried out on a TGA/SDTA 851e Mettler Toledo equipment using an oxidant atmosphere (Air, 80 mL/min) with a heating program consisting on a heating ramp of 10 °C per minute from 393 K to 1273 K and an isothermal heating step at this temperature for 30 minutes. TEM images were taken with a JEOL TEM-1010 Electron microscope working at 100 kV. N_2 adsorption-desorption isotherms

were recorded on a Micromeritics ASAP2010 automated sorption analyser. The samples were degassed at 120 °C in vacuum overnight. The specific surfaces areas were calculated from the adsorption data in the low pressures range using the BET model. Pore size was determined following the BJH method. Fluorescence spectroscopy was carried out on a Jasco FP-8300 Spectrometer and UV-visible spectroscopy was carried out with a Jasco V-630 Spectrometer.

Synthesis of the silica mesoporous nanoparticles support (SMPS):

n-cetyltrimethylammoniumbromide (CTABr, 1.00 g, 2.74 mmol) was first dissolved in 480 mL of distilled water. Then a 3.5 mL of NaOH 2.00 M in distilled water was added to the CTABr solution, followed by adjusting the solution temperature to 80 °C. TEOS (5 mL, 2.57x10 $^{-2}$ mol) was then added dropwise to the surfactant solution. The mixture was stirred for 2 h and white precipitate was obtained. Finally the precipitate was centrifuged, washed with distilled water and dried at 60 °C (MCM-41 as-synthesized). To prepare the final porous material (MCM-41), the as-synthesized solid was calcined at 550 °C using oxidant atmosphere for 5 h in order to remove the template phase.

Synthesis of S1:

500 mg of calcined MCM-41 and safranin O dye (140.34 mg, 0.40 mmol) were suspended in acetonitrile (17 mL) in a round-bottomed flask. The mixture was stirred for 24 h at room temperature, filtered off and dried under vacuum. Afterward, this loaded solid (250 mg) was re-suspended in acetonitrile (8.5 mL) in the presence of an excess of safranin O and (3-mercaptopropyl) trimethoxysilane (464.38 µL, 2.5 mmol) was added. The suspension was stirred for 5.5 h at room temperature and then, 2,2'-dipyridyl disulfide (550.77 mg, 2.5 mmol) was added to the reaction mixture. After stirring for 12 h at room temperature, the resulting solid was filtered off and dried under vacuum. Finally, a mixture of this prepared solid (50 mg) and *O*-(2-Mercaptoethyl)-*O*'-methyl-hexa(ethylene glycol) (0.14 mmol) were suspended in acetonitrile (3.33 mL) in the presence of an excess of

safranin O. The mixture was stirred for 12 h and the final support **S1** was isolated by centrifugation, washed with abundant water and dried at 40 ^{o}C for 12 h.

Materials Characterization:

MCM-41, calcined MCM-41, and **S1** were characterized through standard techniques. Figure S1 shows the X-ray diffraction (XRD) patterns of the as-synthesized MCM-41 matrix, the calcined MCM-41, and the final **S1** solid. Plain MCM-41 curve a) displayed the four typical low-angle reflections of a hexagonal-ordered matrix indexed at (100), (110), (200) and (210) Bragg peaks. In curve b) calcined MCM-41 shows a significant shift of the (100) peak in the PXRD and a broadening of the (100) and (200) peaks. These changes are due to the condensation of silanols in the calcination step which caused an approximate cell contraction of 4 Å. Finally, curve c) shows the PXRD pattern of **S1** solid. For this material, reflections (110) and (200) were mostly lost due to a reduction in contrast related to the functionalization process and to the filling of mesopores with safranin O. Even so, the intensity of the (100) peak in this pattern strongly indicates that the loading process with the dye and the additional functionalization with the oligo(ethylene glycol) chains did not modify the mesoporous MCM -41 scaffold.

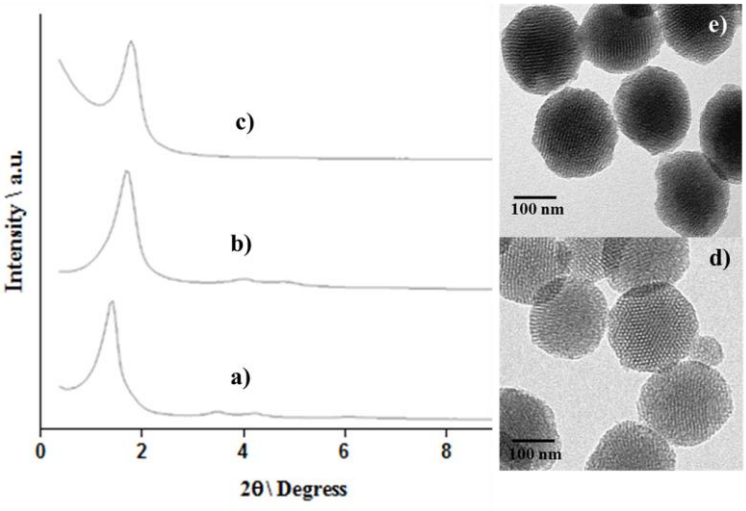

Figure S1. *X-ray patterns of (a) MCM-41, (b) calcined MCM-41 and (c)* ***S1****. TEM images of calcined MCM-41 (d) and* ***S1*** *(e).*

Moreover, TEM images of the investigated solid materials show the typical channels of the MCM-41 matrix as alternate black and white stripes. The typical hexagonal porosity of the calcined MCM-41 material can also be observed (Figure S1-d). TEM images also show that calcined MCM-41 was obtained as spherical nanoparticles with diameters between 80 and 100 nm. Shape and dimension of nanoparticles were preserved even after loading and functionalization processes (Figure S1-d-e).

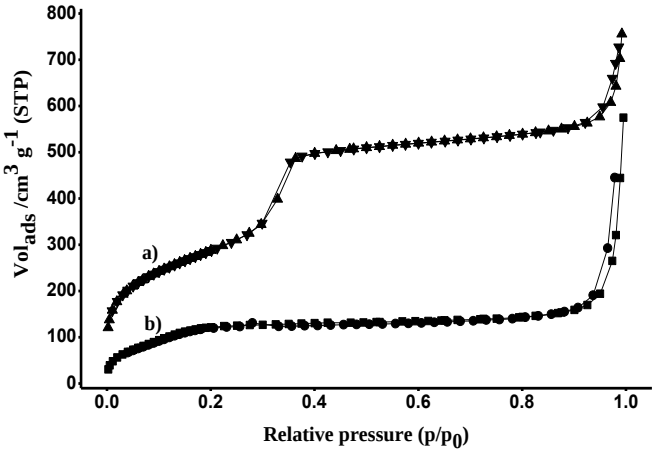

Figure S2. *Nitrogen adsorption-desorption isotherms for (a) MCM-41 mesoporous material and (b)* ***S1*** *material.*

Figure S2 (curve a) shows the N_2 adsorption-desorption isotherms of the calcined MCM-41 nanoparticles. This curve displays an adsorption step with a P/P_0 value between 0.2 and 0.35, corresponding to a type IV isotherm, which is typical of mesoporous materials. This first step is due to nitrogen condensation in the mesopore inlets. With the BJH model on the adsorption curve of the isotherm, the pore diameter and pore volume were calculated to be 2.76 nm and 0.9 cm^3 g^{-1} respectively. The absence of a hysteresis loop in this pressure range and the low BJH pore distribution is due to the cylindrical uniformity of mesopores. The total specific area was 1045.70 m^2 g^{-1} calculated with the BET model. The a_0 cell parameter (44.58 nm) and the wall thickness (16.98 Å) were calculated from the PXRD, porosimetry and TEM measurements. Other important

feature of the curve is the characteristic H1 hysteresis loop that appears in the isotherm at a high relative pressure (P/P_0> 0.8), which can be closely associated with a wide pore size distribution. This corresponds to the filling of the large pores among the nanoparticles (0.75 $cm^3\ g^{-1}$ calculated by the BJH model) due to textural porosity. On the other hand, for the S1 material, the N_2 adsorption-desorption isotherm is typical of mesoporous systems with partially filled pores (see Figure S2, curve b). In this way, and as it can be expected, a lower N_2 adsorbed volume (BJH mesopore volume = 0.28 $cm^3\ g^{-1}$) and surface area (491.1 $m^2\ g^{-1}$) were found when compared with the initial MCM-41 material. As observed, this solid presents a curve with no gaps at low relative pressure values if compared to the mother MCM-41 matrix (curve a). Another important feature of **S1** is that no maximum was observed in the pore size distribution curve, which can be explained by the presence of closed pores (see Figure S3 for pore size distributions).

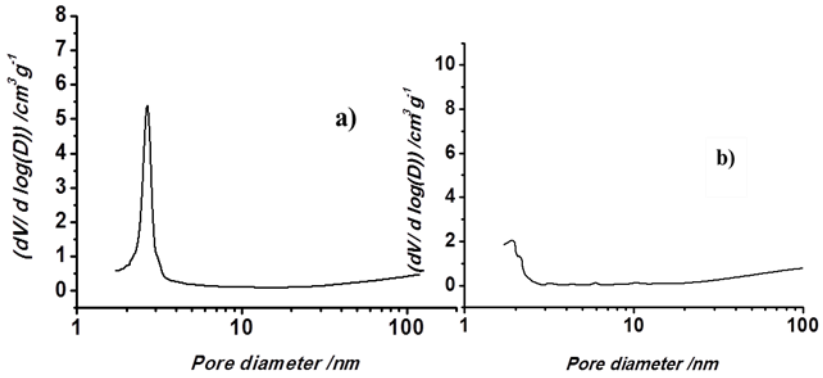

Figure S3*. Pore size distributions for (a) Calcined MCM-41mesoporous material (b)* ***S1****.*

Thermogravimetric studies of **S1** showed the existence of three weights loss steps *i.e*. weight losses of 6.74 % (T < 150 ^oC, corresponding to solvent elimination), 28.10 % (300 < T < 550 ^oC) due to combustion of organics) and 2.09 % (T > 550 ^oC, attributed to condensation of silanols in the siliceous surface) were observed. Also dynamic light scattering studies with MCM-41 calcined and the final **S1** solid were carried out (see Figure S4). As seen in the figure MCM-41 calcined and **S1** presented mean diameters of *ca*. 85 and 150 nm respectively.

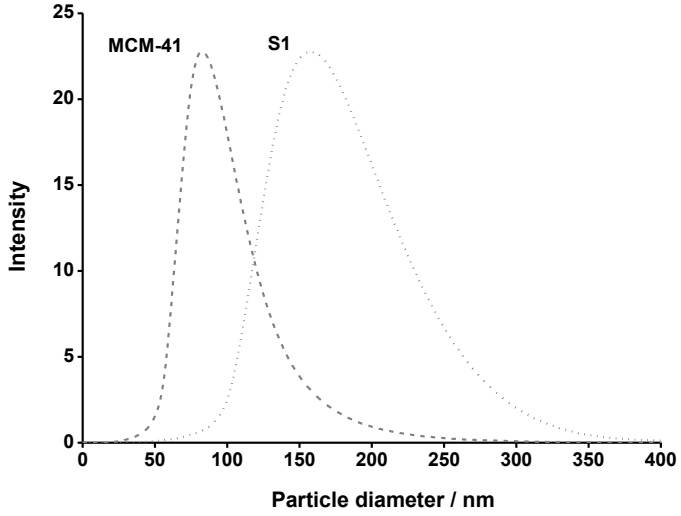

***Figure S4**. Size distribution by number of particles obtained by DLS studies for calcined MCM-41 and **S1** solids.*

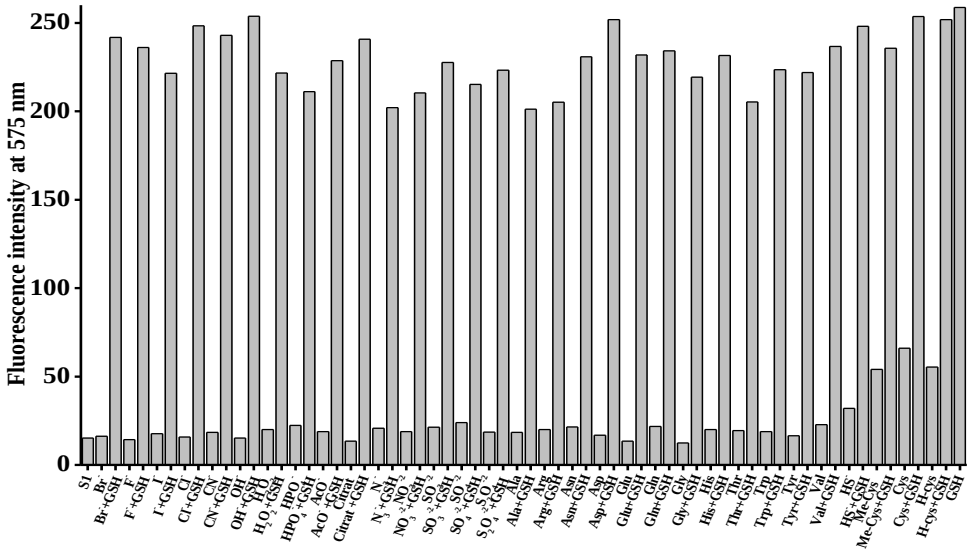

***Figure S5.** Fluorescence intensity at 575 nm (λ_{ex} 520 nm) of safranin O dye released from **S1** in water pH 7.0 after 30 min upon addition of 10 mM of GSH alone and in the prescence of 10 mM of GSH + 10 mM of anions, cations oxidants, reducing agents, phosphates , amino acids, Me-Cys, Cys, Hcy and GSH.*

Selectivity of the method was studied via monitoring the response of **S1** in the presence of 10 mM of selected anions (HS^-, F^-, Br^-, Cl^-, I^-, CN^-, OH^-, HPO_4^-, AcO^-, Citrate, N_3^-, NO_3^{2-}, SO_3^{2-}, SO_4^{2-} and $S_2O_4^{2-}$), oxidants (H_2O_2), amino acids (Hcy, Cys, Me-Cys, Ala, Arg, Asn, Asp, Glu, Gln, Gly, His, Thr, Trp, Tyr and Val), GSH, ME and DTT. Dye delivery from **S1** after 30 min upon guest addition is shown in Figure 3 in the main text. Moreover Figure S5 shows the response of **S1** to GSH in competitive experiments for mixtures of GSH (10 mM) alone and mixtures containing GSH (10 mM) and 10 mM of different anions, oxidants, amino acids and Me-Cys, Cys or Hcy.

Human serum GSH serve as an accurate indicator of GSH status in human subjects and play an important role in some diseases. Thus, the development of simple and accurate analytical method for the determination of GSH is of interest. We attempted to detect GSH using **S1** in more complex systems and selected human serum and artificial serum as more realistic environment. Results obtained using human serum are shown in Table 1 of the manuscript. Moreover here we describe the results obtained in artificial serum. Artificial serum was prepared according to a well-established protocol [1] and it was spiked with conventional quantities of biothiols (Cys: 178.4 μM; Hcy: 5.9 μM and GSH (2.5, 4, 6, 10 μM)). GSH content in the samples was determined using **S1** and following the method of standard addition. Results are shown in Table S1. As seen in the table, **S1** was satisfactorily applied to the detection of GSH with high recovery ratios ranging from 92 to 118 %.

Table S1. *Determination of GSH in artificial serum.*

Sample	GSH spiked (μM)	GSH measured (μM)	Recovery (%)
1	2.5	2.3±0.15	92
2	4.0	4.3±0.24	107
3	6.0	7.1±0.35	118
4	10.0	9.4±0.86	94

1. For serum preparation see: M. R. C. Marques, R. Loebenberg, M. Almukainzi, *Dissolution Technol.*, 2011, **18**, 15.

Hexametaphosphate-capped silica mesoporous nanoparticles containing Cu^{II} complexes for the selective and sensitive optical detection of hydrogen sulfide in water

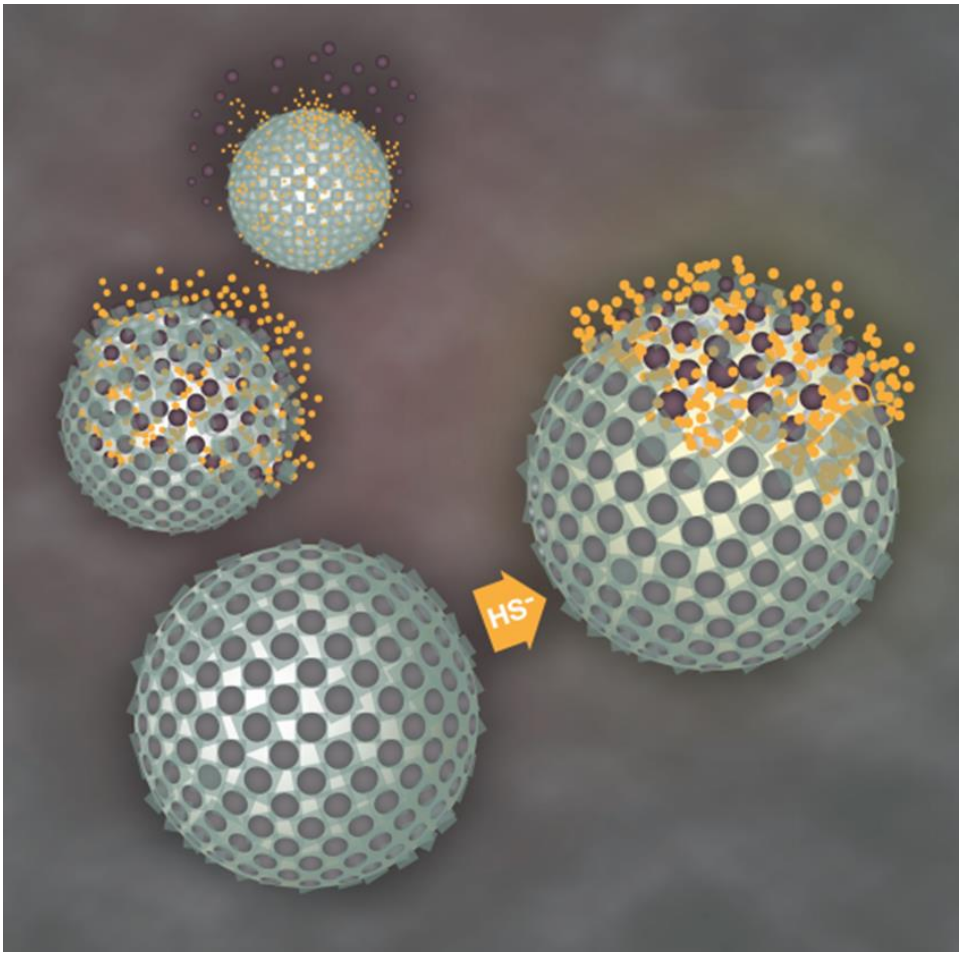

Hexametaphosphate-capped silica mesoporous nanoparticles containing Cu^{II} complexes for the selective and sensitive optical detection of hydrogen sulfide in water

Sameh El Sayed,[a,b,c,d] Michele Milani,[d] Maurizio Licchelli,[d] Ramón Martínez-Máñez[a,b,c] and Félix Sancenón[a,b,c]*

[a] Centro de Reconocimiento Molecular y Desarrollo Tecnológico (IDM), Unidad Mixta Universidad Politécnica de Valencia-Universidad de Valencia.
[b] Departamento de Química, Universidad Politécnica de Valencia
Camino de Vera s/n, 46022, Valencia, Spain
E-mail: rmaez@qim.upv.es
[c] CIBER de Bioingeniería, Biomateriales y Nanomedicina (CIBER-BBN)
[d] Dipartimento di Chimica, Università di Pavia, via Taramelli 12, I-27100 Pavia, Italy.
E-mail: maurizio.licchelli@unipv.it

Received: *29 January 2015*
First published on the web: *10 March 2015*

Chem. Eur.J. **2015**, *21*, 7002 –7006

(Reproduced with permission of WILEY-VCH Verlag GmbH & Co. KGaA, Weinheim© 2015)

Cu^{II}-macrocycle functionalized hexametaphosphate-capped silica mesoporous nanoparticles have been prepared and used for the selective and sensitive detection of hydrogen sulfide in aqueous environments.

Hydrogen sulfide, a colourless and flammable gas, is well known for its toxicity, for its presence in several environmental sites and for its use in certain industrial protocols. Moreover, the role of hydrogen sulfide as endogenous gasotransmitter and its participation in relevant biological processes (neurotransmission, vasorelaxation, cardioprotection, anti-inflammation) has been discovered in recent years.[1] Besides, certain diseases (such as chronic kidney disease, liver cirrhosis, Alzheimer[2] and Down's syndrome[3]) have been associated to abnormal hydrogen sulfide levels.[4] Taking into account the above mentioned roles, the development of selective and sensitive probes for the optical detection of hydrogen sulfide has recently received great attention.

In this context, some probes constructed under the chemodosimeter paradigm for the chromo-fluorogenic detection of hydrogen sulfide have been described in the last years. These probes used reduction (of azide,[5,6] hydroxylamine[7] or nitro moieties[8] to amine) and hydrolysis (of disulfide bonds,[9] dinitrophenyl ethers[10] or cyanovinyl moieties[11]) reactions as main mechanisms for the optical recognition of hydrogen sulfide. Unfortunately, some of these probes presented certain drawbacks such as poor selectivity and cross-reactivity with other thiol-containing biomolecules (such as Cys, Hcy and GSH) and anions (SO_3^{2-} and $S_2O_3^{2-}$).[12] An interesting alternative, recently developed, consisted on the use of hydrogen sulfide-induced demetallation reactions of non-fluorescent complexes that become emissive upon reaction with HS^-.[13]

From another point of view, there is an increasing interest in the design and synthesis of gated nanoscopic hybrid materials with the ability to release an entrapped guest upon application of certain external stimuli.[14] These nanodevices are usually formed by a silica mesoporous support (in which the guest is stored) and molecular or supramolecular entities attached on the external surface than

act as “gates” allowing the controlled release of the entrapped cargo at will. These functional materials have been used for drug delivery applications but we have recently suggested the use of gated materials in optical recognition protocols.[15] Here the underlying idea is that coordination or reaction of a target analyte with the “gate” could modulate dye delivery from the pores to the solution resulting in an optical response. The potential existence of amplification features is one of the advantages of these solids. In particular, it has been reported that the presence of few analyte molecules may induce the release of a relatively high amount of entrapped dye molecules. In spite of these interesting features, the use of gated solids for sensing purposes is still a barely studied area of research especially for the detection of anions.

Given our interest in the development of capped mesoporous materials and their application in recognition and sensing protocols[16] we report herein the design of silica mesoporous nanoparticles functionalized with a Cu^{II} complex, capped with the anion hexametaphosphate and the use of such ensemble for the selective and sensitive detection of hydrogen sulfide. Our proposed sensing protocol is depicted in Scheme 1. MCM-41 mesoporous silica nanoparticles (MSN) of *ca*. 100 nm diameter were selected as inorganic scaffold. The pores of the MSN were loaded with a suitable dye (in this case $[Ru(bipy)_3]^{2+}$ and the outer surface was additionally functionalized with a Cu^{II}-macrocyclic complex (solid **S1**). The final capped sensing solid was prepared via strong electrostatic interactions of the highly charged anion hexametaphosphate with the positively charged anchored Cu^{II} complexes. The signaling paradigm relies on a demetallation of the Cu^{II} complex from the grafted macrocycle in the presence of hydrogen sulfide, which would uncap the pores and induce release of the entrapped dye. Demetallation reactions have been commonly used in the development of hydrogen sulfide molecular fluorogenic probes[17] but, as far as we know, this is the first time that hybrid capped material uses this sensing mechanism.

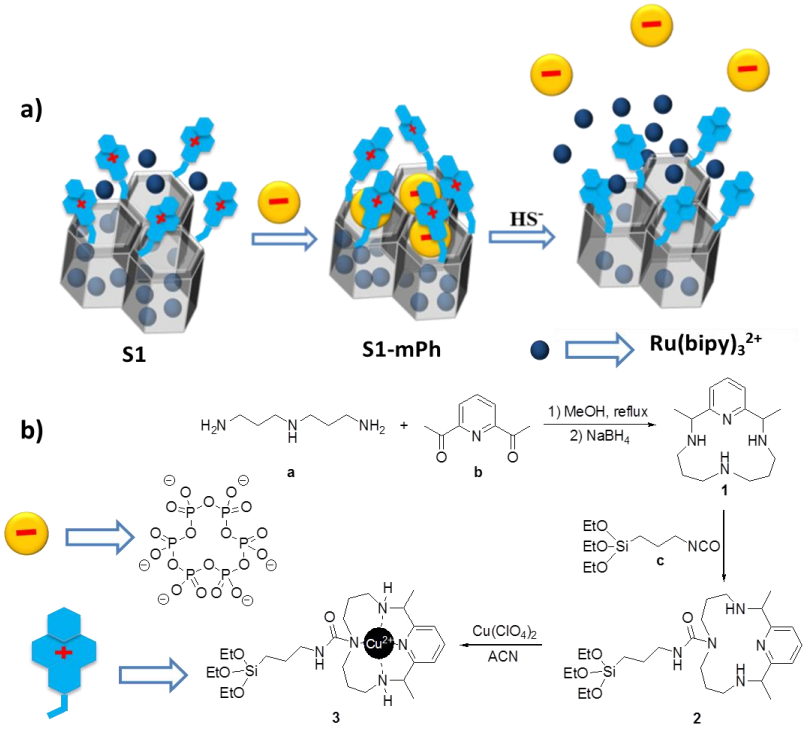

Scheme 1. *(a) Schematic representation of the sensing paradigm of HS^- anion using solid* ***S1-mPh****. (b) Synthesis of macrocycle* ***2*** *and complex* ***3****.*

MCM-41 mesoporous nanoparticles were synthesized according to well-known procedures and then, the pores of the calcined mesoporous scaffold were loaded with $[Ru(bipy)_3]^{2+}$ by simply stirring a suspension of the nanoparticles in an acetonitrile solution of the dye. In a second step, the external surface of the nanoparticles was functionalized with the Cu^{II}-macrocyclic complex **3** yielding solid **S1**. Complex **3** was synthesized using a three step procedure (see Supporting Information for details). In a first step 3,3'-iminobis(propylamine) (**a**) was reacted with 2,6-diacetylpyridine (**b**) in methanol yielding compound **1** after reduction of the diimine formed with $NaBH_4$ (see Scheme 1). In a second step **1** was reacted with (3-isocyanatopropyl)triethoxysilane (**c**) in order to prepare compound **2** that finally, yielded complex **3** upon reaction with copper(II) perchlorate. The final sensing solid **S1-mPh** was prepared by simply mixing **S1** in a solution containing an excess of the highly charged anion hexametaphosphate.

The starting MCM-41 scaffold and solids **S1** and **S1-mPh** were characterized following standard procedures (see Supporting Information for details). Powder X-ray diffraction (PXRD) and transmission electron microscopy (TEM) carried out on the MCM-41 starting nanoparticles showed clearly the presence of a mesoporous structure that persisted in the final solid **S1**-**mPh** regardless of the loading process with the dye, further functionalization with the Cu^{II}-macrocyclic complex **3** and capping with hexametaphosphate (see Figure 1). Besides, from SEM, thermogravimetric and elemental analyses contents of $[Ru(bipy)_3]^{2+}$, complex **3** and hexametaphosphate were determined and are shown in Table 1. Moreover Table 2 list main structural properties such as particle diameter, BET specific surface area, pore volumes and pore sizes obtained for MCM-41 starting nanoparticles, **S1** and **S1**-**mPh**.

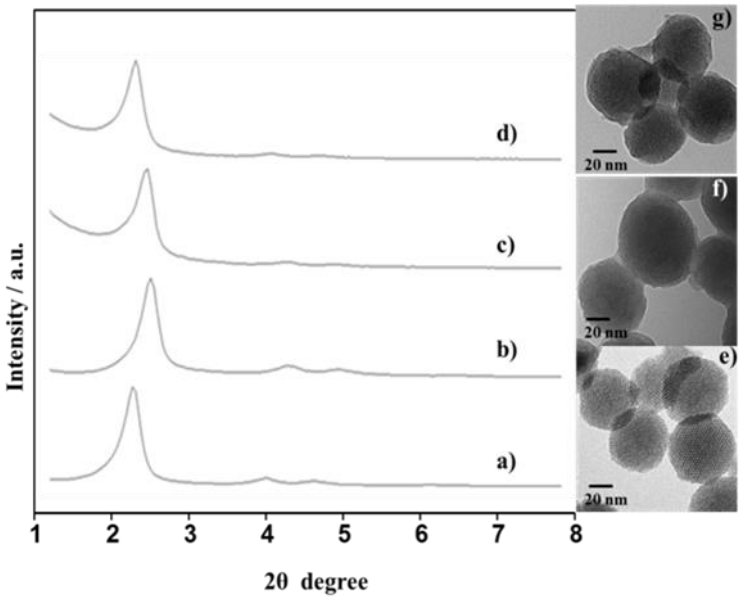

Figure 1. *Left: powder X-ray patterns of the solids (a) MCM-41 as synthesized (b) calcined MCM-41, (c) solid **S1** and (d) solid **S1-mPh**. Right: TEM images of (e) calcined MCM-41 sample, (f) solid **S1** and (g) **S1-mPh** showing the typical hexagonal porosity of the MCM-41 mesoporous matrix.*

Table 1. *Content (α) of anchored molecules and dye in mmol g^{-1} of SiO_2.*

Solid	$\alpha_{complex\ 3}$ [mmol g^{-1} SiO_2]	α_{dye} [mmol g^{-1} SiO_2]	$\alpha_{m\text{-}phosphate}$ [mmol g^{-1} SiO_2]
S1	0.107	0.39	-
S1-mPh	0.105	0.38	0.040

Table 2. *Main structural properties calculated from TEM, PXRD and N_2 adsorption analysis.*

Sample	Diameter particle[a] (nm)	S_{BET} (m^2 g^{-1})	Pore Volume[b] (cm^3 g^{-1})	Pore size[a] (nm)
MCM-41	94.0 ± 5.0	980.9	0.79	2.58
S1	95.0 ± 8.0	320.1	0.28	-
S1-mPh	98.0 ± 6.0	268.5	0.18	-

[a] Measured by TEM. [b] BJH model.

In a typical sensing experiment, 1 mg of **S1-mPh** was suspended in 2 mL of buffered solution (pH 7.5, HEPES 10 mM) in absence and in the presence of HS^- anion. In both cases, suspensions were stirred at room temperature. Dye delivery to the bulk solution was easily detected by monitoring the emission band of $[Ru(bipy)_3]^{2+}$ at 610 nm upon excitation in the spin allowed d-π metal-to-ligand charge transfer (MLCT) transition at 451 nm.[18] The obtained results are depicted in Figure 2. As it can be seen, in the absence of HS^- a negligible dye release was found due to tight pore closure due to strong electrostatic interactions between the hexametaphosphate anion and the grafted Cu^{II}-macrocyclic complex. However, when HS^- anion was present a remarkable dye delivery and chromo-fluorogenic response in *ca*. 30 minutes was observed. The release of the entrapped dye from the pore voids was attributed to a HS^--induced demetallation reaction of the grafted Cu^{II} macrocyclic complex.

Moreover, the crucial role played by Cu^{II} cation in the capping protocol was demonstrated by the preparation of solid **S2** (see Supporting Information for details). This material contains the $[Ru(bipy)_3]^{2+}$ complex in the inner of the pores and the macrocycle **2** (that lacks Cu^{II}) in the outer surface. None of the anions

tested in water (including hexametaphosphate) were able to block the pores an inhibit dye release to a significant extent (data not shown).

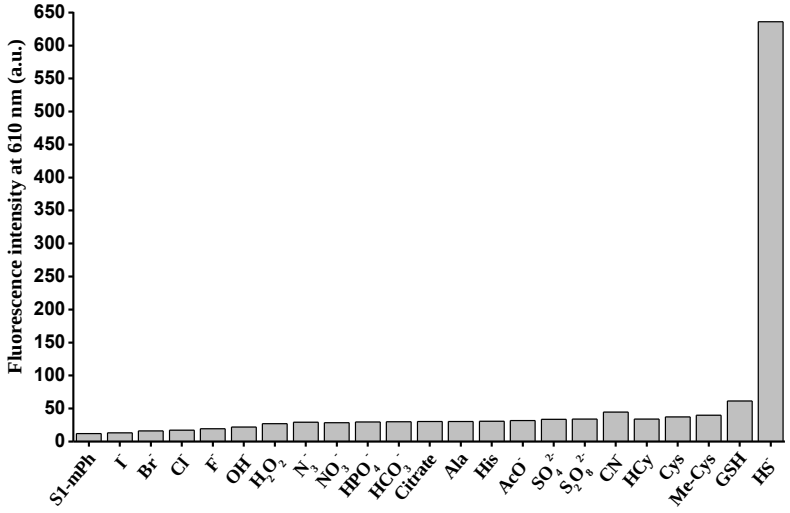

Figure 2. *Fluorescence intensity at 610 nm of $[Ru(bipy)_3]^{2+}$ dye released from **S1-mPh** (HEPES 10 mM at pH 7.5) after 6 h of adding 1 mM of selected anions, amino acids and oxidants.*

To assess the selectivity of the method, the response of solid **S1-mPh** in the presence of selected anions (HS^-, F^-, Cl^-, Br^-, I^-, N_3^-, CN^-, OH^-, HPO_4^-, NO_3^-, HCO_3^-, SO_4^{2-}, $AcO^-$and citrate), amino acids (Ala, His), thiol-containing biomolecules (Cys, HCy, GSH, Me-Cys) and oxidants (H_2O_2 and $S_2O_8^{2-}$) was studied. Figure 2 shows the emission of the ruthenium dye in the solution at 610 nm upon addition of these selected chemicals (1 mM) to buffered suspensions of **S1-mPh**. As seen, these species were unable to induce cargo delivery, showing that **S1-mPh** displays a remarkable highly selective response to HS^-.

In a second step, the fluorogenic response of solid **S1-mPh** was tested upon addition of increasing quantities of HS^- anion by using a similar protocol to that descried above. As seen in Figure 3, a clear correlation between the concentration of HS^- and the dye delivered was observed in agreement with an uncapping protocol involving a demetallation reaction. From the titration profile shown in Figure 3 a remarkable limit of detection for HS^- as low as 1.85 μM was

determined. As stated above one appealing characteristic of analyte-induced uncapping protocols in gated mesoporous supports is the possibility to observe signal amplification. In particular in our case it was confirmed that the presence of one HS^- molecule (at a concentration of *ca*. 1.0 x 10^{-5} mol dm^{-3}) results in the release of *ca*. 220 molecules of the $[Ru(bipy)_3]^{2+}$ dye.

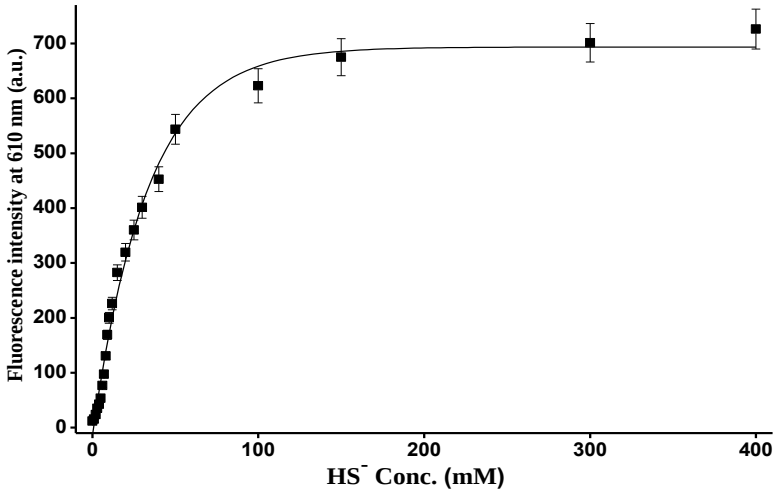

Figure 3. *Calibration curve of $[Ru(bipy)_3]^{2+}$ dye released from **S1-mPh** (HEPES 10 mM, pH 7.5) upon addition of increasing quantities of HS^-.*

Encouraged by these resultes we attempted to detect HS^- in a more complex and realistic environment. For this purpose, tap water was spiked with known amounts of HS^- and the concentration was determined using **S1-mPh** following the method of standard addition. Results are shown in Table 3. As it can be seen, **S1-mPh** was satisfactorily applied to the detection of HS^- with rather high recovery ratios ranging from 83 to 92 %.

Table 3*. Determination of HS^- spiked in tap water samples using **S1-mPh.***

Sample	HS^- spiked (μM)	HS^- determined (μM)	Recovery (%)
1	2.5	2.08 ± 0.34	83
2	4.0	3.58 ± 1.03	89
3	8.0	7.40 ± 2.86	92

In summary, we reported herein the synthesis, characterization and sensing behaviour of a new hybrid material functionalized with a Cu^{II}-macrocyclic derivative and capped through electrostatic interactions with the bulky anion hexametaphosphate. Of all the chemicals tested, only HS^- was able to induce pore opening and dye release. The fluorogenic response obtained was ascribed to a demetallation reaction selectively induced by HS^- anion. The response of the capped hybrid material was highly selective and sensitive to HS^- anion with a limit of detection of 1.85 μM. Moreover, the possible use of different metal complexes combined with different capping anions and choice of different dyes or other sensing molecules as indicators makes this new protocol highly appealing for the preparation of new sensing systems for sulfide detection in different environments.

Acknowledgements

Financial support from the Spanish Government (Project MAT2012-38429-C04-01) and the Generalitat Valencia (Project PROMETEOII/2014/047) is gratefully acknowledged. S.E. is grateful to the Generalitat Valenciana for his Santiago Grisolia fellow.

Keywords: gated materials • sensing • hydrogen sulfide • displacement reaction • signal amplification

Refrences

1. a) L. Li, P. Rose, P. K. Moore, *Annu. Rev. Pharmacol. Toxicol*., **2011**, *51*, 169; b) K. R. Olson, *Am. J. Physiol. Regul. Integr. Comp. Physiol*., **2011**, *301*, R297; c) M. Lavu, S. Bhushan, D. Lefer, *J. Clin. Sci*., **2011**, *120*, 219; d) M. Whiteman, P. K. Moore, *J. Cell. Mol. Med*., **2009**, *13*, 488.
2. K. Eto, T. Asada, K. Arima, T. Makifuchi, H. Kimura, *Biochem. Biophys. Res. Commun.*, **2002**, *293*, 1485.

3. P. Kamoun, M.-C. Belardinelli, A. Chabli, K. Lallouchi, B. Chadefaux-Vekemans, *Am. J. Med. Genet*., **2003**, *116A*, 310.
4. a) C. Szabo, *Nat. Rev. Drug. Discov.,* **2007**, *6*, 917; b) S. Fiorucci, E. Antonelli, A. Mencarelli, S. Orlandi, B. Renga, G. Rizzo, E. Distrutti, V. Shah, A. Morelli, *Hepatology.,* **2005**, *42*, 539.
5. a) Choi, M. M. F. *Analyst*., **1998**, *123*, 1631; b) A. R. Lippert, E. J. New, C. J. Chang, *J. Am. Chem. Soc*., **2011**, *133*, 10078; c) H. Peng, Y. Cheng, C. Dai, A. L. King, B. L. Predmore, D. J. Lefer, B. Wang, *Angew. Chem. Int. Ed.,* **2011**, *50*, 9672; d) F. Yu, P. Li, P. Song, B. Wang, J. Zhao, K. Han, *Chem. Commun.*, **2012**, *48*, 2852; e) L. A. Montoya, M. D. Pluth, *Chem. Commun.*, **2012**, *48*, 4767; f) S. K. Das, C. S.Lim, S. Y. Yang, J. H. Han, B. R. Cho, *Chem. Commun.*, **2012**, *48*, 8395; g) W. Sun, J. Fan, C. Hu, J. Cao, H. Zhang, X. Xiong, J. Wang, S. Cui, S. Sun, X. Peng, *Chem. Commun.*, **2013**, *49*, 3890; h) T. Saha, D. Kand, P. Talukdar, *Org. Biomol. Chem.,* **2013**, *11*, 8166; i) G. Zhou, H. Wang, Y. Ma, X. Chen, *Tetrahedron.*, **2013**, *69*, 867; j) C. Yu, X. Li, F. Zeng, F. Zheng, S. Wu, *Chem. Commun.*, **2013**, *49*, 403; k) J. Zhang, W. Guo, *Chem. Commun.*, **2014**, *50*, 4214; l) M. Tropiano, S. Faulkner, *Chem. Commun.*, **2014**, *50*, 4696; m) T. Ozdemir, F. Sozmen, S. Mamur, T. Tekinay, E. U. Akkaya, *Chem. Commun.*, **2014**, *50*, 5455; n) L. He, W. Lin, Q. Xu, H. Wei, *Chem. Commun.*, **2015**, *51*, 1510; o) J. Zhou, Y. Luo, Q. Li, J. Shen, R. Wang, Y. Xu, X. Qian, *New J. Chem.*, **2014**, *38*, 2770; p) B. Chen, P. Wang, Q. Jin, X. Tang, *Org. Biomol. Chem.*, **2014**, *12*, 5629.
6. S. El Sayed, C. de la Torre, L. E. Santos-Figueroa, C. Marín-Hernández, R. Martínez-Máñez, F. Sancenón, A. M. Costero, M. Parra, S. Gil, *Sensor. Actuat. B-Chem.*, **2015**, *207*, 987.
7. W. Xuan, R. Pan, Y. Cao, K. Liu, W. Wang, *Chem. Commun*., **2012**, *48*, 10669.
8. a) M. Y. Wu, K. Li, J. T. Hou, Z. Huang, X. Q. Yu, *Org. Biomol. Chem.*, **2012**, *10*, 8342; b) J. Bae, M. G. Choi, J. Choi, S. K. Chang, *Dyes Pigm.*, **2013**, *99*, 748.
9. a) C. Wei, Q. Zhu, W. Liu, W. Chen, Z. Xi, L. Yi, *Org. Biomol. Chem*., **2013**, *11*, 479; b) C. Wei, L. Wei, Z. Xi, L. Yi, *Tetrahedron Lett*., **2013**, *54*, 6937; c) X.–F. Yang, L. Wang, H. Xu, M. Zhao, *Anal. Chim. Acta*., **2009**, *631*, 91.
10. a) X. Cao, W. Lin, K. Zheng, L. He, *Chem. Commun*., **2012**, *48*, 10529; b) T. Liu, Z. Xu, D. R. Spring, J. Cui, *Org. Lett*., **2013**, *15*, 2310; c) Y. Liu, G. Feng, *Org. Biomol*. *Chem*., **2014**, *12*, 438; d) S. El Sayed, C. de la Torre, L.E. Santos-Figueroa, R. Martínez-Máñez, F. Sancenón, A.M. Costero, M. Parra, S. Gil, *RSC Adv*., **2013**, *3*, 25690; e) S. El Sayed, C. de la Torre, L. E. Santos-Figueroa, R. Martínez-Máñez, F. Sancenón, M. Ozráez, A.M. Costero, M. Parra, S. Gil, *Supramole. Chem.*, **2015**, *4*, 244; f) Z. Huang, S. Ding, D. Yu, F. Huang, G. Feng, *Chem. Commun.*, **2014**, *50*, 9185.
11. Y. Zhao, X. Zhu, H. Kan, W. Wang, B. Zhu, B. Du, X. Zhang, *Analyst*., **2012**, *137*, 5576
12. a) C. Liu, B. Peng, S. Li, C. M. Park, A.R. Whorton, M. Xian, *Org. Lett*., **2012**, *14*, 2184; b) C. Liu, J. Pan, S. Li, Y. Zhao, L. Y. Wu, C. E. Berkman, A. R. Whorton, M. Xian., *Angew. Chem. Int. Ed*., **2011**, *50*, 10327; c) Z. Xu, L. Xu, J. Zhou, Y. Xu, W. Zhu, X. Qian., *Chem. Commun*., **2012**, *48*, 10871; d) F. Yu, X. Han, L. Chen, *Chem. Commun.*, **2014**, *50*, 12234.
13. a) J. Liu, Y. -Q. Sun, J. Zhang, T. Yang, J. Cao, L. Zhang, W. Guo., *Chem. Eur. J*., **2013**, *19*, 4717; b) L. E. Santos-Figueroa, C. de la Torre, S. El Sayed, F. Sancenón, R. Martínez-Máñez, A. M. Costero, S. Gil, M. Parra, *Eur. J. Inorg. Chem.*, **2014**, 41; c) K. Sasakura, K. Hanaoka, N. Shibuya, Y. Mikami, Y. Kimura, T. Komatsu, T. Ueno, T. Terai, H. Kimura, T. Nagano, *J. Am. Chem. Soc.*, **2011**, *133*, 18003; d) M. –Q. Wang, K. Li, J. –T. Hou, M. –Y. Wu, Z. Huang, X. –Q. Yu, *J. Org. Chem.* **2012**, *77*, 8350; e) I. Takashima, M. Kinoshita, R. Kawagoe, S.

Nakagawa, M. Sugimoto, I. Hamachi, A. Ojida, *Chem. Eur. J.*, **2014**, *20*, 2184; f) Z. Ye, X. An, B. Song, W. Zhang, Z. Dai, J. Yuan, *Dalton Trans.*, **2014**, *43*, 13055.

14. M. W. Ambrogio, C. R. Thomas, Y.-L. Zhao, J. I. Zink, J. F. Stoddart, *Acc. Chem. Res*., **2011**, *44*, 903.
15. C. Coll, A. Bernardos, R. Martínez-Máñez, F. Sancenón, *Acc. Chem. Res*., **2013**, *46*, 339.
16. a) S. El Sayed, C. Giménez, E. Aznar, R. Martínez-Máñez, F. Sancenón, M. Licchell, *Org. Biomol. Chem.*, **2015**,*13*, 1017; b) I. Candel, A. Bernardos, E. Climent, M. D. Marcos, R. Martínez-Máñez, F. Sancenón, J. Soto, A. Costero, S. Gil, M. Parra, *Chem. Commun*., **2011**, *47*, 8313; c) Y. Salinas, R. Martínez-Máñez, J. O. Jeppesen, L. H. Petersen, F. Sancenón, M. D. Marcos, J. Soto, C. Guillem, P. Amorós, *ACS Appl. Mater. Inter.*, **2013**, ***5***, 1538; d) E. Climent, A. Bernardos, R. Martínez-Máñez, A. Maquieira, M. D. Marcos, N. Pastor-Navarro, F. Sancenón, J. Soto, P. Amorós*, J. Am. Chem. Soc*., **2009**, *131***,** 14075.
17. a) X. Qu, C. Li, H. Chen, J. Mack, Z. Guo, Z. Shen, *Chem. Commun.,* **2013**, *49*, 7510; b) C. Kar, M. D. Adhikari, A. Ramesh, G. Das, *Inorg. Chem.,* **2013**, *52*, 743.
18. a) F. Felix, J. Ferguson, H. U. Guedel, A. Ludi, *J. Am. Chem. Soc.*, **1980**, *102*, 4096; b) F. E. Lytle, D. M. Hercules, *J. Am. Chem. Soc.*, **1969**, *91*, 253.

SUPPORTING INFORMATION

Hexametaphosphate-capped silica mesoporous nanoparticles containing Cu^{II} complexes for the selective and sensitive optical detection of hydrogen sulfide in water

Sameh El Sayed, Michele Milani, Maurizio Licchelli, Ramón Martínez-Máñez and Félix Sancenón

Reagents:

2,6-diacetylpyridine, $NaBH_4$, 3,3'-iminobis(propylamine), (3-isocyanatepropyl) triethoxysilane, copper perchlorate, tetraethylorthosilicate (TEOS), n-cetyltrimethylammonium bromide (CTABr), $[Ru(bipy)_3]^{2+}$, sodium hydroxide (NaOH), sodium hexametaphosphate, selected amino acids, and all other chemicals were provided by Sigma-Aldrich. Analytical-grade solvents were from Scharlab. All reagents were used as received.

Methods:

^1H NMR spectra were recorded with a Varian Gemini 300 MHz NMR spectrometer. Mass spectra were acquired on a Thermo-Finnigan ion-trap LCQ Advantage Max instrument equipped with an ESI source. UV/Vis absorption measurements were measured with a Perkin–Elmer Lambda-35 spectrometer. The fluorescence behaviour was studied with an FS900CDT Steady State T-Geometry Fluorimeter from Edinburgh Analytical Instruments. X-ray measurements were performed on a Bruker AXS D8 Advance diffractometer

using Cu-Kα radiation. Thermogravimetric analysis were carried out on a TGA/SDTA 851e Mettler Toledo equipment, using an oxidant atmosphere (Air, 80 mL/min) with a heating program consisting on a heating ramp of 10 °C per minute from 393 K to 1273 K and an isothermal heating step at this temperature during 30 minutes. TEM images were taken with a JEOL TEM-1010 Electron microscope working at 100 kV. N_2 adsorption-desorption isotherms were recorded on a Micromeritics ASAP2010 automated sorption analyser. The samples were degassed at 120 °C in vacuum overnight. The specific surfaces areas were calculated from the adsorption data in the low pressures range using the BET model. Pore size was determined following the BJH method.

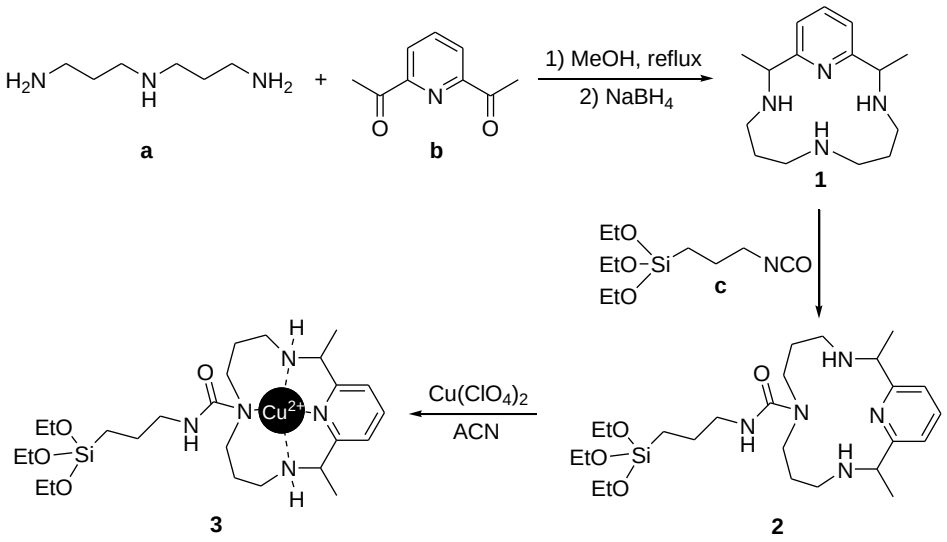

Scheme S1. *Schematic representation of the synthesis of **1**, macrocycle **2** and complex **3**.*

Synthesis of 1:

3,3'-iminobis(propylamine) (**a**, 0.658 g, 5.02 mmol) was dissolved in MeOH (50 mL) and slowly added to a stirred solution of 2,6-diacetylpyridine (**b**, 0.820 g, 5.02 mmol) in MeOH (200 mL). After refluxing for 1h, $NaBH_4$ (0.570 g, 15.1 mmol) was slowly added and the solution was stirred overnight. Afterward, the solvent was evaporated to yield a sticky oil which was purified with column chromatography

on silica gel with $CHCl_3$/MeOH 75: 25 as eluent to give **1** (1.108 g, 4.20 mmol, 78 % yield).

^{1}H NMR (400 MHz, $CDCl_3$) δ 7.67 – 7.40 (m, 1H), 7.06 (m, *J* = 7.7 Hz, 1H), 6.98 (d, *J* = 7.6 Hz, 1H), 3.82 (t, *J* = 6.7 Hz, 2H), 3.73 (t, *J* = 6.8 Hz, 1H), 2.97 – 2.81 (m, 2H), 2.63 (m, *J* = 7.2, 4.1 Hz, 8H), 2.47 (s, 2H), 2.34 (d, *J* = 3.3 Hz, 2H), 1.39 (dd, *J* = 23.9, 6.7 Hz, 6H).

MS ESI (MeOH) = 263.39 m/z, $(M+1)^+$.

Synthesis of 2:

(3-isocyanatepropyl)triethoxysilane (**c**, 0.328 g, 1.33 mmol) was dissolved in dry acetonitrile (10 mL) and then was slowly added to solution of **1 (**0.350 g, 1.33 mmol) in acetonitrile/toluene/$CHCl_3$ 1:1:0.1 v/v/v mixture (50 mL). The solution was stirred during 1 h at 0 °C and then at room temperature for another 60 min. The solvent was evaporated to give a yellow oil that was precipitated by the addition of diethyl ether (20 mL). The final macrocycle **2** (0.542 g, 1.07 mmol, 80 % yield) was isolated as a yellow solid.

^{1}H NMR (400 MHz, $CDCl_3$) δ 7.62 (t, *J* = 7.7 Hz, 1H), 7.09 (d, *J* = 7.7 Hz, 1H), 7.00 (d, *J* = 7.5 Hz, 1H), 3.95 – 3.83 (m, 1H), 3.71 (d, *J* = 7.0 Hz, 4H), 2.94 (d, *J* = 8.9 Hz, 1H), 2.80 – 2.56 (m, 4H), 2.52 (s, 1H), 2.37 (s, 1H), 1.83 (d, *J* = 30.1 Hz, 5H), 1.45 (d, *J* = 6.7 Hz, 4H), 1.38 (d, *J* = 6.7 Hz, 3H), 1.24 (s, 6H).

MS ESI (MeOH) = 510.00 m/z, $(M+1)^+$.

Synthesis of complex 3:

Macrocycle **2** (0.800 g, 1.56 mmol) was dissolved in dry acetonitrile (30 mL) and then copper(II) perchlorate (0.600 g, 1.62 mmol) was added. The final mixture was stirred at room temprature for 2 h. The solvent evaporated and complex **3** obtained as blue solid (1.330 g, 1.97 mmol, 95 % yield).

MS ESI (MeOH) = 673.56 m/z, $(M+1)^+$.

Synthesis of the MCM-41 mesoporous silica nanoparticles:

n-cetyltrimethylammonium bromide (CTABr, 1.00 g, 2.74 mmol) was first dissolved in distilled water (480 mL). Then NaOH 2.00 M in distilled water (3.5 mL) was added to the CTABr solution and the temperature was kept at 80 °C. TEOS (5 mL, 2.57 x 10^{-2} mol) was then added dropwise to the surfactant solution. The mixture was stirred for 2 h to give a white precipitate. Finally the solid product was centrifuged, washed with distilled water and dried at 60 °C (MCM-41 as-synthesized). To prepare the final porous material (MCM-41), the as-synthesized solid was calcined at 550 °C using oxidant atmosphere for 5 h in order to remove the template phase.

Synthesis of S1:

Calcined MCM-41 (500 mg) and $[Ru(bipy)_3]^{2+}$ dye (140.34 mg, 0.40 mmol) were suspended in acetonitrile (20 mL) in a round-bottomed flask. The mixture was stirred for 24 h at room temperature, filtered off and dried under vacuum. Afterward, this loaded solid (400 mg) was re-suspended in acetonitrile (10 mL) containing $[Ru(bipy)_3]^{2+}$ (30 mg) and complex **3** (0.900 g, 1.7 mmol) was added. After stirring for 12 h at room temperature the resulting solid was filtered off, dried under vacuum, washed with acetonitrile (10 mL) and diethyl ether (10 mL) and, finally, dried at 40 ^{o}C for 12 h.

Synthesis of S1-mPh:

S1 (300 mg) was suspended in distilled water (5 mL) containing $[Ru(bipy)_3]^{2+}$ (10 mg) and sodium hexametaphosphate (1 g, 1.7 mmol) and stirred at room temperature for 2 hours, filtered and dried under vacuum for 12 hours.

Synthesis of S2:

MCM-41 loaded with $[Ru(bipy)_3]^{2+}$ (200 mg) solid was suspended in acetonitrile (10 mL) containing $[Ru(bipy)_3]^{2+}$ (30 mg) and macrocycle **2** (0.600 g, 0.98 mmol). After stirring for 12 h at room temperature the resulting solid was filtered off, dried under vacuum, washed with acetonitrile (10 mL) and diethyl ether (10 mL) and finally dried at 40 ^{o}C for 12 h.

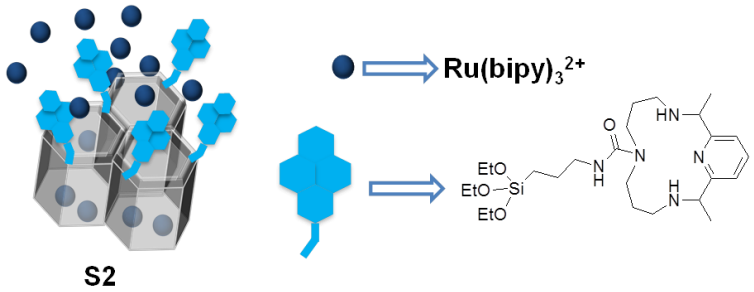

Scheme S2. *Schematic representation of solid* ***S2****.*

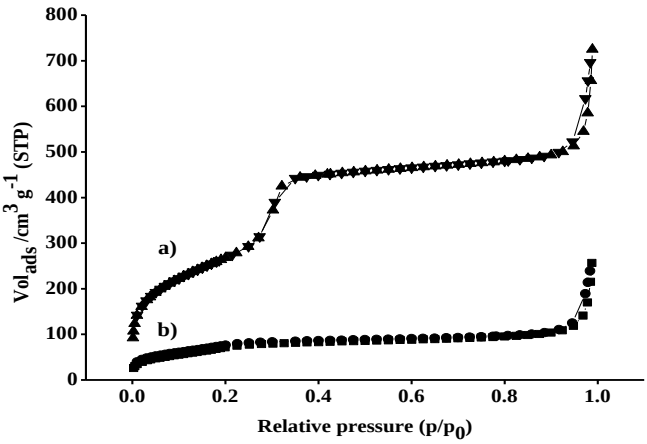

Figure S1. *Nitrogen adsorption-desorption isotherms of (a) calcined MCM-41mesoporous material and (b)* ***S1-mPh*** *material.*

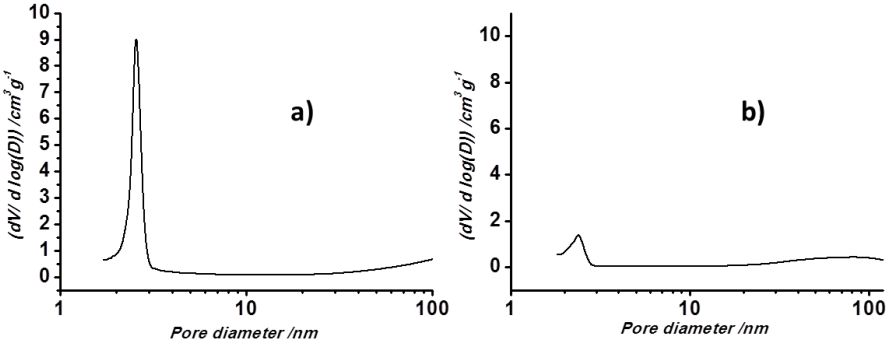

Figure S2. *Pore size distributions of (a) calcined MCM-41mesoporous material (b)* ***S1-mPh*** *material.*

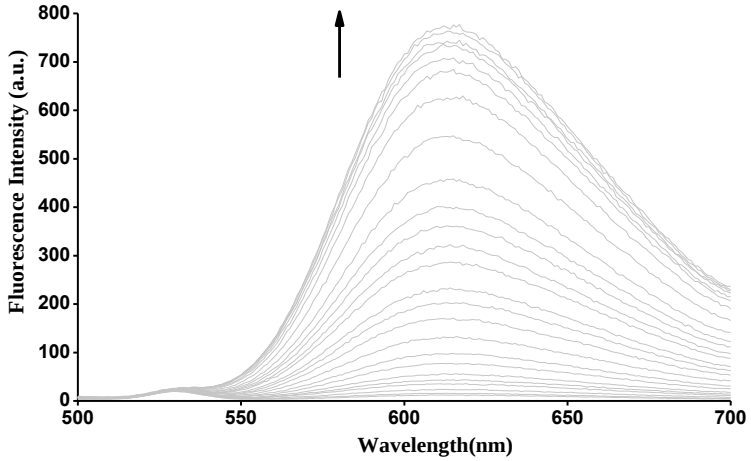

Figure S3. *Fluorescence intensity at 610 nm of $[Ru(bipy)_3]^{2+}$ dye released from* ***S1-mPh*** *(pH 7.5, buffered with HEPES 10mM) upon increasing the concentration of HS^-.*

4. Conclusions and perspectives

Chemical sensing of hazardous species using molecular based probes designed taking into account supramolecular chemistry principles, has attracted great attention in the last years. In addition, very recently, the use of nanoscopic hybrid organic-inorganic materials in recognition and sensing protocols has been described. Bearing in mind the above mentioned facts, the objectives of this PhD thesis were to contribute to the evolution of both fields. In particular, organic, inorganic and material chemistry are combined in order to prepare molecular and hybrid probes for the optical detection of anions and neutral species of environmental and biological significance.

The ***first chapter*** of this PhD thesis was devoted to the introduction of the fundamental principles and recent developments in supramolecular chemistry, especially applied to molecular recognition events and self-assembly process.

Chapter two was focused on the preparation of molecular-based sensors for the optical (chromo and fluorogenic) detection of fluoride, the nerve agent simulant diisopropyl fluorophosphate (DFP) and hydrogen sulfide anion.

- Detection of fluoride anion was achieved by using a pyridine-based silyl ether-containing probe. Of all the anions tested, only fluoride was able to induce a color change from colorless to yellow with a remarkable enhancement in emission intensity. The optical changes were ascribed to a fluoride-induced hydrolysis of the silyl ether moiety.
- A stilbene based pyridinium derivative functionalized with hydroxyl and silyl ether moieties was used as selective sensor for DFP. DFP addition to aqueous solution of the probe induced a color change from colorless to yellow which was ascribed to a hydroxyl phosphorylation followed by a fluoride-induced hydrolysis of the silyl ether group. Besides, the probe was implemented in test strips and DFP detection in gas phase was accomplished.
- Fluorogenic recognition of hydrogen sulfide anion was achieved using different fluorophores (*i.e*. styryl pyridine, naphthalene, quinoline and

fluoresceine) functionalized with 2,4-dinitrophenyl ether moieties. The prepared probes were neraly non-emissive but remarkable selective emission enhancements upon addition of hydrogen sulfide were observed (ascribed to a selective sulfide-induced hydrolysis of the 2,4-dinitrophenyl ether moieties).

- The sensing of hydrogen sulfide anion was also achieved by using fluorophores (coumarin and naphthalene) containing azide and sulfonylazide moieties. Probes were non-fluorescent but upon addition of hydrogen sulfide, an important enhancement in emission was observed. The selective response was ascribed to a reduction of the azide and sulfonylazide moieties to amine and sulfonylamide induced by hydrogen sulfide anion.

The ***third chapter*** of this PhD thesis was devoted to the preparation of nanoscopic gated materials and their application in sensing protocols. By using this original approach, the optical detection of glutathione (GSH) and hydrogen sulfide anion was achieved.

- The first sensory material used MCM-41 mesoporous silca nanoparticles as inorganic scaffold with the pores loaded with safranine O and the external surface functionalized with disulfide-containing oligo(ethylene glycol) moieties. Addition of GSH induced pore opening and dye delivery due to the selective reduction of the disulfide bond. This hybrid material was highly selective to the presence of GSH over other relevant bio-thiols (*i.e*. Hcy, Cys and Me-Cys).
- Capped organic-inorganic hybrid materials for the selective detection of hydrogen sulfide were also prepared. In particular MCM-41 support was loaded with $[Ru(bipy)_3]^{2+}$ dye and the external surface was functionalized with Cu(II)-macorcyclic complexes. Finally, the pores were capped by the addition of the bulky anion hexametaphosphate. Aqueous suspensions of this material showed negligible dye release whereas in the presence of hydrogen sulfide anion a remarkable colour change was observed. This

optical response was ascribed to a demetallation process of the Cu(II) complex induced by hydrogen sulfide.

The results obtained during this PhD thesis provided new insights into the optical detection of anions and neutral molecules of environmental and biological interest. More in detail, the detection of fluoride and hydrogen sulfide in aqueous environment opens the way to apply the prepared probes in analysis of real samples. Also the prospective use of the probes functionalized with 2,4-dintrophenyl ether, azide and sulfonylazide moieties for real time monitoring of hydrogen sulfide in cells has been demonstrated.

The easy fabrication of nerve gases (Sarin, Soman and Tabun) and their indiscriminate use by certain nations and by terrorist groups have increased the efforts of the scientific community toward the detection and remediation of these deadly chemicals. Recently, as an alternative to instrumental methods, the development of fluorogenic and chromogenic probes has gained increasing interest. In this sense, the prepared probe, that allowed the selective optical detection of DFP (a Sarin and Soman mimic), can be of significance. In this context, it is important to note that although the emergency response protocol for Sarin, Soman and Tabun is similar, there are evidences that some antidotes are effective only for certain nerve gases indicating the importance of distinguishing one specific agent within this family of deadly compounds. In this field there are very few examples of probes capable to selectively discriminate DCNP (Tabun mimic) and DFP (Sarin-Soman mimics) indicating the significance of the results obtained with our DFP-selective probe.

Moreover, the design and synthesis of new nanoscopic gated materials for application in sensing protocols are of special interest. One advantage of this approach is the potential existence of amplification features; in particular, the presence of few analyte molecules may induce the release of a relatively high amount of entrapped dye molecules. This could yield sensory materials with higher sensitivities than those reported for the classic molecular-based probes. Also, given the possible use of different porous supports, diverse guest-selective

gate-like systems and a wide range of indicator dyes, this strategy, which has still to be fully studied, displays enormous potential for the development of novel signaling systems.

Gracias al Generalitat Valenciana por concederme una beca SANTIAGO GRISOLÍA.